

**PHOTOCROSSLINKABLE HYDROGELS FOR  
CARTILAGE TISSUE ENGINEERING**

Peter Levett

2015

## **Photocrosslinkable hydrogels for cartilage tissue engineering**

Peter A. Levett

ISBN: 978-0-646-94180-6

Cover by Arabella Waghorn

© 2015 Peter Levett, Brisbane, Australia

No part of this thesis may be reproduced without written permission of the copyright owner.

Principle supervisor:	Dr. Travis J. Klein
Associate supervisors:	Prof. Dietmar W. Hutmacher
	Dr. Jos Malda
	Prof. Whouter J. A. Dhert

The work described in this thesis was completed at the Institute of Biomedical Innovation at the Queensland University of Technology, Australia and the Department of Orthopaedics at the University Medical Center, Utrecht, The Netherlands. The research was funded by the Australian Research Council and the Australasian Society for Biomaterials and Tissue Engineering. The publication of this thesis was sponsored by the Australian Postgraduate Award Scheme.

# **PHOTOCROSSLINKABLE HYDROGELS FOR CARTILAGE TISSUE ENGINEERING**

Foto-crosslinkbare hydrogelen voor het kweken van  
kraakbeenweefsel

(met een samenvatting in het Nederlands)

Proefschrift

ter verkrijging van de graad van doctor aan de Universiteit Utrecht op gezag van  
de rector magnificus, prof.dr. G.J. van der Zwaan, ingevolge het besluit van het  
college voor promoties in het openbaar te verdedigen op maandag 24 augustus  
2015 des avonds te 6.00 uur

door

Peter Andrew Levett

geboren op 14 augustus 1987 te Goroka, Papua New Guinea

Promotoren: Prof.dr. W. J. A. Dhert  
Prof.dr. D. W. Hutmacher

Copromotoren: Dr.ir. J. Malda  
Dr. T. J. Klein

# **PHOTOCROSSLINKABLE HYDROGELS FOR CARTILAGE TISSUE ENGINEERING**

Peter Andrew Levett

Submitted in fulfilment of the requirements for the degree of  
Doctor of Philosophy

Institute of Health and Biomedical Innovation  
Science and Engineering Faculty  
Queensland University of Technology

and

Utrecht University  
Utrecht  
The Netherlands

August 2015

## Abstract

---

For millions of people, damaged cartilage is a major source of pain and disability. As those people often discover upon seeking medical treatment, once damaged, cartilage is very difficult to repair. Finding better clinical therapies for damaged cartilage has generated a huge amount of research interest, and has led to the studies detailed in this thesis. This work was broadly motivated by the aim of advancing our understanding of cartilage tissue engineering – that is, the creation of new cartilage from a combination of biomaterials, cells and growth factors.

Biomaterials are a key part of cartilage tissue engineering therapies. Historically the main purpose of using biomaterials in these therapies was to provide structural support for cells while the damaged tissue regenerated. More recently, it has been recognised that the composition and properties of the biomaterial influence the cell responses and quality of the newly formed tissue. This has led to the development of biomaterials for the specific application of cartilage tissue engineering.

In this thesis, the focus was on hydrogel biomaterials derived from natural polymers. The polymers, including gelatin, hyaluronic acid (HA) and chondroitin sulfate (CS), were chemically modified to become gelatin methacrylamide (Gel-MA), hyaluronic acid methacrylate (HA-MA) and chondroitin sulfate methacrylate (CS-MA) respectively, allowing them to be crosslinked by UV light in the presence of living cells. Using these materials, we investigated *in vitro* the viability of the encapsulated cells, the cell phenotype, and the quantity, composition and mechanical properties of the extracellular matrix they produced.

Compared to encapsulation in other widely used hydrogels such as alginate, chondrocytes produced substantially more cartilage matrix when encapsulated in Gel-MA, and the matrix was much stiffer than that in other materials. However, chondrocyte redifferentiation in Gel-MA was poor. Characterisation of cell-free Gel-MA hydrogels showed that the compressive modulus properties can be controlled over a wide range – approximately 5 to 180 kPa – and that by increasing the viscosity of Gel-MA by supplementing it with hyaluronic acid, Gel-MA structures with defined architecture and porosity could be printed.

To address the poor redifferentiation in Gel-MA, biomimetic constructs containing HA-MA and/or CS-MA were evaluated. By including a small

quantity of HA-MA in Gel-MA hydrogels (9.5% Gel-MA and 0.5% HA-MA), chondrocytes redifferentiated to their normal phenotype to a greater extent, with more rounded cell morphologies and chondrogenic gene expression patterns. Collagen type II and aggrecan were distributed throughout the gels more evenly in the presence of HA-MA. Crucially for cartilage, the developed mechanical properties of constructs with HA-MA were greatly improved compared to Gel-MA controls.

The effect of HA-MA on the developed mechanical properties of tissue-engineered cartilage constructs was further investigated using a range of HA-MA concentrations. The developed mechanical properties were highly dependent on HA-MA concentration, with higher HA-MA concentrations leading to stiffer constructs. In addition to stiffness, the failure strength was increased in gels with HA-MA. Collagen type X deposition, which is an unwanted but commonly produced protein in cartilage repair tissue, was observed in all gels. This reinforces the existing evidence that shows that prolonged growth factor exposure combined with the reactive oxygen species that are generated during crosslinking may induce chondrocyte hypertrophy.

Gel-MA hydrogels were modified with processed cartilage, tissue or tendon tissue extracts (all equine origin). The tissues were digested with pepsin and modified with photocrosslinkable groups to allow the extracts to form stable hydrogels or be incorporated into Gel-MA hydrogels. Mesenchymal stromal cells (MSCs) responded more favourably to the tissue extracts than chondrocytes. Chondrocytes showed increased catabolic processes in the presence of tissue extracts, which is consistent with other research using collagen fragments.

In summary, hydrogels formed from mixtures of Gel-MA and HA-MA showed significant promise as materials for tissue engineering models, and would be interesting materials to investigate in *in vivo* settings.

**Keywords:** Tissue engineering, cartilage, hydrogels, hyaluronic acid, gelatin

# Publications

---

## Peer-Reviewed Journal Articles

- Levett PA, Melchels FPW, Schrobback K, Hutmacher DW, Malda J, Klein TJ. Chondrocyte redifferentiation and construct mechanical property development in single-component photocrosslinkable hydrogels. *Journal of Biomedical Materials Research - Part A* 2013;102:2544-53.
- Schuurman W, Levett PA, Pot MW, Weeren PRv, Dhert WJA, Hutmacher DW, et al. Gelatin-methacrylamide hydrogels as potential biomaterials for fabrication of tissue engineered cartilage constructs. *Macromolecular Bioscience* 2013;13:551-61.
- Levett PA, Melchels FPW, Schrobback K, Hutmacher DW, Malda J, Klein TJ. A biomimetic extracellular matrix for cartilage tissue engineering centered on photocurable gelatin, hyaluronic acid and chondroitin sulfate. *Acta Biomaterialia* 2014;10:214-23.
- Levett P, Hutmacher D, Malda J, Klein T. Hyaluronic acid enhances the mechanical properties of tissue-engineered cartilage constructs. *Plos One* 2014;9:e113216.
- Visser J, Levett P, te Moller N, Besems J, Boere K, van Rigen M, et al. Crosslinkable hydrogels derived from cartilage, meniscus and tendon tissue. *Tissue Engineering - Part A* 2015;21:1195-206.
- Babur BK, Ghanavi P, Levett P, Lott W, Klein T, Cooper-White J, et al. The interplay between chondrocyte redifferentiation, pellet size and oxygen concentration. *PLoS One* 2013;8:e58865.

## Conference Presentations

- Levett P, Hutmacher D, Klein T. Effects of hyaluronic acid and hydrogel stiffness on human zonal chondrocytes encapsulated in degradable polyethylene hydrogels. In: Dias G, Woodfield T, editors. *Australasian Society for Biomaterials and Tissue Engineering*. Queenstown, New Zealand 2011.



- Levett P, Melchels FP, Schrobback K, Hutmacher D, Malda J, Klein T. Photocrosslinkable hydrogels for cartilage tissue engineering. In: Zhang X, editor. World Biomaterials Congress. Chengdu, China 2012.
- Levett P, Melchels F, Schrobback K, Hutmacher D, Malda J, Klein T. Photocrosslinkable hydrogels for cartilage tissue engineering. In: Redl H, editor. Tissue Engineering and Regenerative Medicine World Congress. Vienna, Austria 2011.
- Levett P, Melchels FP, Schrobback K, Hutmacher D, Malda J, Klein T. Photocrosslinkable gelatin, hyaluronic acid and chondroitin sulfate hydrogels for cartilage tissue engineering. In: de Boer J, editor. Nederlandse Vereniging voor Biomaterialen en Tissue Engineering. Lunteren 2012.

## Abbreviations

---

ACAN	Aggrecan gene
ACI	Autologous chondrocyte implanation
AL-MA	Alginate methacrylate
ATMP	Advanced Therapy Medicinal Product
BMP	Bone morphogenetic protein
CS	Chondroitin sulfate
DMEM	Dulbello's modified eagle medium
DMMB	Dimethylmethylene blue
DNA	Deoxyribonucleic acid
ECM	Extracellular matrix
FGF	Fibroblast growth factor
GAG	Glycosaminoglycan
Gel-MA	Gelatin-methacrylamide
HA	Hyaluronic acid
HA-MA	Hyaluronic acid methacrylate
Hep-MA	Heparin methacrylate
KS	Keratan sulfate
MAAh	Methacrylic anhydride
MMP	Matrix metalloproteinase
MSC	Mesenchymal stromal cell
NMR ( <sup>1</sup> H NMR)	Nuclear magnetic resonance (Proton NMR)
OA	Osteoarthritis/osteoarthritic
PCL	Polycaprolactone
PCR	Polymerase chain reaction
PEG	Polyethylene glycol
PBS	Phosphate buffered saline
RNA (mRNA)	Ribonucleic acid (messenger RNA)
ROS	Reactive oxygen species
TGF-β	Transforming growth factor β
UV	Ultraviolet
VEGF	Vascular endothelial growth factor

## Aknowledgements

---

Firstly, I would like to thank my late father, Malcolm who many years ago started encouraging me to do a PhD. It has been a hugely rewarding experience, and I am very glad to have had the opportunity. To my supervisors, Travis, Dietmar and Jos, I am very grateful for your seemingly endless support, patience and guidance. Travis, your patience and insight is infallible; Dietmar, your clear vision & direction when mine were clouded was always appreciated, and Jos, thank you for your motivation and support throughout, and also for taking care of us in Holland (and all the great meals!). Prof. Dhert, thank you for your support in Utrecht and making the dual degree possible. Ferry, thank you for introducing me to Gel-MA, for showing me the ropes in the lab, and for the Nederlandse Les! It was a pleasure to work in the Cartilage Regeneration Lab – the list is long, but in particular to Christoph, Karsten & June, it was great to work with you all. To my wife, Libby, I am always thankful for your encouragement and empathy – I think you had the hardest job of all! Finally, thank you to my mother, Linda, and the rest of my family, Melissa, Alan & Ian for all your help, support and fun over the last few years.



# Contents

---

<b>Chapter 1</b>	General introduction & aims	1
<b>Chapter 2</b>	Photocrosslinkable hydrogels for cartilage tissue engineering: A review of the literature	13
<b>Chapter 3</b>	Chondrocyte redifferentiation and construct mechanical property development in single component photocrosslinkable hydrogels	31
<b>Chapter 4</b>	Gelatin-methacrylamide hydrogels as potential biomaterials for fabrication of tissue engineered constructs	51
<b>Chapter 5</b>	A biomimetic extracellular matrix for cartilage regeneration centered on photo-curable gelatin, hyaluronic acid and chondroitin sulfate	71
<b>Chapter 6</b>	Hyaluronic acid enhances the mechanical properties of tissue engineered cartilage constructs	95
<b>Chapter 7</b>	Crosslinkable hydrogels derived from cartilage, meniscus and tendon tissue	123
<b>Chapter 8</b>	Discussion & future work	145
<b>Summary</b>		171
<b>Samenvatting</b>		175
<b>References</b>		179
<b>Appendix A</b>		203
<b>Appendix B</b>		211



## **Chapter 1**

### **General introduction & aims**

---

## 1.1 Biomaterials and tissue engineering

Several thousand years ago, skilled craftsmen used gold to stabilise loose teeth, crown damaged ones and even replace lost teeth altogether [1]. This was, most likely, the beginning of biomaterial technology. Following these pioneering exploits in dentistry, the course of biomaterial development was slow for many centuries. Though doctors continued to experiment with metallic materials as prostheses for many other body parts [2], a lack of understanding of the need for sanitation, along with a lack of means for sanitation, hampered success rates [3].

The invention of polymeric materials in the 20<sup>th</sup> century, along with other advances in healthcare, paved the way for the modern era of biomaterials. Initially these were off-the-shelf materials taken from other industries, but the 1960s saw a shift towards the large scale use of materials designed specifically for medical purposes [3]. Decades of systematic and widespread research in biomaterials followed, and it is now a market worth approximately \$US44 billion per year, and growing at 15% annually [4].

Up until approximately the 1980s, biomaterials were first envisioned to replace or augment damaged tissues, while the original tissue was sacrificed and discarded. Although these transfers were often initially successful, most materials tended to degrade in the body, and the material often did not last the life of the patient. Concurrently, whole tissue and organ transplantations were increasingly used for the treatment of critical patients, although success was (and continues to be) constrained by the need for prolonged immunosuppressant medication and a demand for transplanted organs that far outstrips supply. The contribution of both biomaterials and organ transplants to modern medicine healthcare should not be understated, but the limitations of both fields led to ongoing research and innovations in pursuit of improved technologies. The last decades of the 20<sup>th</sup> century saw the emergence of a new paradigm in medicine: tissue engineering [5]. The concept was novel yet fundamentally simple: rather than replace a damaged tissue with an inert, non-viable material, or healthy tissue from a donor, why not use a combination of biomaterials, cells and biological signalling factors to facilitate the regeneration of the new, healthy tissue?

The terms *tissue engineering* and *regenerative medicine* are frequently used interchangeably to encompass the research and clinical efforts to repair or regenerate damaged or diseased tissues. In this thesis, the term *tissue engineering* will generally be adopted. Tissue engineering is an interdisciplinary field that lies at the intersection of materials science and engineering, biology,



chemistry and medicine. The scope for tissue engineering is driven by the shortcomings of clinical medicine, while chemistry and materials science provide the tools to manufacture the materials, and biology provides both the specific requirements for material design and the potential to engineer biological systems. It is a field with the capacity to address many of the challenges in medicine and attempts have been made to engineer many different tissues, including bone, cartilage, skin, liver, kidney, heart, retina, pancreas, and many others. In large part, however, the field has yet to really prove itself, and currently there are relatively few cases of long term, successful clinical application.

Two decades ago, Langer and Vacanti published a landmark paper outlining the concepts and potential of tissue engineering [5]. From this and other studies, three generic components have been identified as the foundations of tissue engineering therapies: biomaterials, cells and signalling factors [5]. As one of the core components, biomaterials have received a great deal of attention in tissue engineering research, and much of the progress of tissue engineering is attributable to the development of biomaterials.

The term biocompatibility describes the interaction or suitability of a biomaterial in a specific biological system. Many definitions exist, but given the broad nature of the field, the generic definition proposed by Williams is perhaps most apt: “The ability of a material to perform with an appropriate host response in a specific application” [6]. Critically, this definition does not simply imply non-toxicity or non-immunogenicity, but also allows for specific responses and cell-material interactions, should such responses be appropriate or desirable in the given application.

## **1.2 Cartilage**

Articular cartilage is a soft, frequently damaged tissue and unlike many tissues, almost completely lacks the capacity to heal itself once it is damaged. These properties have made it an important target for tissue engineering. There are currently no completely effective clinical solutions to cartilage repair, and for this reason the pursuit of an appropriate biomaterial for regeneration of cartilage is a primary aim of many research groups worldwide, as well as the subject of this thesis.

Articular cartilage is a hyaline tissue that covers the ends of long bones in mammalian, diarthrodial joints. It cushions impacts, distributes loads and provides a near frictionless surface for articulation. The extracellular matrix

(ECM) has three major components: a collagen network, proteoglycans and fluid [7]. The bulk composition of cartilage is approximately 70-80% water and 20-30% matrix by weight. Structurally, cartilage is a relatively simple tissue that lacks nerves, blood vessels, and lymphatic vessels. The tissue contains only one cell type, the chondrocyte, at a remarkably low density; in human cartilage, chondrocytes account for only 1-5% of the total volume [8, 9]. Chondrocytes are a terminally differentiated, specialised cell type whose primary function is to produce and maintain the ECM [10, 11].

### 1.3 Cartilage composition

Collagen is the major component of the solid phase of articular cartilage, accounting for approximately 60% of the matrix dry weight [7]. Collagen type II is by far the most abundant, accounting for 90-95% of the total collagen content [12]. Collagen types VI, IX, X, XI, XII and XIV are embedded in the network in smaller quantities, although the functions of each type are not yet fully understood [13]. Of these, types II, IX and XI are unique to cartilage [14].

Hyaluronic acid (HA) is a polysaccharide of particular biological importance. It belongs to a class of compounds known as glycosaminoglycans (GAG), but notable distinctions between HA and other GAGs exist. In vertebrates, glycosaminoglycans typically contain large numbers of sulfate and carboxyl groups, and therefore contain a high level of negative charge at physiological pH [15]. Uniquely, HA is an unsulfated GAG, composed of repeating disaccharide units of N-acetyl-D-glucosamine and D-glucuronic acid [16]. In contrast to other GAGs, which are synthesised in the rough endoplasmic reticulum and processed in the golgi apparatus for incorporation into proteoglycans, HA is produced in the plasma membrane, and contains no amino acid sequences in its final structure [17, 18]. HA forms extensive linear chains, with a molecular mass in the range  $10^3 - 10^4$  kDa, corresponding to 2000 – 25,000 repeat units and a length of 2 – 25  $\mu\text{m}$  [18].

HA is ubiquitous in the extracellular matrices of higher animals, and appears in particularly high concentrations in soft connective tissues [16]. Despite its simple structure, it has many functions in cartilage and other tissues. HA is implicated in embryonic development, wound healing, immune responses, inflammation and cancer development [18, 19]. In cartilage, chondrocytes can directly detect and bind to HA via various receptor domains expressed on the cell surface, such as CD44 and the receptor for hyaluronic acid mediated motility (RHAMM) [20]. In addition, HA forms strong associations with collagen type VI [21, 22], and is a key component of the large proteoglycan

aggregates that contribute to the compressive strength of cartilage. It is also involved in the regulation of several growth factors [23], and there are likely many functions yet to be discovered.

Proteoglycans are the second most abundant organic component of articular cartilage, accounting for 30% of the matrix dry weight [7]. Proteoglycans are molecules in which a large number of GAG chains are covalently linked to a core protein [15]. The compressive strength of cartilage is provided primarily by the large aggregating proteoglycan called aggrecan [14]. The core protein has a mass of approximately 230 kDa, and is organised into three globular domains, G1-G3 [14]. Located between the G2-G3 domains are sites for attachment of the GAGs chondroitin sulfate (CS) and keratan sulfate (KS). Up to 130 CS and KS chains may be covalently bonded to the core protein, resulting in a molecule with a molecular mass of up to 2.2 MDa [24]. Up to 100 of these proteoglycans are further bound to hyaluronic acid, creating a superaggregate with a molecular mass in the region of 200 million Daltons, of which greater than 90% is carbohydrate [7, 15]. Link protein (molecular weight 41 – 48 kDa) stabilises the non-covalent interaction between the individual aggrecan molecules and HA [25] (Figure 1.1B).

The high level of fixed negative charge in aggrecan contributes to the biomechanical properties of cartilage in a number of ways. Adjacent charged groups are sufficiently close (approximately 1 – 1.5 nm apart) to allow electrostatic interactions and the resulting repulsive forces contribute significantly to swelling of the matrix [24]. In addition, the level of fixed charge mediates a high level of hydration, and results in a high concentration of cations (primarily sodium) in the fluid phase. The elevated cation concentration relative to the surrounding synovial fluid yields a Donnan osmotic pressure, causing a swelling pressure in the order of several atmospheres [26]. Finally, aggrecan, particularly through CS, bestows cartilage with a low hydraulic permeability, which limits the loss of fluid under compression and aids in compression resistance [27, 28].

#### **1.4 Zonal organisation**

The composition and structure of cartilage is organised according to depth, and this depth variation has been studied for over half a century [29]. The tissue is typically considered in four distinct zones, classified as the superficial, middle, deep and calcified zones with increasing depth from the articular surface [29, 30]. The biochemical and biomechanical properties of cartilage, along with chondrocyte phenotype, vary significantly between zones (Figure 1.1). While

the structures in the superficial, intermediate and deep zones are distinct, there is a gradual transition between adjacent zones, with no clear boundaries [31].

The superficial zone accounts for 10 – 20% of the total thickness nearest the articular surface. The collagen network is aligned parallel to the articular surface (Figure 1A), and collagen content is highest in the superficial zone (85% dry weight). The proteoglycan content is lowest (15% dry weight), which results in this zone having the highest tensile strength and lowest compressive modulus [32]. The low compressive modulus permits substantial deformation of the tissue during loading [33]. Single chondrocytes are dispersed throughout the matrix, and secrete proteoglycan 4 (PRG4) which acts as a lubricant to reduce friction at the joint surface [8].

#### *Superficial zone*

The network orientation of the superficial zone provides a high tensile strength, which serves to maintain the fluid pressure of the deeper zones, and is often described as analogous to the wall of a pressure vessel [31]. The tensile strength of the network in this outer region opposes the swelling tendency of the deeper regions, thus preventing overexpansion of the tissue, and maintaining a positive fluid pressure in the lower zones.

#### *Middle/intermediate zone*

In the middle/intermediate zone (30-50% of total thickness) the collagen matrix is randomly oriented, and appears as a tangled mesh. The proteoglycan content is approximately 25% dry weight, resulting in a higher compressive modulus than the superficial zone [32]. Upon loading, the compressive strain aligns the fibres parallel to the surface. Chondrocytes in this zone are oval in shape, and are commonly found as singles or in pairs [34].

#### *Deep zone*

The collagen network of the deep zone (30-50% of total thickness) is oriented perpendicularly to the calcified cartilage and underlying subchondral bone, and the proteoglycan level is greatest in this zone, resulting in a compressive modulus an order of magnitude greater than the superficial zone [33]. When loaded, the high charge density prevents significant compression of the tissue by retention of water, and when unloaded, the aligned collagen matrix provides the tensile strength required to prevent excessive expansion [35]. Chondrocytes in the deep zone are arranged in columns of cells which are aligned parallel to the collagen network [36].

### Calcified zone

The calcified layer is very thin, ( $\sim 100 \mu\text{m}$ ), and its function is to provide a strong interface for attachment of cartilage to the subchondral bone beneath [30]. Collagen fibrils from the deep zone penetrate and are firmly embedded in the calcified zone [7]. The chondrocytes produce collagen type X, which serves to calcify the matrix.

## 1.5 Matrix organisation around chondrocytes

On a smaller scale, the ECM of cartilage is organised around chondrocytes into defined structures. With increasing distance from chondrocytes, the matrix is classified as pericellular, territorial or interterritorial [37] (Figure 1.1C). The interterritorial matrix is continuous, and provides the bulk of the mechanical properties. The exact function of the pericellular matrix is unclear, but it has been implicated in the protection of chondrocytes from mechanical stresses, while allowing transduction of mechanical stimuli and molecular signalling [12, 38]. In addition, the presence of the four defining components of basement membranes – laminin, collagen IV, nidogen and perlecan – provides some indication that the pericellular matrix may be the functional equivalent of a basement membrane [39].

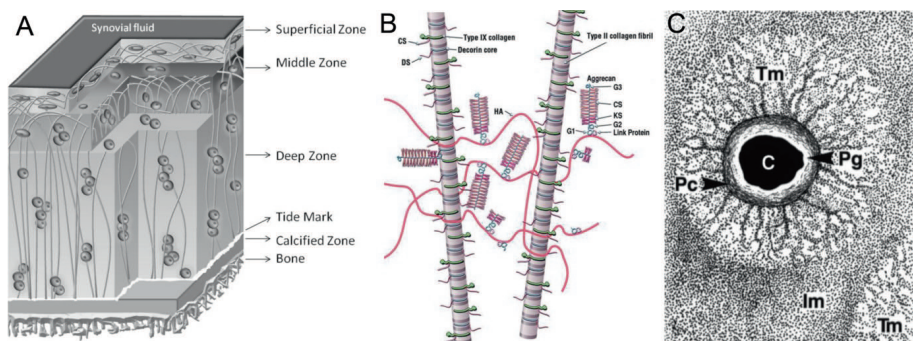


**Figure 1.1: Matrix structures in articular cartilage.** (A) Schematic representation of the zonal structure of articular cartilage (adapted from [40]); (B) the major components of articular cartilage (adapted from [12]), and (C) an electron micrograph showing the ultrastructure of matrix surrounding a deep zone chondrocyte (from [41]). In (C), the tissue surrounding the chondrocyte (labelled C) is organised into the pericellular matrix (Pg), pericellular capsule (Pc), territorial matrix (Tm) and interterritorial matrix (Im).

## 1.6 Cartilage: a challenge for tissue engineering

Unfortunately, cartilage is susceptible to damage through trauma, such as sports injuries or motor vehicle accidents, and disease, the most prevalent of which is osteoarthritis (OA) [42]. Damaged cartilage has very little capacity for self repair, an attribute that has been exhaustively noted in the cartilage literature, most notably by William Hunter, a Scottish physician who made broad contributions to the understanding of human anatomy and physiology (Figure 1.2) [43].

**If we consult the standard Chirurgical Writers from *Hippocrates* down to the present Age, we shall find, that an ulcerated Cartilage is universally allowed to be a very troublesome Disease; that it admits of a Cure with more Difficulty than a carious Bone; and that, when destroyed, it is never recovered.**

**Figure 1.2: Excerpt from William Hunter's 1743 article *On the structure and diseases of articulating cartilage* [44].**

Cartilage damage is classified as either partial thickness if it is entirely contained within the cartilage volume, or full-thickness if it extends into the subchondral bone. Partial thickness injuries display effectively no healing response, making medical interventions particularly important. Whereas in full-thickness defects, blood from the bone marrow can enter the damaged cartilage, and some, albeit imperfect, healing response is observed [45]. The repair tissue that forms in full-thickness defects is akin to the scar tissue that commonly replaces damaged skin; it is highly fibrous, and like scars of the skin, displays little resemblance to the composition, structure and function of the original tissue. The fibrous cartilage that fills full-thickness defects does not have the mechanical strength or low-friction properties of hyaline cartilage, and at best offers only temporary relief from symptoms. Regenerating cartilage with the same composition, structure and functional of the original tissue has proven far more difficult than first envisioned [46-48].

Despite the limitations, the repair mechanism of full-thickness defects forms the basis for some of the most widely used treatments for cartilage injuries. The current gold standard and first line treatment for small, isolated chondral defects is microfracture [49]. This procedure involves debridement of the defect to remove loose or damaged cartilage along with the calcified layer, followed by perforating the subchondral bone with an awl to allow blood flow and induce

the healing response observed in full thickness defects. Microfracture is a simple, fast and low-cost procedure, and is routinely used for treatment for small defects ( $<2.5 \text{ cm}^2$ ) [49]. As expected, short terms outcomes are generally good, however the longer-term prognosis is poor. For larger defects, osteochondral plugs can be harvested from the less weight bearing regions of the same joint or from donor tissue and used to fill the defect. While the results are generally good, the lack of donor tissue, and the additional damage caused by harvesting the plugs are significant limitations [49].

Cartilage tissue engineering therapies aim to address the limitations of microfracture and osteochondral transfers. The earliest iteration, autologous chondrocyte implantation (ACI), was introduced by Brittberg et al. in 1994 (Figure 1.3) [50]. The original conception of ACI required patients to undergo two surgeries, and has consequently now been classified as a two-stage procedure. During the first operation the defect is tidied by removing loose and damaged cartilage, and a small section of healthy cartilage is harvested from a non-weight bearing region. The chondrocytes are enzymatically released from the healthy cartilage and expanded *in vitro* for several weeks, with an approximately  $\sim 10$  fold increase in the total number of cells. During the second surgery the expanded chondrocytes are injected as a slurry into the defect and covered with a periosteal flap or collagen membrane, with the hypothesis that the injected cells will remain viable, and over time synthesise new, healthy cartilage to replace the tissue that has been lost or damaged.

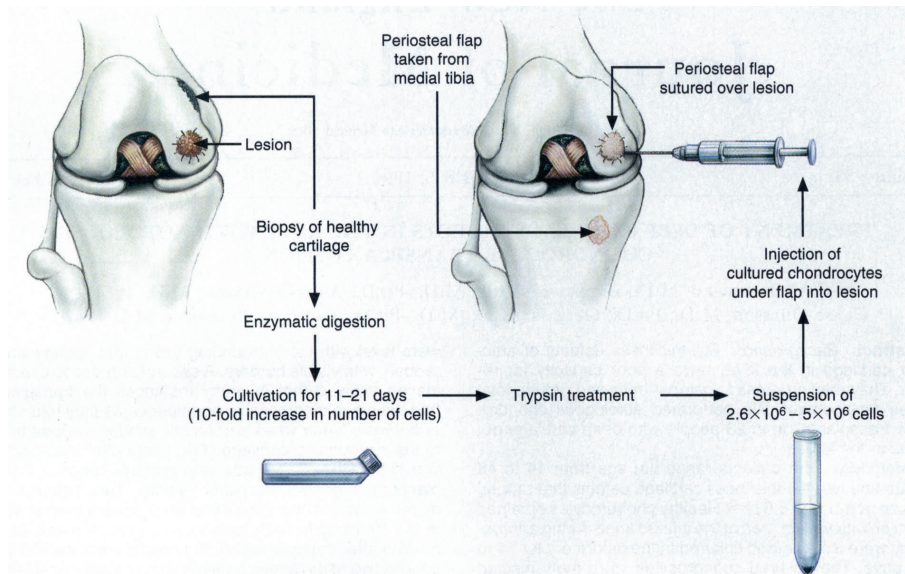


**Figure 1.3: Schematic representation of autologous chondrocyte implantation.** Healthy, non-weight bearing cartilage is harvested, the chondrocytes are isolated and expanded *in vitro*, then injected into the original defect (from [50]).

The primary shortcoming of ACI is that the repair tissue is more similar to fibrocartilage than the original hyaline cartilage. Chondrocytes lose their distinctive phenotype during *in vitro* expansion, with a shift from producing collagen type II, which is the major component of hyaline cartilage, to collagen type I, which is the major component of fibrocartilage. It is likely that the synthesis of fibrocartilage is a result of the inability to adequately reverse the dedifferentiation process and to restore the original chondrocyte phenotype.

It is now two decades since the original ACI procedure was first used in humans, and cartilage tissue engineering has evolved into a number of diverse therapies that owe their origins in some way to this original concept [51]. The use of biomaterials has been a common evolution of the original ACI procedure, and a vast variety of materials have been evaluated for this purpose. Biomaterials can be used to deliver cells to the defect, thus providing a framework for holding cells in place and acting as a temporary support structure for filling the defect until the new cartilage has been synthesised. In addition, more recently, a goal of research efforts has been to develop materials that promote both restoration of the original chondrocyte phenotype and production of new, hyaline tissue. This can be achieved by incorporating bioactive signalling molecules creating materials that mimic hyaline cartilage.



Throughout this thesis, *in vitro* hydrogel models have been used to assess hydrogels materials for their suitability for cartilage tissue engineering, and in particular, the cell differentiation state, along with quantity and quality of matrix production

## 1.7 Hypotheses

The central hypothesis of this thesis was that gelatin-based hydrogels can be developed for cartilage tissue engineering using *in vitro* models. We hypothesised that by functionalising gelatin with photocrosslinkable domains, hydrogels with a broad range of mechanical properties could be fabricated, and that the thermosensitivity of gelatin could be exploited to print hydrogel structures. We also hypothesised that through the incorporation of GAGs and tissue-derived supplements, the hydrogels would create a biomimetic environment for enhanced chondrogenic (re)differentiation and ECM formation. To allow gelatin hydrogels to be photocrosslinked, we produced gelatin-methacrylamide using a process originally described by Van den Bulcke et al. [52].

## 1.8 Aims

There were four main aims to address these hypotheses:

- i. To evaluate Gel-MA hydrogels in parallel with other widely used hydrogels for cartilage tissue engineering;
- ii. To characterise the mechanical properties of Gel-MA hydrogels, and evaluate the printability of Gel-MA based hydrogels;
- iii. To incorporate GAGs into Gel-MA hydrogels to enhance chondrogenic differentiation, and optimise the composition of the hydrogels; and
- iv. To test whether chondrogenesis and matrix formation can be enhanced by incorporating extracts from three collagen-based tissues: cartilage, meniscus, and tendon.

## 1.9 Thesis overview

Significant research efforts have been directed towards developing hydrogels for cartilage regeneration. This literature is reviewed in **Chapter 2**, with a particular focus on photocrosslinkable hydrogels and functionalisation strategies that enhance chondrogenesis and matrix formation.

Chapters 3 to 7 contain the experimental contributions that address the aims and hypotheses. This begins with a direct comparison of four photocrosslinkable

hydrogels in **Chapter 3**. This comparison highlighted the potential utility of Gel-MA hydrogels, which form the focus of the subsequent chapters. In **Chapter 4**, Gel-MA hydrogels are evaluated more closely, including characterisation of the swelling and mechanical properties of hydrogels crosslinked under different conditions and formed from different concentrations of Gel-MA. Possibilities for printing Gel-MA constructs are also investigated. In **Chapter 5** we assess the effect of incorporating photocrosslinkable HA and/or CS into Gel-MA hydrogels on chondrogenesis and matrix formation. In **Chapter 6** we investigate in further detail how HA concentration influences the development of mechanical properties during culture. In **Chapter 7** we have developed a process for functionalising tissue derived matrices with photocrosslinkable domains. Using chondrocytes and mesenchymal stromal cells (MSCs), we investigate if the addition of photocrosslinkable tissue matrices derived from three equine tissues, cartilage, meniscus or tendon, can enhance matrix production or chondrogenesis. The findings of this thesis are discussed in **Chapter 8**, along with potential avenues for future work. Following Chapter 8 the major findings are summarised in English and Dutch.

## **Chapter 2**

# Photocrosslinkable hydrogels for cartilage tissue engineering: A review of the literature

---

## Abstract

Hydrogels share many properties with cartilage, and chondrocytes were shown to respond favourably to encapsulation in hydrogels over 20 years ago. Early hydrogel studies typically used physically crosslinked, naturally derived hydrogels, such as agarose and alginate. Since the year 2000, the development of new hydrogel systems has been an active area of research, with many broad goals, such as the synthesis of new materials, increased mechanical strength, and reduced cell-toxicity. Of particular significance has been the emergence of photocrosslinkable hydrogels, which are covalently crosslinked by exposure to light. These materials can be produced from synthetic or naturally derived hydrogels, or a combination of both, and provide a versatile platform for further functionalisation and modification. Accordingly, a major avenue of cartilage research has been identifying bioactive molecules, such as peptides, proteins, polysaccharides, proteoglycans and growth factors that enhance chondrogenesis and matrix synthesis. Some photocrosslinkable hydrogels are now making early inroads into commercial translation to therapies for clinical cartilage repair. Recently, new photocrosslinkable chemical groups with improved kinetics and potentially reduced adverse cell effects have also been developed, along with new photoinitiators that allow the use of visible light to achieve crosslinking, overcoming the need to use potentially harmful ultraviolet light. Photocrosslinkable hydrogels offer many advantages over other materials, and their use in both cartilage tissue engineering research and clinical application are expected to grow in the future.

**Keywords:** Hydrogels; photopolymerisation; cartilage; tissue engineering.

## 2.1 Introduction

Biomaterials, cells and signalling factors form the three key components of tissue engineering. The study of biomaterials is a diverse field, ranging from metallic and ceramic materials used in bone applications, to pastes and gels used for soft tissue repair. For cartilage regeneration, hydrogels are a key subset of biomaterials being investigated and developed, since they share many properties with healthy cartilage. They are formed from crosslinked networks of water-swollen polymers, and typically contain 80-99% water by mass. The high water content allows for diffusion of metabolites through the network, allowing cells to survive when encapsulated in the hydrogel. Following the early finding that dedifferentiated chondrocytes regain aspects of their original phenotype when encapsulated in agarose hydrogels [53], much effort has been directed at developing hydrogels that are specifically targeted for cartilage tissue engineering [54].

One of the fundamental benefits of hydrogels for cartilage repair is that through *in situ* crosslinking of a cell suspension in solution of a precursor polymer, the cells can be encapsulated in a genuinely three-dimensional environment that promotes a rounded morphology. The commonly used alternative, seeding cells onto a preformed scaffold or matrix, also provides a three-dimensional environment on a larger scale, but if the pore sizes are large enough to allow cells to penetrate into the scaffold, then they are also large enough to allow cells within the scaffold to spread significantly.

The objective of this literature review is to summarise the advances in photocrosslinkable hydrogel materials intended for cartilage tissue engineering, including functionalisation of hydrogels with bioactive motifs to improve the quantity and quality for newly formed cartilage tissue.

## 2.2 Mechanics of photocrosslinking

There are two main requirements for a polymer solution to become covalently crosslinked when exposed to light. The first is a photoinitiator that produces radicals upon light exposure, and the second is that the polymer must contain reactive groups that undergo a crosslinking reaction in the presence of the photogenerated radical.

Since the year 2000, cell encapsulation within photocrosslinkable hydrogels has been explored as a potential means for chondrocyte delivery [55]. Early studies focused primarily on PEG and PVA hydrogels, and crosslinking was almost exclusively achieved via photoinitiated radical polymerisation of polymers

functionalised with (meth)acrylate groups. These early studies showed that chondrocytes tolerated the photocrosslinking process, and were well suited for encapsulation within these bioinert hydrogels [55].

### **2.2.1 Photoreactive chemical species**

The majority of polymers used in photocrosslinkable hydrogels systems are functionalised with acrylate or methacrylate groups. Polymers containing primary or secondary hydroxyl groups can be easily be modified to include acrylate or methacrylate groups using reactive derivatives of acrylic acid or methacrylic acid, respectively. Similarly, these reagents react with primary amines to form acrylamide and methacrylamide, which, due to resonance stabilisation, are less reactive than the corresponding (meth)acrylate groups. This simple and versatile chemical process has been used to functionalise a large number of synthetic and natural polymers with photocrosslinkable domains [56].

Acrylate and methacrylate remain among the most widely chemical groups in photocrosslinked hydrogels, but more recently other systems with different crosslinking rates, mechanisms and conditions have been developed. These include the orthogonal systems, in which two different chemical groups are covalently bound during polymerisation. Usually, one of these groups is a thiol (S-H). The photogenerated radicals remove or abstract hydrogen from the thiol, leaving a reactive thiyl radical on the polymer chain. Thiyl radicals react readily with unsaturated groups containing double or triple bonds, termed thiol-ene and thiol-yne reactions, respectively. In addition, thiyl groups can react with acrylate and methacrylate, allowing different combinations of polymers to be incorporated into the hydrogel. There are several potential advantages of thiol-systems compared to (meth)acrylate systems, and these are discussed in Chapter 8.

### **2.2.2 Photoinitiators and safety**

UV crosslinked biomaterials have been used in dentistry since the early 1970s, making dentistry an ideal field to review for insights into the safety of UV photopolymerisation. Polymer-based materials were developed to restore damaged or drilled teeth. These were applied as a viscous paste, shaped as required, then cured to form a solid upon exposure to light. Initially, light with a wavelength of approximately 365 nm was used and crosslinking was initiated using benzoin methyl ether [57]. The uptake of these systems was fast and widespread, but within a few years, concerns were raised regarding potential

biological damage to the oral mucosa of the patient and eyes of the physician [58]. This resulted in a rapid transition to visible light (400 – 550 nm) initiation, using the initiator camphorquinone together with amine accelerators [57]. Subsequently, potential risks to retinal damage from the lower regions of the visible spectra were identified [59], and if desired, physicians could use filters to remove wavelengths under 500 nm. This system has now proven itself over a long period, with visible light polymerisation using camphorquinone being a mainstay of dentistry for over 20 years.

As previously mentioned, photocrosslinking requires the presence of a photoinitiator. Photoinitiators can be classified as radical or cationic depending on their mechanism of action. Generally speaking, cationic initiators are incompatible with aqueous systems, so *in situ* polymerisation necessitates the use of radical initiators. When light is absorbed by a radical photoinitiator, the molecule undergoes photolysis, forming two radicals. When they come into contact with unsaturated vinyl groups or other reactive moieties, these radicals initiate polymerisation and thus crosslinking occurs.

Different photoinitiators are active at different wavelengths, and they are broadly grouped depending on whether they are active in the UV or visible region of the electromagnetic spectrum. The ultraviolet spectrum is further divided into three bands according to wavelength: UVA (320 – 400 nm), UVB (280 – 320 nm) and UVC (<280 nm) [60]. Solar radiation contains all of UVA, UVB and UVC, however not all of the UV radiation reaches the earth. UVC is almost completely absorbed by stratospheric oxygen, resulting in the production of ozone (O<sub>3</sub>), which in turn can absorb and filter UVB [61]. Consequently, UVA accounts for approximately 95% of the solar UV radiation falling on the Earth's surface, with the majority of the remainder being UVB.

UVA penetrates further into human skin than the shorter-wavelength UVB light, but importantly, has a lower energy. UVB has sufficient energy to cause direct DNA damage and mutations, and is the major cause of light-induced mutagenic DNA modifications [62], which effectively excludes UVB light from any photoinitiation systems involving cells. In comparison, DNA absorbs light only minimally in the UVA and visible regions; so direct damage to DNA upon UVA exposure is very limited [60]. Nevertheless, DNA damage through indirect mechanisms, such as reactive oxygen species (ROS), is still possible, and therefore safety concerns of UVA radiation cannot and should not be dismissed [61].

In addition to the potentially deleterious effects of UV radiation, there are a limited number of photoinitiators that have acceptable toxicity for use in direct contact with cells. In order for a photoinitiator to be suitable, it must be water soluble, non-toxic (or minimally toxic) and active under either visible or UVA light. In addition, the photogenerated radicals must have an acceptable toxicity profile. The vast majority of photoinitiators have been developed for the chemical industry and are not soluble in water, which leaves a relatively small pool that may be suitable for hydrogel crosslinking.

An early study on the biocompatibility of different photoinitiators compared five photoinitiation systems [63] which were either active under visible or UVA light. Of the five, Irgacure 2959 was demonstrated to have a considerably better cytotoxicity profile than the others [63], and these findings led to the near universal and exclusive use of Irgacure 2959 for cell encapsulation in photocrosslinkable hydrogels [63]. Irgacure 2959 has an absorption peak at approximately 280 nm (Figure 8.4, in Chapter 8), but since this wavelength is in the UVB region, it is incompatible for with cells. As a compromise, the initiating light is often restricted to a safer wavelength of approximately 360-365 nm, with a substantial drop in the molar extinction coefficient, and thus efficiency of the photoinitiating system [64]. Complete safety of this initiator has not yet been shown, and further studies, including long term *in vivo* studies, are required to obtain a clearer picture of the safety and risks of cell encapsulation with UVA light.

Although photocrosslinking has a long history in dentistry, fundamental differences exist between using light to crosslink cell-free biomaterials compared to directly exposing cells to light during photocrosslinking. In addition, significant differences have been found between exposing cells in monolayer cultures to photoinitiated radicals compared to cells in hydrogels during crosslinking [65]. In a study using MSCs, UV exposure and Irgacure 2959 had adverse effects on monolayer cultures, including reduced viability, reduced proliferation and reduced differentiation potential. During encapsulation, however, these negative effects were almost completely eliminated [65]. It was suggested that in monolayer cultures, in the absence of other reactive chemical species, the majority of the radicals formed react with cells. In contrast, during encapsulation, the radicals initiate crosslinking reactions, and are therefore less likely cause cell damage. This is a plausible explanation for the difference between the culture systems, but still suggests that optimising Irgacure concentration, UV exposure time and UV intensity are necessary for minimising cell harm. If radicals continue to be produced once



crosslinking is complete then presumably they would be likely to cause cell damage. Overall, the risks need to be evaluated for each hydrogel system and the process parameters need to be selected such that risks are minimised, at least to an acceptable level for clinical use. Further details and recent advances in photoinitiators are given in Chapter 8.

### 2.2.3 Versatility

One advantage that photocrosslinkable hydrogels have over other widely used systems, such as alginate or agarose, is that crosslinking can be triggered on demand. This gives a high level of spatial and temporal control over crosslinking. For example, spatial patterning can be achieved by placing a micro-fabricated template or stencil between the hydrogel and the light source. This has many possible applications, and as an example, surfaces can be selectively coated with different hydrogels, as shown in Figure 2.1 [66]. Photocrosslinkable hydrogels can potentially be used for injectable cell or drug delivery, and crosslinked by shining light through the skin [67].

In addition, photocrosslinking is not heavily dependent on the size of the hydrogel, and the extent of crosslinking is typically relatively even throughout the hydrogel. In comparison, alginate hydrogels are crosslinked by diffusion of calcium ions into the gel, so the total time required for crosslinking rate is strongly dependent on hydrogel size, and the rate of crosslinking varies as crosslinking occurs, since calcium diffusion is slowed as crosslinking proceeds.

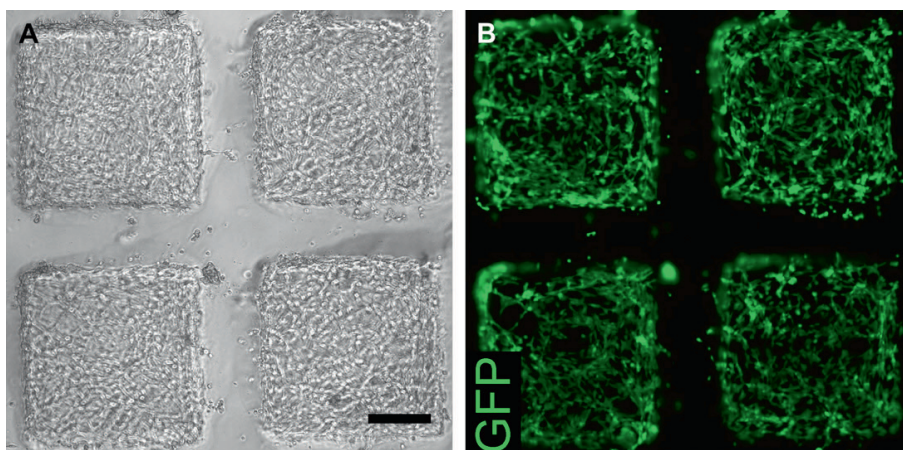


**Figure 2.1: Gel-MA micro-patterned onto a PEG substrate.** Cells adhere strongly to regions coated with Gel-MA, but not surfaces coated with PEG. Scalebar represents 200  $\mu\text{m}$ ; Figure from [66].

## **2.3 Hydrogels for cartilage tissue engineering**

The similarities between hydrogels and cartilage make hydrogels a natural choice for use in cartilage tissue engineering. Both are predominantly water by weight, and both maintain a swollen state by attracting water to the hydrophilic chemical groups. Hydrogels can be broadly categorised and naturally derived or synthetic, with each class having its own benefits and disadvantages.

Depending on the materials, crosslinking mechanisms and functional groups, hydrogels can have a wide variety of properties. As expected, different properties are beneficial in different applications and the development of hydrogels that are inductive for cartilage repair is a key goal of many research groups and institutes. Several cartilage repair products that use photocrosslinkable hydrogel systems have progressed to human clinical trials, some of which use ‘off-the-shelf’ hydrogels such as fibrin, and others use hydrogels specifically developed for cartilage applications. Although it is too early to definitively evaluate the success of these products, some of the results have been promising. Further details are given in Chapter 8.

### **2.3.1 Naturally derived hydrogels**

Many materials naturally form hydrogels, and these materials formed the basis for early hydrogel research. Common examples include alginate, agarose, gellan gum. One of the key challenges of handling chondrocytes is that they rapidly lose their characteristic phenotype when placed on two-dimensional surfaces, a process called dedifferentiation. A landmark study in 1982 identified that when dedifferentiated chondrocytes were encapsulated within agarose hydrogels the cells could regain aspects of their differentiated phenotype [53].

Most natural hydrogels are non-covalently crosslinked, either through ionic or temperature dependent crosslinking. Some polymers, such as gellan gum, can be both ionically and/or thermally crosslinked. One disadvantage of ionic and temperature dependent crosslinking is that it is reversible: removing the crosslinking ions or reversing the temperature change will remove the crosslinks. To capitalise on the advantages of photocrosslinking, many natural materials have been modified with photocrosslinkable domains, allowing relatively robust, covalently crosslinked hydrogels to be synthesised. The most notable of these include alginate [56, 68], gelatin [52], hyaluronic acid (HA) [56, 69], chitosan [70], dextran [71], and gellan gum [72], along with mixtures of these.

HA is an important component of cartilage, and has been widely studied for cartilage repair. HA can be used in its natural, unmodified state [73, 74], or chemically modified to allow scaffolds [75] or hydrogels to be fabricated [69]. The synthesis of photocrosslinked hyaluronic acid methacrylate (HA-MA) hydrogels was first described in 2000 [56], along with an analogous method for producing alginate methacrylate (AL-MA). Several years later, chondrocytes were encapsulated in HA-MA and using an osteochondral defect model, were shown to be superior to empty defects [76]. In a later study, passage 0 and 1 auricular chondrocytes encapsulated in HA-MA showed similar levels of neocartilage formation in a subcutaneous model [77], indicating that these cells could potentially tolerate a degree of monolayer expansion. HA-MA hydrogels provide a conducive environment for chondrogenic differentiation of mesenchymal [78] and embryonic stem cells [79], along with synthesis and retention of new cartilage matrix. Although differentiation is predominantly driven by potent soluble factors, such as transforming growth factor  $\beta$  (TGF- $\beta$ ), HA-MA hydrogels are nevertheless promising materials for cartilage repair.

Alginate has a long history of use in cartilage tissue engineering research and has come to be regarded as a benchmark or gold standard for chondrocyte redifferentiation [80]. AL-MA has been investigated for nucleus pulposus tissue engineering [68], but little work has been done to evaluate AL-MA for engineering articular cartilage.

Gelatin is a polymer of amino acids that is produced by hydrolysis of animal connective tissues. It has a long history of use in foodstuffs, and has more recently its potential for use as a biomaterial has been explored. The synthesis and properties of photocrosslinkable gelatin-methacrylamide (Gel-MA, also referred to as methacryloyl substituted gelatin, or occasionally as gelatin-methacrylate) were first described in detail in 2000 [52]. In this original publication, no mention was made of the possibility to encapsulate cells within the gel. It was not until 10 years later that cell encapsulation was reported and this has sparked a rapid rise in the interest of Gel-MA hydrogels for various tissue engineering applications [66]. The use of Gel-MA hydrogels in cartilage tissue engineering research remains quite limited, and this application is the major focus of this thesis.

### **2.3.2 Synthetic hydrogels**

Synthetic hydrogels are a different proposition to naturally derived hydrogels. Synthetic hydrogels can be designed and synthesised at a molecular level – allowing a huge degree of control over molecular weight, polymer structure, and

functionalities. In addition, whereas natural polymers show a degree of batch-to-batch variation and carry a small risk of disease or microbial transmission, synthetic polymers can theoretically be produced without these drawbacks.

Polyethylene glycol (PEG) is by far the most common synthetic polymer used to produce hydrogels for cartilage tissue engineering. It can be synthesised in a wide range of molecular weights, with a number of different functional groups, and as either linear or branched polymers. One of the advantages of synthetic hydrogels is the opportunity to tailor the physical and biochemical properties. In particular, modern technology allows synthetic peptides that perform biological functions to be incorporated into hydrogels, thus synthetic hydrogel systems can act as a platform for producing tailored hydrogels with specific biological functionalities.

### **2.3.3 Physical properties**

Appropriate physical properties are not only important for overall structure and stability, but also for cell-material interactions and ECM production. In load bearing applications, physical properties are often a limitation for hydrogels, which are, by their nature, generally soft and watery materials [81].

There are a number of commonly measured physical properties for hydrogels, such as Young's modulus, dynamic modulus, equilibrium modulus, fracture strength and fracture energy, each of which represents a slightly different aspect of the gel properties. The stiffness of a hydrogel is a measure of the force required to compress (or stretch) the hydrogel by a certain amount. The Young's modulus is the most common measure of stiffness, and can be measured by stretching or compressing the gel. When measured under compression, the Young's modulus is commonly referred to as the compressive modulus. It is measured by compressing the gel at a slow, constant rate and measuring the force exerted by the gel. It is a measure of both the compression of the solid phase of the gel and the resistance to fluid flow (which depends on the rate at which the gel is compressed). The dynamic modulus is usually measured by applying a sinusoidal waveform to the gel, typically at a higher strain rate than used to measure compressive modulus. Again it is a measure of both the force required to compress the gel and the resistance to fluid flow, but since the strain rate is higher, usually there is more impact of resistance to fluid flow. In addition, because the waveform is repeated, it also shows the recovery of the gel after multiple compressions. The equilibrium modulus is measured by compressing the gel to a fixed strain (eg 10%), then waiting until the force exerted by the gel is effectively no longer changing, and recording this

equilibrium force. The strain is then increased (to say 15%), and again the equilibrium force is recorded. When the equilibrium force is converted to stress and plotted against strain, the slope of the stress strain curve gives the equilibrium modulus. Fracture strength (or failure strength) is usually measured by compressing the gel at a fixed rate until the gel fractures, then determining the stress at the point of failure. The fracture energy is the amount of energy required to require this point. Fracture strength is not necessarily related to stiffness, since some gels may tolerate 90% strain (or more) before they fracture, while others may fracture at 50% strain.

Despite physical properties being a limitation for hydrogels, research has identified ways to control the physical properties of hydrogels over extraordinary ranges, and the stiffness of some hydrogels can approach or even exceed that of cartilage [82]. For example, by changing the molecular weight and concentration, PEG-DA hydrogels can be produced with dynamic compressive stiffness ranging from 55 kPa to 42 MPa [82]. An elegant way to improve the mechanical strength is through so-called double-network hydrogels, in which different polymers are combined in different ratios, and crosslinked at different times, to form an interpenetrated network with a mechanical strength that vastly exceeds that of either network individually [83]. Double network hydrogels are discussed further in Chapter 8. For both of these strategies, the challenge for tissue engineering is to encapsulate cells in these hydrogels while achieving high cell viabilities and providing an environment that is conducive to cartilage formation.

The initial physical properties of a hydrogel are important for 2 main reasons. Firstly, the loads that the hydrogel can withstand are determined by these properties, and secondly, the extent to which cells are able to form a mechanically functional, interconnected tissue is dependent on the initial mechanical properties. The current hypothesis is that softer hydrogels have a larger mesh/pore size, and that the larger pore size allows for more diffusion, distribution and interconnectivity of the newly synthesised matrix throughout the hydrogel. Several studies have confirmed this pattern using hydrogels formed from PEG [80, 84], alginate [80] agarose [85] and HA-MA [78]. The initial mechanical properties must be chosen to select the optimal balance for this apparent conflict. The material must be sufficiently strong to withstand the mechanical loads that are applied, yet not so tightly crosslinked that it prevents the effective formation of new tissue.

### 2.3.4 Functionalisation and cell adhesion

Functionalisation of hydrogels with biochemical moieties to increase cell-biomaterial interactions, with the aim of enhancing differentiation and/or function has been a common theme of hydrogel research. For cartilage applications, both natural and synthetic hydrogels have been functionalised with a wide range of biomolecules, such as polysaccharides, peptides, cell adhesion motifs, degradation sites and growth factors. These functionalisations have generally resulted in incremental increases or decreases in chondrogenesis and/or matrix production, but revolutionary improvements have been limited. Often, as shown in Table 2.1 for HA, the results are highly dependent on the context in which the biomolecule is applied, making direct comparisons very difficult. For example HA may have quite different effects depending on the molecular weight, the cell type(s) used, the presence of other materials/growth factors, the nature and degree of modification, and whether it is supplemented into the media or incorporated into the gel. In addition, the significant challenge of biological or donor-to-donor variation adds further complexity. As a consequence, drawing general conclusions about the significance or benefit of a given functionalisation is at best difficult and requires care.

Since most cell types require cell attachment in order to survive and function, cell adhesion domains have been one of the most commonly investigated hydrogel functionalisations. Cell attachment is often assessed by incorporating the fibronectin-derived adhesion peptide RGD (arginine-glycine-aspartic acid) [86] into the hydrogel, which allows cells to attach and spread. However, a distinguishing physical feature of chondrocytes is their rounded morphology, so the value of RGD functionalisation is unclear for chondrocytes, since cell attachment and spreading is typically detrimental to chondrogenesis.

When chondrocytes are encapsulated in hydrogels functionalised with the cell adhesion peptide RGD they display spreading [80], dedifferentiation [87] and even apoptosis [88]. Collectively, these suggest that RGD has a negative effect for chondrocyte encapsulation. When encapsulated in a photocrosslinkable PEG hydrogel with a gradient in RGD concentration, chondrogenesis and matrix formation were reduced as RGD concentration increased [89]. These effects, however, can be reversed when combined with mechanical loading, with the combination of RGD functionalisation and mechanical loading in fact leading to enhanced chondrogenesis [90]. RGD has been identified as an important element of mechanotransduction in dynamically compressed cartilage constructs [91], so may be of some benefit when combined with mechanical loading.

In general, hydrogels that lack cell-adhesion domains, such as agarose, alginate, PEG and HA account for the majority of hydrogels used for chondrocyte encapsulation. However, although chondrocytes generally respond favourably to encapsulation in hydrogels that lack adhesion sites, other cell types, such as MSCs, do not, and over time viability and metabolic activity become reduced [92]. Thus for cells other than chondrocytes, RGD may be advantageous for maintaining survival and allowing the early stages of chondrogenic differentiation to occur. This has led to systems in which the presentation of RGD can be temporally controlled, for example by tethering the RGD peptide onto a degradable linkage [93]. Using this approach, chondrogenesis of MSCs can be enhanced when the RGD sequences are cleavable by MMP13 compared to non-cleavable RGD [93]. Thus like many functionalisations, a blanket conclusion cannot be drawn for RGD, since it may be beneficial in specific circumstances.

Modification of hydrogels to allow enzymatic or hydrolytic degradation has also been widely investigated. For cartilage regeneration, the inclusion of enzymatic degradation sites in PEG hydrogels resulted in increased distribution of cell-secreted matrix throughout the gel [94], which is highly beneficial. Hydrolytically degradable HA-MA hydrogels have been synthesised by synthesising a co-polymer of HA-MA and polycaprolactone [95]. The most notable outcomes were observed between the following two groups: 2% (w/v) HA-MA and 1% (w/v) HA-MA combined with 1% (w/v) of the HA-MA polycaprolactone copolymer. The hydrogels with a degradable component showed increased collagen type II and aggrecan gene expression compared with the 2% HA-MA gels, and also showed greater increases in compressive modulus during culture [95].

In the same way that the peptide RGD has been identified as a functional sequence for cell adhesion, other short peptides of other matrix proteins and proteoglycans have been identified for other biological functions. The collagen-derived sequence (Hyp-P-G)<sub>n</sub> has been shown to effectively mimic some of the features of collagen, including triple helical formation [96]. When incorporated into PEG-DA hydrogels, the peptide enhances the chondrogenic differentiation of MSCs, increases matrix production, and suppresses hypertrophy markers [97]. Similarly, the collagen binding peptide KLER, derived from the proteoglycan decorin, may also improve chondrogenic differentiation of MSCs and support matrix retention [98]. The collagen mimetic peptide GFOGER can also enhance chondrogenic differentiation of MSCs in PEG-based hydrogels

[99], however given the high level of cell spreading induced by this peptide, it is unlikely that chondrocytes would benefit substantially.

This research area is still in its early stages. The limiting factor is the biological complexity, and the incomplete understanding we have over the biological roles of different molecules. As they key molecules are identified, the tools and methods to synthesise and incorporate them into hydrogels are well established. For other cell types and applications, Zhu et al. have reviewed in detail different peptide functionalisations of PEG hydrogels [100].



**Table 2.1: influence of hyaluronic acid on chondrogenic differentiation and matrix accumulation *in vitro*.**

Study	Hydrogel/ scaffold	Cell Details	Notable Findings
Allemann et al. (2001) [101]	Lyophilised HA/collagen type 1 sponges, with HA accounting for 0 or 2% of dry weight.	Juvenile, primary, bovine chondrocytes; 3 or 5 million cells per sponge. Cultured for 7 days with 10% FBS	Fourfold higher collagen II expression and twofold higher aggrecan expression in sponges with HA.
Grigolo et al. (2002) [102]	HYAFF® 11 scaffolds – benzyl ester of HA.	Expanded (P3/4) human chondrocytes (non-OA); 10 <sup>6</sup> cells per scaffold. 14 days culture with 10% FBS, 1 ng/mL TGF-β1, 1 ng/mL EGF, 10 ng/mL b-FGF	Relative to day 0, collagen II expression increased in 4 out of 4 patients; collagen I expression decreased in all patients; changes in aggrecan expression were mixed (2 up, 2 down).
Liao et al. (2007) [103]	Collagen I hydrogels with HA (3 MDa) accounting for 0, 1, 2, 5 or 10% of dry weight. [HA conc. in 10% gels = 0.47 mg/mL].	Non-expanded porcine chondrocytes; 3.5 × 10 <sup>6</sup> cells/mL. Cultured for 14 days with 10% FBS.	Very slight increase in GAG/DNA in gels with 5% HA.
Ko et al. (2008) [104]	Collagen II sponges and sponges with HA and CS.	Passage 3, non-OA human chondrocytes; 1.5 × 10 <sup>6</sup> cells per scaffold. Cultured for 14 days 10 mg/mL TGF- β3 (assumed 10 ng/mL)	The inclusion of HA and CS strongly increased aggrecan expression and slightly increased collagen type II expression. Cells were not encapsulated.
Angele et al. (2009) [105]	Esterified HA with 0, 5 or 30% (w/w) gelatin. Sterilised by beta irradiation.	Human bone marrow MSCs isolated by adherence to plastic substrate; cell density not stated. Cultured for 28 days with unspecified level of TGF- β1.	Gelatin caused a significant increase in cell spreading on 2D films, and increased GAG/DNA ratios in hydrogels.
Hwang et al. (2007) [106]	10% PEG-DA or 10% PEG-DA with 0.25% HA	Zonal chondrocytes from immature bovine joints; 2 × 10 <sup>7</sup> cells/mL. Cultured for 21 days with 10% FBS.	HA increased aggrecan expression ~2 fold in superficial cells and decreased expression ~2 fold in deep zone cells. Expression of collagen type II and link protein both unchanged.
Hwang et al. (2011) [107]	10% PEG-DA or 10% PEG-DA with 0.25% HA	Bone marrow MSCs from adult goats; 2 × 10 <sup>7</sup> cells/mL. Cultured for 6 weeks with 10 ng/mL TGF- β1.	HA significantly reduced GAG accumulation after 6 weeks. At day 5, HA appeared to reduce aggrecan expression and increase osteogenic markers.
Skaalure et al. (2014) [74]	15% PEG-LA-DA with 0.05% or 0.5% of 30 or 2,000 kDa HA	Bovine chondrocytes from skeletally mature animals; 20 × 10 <sup>7</sup> cells/mL. Cultured for 29 days with 10% FBS	At day 8, all HA formulations increased the proportion of cells stained for collagen type II. Minimal impact of HA at day 29.

## 2.4 Photocrosslinkable hydrogels: Application in Bioprinting

Photosensitive resins have been extensively used in stereolithography, an additive manufacturing technique in which light is used to cure a resin in a layer-by-layer approach, allowing precise control over scaffold architecture. In the rapidly developing field of bioprinting, early studies typically used a combination of two or more rheological properties or crosslinking mechanisms are used to print constructs with defined structures. During deposition, the printed hydrogel structure must somehow retain its shape until it is crosslinked. This step exploits the first rheological or crosslinking property, and, for example, can be provided by high viscosity or temperature dependent gelation. Subsequently, the construct is crosslinked to stabilise its shape and structure. Alginate has been commonly used for bioprinting since its rheological and crosslinking properties lend themselves make it somewhat suitable. During printing, its high viscosity maintains the desired structure, and once the finished structure has been printed, it is easily crosslinked by submersion in a solution of  $\text{Ca}^{2+}$ . The fidelity of the printed structures is usually limited, since high viscosities are not sufficient to completely prevent flow of the printed construct.

One of the challenges for bioprinting has been a lack of hydrogels that are appropriate for *both* cell culture and have the properties required for printing. When using alginate for cell culture, concentrations of 1-2% (w/v) are typically used, since these low concentrations support high cell viability and nutrient diffusion. For printing, though, higher concentrations give higher viscosity, making higher concentrations (4-10% w/v) most suited for printing. This had led to the popular concept of a bioprinting window – that is the working range in which a material can be both printed and be used as an effective biomaterial. So while alginate can be printed, it clear has some limitations for printing well-defined or large structures. Other polymers, in comparison, such as lutrol and pluronic F127, are very well suited for printing, but are of limited practical use for cell culture [108].

New materials are being developed and applied specifically for use in bioprinting. In particular, fluids with properties approaching those of Bingham fluids are ideal for temporarily holding the structure of the printed construct, since Bingham fluids usually do not flow under gravity alone. Gellan gum, for example, is a useful addition to Gel-MA for bioprinting, because it provides a yield stress at relatively low concentrations [109]. Photocrosslinking is a useful means to permanently crosslink the printed structure.

Alternative approaches that remove, or reduce, the requirement for viscosity or temperature sensitivity to maintain the initial structure have also been investigated. Skardal et al. have printed partially crosslinked mixtures of photocrosslinkable 1.2% (w/v) hyaluronic acid and 0.3% (w/v) gelatin [110]. Prior to printing, the hydrogel precursor solution, containing  $25 \times 10^6$  cells/mL, was exposed to UV for two minutes. Following printing, the constructs were further UV crosslinked for one minute per layer. This provides additional support for the printed structure, but it is uncertain how this two-stage crosslinking would influence the network structure, mechanical strength and layer-to-layer integration.

Cui et al. have used simultaneous inkjet printing and UV crosslinking to print PEGDA, which has a low viscosity and no thermal sensitivity [111]. In this way, the gel is crosslinked as it is deposited, which has the advantage that cells do not settle between printing and crosslinking. However, the objective was to entirely fill a cylindrical chondral defect, so the added value of printing, as opposed to a syringe or pipette, is unclear. Billiet et al. have modified a commercial printing system (Bioplotter, EnvisionTEC, Germany) to enable a high degree of control over the temperature at the needle outlet, which allows Gel-MA to be printed at the upper critical solution temperature (UCST) [112]. This study highlights the critical importance of temperature control if temperature sensitivity plays a substantial part of the printing process.

## 2.5 Conclusion

Photocrosslinkable hydrogels have been extensively evaluated for cartilage tissue engineering, but optimal materials have not yet been found. PEG hydrogels have provided a versatile and valuable platform for evaluating bioactive moieties, but have generally failed to match the level of chondrogenesis seen in naturally derived hydrogels. Recently, natural polymers that have been functionalised with photocrosslinkable domains have attracted increasing interest for cartilage tissue engineering, and HA in particular has generated significant research interest. Despite its widespread use, there is very little consensus on the impact of HA, which appears to depend on many other factors, such as the origin of the cells, the presence of other materials and growth factors, the HA concentration and molecular weight, and how the HA is crosslinked, if at all. Although the outcomes have been variable, many studies have shown promising effects of HA, which are expected to continue to create interest in this biopolymer.



## Chapter 3

# Chondrocyte redifferentiation and construct mechanical property development in single-component photocrosslinkable hydrogels

---

Peter A. Levett<sup>1,2</sup>, Ferry P. W. Melchels<sup>1,2</sup>, Karsten Schrobback<sup>1</sup>, Dietmar W. Hutmacher<sup>1,3</sup>, Jos Malda<sup>1,2</sup> and Travis J. Klein<sup>1</sup>

Journal of Biomedical Materials Research – Part A (2013), Vol. 102, No. 8, p. 2544-2553.

<sup>1</sup> *Institute of Health and Biomedical Innovation, Queensland University of Technology, 60 Musk Ave, Kelvin Grove, QLD 4059, Australia*

<sup>2</sup> *Department of Orthopaedics, University Medical Center, Utrecht, P.O. Box 85500, 3508 GA, The Netherlands*

<sup>3</sup> *George W Woodruff School of Mechanical Engineering, Georgia Institute of Technology, Atlanta, Georgia, USA*

## Abstract

Hydrogels are promising materials for cartilage repair, but the properties required for optimal functional outcomes are not yet known. In this study, we functionalised four materials that are commonly used in cartilage tissue engineering and evaluated them using *in vitro* cultures. Gelatin, hyaluronic acid, polyethylene glycol, and alginate were functionalised with methacrylic anhydride to make them photocrosslinkable. We found that the responses of encapsulated human chondrocytes were highly dependent on hydrogel type. Gelatin hydrogels supported cell proliferation and the deposition of a glycosaminoglycan-rich matrix with significant mechanical functionality. However, cells had a dedifferentiated phenotype, with high expression of collagen type I. Chondrocytes showed the best redifferentiation in hyaluronic acid hydrogels, but the newly formed matrix was highly localised to the pericellular regions, and these gels degraded rapidly. Polyethylene glycol hydrogels, as a bioinert control, did not promote any strong responses. Alginate hydrogels did not support the deposition of new matrix, and the stiffness decreased during culture. The markedly different response of chondrocytes to these four photocrosslinkable hydrogels demonstrates the importance of material properties for chondrogenesis and extracellular matrix production, which are critical for effective cartilage repair.

**Keywords:** cartilage; hydrogels; photopolymerisation; chondrogenesis; tissue engineering

### 3.1 Introduction

Articular cartilage has a low capacity for self-repair, and treatment of cartilage defects remains a clinical and economic burden [49]. Current therapies such as microfracture and autologous chondrocyte implantation (ACI) frequently result in a fibrous repair tissue that is rich in collagen type I, and lacking the mechanical properties and zonal organisation of normal articular cartilage [113, 114]. Cell-based cartilage tissue engineering aims to overcome the current limitations in cartilage therapies by restoring damaged tissue with hyaline cartilage that is rich in collagen type II and aggrecan [115].

Cell-based cartilage tissue engineering strategies most commonly use autologous chondrocytes that are harvested during a biopsy and expanded in culture [50]. A major limitation of this approach is that chondrocytes dedifferentiate during expansion, adopting a fibroblastic morphology, and replacing collagen type II expression with collagen type I expression [53, 116]. This dedifferentiation is likely responsible for repair tissue that is rich in collagen type I and mechanically inferior to the original cartilage. Thus, in order for the repair tissue to have similar structure and function as the original tissue, the chondrogenic phenotype of the cells must be restored [117]. One approach to achieve this goal is the development of biomaterials to direct the chondrocyte phenotype, and ultimately enhance the quality of the repair tissue.

Dedifferentiated chondrocytes can regain their differentiated phenotype when cultured in three-dimensional hydrogels [53], which are water-swollen, crosslinked networks of hydrophilic polymers. The design of optimal hydrogel biomaterials to restore the chondrocyte phenotype and guide cartilage regeneration is a current challenge [118, 119], and there are a number of requirements that must be met. Ideally, the hydrogel should promote chondrogenesis, with the newly formed matrix resembling the original hyaline cartilage, which is rich in collagen type II and aggrecan [118]. Furthermore, the matrix should be spread throughout the hydrogel, rather than concentrated in the pericellular regions, and should facilitate the regeneration of the complex zonal organisation of native cartilage [118]. Finally, it must be practical to use it in a clinical setting: it must be sterilisable, easy to handle, and crosslink relatively rapidly.

Photocrosslinkable hydrogels are covalently crosslinked by exposing a precursor polymer solution to light in the presence of a photoinitiator. The reaction proceeds relatively rapidly under physiological conditions, allowing *in situ* crosslinking and cell encapsulation with high viabilities [120]. In this study,

we compared four photocrosslinkable hydrogels with distinctly different properties to elucidate which cell-material interactions are likely to be beneficial for cartilage tissue engineering, and which are not. The hydrogels provided a wide range of functionalities (Table 3.1). Polyethylene glycol dimethacrylate (PEG-MA) is synthetic and highly hydrophilic, and since it is bioinert, it serves as a useful control. Like the matrix of native cartilage, alginate methacrylate (AL-MA) is negatively charged, and alginate hydrogels have frequently been used in chondrogenic differentiation models [80]. Hyaluronic acid-methacrylate (HA-MA) is based on a major component of articular cartilage that interacts with both chondrocytes, through CD44 receptors [20], and components of the extracellular matrix (ECM), such as aggrecan, via link protein [25]. Gelatin-methacrylamide (Gel-MA) hydrogels are produced from hydrolysed collagen, retain cell adhesion domains, and are sensitive to cell-mediated degradation by matrix metalloproteinases (MMPs) [52, 66].

**Table 3.1: Hydrogel source and properties.**

<b>Hydrogel</b>	<b>Source</b>	<b>Properties</b>
Gel-MA	ECM collagens	Protein hydrogel, cell attachment domains, degradable
PEG-MA	Synthetic	Bioinert, highly hydrophilic
HA-MA	Recombinant	Direct interaction with chondrocytes through CD44 receptors, hydrolytically and enzymatically degradable
AL-MA	Seaweed	Negatively charged, non-adhesive to cells, non-degradable

## 3.2 Materials and Methods

### 3.2.1 Macromer Synthesis

Type A gelatin (molecular weight [MW] ~90 kDa), medium viscosity alginate (MW ~260 kDa [121]), PEG (MW 8 kDa), and methacrylic anhydride (MAAh) were purchased from Sigma Aldrich (St Louis, Mo). Hyaluronic acid (MW 860 kDa) was generously provided by Novozymes. Polymers were modified to include photocrosslinkable groups by reaction with MAAh, based on previously published methods, which vary slightly between polymers to account for their different chemistries. Gelatin was dissolved in phosphate buffered saline (PBS, Invitrogen, Carlsbad, CA) at 100 mg/mL and reacted with 0.6 g MAAh per gram of gelatin for 1 h at 50 °C under constant stirring [52]. Alginate and HA were dissolved in distilled water at 20 mg/mL, and reacted with MAAh for 24 h



on ice [56]. For HA and alginate, five- and 10-fold molar excesses of MAAh to total hydroxyl groups were used, respectively, and the pH was regularly adjusted to 8 using 5 M NaOH. PEG was dissolved in dichloromethane (Thermo Fisher, Australia) at 300 mg/mL, and functionalised with MAAh (100% molar excess relative to hydroxyl groups) in the presence of triethylamine (25% molar excess). After reaction for 10 days at room temperature the PEG-MA was precipitated in diethyl ether (Merck, Darmstadt, Germany) and dried. For all other polymers, insoluble MAAh was removed by centrifugation, and remaining MAAh was removed by dialysis against distilled water (12 kDa molecular weight cut off cellulose dialysis membrane, Sigma). Functionalised polymers were lyophilised.

Chemical modification of the hydrogel precursors was confirmed using proton nuclear magnetic resonance ( $^1\text{H}$  NMR, spectra not shown) using a Bruker Avance 400 MHz instrument at room temperature. The  $^1\text{H}$  NMR spectra for all unmodified polymers in  $\text{D}_2\text{O}$  (Sigma) showed no signal in the range 5.5–6.5 ppm, whereas the spectra of the modified polymers gave peaks in this region, corresponding to the vinyl protons of the methacrylate or methacrylamide groups [56].

### **3.2.2 Cell Isolation and Expansion**

Cartilage was harvested from the macroscopically normal regions of the femoral condyles of a 72-year-old female patient undergoing knee replacement surgery. Chondrocytes were isolated as previously described [80]. The patient provided informed consent, and ethics approval was granted by Queensland University of Technology and the Prince Charles Hospital. Expansion media contained low glucose DMEM with 2 mM GlutaMAX<sup>TM</sup> (Invitrogen), supplemented with 10% fetal bovine serum (Lonza, Waverly Australia), 10 mM 4-(2-hydroxyethyl)-1-piperazineethanesulfonic acid, 0.1 mM non-essential amino acids, 0.5  $\mu\text{g}/\text{mL}$  amphotericin B (Fungizone), 50 U/mL penicillin G sodium, 50  $\mu\text{g}/\text{mL}$  streptomycin (all Invitrogen), 0.4 mM L-proline and 0.1 mM ascorbic acid (both Sigma).

### **3.2.3 Cell Encapsulation and Culture**

Cells were released from the tissue culture plastic by 5 minutes incubation in 0.25% trypsin with 1 mM ethylenediamine tetraacetic acid (Invitrogen). Passage 1 cells were washed, split equally into four groups, centrifuged, and resuspended at a density of  $10^7$  cells/mL in hydrogel precursor solutions in PBS containing 0.5 mg/mL Irgacure 2959 (BASF, Ludwigshafen, Germany). It was

necessary to vary the concentrations of polymer precursors according to solubility and hydrogel formation. For example, PEG-MA hydrogels are commonly formed from precursor solutions approximately 20% (w/v) PEG-MA, which is above the solubility limit of many polysaccharides, such as alginate, which is commonly used at approximately 1–3% (w/v). Precursor concentrations for Gel-MA, PEG-MA, HA-MA, and AL-MA were 9%, 18%, 2%, and 3%, respectively (w/v). Cylindrical hydrogels with an initial volume of 100  $\mu\text{L}$ , and height of 2 mm were crosslinked by 5 minutes exposure to 365 nm UV light at an intensity of 12  $\text{mW}/\text{cm}^2$  (OmniCure®, Lumen Dynamics). Hydrogels were then cut into four even pieces, and were cultured for up to 4 weeks in serum-free, high glucose DMEM (Invitrogen) differentiation media. In addition to the supplements in expansion medium, differentiation media contained ITS+1 (100  $\times$  dilution), 1.25 mg/mL bovine serum albumin (BSA), 0.1  $\mu\text{M}$  dexamethasone (all Sigma), and 10 ng/mL TGF- $\beta$ 3 (GroPep, Australia). Cultures were maintained at 37  $^{\circ}\text{C}$  in an atmosphere of 21% oxygen and 5% carbon dioxide.

### 3.2.4 Viability assay

Cell-hydrogel constructs were incubated in PBS containing 10  $\mu\text{g}/\text{mL}$  fluorescein diacetate and 5  $\mu\text{g}/\text{mL}$  propidium iodide (both Sigma), which stain living and dead cells green and red, respectively. Images were taken using a Nikon Eclipse fluorescence microscope.

### 3.2.5 Mechanical testing

Compressive testing was performed using an Instron 5848 microtester with a 5 N load cell (Instron, Melbourne, Australia) in an unconfined arrangement. During testing, hydrogels were submerged in PBS at 37  $^{\circ}\text{C}$ . A displacement rate of 0.0025 mm/s was applied using a non-porous indenter. Constructs were weighed after testing using an analytical balance, and the cross-sectional area was determined as the ratio of wet weight to height. The compressive modulus was taken as the slope of the linear region of the stress-strain curve from 10 to 15% strain, since comparable strain regions have been shown to be suitable for measuring similar hydrogel constructs [122-124].

### 3.2.6 Biochemical analyses

For GAG and DNA analyses, hydrogel constructs were lyophilised and digested in proteinase K solution (Invitrogen) for 16 h at 56  $^{\circ}\text{C}$ . The concentration of GAGs in the digests was measured using the dimethylmethylene blue assay (pH 1.5) in a 96 well-plate format [125]. GAG concentration in the conditioned

media was assayed at each media change. Results from the first media change were excluded because uncrosslinked alginate diffuses out of AL-MA gels during swelling. DNA concentration in the digests was measured using the Quant-iT<sup>TM</sup> PicoGreen® dsDNA quantification assay (Invitrogen).

### **3.2.7 Immunofluorescence and Histology**

Immunofluorescence for aggrecan and collagen types I and II were performed on sections of fresh-frozen constructs, which were fixed by 10 min contact with ice-cold acetone. Sections were treated with 0.1% hyaluronidase (Sigma) in PBS for 30 min, then blocked in 2% BSA in PBS for 1 h. Antibodies for collagen type II (II-II6B3, DSHB, 1:200 dilution), collagen type I (I-8H5, MP Biomedicals, Australia, 1:300 dilution), and aggrecan (MA75A95, Abcam, 1:4 dilution) were diluted in PBS with 2% BSA, and applied overnight at 4 °C. The secondary antibody (Alexa Fluor® 488, Invitrogen) was applied for 1 h in PBS with 2% BSA and 0.5 µg/mL DAPI. The secondary antibody alone was used as a negative control. Sulfated GAGs were stained with 0.5% Alcian blue (Sigma, pH 1) for 10 min at room temperature.

### **3.2.8 Confocal microscopy**

Cell morphology was visualised using confocal microscopy in constructs cultured for 4 weeks. Constructs were fixed and permeabilised in 4% paraformaldehyde (Electron Microscopy Sciences, Hatfield, PA) with 0.2% Triton X-100 (Merck) in PBS, for 30 min at room temperature. Actin filaments and nuclei were stained for 1 h with 0.8 U/mL rhodamine-labeled phalloidin (Invitrogen) and PicoGreen® (1:200 dilution, Invitrogen), respectively. Images were acquired on a Leica SP5 confocal laser scanning microscope using a 20× objective.

### **3.2.9 Gene expression**

Total RNA was isolated from cells prior to encapsulation in hydrogels (day 0), and from cell-hydrogel constructs on day 21. Cells or hydrogel constructs were homogenised in 1 mL of TRIzol reagent (Invitrogen) and frozen in liquid nitrogen. Total RNA was isolated according to manufacturer's instructions. SuperScript<sup>TM</sup> III First Strand Synthesis System (Invitrogen) was used to synthesise the first strand of complementary DNA (cDNA). DNase and RNase treatments (both Invitrogen) were included before and after cDNA synthesis, respectively. Real time-polymerase chain reaction was performed using SybrGreen® Mastermix (Invitrogen). B2M and RPL13a were selected as housekeeping genes. The primer sequences were either taken from the literature

for RPL13a [126] and COL2A1, COL1A1, COL10A1, ACAN and proteoglycan 4 (PRG4) [127], or designed using Primer-BLAST (NCBI, Bethesda, MD) for: B2M (5'→3' F: ATGAGTATGCCTGCCGTGTGA, R: GGCATCTTCA-AACCTCCATGATG) and MMP13 (5'→3' F: ACTTCACGATGGCATTGCTG, R: CATA-ATTTGGCCCAGGAGGA).

### 3.2.10 EPIC- $\mu$ CT

The distribution of fixed negative charges within the hydrogel constructs was visualised using equilibrium partitioning of an ionic contrast agent microcomputed tomography (EPIC- $\mu$ CT) [128]. Cell-free hydrogels, and fixed, cell-laden constructs cultured for 4 weeks were incubated in a solution of 40% ioxaglate (Hexabrix®, Aspen, Australia) in PBS overnight at 37 °C. Constructs were imaged in a  $\mu$ CT 40 scanner (Scanco Medical, Switzerland) at 45 kV and 177  $\mu$ A, and analysed using Scanco  $\mu$ CT software.

### 3.2.11 Statistics

SPSS software (version 20, IBM corporation, Armonk) was used for statistical analyses. ANOVA and either Tukey's or Dunnett's T3 post hoc tests were used to determine significant differences between hydrogel groups for GAGs, day 1 wet weights, and gene expression data, as appropriate. Independent samples t-tests were used to compare day 1 and day 21 wet weights and moduli data for each hydrogel.

## 3.3 Results

Human chondrocytes showed distinctly different responses in the four hydrogels, indicating the importance of hydrogel properties for guiding cell processes and tissue regeneration. Most cells remained viable in all hydrogels after 4 weeks of culture (Supporting Information Fig. S3.1).

### 3.3.1 Physical Properties

Constructs had an initial wet weight of approximately 25 mg after crosslinking. The hydrophilic properties of PEG-MA caused much greater swelling on day 1 compared to the other gel types (Figure 3.1A, Figure S3.2). The wet weight of HA-MA constructs decreased by almost half in 3 weeks, indicating relatively rapid degradation, while the wet weights of the other hydrogels were unchanged.

The compressive moduli of all constructs changed significantly during 21 days culture (Figure 3.1B). The stiffness of Gel-MA constructs was markedly higher on day 21 (54 kPa) than day 1 (1.5 kPa). Macroscopically, Gel-MA constructs were transparent on day 1, but white and opaque after 3 weeks (Fig. S3.2), indicating ECM accumulation. The compressive moduli of HA-MA constructs also increased during culture, although to a lesser extent than Gel-MA. PEG-MA and AL-MA constructs became softer during culture. On day 1 there were differences in the compressive moduli of hydrogel constructs, due to differences in swelling and crosslink densities. Gel-MA and PEG-MA constructs were softer than HA-MA and AL-MA constructs ( $p < 0.05$ ), and HA-MA constructs were softer than AL-MA constructs (Figure 3.1B,  $p < 0.05$ ).

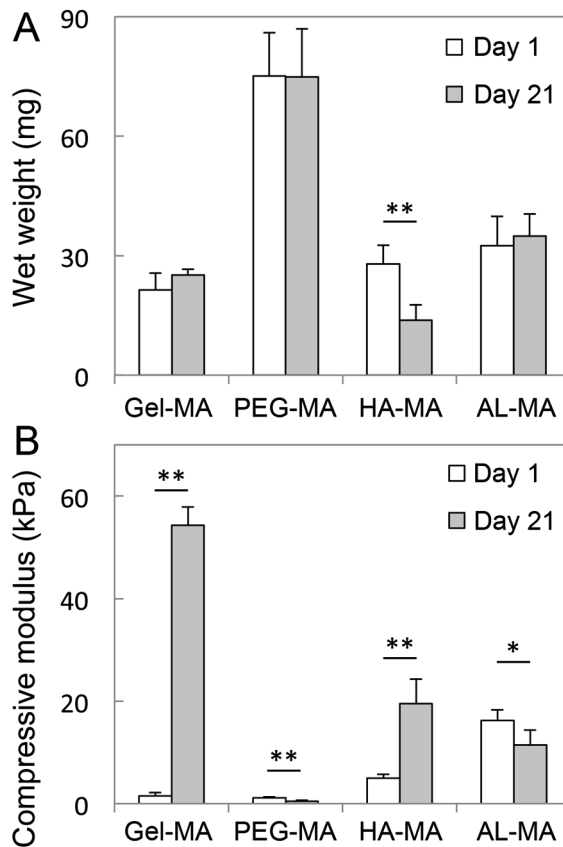


**Figure 3.1: Wet weights (A) and compressive moduli (B) of hydrogel-cell constructs on days 1 and 21.** Bars and error bars show the means and standard deviations of five samples; stars indicate significant differences between days 1 and 21 (\* indicates  $p < 0.05$ , \*\* indicates  $p < 0.005$ ).

### **3.3.2 Cell Proliferation and Morphology**

Hydrogel type was a strong determinant of cell morphology (Figure 3.2). Cells encapsulated in Gel-MA, which contains an abundance of cell adhesion domains, showed highly spread morphologies, indicative of dedifferentiated chondrocytes (Figure 3.2A). Cells were more highly spread on the surface of the gels than when encapsulated, but encapsulated cells also showed stretched actin filaments. Chondrocytes only proliferated in Gel-MA gels, with total DNA content increasing approximately three-fold during 3 weeks culture (Figure 3.2E). Cells did not spread significantly in the other gels, although small cell extensions were seen spreading from cell clusters in PEG-MA hydrogels (Figure 3.2B).

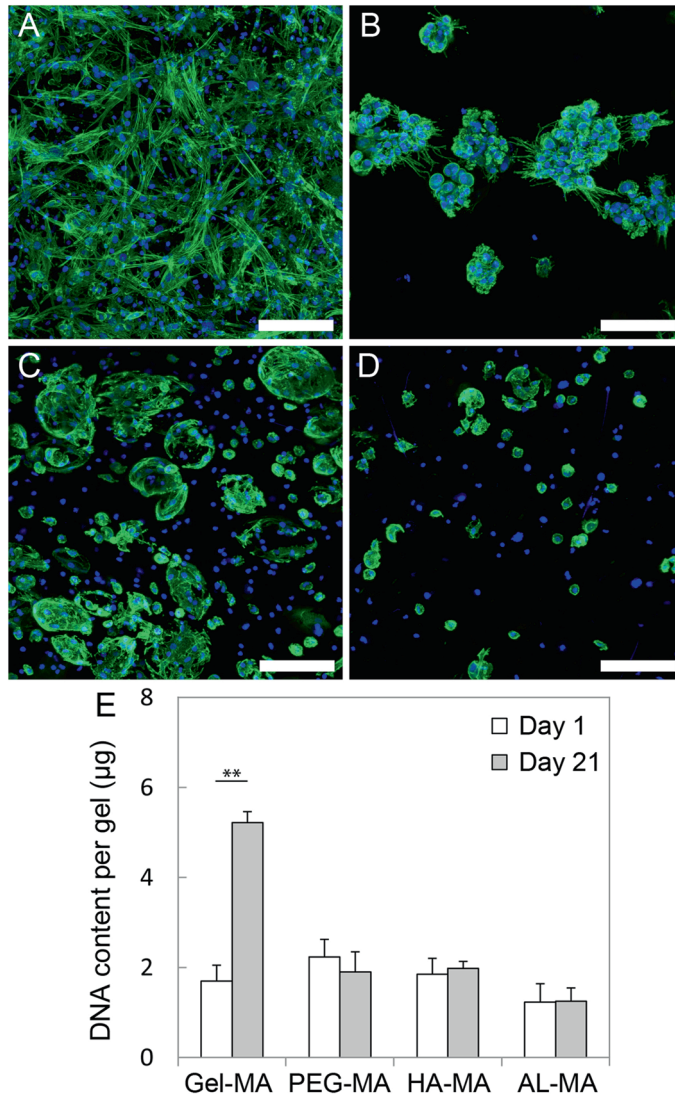


**Figure 3.2: Confocal microscopy images showing organisation of actin filaments (green) and cell nuclei (blue) in Gel-MA (A), PEG-MA (B), HA-MA (C), and AL-MA (D) hydrogel-cell constructs after 4 weeks culture. Scale bars: 100 µm. Total DNA content (E) showed that cells only proliferated significantly in Gel-MA constructs ( $p < 0.005$ ). Bars and error bars show the means and standard deviations of five samples.**

### 3.3.3 Gene Expression

The expression levels of key chondrogenic genes were measured to determine the degree of chondrogenesis in each of the hydrogels (Figure 3.3). Compared to day 0 levels, COL2A1 expression was upregulated in all hydrogels, but to the lowest extent in PEG-MA (Figure 3.3A). Aggrecan expression was upregulated only in HA-MA gels compared to day 0 (Figure 3.3B). Expression of the dedifferentiation marker COL1A1 was highly upregulated in Gel-MA, and unchanged from the day 0 level in other gels (Figure 3.3C). The superficial zone marker PRG4 was upregulated in all hydrogels, but to the highest extent in HA-MA (Figure 3.3D), while expression of the deep zone marker COL10A1 was markedly upregulated in Gel-MA hydrogels (Figure 3.3E). MMP13 was also strongly upregulated in Gel-MA (Figure 3.3F), which together with COL10A1, indicates that cells in Gel-MA may be undergoing hypertrophy.

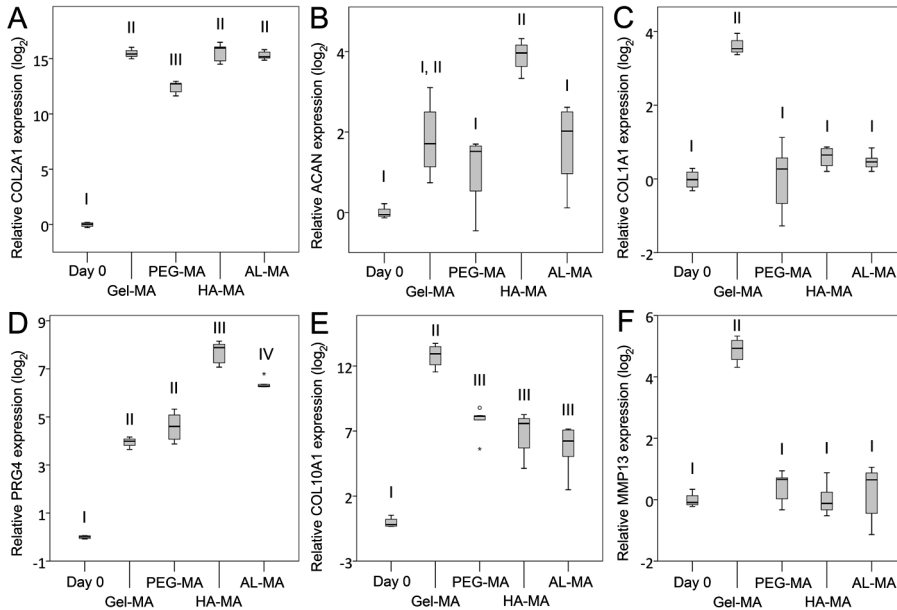


**Figure 3.3: Gene expression profile of chondrocytes after 3 weeks culture, normalised to day 0 expression levels.** Expression of chondrogenic markers COL2A1 (A) and ACAN (B), the dedifferentiation marker COL1A1 (C), superficial zone marker PRG4 (D), deep zone marker COL10A1 (E), and hypertrophy marker MMP13 (F). Box plots show the mean, lower and upper quartiles, and range from five samples; different Roman numerals indicate statistically significant differences between groups ( $p < 0.05$ ).



### 3.3.4 Matrix Production and Accumulation

Total GAG production was determined as the sum of the GAGs retained in the hydrogel and GAGs secreted into the media. GAG production was highest in Gel-MA hydrogels, with two-fold more GAGs retained in Gel-MA compared to the other hydrogels (Figure 3.4A). The amount of GAGs retained was similar in PEG-MA, HA-MA, and AL-MA, with minor variations in the amounts secreted (Figure 3.4A). The fraction of total GAGs that were retained in the hydrogels was highest in AL-MA and HA-MA hydrogels, and lowest in PEG-MA hydrogels (Figure 3.4B). When normalised to the DNA content on day 21, GAG/DNA ratios were highest in Gel-MA and PEG-MA constructs (Figure 3.4C).

On day 1, HA-MA and AL-MA gels showed more Alcian blue staining than Gel-MA and PEG-MA, due to the negative charges on these polymers (Figure 3.4D). After 21 days of culture, Alcian blue staining was strong and homogeneous in Gel-MA constructs. Conversely, staining was highly heterogeneous in HA-MA constructs, with intensely stained pockets of approximately 50  $\mu\text{m}$  in diameter distributed throughout the construct, and overall less intense staining than in Gel-MA.

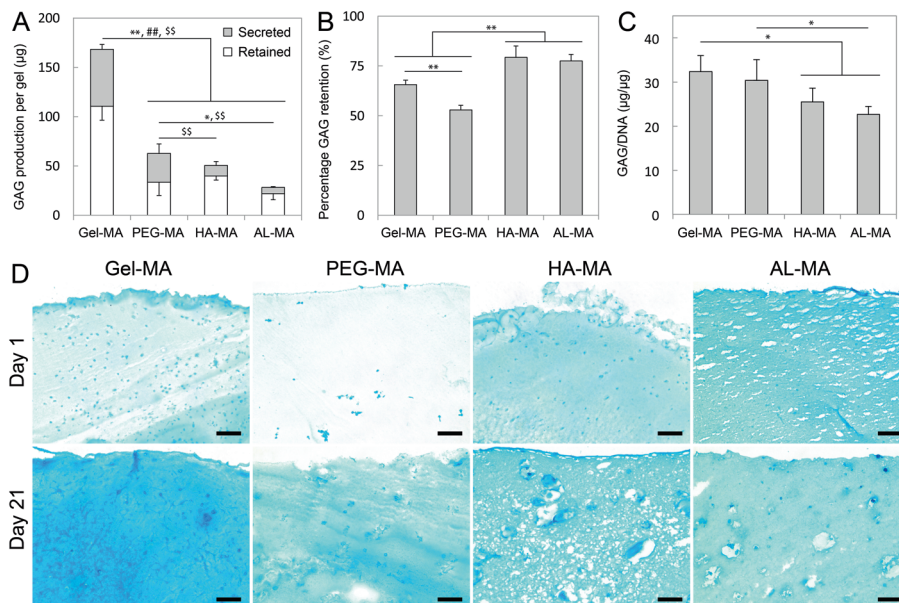


**Figure 3.4: Production and retention of GAGs by chondrocytes encapsulated in the hydrogel constructs.** Amount of GAGs secreted into the media or retained in the constructs during 21 days culture (A), the percentage of GAGs produced that were retained in the constructs (B), the total GAG normalised to the DNA content on day 21 (C), and sections of cell-hydrogel constructs stained for GAGs with pH 1 Alcian blue (D). Bars and error bars show the mean and standard deviation of five samples. In A, \* and \*\* indicate statistical significance for total (secreted + retained) GAG production ( $p < 0.05$  and  $0.005$  respectively), ## indicates significance for GAGs retained ( $p < 0.005$ ), and \$\$ represents significance for GAGs secreted ( $p < 0.005$ ). Scale bars:  $100 \mu\text{m}$ .

EPIC- $\mu\text{CT}$  scans of cell-free hydrogels and cell-laden hydrogels after 28 days show intrinsic differences in the fixed negative charges in different hydrogels, as well as changes resulting from GAG deposition by encapsulated cells (Figure 3.5). Attenuation values correlate with ioxaglate concentration, and are inversely correlated with the fixed negative charge in the construct, due to the negative charge of ioxaglate [128]. Clear differences were apparent between the four cell-free hydrogels (Figure 3.5A-D), with lower attenuation values recorded in the negatively charged gels. Changes were also apparent between cell-free gels and cultured constructs. In Gel-MA constructs, attenuation was strongly reduced in the cultured constructs as a result of the GAG accumulation in these gels (Figure 3.5), while the other gels, with lower GAG accumulation, showed less distinct differences. The perimeter of cultured HA-MA constructs showed regions of localised degradation (Figure 3.5G).

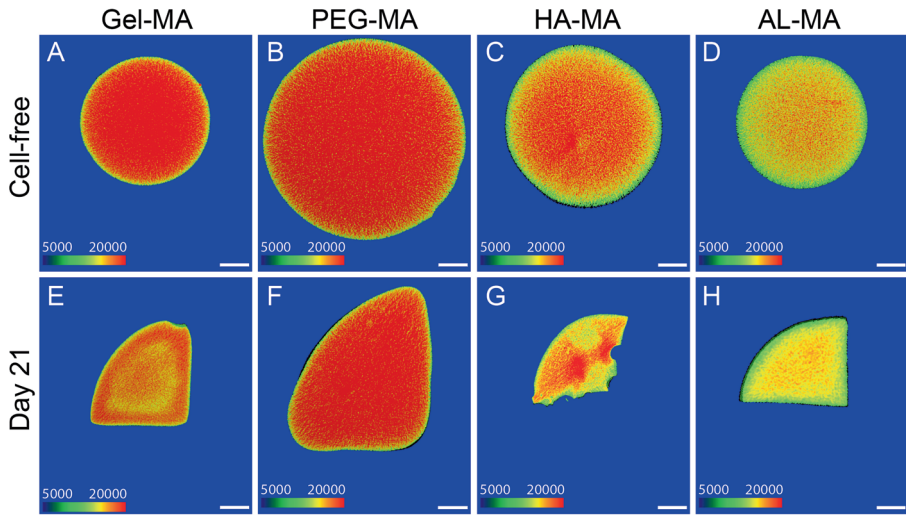


**Figure 3.5: EPIC- $\mu$ CT images of negative charge and charge distribution in cell-free (circular cross-sections, A–D) or cell-laden (quarter-circle cross-sections, E–F) Gel-MA, PEG-MA, HA-MA and AL-MA hydrogel constructs, which were cultured for 4 weeks. Scale bars indicate 1 mm; different sizes result from differences in swelling between the constructs. The colour indicates the signal intensity (5,000 to 20,000) of the contrast agent ioxaglate. Higher ioxaglate intensity indicates lower fixed negative charge.**

Immunofluorescence was used to detect the presence of the chondrogenic markers collagen type II and aggrecan, and the dedifferentiation marker collagen type I (Figure 3.6). Collagen type II immunofluorescence was strong in Gel-MA and HA-MA constructs (Figure 3.6 A1, C1), however, was more evenly spread throughout Gel-MA constructs than in HA-MA constructs. In HA-MA constructs, both collagen II and aggrecan were intensely stained around cells and cell clusters. Aggrecan staining was strongest in HA-MA, with only low levels of staining in the other gels. Strong collagen type I immunofluorescence was observed in Gel-MA constructs (Figure 3.6 A3). Immunofluorescence showed relatively low levels of aggrecan, and collagen types I and II in PEG-MA and AL-MA constructs.

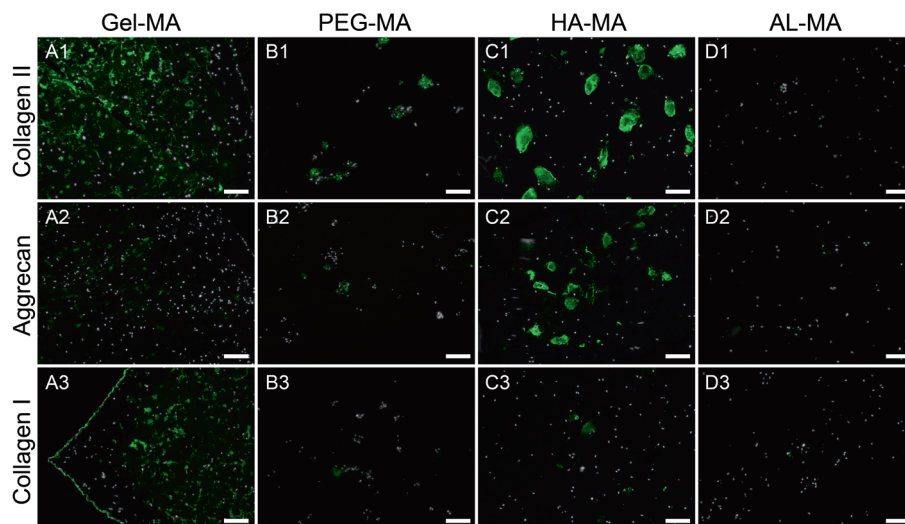


**Figure 3.6:** Immunofluorescence staining for collagen type II, aggrecan, and collagen type I in Gel-MA, PEG-MA, HA-MA, and AL-MA hydrogel constructs cultured for 21 days, with DAPI nuclear stain shown in white. Scale bars: 100  $\mu\text{m}$ .

### 3.4 Discussion

The aim of this study was to determine which hydrogel properties would be beneficial for cartilage tissue engineering. We found that Gel-MA hydrogels promoted a significant amount of ECM production, but chondrocytes had a mixed phenotype, whereas HA-MA hydrogels most effectively promoted chondrocyte redifferentiation. In comparison, the hydrogel properties in AL-MA and PEG-MA did not result in particularly notable outcomes.

Gel-MA hydrogels are a promising biomaterial for engineering various tissues [66]. Here, we show that Gel-MA hydrogels promote encapsulated human chondrocytes to proliferate and form a GAG- and collagen-rich ECM. The ECM generated in Gel-MA constructs had significantly more mechanical functionality compared to the other hydrogels. Mechanical properties are a key metric for evaluating tissue-engineered cartilage [129], and has been a limitation of many attempts to date [130]. Although the final modulus of approximately 55 kPa is substantially lower than that of cartilage, it is a significant increase in a relatively short (3 week) *in vitro* culture period. However, the stretched cell morphologies and upregulation of COL1A1 and hypertrophy makers [131] indicate the cells are not undergoing classical chondrogenesis, and the matrix would not resemble the original hyaline cartilage. Based on these results, for

Gel-MA to be used in cartilage tissue engineering, additional strategies to guide chondrogenesis must be pursued in further studies.

The apparent discrepancy between high GAG deposition and a lack of chondrogenic differentiation in Gel-MA may be accounted for by the lack of specificity of the GAG assay, Alcian blue, and EPIC- $\mu$ CT, which are all measures of negative charge. Cartilage is a proteoglycan rich tissue, but more specifically, aggrecan accounts for 80% of total proteoglycans [34]. Other proteoglycans, for example, versican, decorin, and biglycan, which are not normally produced in cartilage, are upregulated during dedifferentiation [132]. In this study, the newly formed ECM in Gel-MA constructs was rich in GAGs, but immunofluorescence showed that very little aggrecan was produced. Similarly, while GAGs were produced in PEG-MA and AL-MA constructs, there was very little aggrecan staining in these constructs. From a practical perspective, these results highlight the need for multiple means of analyses in cartilage tissue engineering research, as the most widely used methods, GAG production and Alcian blue staining, do not necessarily correlate with chondrogenesis.

Chondrogenic redifferentiation was most complete in HA-MA constructs. Expression levels of aggrecan were highest in HA-MA, and immunofluorescence for collagen type II and aggrecan were the strongest in this gel. PRG4 expression was also highest in HA-MA. Correlations between PRG4 expression and chondrogenesis have been observed [127], so it may serve as a putative chondrogenic marker, but is also used as a marker of superficial zone chondrocyte phenotype. Together with HA, PRG4 is an important component of the lubricating system in synovial joints, and these molecules have been shown to have synergistic effects on lubrication and to interact in solution [133]. The addition of HA to alginate hydrogels also upregulated PRG4 expression in primary bovine chondrocytes undergoing dedifferentiation, indicating that HA may be more directly involved in PRG4 metabolism [134].

An important limitation of HA-MA hydrogels for tissue engineering was the lack of matrix distribution, as collagen type II and aggrecan were entirely limited to the pericellular space, and improvements in construct mechanical properties were significantly lower than in Gel-MA constructs. Increasing the cell density could result in better integration and functionality of the newly formed matrix [135], along with reducing the initial crosslink density in the hydrogel constructs [122]. HA-MA gels degraded relatively rapidly, with gels losing approximately 50% of their initial wet weight after 3 weeks culture,

whereas the wet weights of the other hydrogels remained unchanged. HA is susceptible to both hydrolytic and enzymatic degradation, making *in vivo* degradation times difficult to model precisely. It appears that enzymatic degradation was the predominant mechanism in our hydrogels, as cell-free gels did not change in shape or weight with time in culture (data not shown). Strategies to increase the stability of HA hydrogels have been developed, but some, such as esterification, appear to also alter its biological properties [69, 136, 137].

Like HA-MA, AL-MA is a polysaccharide polymer with a fixed negative charge, however, is non-degradable. Cells responded very differently in these two gels, with only minimal matrix formation observed in AL-MA constructs. This could be a consequence of localised HA-MA degradation providing a more permissive environment for matrix deposition, or HA-MA promoting chondrogenesis through CD44 receptor mediated signaling [20]. It may also be a result of the differences in the initial crosslink densities and mesh sizes of the hydrogels.

On day 1, significant differences existed in the compressive moduli, and hence crosslink densities and mesh sizes, of the different hydrogels. Other studies have shown that matrix properties are influenced by crosslink density, with increased matrix production and distribution occurring with lower crosslink densities [120, 122]. Matrix production was low in AL-MA constructs, and this could be partly attributable to these gels being the stiffest on day 1 [80, 122]. Similarly, the lower retention of GAGs in PEG-MA hydrogels may be a consequence of these gels being relatively soft on day 1. However, material properties appear to be of greater importance than crosslink densities. In a previous study in which PEG and alginate with different crosslink densities were compared, the differences between PEG and alginate were more pronounced than differences in crosslink densities for each material [80]. Nevertheless, the differences in the initial mechanical properties of the hydrogels are expected to have some influence over cell-fate and matrix production, and the role that initial mechanical properties and crosslink densities play is the subject of further studies in our laboratory. The impact of UV exposure on cells during hydrogel cross-linking is not fully understood [65], so we believe it is imperative that each group receives the same level of UV exposure.

Biomaterials play a key role in next-generation ACI-based therapies. Different biomaterials have the capacity to influence the properties of the repair tissue. For example, differences in the repair tissue formed from cartilage therapies

using either HA or collagen-based materials were still detectable 2 years post operatively [114]. Thus, there is significant scope for material properties to influence outcomes of cartilage tissue therapies, and further research is required to develop and optimise these materials or their combinations for use in cartilage tissue engineering therapies.

### **3.5 Conclusions**

Photocrosslinkable hydrogels have the potential to improve cell-based cartilage tissue engineering therapies. Here, we identified key differences in cellular response between several single-component hydrogel systems. Gel-MA hydrogels promoted the rapid formation of a cell-secreted, and mechanically functional ECM, thus reinforcing the interest in Gel-MA for tissue engineering applications. However, several measures showed that chondrocytes had a mixed phenotype in these gels. Meanwhile, HA-MA hydrogels promoted chondrogenic differentiation, but the limited matrix distribution and rapid degradation were clear limitations. As each material showed specific advantages and disadvantages, combinations of materials should be a focus in future attempts to recapitulate the composition, structure and function of articular cartilage.

### **Acknowledgements**

The authors would like to thank Prof. Ross Crawford for facilitating the supply of cartilage tissue, and Dr. Mark Wellard for assistance with NMR. The antibody against collagen type II, developed by T.F. Linsenmayer was obtained from the Developmental Studies Hybridoma Bank developed under the auspices of the NICHD and is maintained by the University of Iowa, Department of Biology, Iowa City, IA, 52242.





## Chapter 4

# Gelatin-methacrylamide hydrogels as potential biomaterials for fabrication of tissue engineered cartilage constructs

---

Wouter Schuurman<sup>1,2,†</sup>, Peter A. Levett<sup>1,3,†</sup>, Michiel W. Pot<sup>1,4</sup>, Paul René van Weeren<sup>2</sup>, Wouter J. A. Dhert<sup>1,5</sup>, Dietmar W. Huttmacher<sup>3</sup>, Ferry P. W. Melchels<sup>1,3</sup>, Travis J. Klein<sup>3</sup> and Jos Malda<sup>1,2,3</sup>

*† Wouter Schuurman and Peter Levett contributed equally and are joint first authors*

Macromolecular Bioscience (2013), Vol. 13, No. 5, p. 551-561.

<sup>1</sup> *Department of Orthopaedics, University Medical Center, Utrecht, P.O. Box 85500, 3508 GA, The Netherlands*

<sup>2</sup> *Department of Equine Sciences, Faculty of Veterinary Medicine, University of Utrecht, The Netherlands*

<sup>3</sup> *Institute of Health and Biomedical Innovation, Queensland University of Technology, Kelvin Grove 4059, Australia*

<sup>4</sup> *Technical Medicine, MIRA (Institute for Biomedical Technology and Technical Medicine), University of Twente, Enschede, The Netherlands*

<sup>5</sup> *Faculty of Veterinary Medicine, University of Utrecht, The Netherlands*

## **Abstract**

Gelatin-methacrylamide (Gel-MA) hydrogels are shown to support chondrocyte viability and differentiation and give wide ranging mechanical properties depending on several cross-linking parameters. Polymer concentration, UV exposure time, and thermal gelation prior to UV exposure allow for control over hydrogel stiffness and swelling properties. Gel-MA solutions have a low viscosity at 37 °C, which is incompatible with most biofabrication approaches. However, incorporation of hyaluronic acid (HA) and/or co-deposition with thermoplastics allows Gel-MA to be used in biofabrication processes. These attributes may allow engineered constructs to match the natural functional variations in cartilage mechanical and geometrical properties.

**Keywords:** additive manufacturing; cartilage; gelatin; hydrogels; tissue engineering

## 4.1 Introduction

Regenerative medicine aims to restore or replace damaged tissues or organs, using a combination of cells, scaffolding materials, and growth factors. Scaffolding materials, acting as a temporary extracellular matrix, must both provide a support structure for the cells and at the same time provide a niche that allows the cells to deposit their specific extracellular matrix [5, 138]. Besides the material composition, structural characteristics, including architecture and mechanical properties will also affect its functionality. In native cartilage tissue, mechanical properties vary with distance from the surface. For example, stiffness increases with depth by more than an order of magnitude from the superficial to the deep zone [33]. The ability to regenerate articular cartilage with a zonal structure featuring different characteristics with changing depth would mark a significant advancement in the treatment of chondral defects [118]. Development of hydrogels with tunable mechanical properties is an important step toward this aim.

Additive manufacturing techniques are recognised as promising innovative technologies in the emerging field of regenerative medicine, as they allow the fabrication of constructs of well-defined shape and internal structure, employing medical imaging and computer-aided design [139-141]. Bioprinting is a subclass of additive manufacturing techniques that involves the organised and specific placement of cells and materials, with or without a carrier material, to recreate the complex organisation of tissues and organs [142-144]. The possibility of combining different cell types and materials makes this approach particularly interesting for cartilage tissue engineering, since it can aid in the replication of the native zonal organisation of the tissue.

In bioprinting, hydrogels are most often used as a cell carrier. These hydrogel materials need to meet a number of requirements in order to be suitable for bioprinting [145, 146]. First, the rheological properties of the material must enable the deposition of strands. Second, the material must have adequate mechanical properties to allow the construct to retain its shape after printing. Third, the gel must be cytocompatible and allow for differentiation of the encapsulated cells. Finally, the swelling characteristics of hydrogels must be known to predict the final shape and size of a bioprinted construct after swelling.

Gelatin is a water-soluble protein obtained by the denaturation of collagen. Due to its biodegradability [147], biocompatibility [148], and ability to form hydrogels, gelatin plays a significant role in biomedical materials research and

specifically for three-dimensional (3D) cell culture models and tissue engineering applications. Aqueous solutions of gelatin form thermoreversible hydrogels below their upper critical solution temperature (UCST) of 25–35 °C [149, 150]. This thermo-responsive behavior could be employed in bioprinting, as thermal gelation would aid in retaining the shape of printed constructs [151]. Functionalisation of gelatin with unsaturated methacrylamide groups results in gelatin-methacrylamide (Gel-MA), which can form covalently crosslinked hydrogels under mild conditions [52, 152] and be cultured with encapsulated cells [153-155]. The addition of more viscous components, such as hyaluronic acid (HA), could potentially further improve properties important for printing of hydrogel systems [156]. Moreover, the presence of HA may be especially beneficial for cartilage tissue engineering given its abundance in native cartilage and its anabolic effect on extracellular matrix synthesis [157, 158].

In this work, we characterised how the macromer concentration, UV dose, and crosslinking temperature influence the mechanical and swelling properties of Gel-MA hydrogels. Subsequently, we investigated two strategies to allow Gel-MA to be used as the “ink” in bioprinting. The first was to combine Gel-MA with HA to increase the viscosity, and the second was to utilise a thermoplastic polymer to provide structural support in printed hybrid constructs. Lastly, we assessed the suitability of Gel-MA for engineering of cartilaginous tissue by culturing encapsulated chondrocytes in photocrosslinked Gel-MA and Gel-MA/HA hydrogels.

## **4.2 Experimental Section**

### **4.2.1 Preparation of Gel-MA**

Gel-MA was prepared by reaction of type A gelatin (Sigma–Aldrich, St. Louis, Missouri, USA) with methacrylic anhydride (Sigma–Aldrich) at 50 °C for 1 h, as previously described [52]. Briefly, methacrylic anhydride was added dropwise to a 10% solution of gelatin in phosphate-buffered saline (PBS) (Invitrogen, Carlsbad, California, USA) under constant stirring. To achieve a high degree of functionalisation (DoF), 0.6 g of methacrylic anhydride was added per gram of gelatin [124]. The functionalised polymer was dialysed against distilled water for 3 d at 40 °C to remove methacrylic acid and anhydride, neutralised with 10% sodium bicarbonate (Merck, Darmstadt, Germany), freeze-dried and stored at ~20 °C before use. The DoF was determined as previously described [159], by using ninhydrin to quantify the concentration of residual free amine groups in the synthesised Gel-MA relative to the starting material.

### **4.2.2 Preparation of cell-free gels**

Unless otherwise stated, all concentrations given as a percentage are percent weight per volume (w/v). Hydrogel precursor solutions were prepared in PBS, with a final concentration of the photoinitiator Irgacure 2959 (BASF, Ludwigshafen, Germany) of 0.05% and photocrosslinked in a custom-built Teflon mold using 365 nm light at an intensity of 2.7 mW/cm<sup>2</sup> in a UVP CL-1000L crosslinker (UVP, Upland, California, USA). The mold produces gels with dimensions of 4 × 4 × 2 mm; n = 4 per condition. Gel-MA gels were either crosslinked as solutions at 37 °C, or allowed to form physically crosslinked gels at room temperature for 15 min, and then UV crosslinked.

### **4.2.3 Physical Properties**

To determine the effective swelling, gels were weighed immediately after crosslinking and again after swelling overnight in PBS at 37 °C. The difference in wet weights was expressed as a percentage, and referred to hereafter as effective swelling. To assess the mass swelling ratio, swollen gels were weighed, then lyophilised to determine their dry mass. The mass swelling ratio was determined by the ratio of equilibrium wet weight to dry weight. The compressive moduli of swollen Gel-MA hydrogels were measured using an Instron 5848 microtester (Instron, Norwood, Massachusetts, USA) with a 5 N load cell. The hydrogels were tested in an unconfined arrangement while submerged in PBS at 37 °C. The gels were compressed at a displacement rate of 0.01 mm/s between flat, non-porous surfaces. Gels were weighed after testing, and the cross-sectional area of each gel was calculated as the ratio of wet weight to height. The Young's modulus was taken as the slope of the stress–strain curve from 10 to 15% strain.

### **4.2.4 Bioprinting**

Three-dimensional (3D) models for the constructs were designed using Rhino 3D software (McNeel, Seattle, Washington, USA), loaded via computer-aided manufacturing (CAM) software (PrimCAM, Einsiedeln, Switzerland), and constructs were printed using the BioScaffolder dispensing system (SYS + ENG, Salzgitter-Bad, Germany). Briefly, the BioScaffolder is a three-axis dispensing machine, which can build 3D constructs by coordinated motion of one or more syringe dispensers (for dispensing hydrogel) and a polymer dispenser, which deposit the polymer solution on a stationary platform. Manufacturing was performed at room temperature while keeping the hydrogel dispensing heads at 37 °C.

Printing of hydrogel-only constructs was attempted using 10% Gel-MA, 20% Gel-MA, and 20% Gel-MA supplemented with 2.4% HA (HA sodium salt from *Streptococcus equi*, Sigma–Aldrich). Hydrogel-only constructs were printed using a 27 G needle (inner diameter 210  $\mu\text{m}$ ), an XY-plane speed of 1,000 mm/min, a spindle speed of 1.5 (arbitrary units), a strand distance of 1.5 mm, and a layer thickness of 0.3 mm. The spindle speed reflects the flowrate of the hydrogel precursor, and different materials require different XY-plane speeds and flow-rate parameters for printing. The optimal speed of the XY-platform and the flow-rate of the material were determined for each material used in this study.

Hybrid constructs were printed with 10% Gel-MA plus 2.4% HA, alternated with  $\epsilon$ -polycaprolactone (PCL) (MW 70–90 kg/mol, Sigma–Aldrich) as previously described [160]. The PCL was dispensed through a 23 G metal needle (inner diameter 337  $\mu\text{m}$ , DL Technology LLC, Haverhill, MA, USA) at 160 °C and 0.5 MPa, at a deposition speed of 176 mm/min. Gel-MA/HA was dispensed between the PCL fibers at an XY-plane speed of 60 mm/min, spindle speed of 1.10 (arbitrary units), using an 18 G needle (inner diameter 838  $\mu\text{m}$ ). Since porosity was not required in these constructs, the XY-plane speed was significantly lower than for printing of hydrogel-only constructs. For visualisation, the hydrogel was stained using Fast Green or Basic Fuchsin (Sigma–Aldrich), or loaded with Dye-Trak “F” fluorescent blue or lemon beads (Triton technology, San Diego, CA, USA). After the construct was finalised, the Gel-MA was crosslinked by 5 min irradiation with a Superlite S-UV 2001AV lamp (Lumatec, Munchen, Germany). Printed constructs were cut to 6  $\times$  5  $\times$  2 mm and analysed using fluorescence microscopy.

#### **4.2.5 Cell-laden Gelatin Hydrogel Constructs**

Full thickness healthy articular cartilage was harvested from the condyles and patellofemoral grooves of fresh equine cadavers (n=3, age 4–9 years) under aseptic conditions. The cells were obtained (with consent of the owners) from cadavers that died of natural causes in the clinic, and animals were thus not specifically sacrificed for this study. Cells from each donor were kept separate throughout the experiment. After digesting the tissue using 0.15% type II collagenase (Worthington Biochemical Corporation, Lakewood, New Jersey, USA) overnight at 37 °C, the cell suspensions were filtered (100  $\mu\text{m}$  cell strainer, BD Falcon, Bedford, Massachusetts, USA) and washed three times in PBS. Cells were then resuspended in expansion medium (DMEM, Invitrogen) supplemented with 10% fetal bovine serum (FBS, Biowhittaker, Walkersville, Maryland, USA), 100 units/mL penicillin and 100 mg/mL streptomycin

(both Invitrogen), 25 mM HEPES (Invitrogen), and 10 ng/mL FGF-2 (R&D Systems, Minneapolis, Minnesota, USA) and counted using a hemocytometer. Chondrocytes were seeded at a density of 5000 cells/cm<sup>2</sup> and expanded until 90% confluency in monolayer cultures in expansion medium.

After expansion, cells were detached using 0.25% trypsin (Invitrogen), washed with PBS, and P1 cells were resuspended in either a 10% Gel-MA solution or a mixture of 10% Gel-MA and 2.4% HA (Gel-MA/HA) (n = 3 per condition per donor). The Gel-MA hydrogel consisted of 10% Gel-MA and 0.05% Irgacure 2959 (BASF). For the Gel-MA/HA, 2.4% HA was added to the Gel-MA solution, resulting in a highly viscous, translucent mixture. Cells were encapsulated at a density of  $5 \times 10^6$  cells/mL for viability assays and at a density of  $2 \times 10^7$  cells/mL for differentiation assays. Lower cell densities were used to more accurately visualise and quantify live and dead cells, while a higher cell density was used for increased matrix production in differentiation cultures. Constructs of 100  $\mu$ L were fabricated using two sterilised glass slides and two PVC spacers of 2 mm height. The hydrogel-cell suspension was put on a glass, the spacers were placed, and the second glass was put on top of the gel, yielding a cylindrical construct. A Superlite S-UV 2001AV lamp (Lumatec) was used to cross-link the cell-laden hydrogel constructs for 5 min. Constructs were cultured in chondrogenic differentiation medium [DMEM supplemented with 0.2 mM ascorbic acid 2-phosphate (Sigma–Aldrich), 0.5% human serum albumin (Cealb, Sanquin, Utrecht, The Netherlands), 1% v/v insulin–transferrin–selenium mixture (ITS-X, Invitrogen), 100 units/mL penicillin and 100  $\mu$ g/mL streptomycin, and 5 ng/mL TGF- $\beta$ 2 (R&D Systems Abingdon, UK)]. Samples for viability assays were taken after 1 and 3 days. Samples for differentiation were cultured for 4 weeks; medium was refreshed twice per week. Samples (n = 3 per donor) were cut in half, one half was processed for histology and the other half was used for quantitative assays.

#### **4.2.6 Viability Assay**

To visualise cell viability, a LIVE/DEAD Viability Assay (Molecular Probes MP03224, Eugene, Oregon, USA) was performed according to the manufacturer's recommendations, as previously described [151]. The samples were examined using an Olympus BX51 light microscope and photomicrographs taken with an Olympus DP70 camera (both Olympus, USA). The excitation/emission filters were set at 488/530 nm to observe living (green) cells and at 530/580 nm to detect dead (red) cells. Live and dead cells were counted for three samples per time point, at four locations within each construct.

#### **4.2.7 Histological, Immunohistochemical and Biochemical Assays**

For histology, samples were fixed in formalin, processed through graded alcohol series, and embedded in paraffin. Embedded samples were cut to yield 5  $\mu\text{m}$  sections. Sections were stained with Weigert's hematoxylin (Klinipath, Duiven, The Netherlands) for cells, fast green (Merck) for proteins, and Safranin-O (Merck) for proteoglycans. For immunolocalisation of cartilage marker collagen type II, endogenous peroxidase was blocked using a 0.3%  $\text{H}_2\text{O}_2$  solution for 10 min. Samples were washed with PBS/Tween (0.1%), followed by hyaluronidase and pronase antigen retrieval. Samples were blocked with 5% BSA in PBS for 30 min and then incubated overnight with the monoclonal anti-collagen type II antibody [1:100, II-6B3II, Developmental Studies Hybridoma Bank (DSHB), Iowa City, IA, USA]. Samples were then incubated for 60 min with a horseradish peroxidase-conjugated goat anti-mouse antibody. Staining was visualised using DAB solution (Sigma–Aldrich) for 10 min. Counterstaining was performed with hematoxylin. The sections were examined using a light microscope. Isotype controls were performed by using mouse isotype IgG1 monoclonal antibody at concentrations similar to those used for the staining. For biochemical analysis, samples were digested overnight at 56 °C in a solution containing 250  $\mu\text{g}/\text{mL}$  papain (Sigma–Aldrich). Quantification of total DNA was performed by Quant-iT PicoGreen dsDNA kit (Invitrogen) using a spectrofluorometer (BioRad, Hercules, California, USA). The amount of glycosaminoglycans (GAGs) was determined spectrophotometrically after reaction with dimethylmethylene blue dye (DMMB, Sigma–Aldrich) [125], pH = 3.0.

Intensity of color change was quantified immediately in a microplate reader (BioRad) by measuring absorbance at 540 and 595 nm. The amount of GAGs was calculated using a standard of chondroitin sulfate C (Sigma–Aldrich) and by calculating the ratio of absorbances. The tissue sections were examined using a light microscope and photomicrographs taken to assess the tissue thickness, the distribution of cells, and GAGs.

#### **4.2.8 Statistics**

All statistical analyses were performed using SPSS 15.0 software (IBM Corporation, Armonk, NY, USA). A one-way ANOVA and Tukey's post hoc test were used for analysis of physical properties. To analyse viability between conditions, a one-way analysis of variance (ANOVA) was used, while for viability in time, a repeated measurements ANOVA was performed. For the



comparison between GAG and GAG per DNA, an independent samples t-test was used. All data are shown as mean values  $\pm$  standard deviation.

### **4.3 Results**

The synthesised and purified Gel-MA had a DoF of  $75 \pm 9\%$ . Transparent Gel-MA hydrogels with a wide range of mechanical and swelling properties were produced by varying the photocrosslinking duration and Gel-MA concentration.

#### **4.3.1 Effect of Macromer Concentration**

To investigate the effect of macromer concentration on swelling and mechanical properties, gels were produced by photocrosslinking 5, 10, 15, and 20% Gel-MA solutions. All gels were photocrosslinked for 30 min to produce completely crosslinked gels. Other studies in our laboratory have shown that up to cell densities of  $7 \times 10^6$  cells/mL, the physical properties of cell-free and cell-laden Gel-MA constructs are similar after crosslinking and swelling overnight (manuscript in preparation), and future studies will investigate how differences in the initial mechanical properties influence outcomes of cell-laden constructs after *in vitro* culture. Gel-MA concentration had a significant impact on hydrogel stiffness (Figure 4.1A) and equilibrium mass swelling (Figure 4.1B), but only a minor influence on the effective swelling (Figure 4.1B). The compressive modulus showed a strong power-law dependence on the Gel-MA precursor concentration. For Gel-MA concentrations between 5 and 20%, the modulus of gels crosslinked for 30 min was given by Equation 4.1, in which  $E_{100}$  is the modulus of a (hypothetic) undiluted gel (100% Gel-MA, no PBS),  $C$  is the Gel-MA concentration (% w/v), and  $n$  is the power constant.

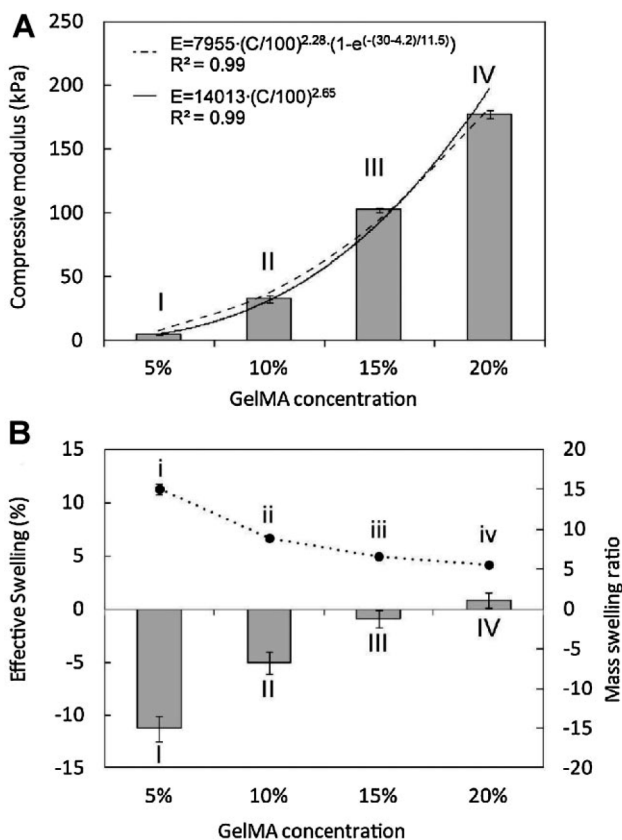


**Figure 4.1: Mechanical and swelling properties of Gel-MA hydrogels crosslinked for 30 minutes.** (A) Compressive modulus shows a power law dependence on concentration (lower equation, solid line). The top equation and dashed line represent the overall model in which the exposure time is included as well (**Equation 4.3**). (B) Effective swelling (bars) and mass swelling ratio (dots) for 5–20% (w/v) Gel-MA hydrogels. Differences in the initial Gel-MA concentrations are maintained after swelling, indicated by distinct mass swelling ratios between groups. Effective swelling (B) increases only moderately with Gel-MA concentration. All groups are statistically significantly different, as indicated by different Roman numerals ( $p < 0.05$ ).

The low degree of effective swelling exhibited by the Gel-MA gels over a broad range of macromer concentrations is favorable for application in bioprinting, as excessive swelling would compromise printing accuracy. Even at the lowest Gel-MA concentration the weight change was only 12% (shrinkage in this case). This corresponds to a volume change of approximately 12% as well, which is less than 4% change in each dimension. Thus hydrogels with different macromer concentrations could potentially be combined in a single construct

with minimal interfacial stress, to obtain spatially defined mechanical properties as is the case in native cartilage [118].

**Equation 4.1: Power law dependence of compressive modulus (E, kPa) on Gel-MA concentration (C, % w/v) of gels crosslinked for 30 min.**

$$E = E_{100} \left( \frac{C}{100} \right)^n$$

### 4.3.2 Effect of UV exposure

Total UV exposure is a sensitive parameter for controlling the stiffness and swelling of Gel-MA hydrogels. The compressive moduli of 20% Gel-MA hydrogels crosslinked for 30 min were over tenfold greater than those crosslinked for 5 min (Figure 4.2A), while hydrogels crosslinked for 10 min were over sixfold greater than those crosslinked for 5 min. The variation of modulus with UV time appeared to follow first order kinetics. Equation 4.2 shows the model used to estimate the modulus of 10 and 20% Gel-MA hydrogels crosslinked for UV times ranging from 5 to 30 min. The modulus of the fully crosslinked hydrogels (at infinite exposure times) are given by  $E_{\infty}$ . A time shift (A, in min) was incorporated to account for retardation (consumption of formed radicals by reaction with dissolved oxygen prior to the onset of crosslinking of the methacrylamide groups) and to achieve the minimum crosslink density necessary for gel formation. The time constant  $\tau$  (minutes), A and  $E_{\infty}$  were determined using Solver in Excel to minimise the sum of squared errors. The values of these parameters for 10 and 20% Gel-MA hydrogels are shown in Table 4.1. For both Gel-MA concentrations, a time shift of approximately 4 min was found, which accounts for the large difference in moduli of hydrogels crosslinked for 5 or 10 min. The time constants,  $\tau$ , were 9.4 and 10.9 min for 10 and 20% Gel-MA hydrogels, respectively, indicating that in each case gels have attained approximately two thirds of their maximum modulus after approximately 10 min UV exposure.

The effective swelling ratio is highly dependent on UV exposure, decreasing from 60% with 5 min exposure to negligible swelling after 25 or more minutes of UV exposure (Figure 4.2B). These data demonstrate that the UV exposure affects the mechanical properties of the hydrogel, but also define the kinetics of the reaction. Near-complete reaction of the functional groups is indicated by both the compressive modulus and the swelling parameters reaching steady-state at 25–30 min. It is important to keep in mind that the total UV exposure, not the UV time, that is the main parameter of importance, and that changing the UV

intensity would also change the necessary UV exposure times. Additionally, the DoF will affect the modulus, swelling parameters, and kinetics of the reaction as well. Preliminary experiments using Gel-MA with lower DoF (~40%) showed lower stiffness, along with swelling ratios up to 160% (data not shown). As these attributes are unsuitable for cartilage tissue engineering applications, all studies described here are based on the Gel-MA with a high DoF ( $75 \pm 9\%$ ).

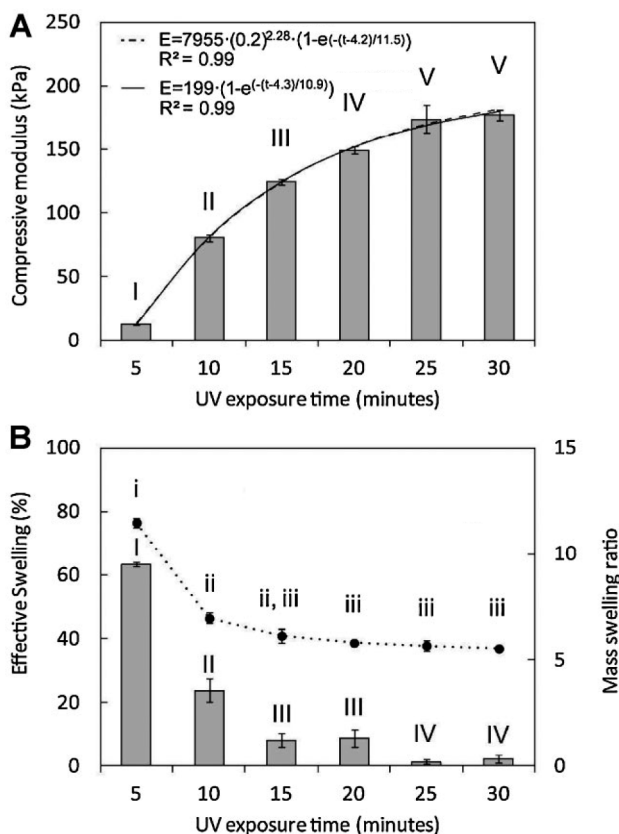


**Figure 4.2: Effect of UV exposure on the mechanical and swelling properties of 20% (w/v) Gel-MA hydrogels.** (A) Compressive modulus increases with UV exposure time in agreement with the exponential model (lower equation, solid line). The top equation and dashed line represent the overall model in which the Gel-MA concentration is included as well (**Equation 4.3**). (B) Effective swelling (bars) and mass swelling ratio (dots) decrease significantly with increased UV exposure. Statistically significant differences ( $p < 0.05$ ) between groups are indicated by different Roman numerals.

Combining Equation 4.1 and Equation 4.2 gave a model for estimating the modulus of Gel-MA hydrogels with varying concentrations and photocrosslinking times (Equation 4.3). This equation was solved using the minimal sum of squared error method for all available combinations of concentration and exposure times, resulting in the generic best-fit parameters listed in Table 4.2. Here, the same parameters  $C$  and  $t$  and the same constants  $n$ ,  $A$ , and  $\tau$  are used as in Equation 4.1 and Equation 4.2.  $E_{\max}$  combines the time-dependent parameter  $E_{100}$  (Equation 4.1) and concentration-dependent  $E_{\infty}$  (Equation 4.2) into one independent parameter,  $E_{\max}$ , which represents the maximum modulus of a 100% Gel-MA gel at infinite exposure time. Its value of approximately 8 MPa is typical for rubbers, reinforcing that (Gel-MA) hydrogels are networks of rubbery polymer chains diluted by water.

**Equation 4.2: Model to approximate the compressive modulus ( $E$ , kPa) of Gel-MA hydrogels with varying UV exposure time ( $t$ , min), for a given concentration of Gel-MA.**

$$E = E_{\infty} (1 - e^{-(t-A)/\tau})$$

**Table 4.1: Best-fit parameters for the compressive modulus model (Equation 4.2) using experimental data of 10 and 20% (w/v) Gel-MA hydrogels.**

<b>Gel-MA Concentration</b> (% w/v)	<b><math>E_{\infty}</math></b> (kPa)	<b>A</b> (min)	<b><math>\tau</math></b> (min)
10	36	4.0	9.4
20	199	4.3	10.9

The mathematical model can be used to guide the selection of concentrations and photocrosslinking times that should be used to give gels with a specific stiffness. It is only valid if other parameters used in this system, such as DoF, photoinitiator concentration, UV intensity, solvent type (PBS here), and crosslinking temperature remain constant. Changes to these conditions will affect the crosslinking kinetics and alter the values of parameters in Equation 3, although it is expected that the underlying model could be fitted to other conditions.

**Equation 4.3: Model for estimating the compressive modulus ( $E$ , kPa) of Gel-MA hydrogels based on Gel-MA concentration ( $C$ , % w/v) and UV exposure time ( $t$ , min).**

$$E = E_{\max} \left( \frac{C}{100} \right)^n (1 - e^{-(t-A)/\tau})$$

$$\text{where} \quad \begin{array}{l} 5 \leq C \leq 20 \\ 5 \leq t \leq 30 \end{array}$$

**Table 4.2: Best-fit parameters for the compressive modulus model (Equation 3) using experimental data of 5–20% (w/v) Gel-MA hydrogels.**

$E_{\max}$ (kPa)	$n$	$A$ (min)	$\tau$ (min)
7995	2.28	4.2	11.5

### 4.3.3 Effect of Temperature

The state of Gel-MA polymer chains during crosslinking, and the mechanical properties of the resulting gels, is dependent on the gelation state during crosslinking (Figure 4.3). Gel-MA solutions that were maintained at 25 °C and were allowed to form thermal gels prior to UV exposure were significantly stiffer than those that were maintained at higher temperature (37 °C). The increased stiffness of gels which were photocrosslinked as physical gels (i.e., at 25 °C) was maintained when the gels were swelled and mechanically tested at 37 °C, indicating that the physical crosslinks that arise from thermal gelation are no longer temperature-responsive after covalent crosslinking. Moreover, gels crosslinked in solution at 37 °C also showed no difference in stiffness when tested at either 25 or 37 °C, confirming that these gels had also lost their temperature-responsiveness (data not shown). Gels crosslinked at 37 °C had similar equilibrium swelling ratios to those crosslinked at room temperature. The thermo-responsive properties of Gel-MA may be utilised during bioprinting to provide mechanical support prior to covalent photocrosslinking of the Gel-MA network. By photocrosslinking the hydrogel in a thermal gel state, the Gel-MA polymer chains maintain a triple helical conformation, and hence their biological relevance [161]. Photocrosslinking after printing and thermal gelation has the advantages of increased stiffness and stability, which is important for its potential application in tissue engineering.

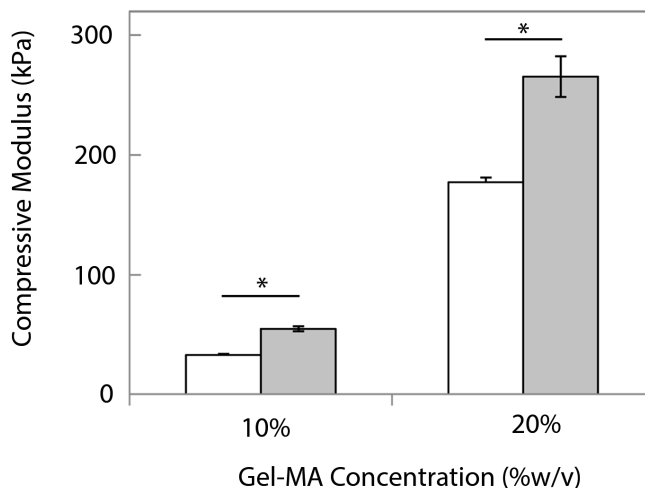


**Figure 4.3: Effect of crosslinking temperature on the stiffness of 10 and 20% Gel-MA hydrogels.** Gels were crosslinked at 37 °C (white bars), or allowed to cool to room temperature then UV crosslinked (gray bars). All gels were tested at 37 °C; \* indicates  $p < 0.05$ .

#### 4.3.4 Bioprinting of Gel-MA and Gel-MA/HA

Bioprinting of Gel-MA was, despite the thermosensitive behavior of the material, hampered by its low viscosity. Upon ejection from the needle, droplets were formed that spread when contacting the building platform (Figure 4.4A, C). At lower temperatures the viscosity increased significantly, but at the cost of irregular flow rates and material inhomogeneity, resulting in blocking of the nozzle. The addition of 2.4% HA to 20% Gel-MA allowed the controlled, homogeneous deposition of hydrogel strands (Figure 4.4B). The strands fused to form mechanically robust porous constructs measuring  $\sim 20 \times 20 \times 1.2$  mm and consisting of four stacked layers with a 0–90° lay-down pattern were fabricated according to the predefined size and shape (Figure 4.4D). The addition of HA increases the viscosity, and can facilitate the printing process and improve shape fidelity, as had been previously shown for dextran-based gels [156]. In this way, large and interconnected pores can be introduced, which is especially important when larger, clinically relevant constructs are to be manufactured [162–164]. Porosity can enhance nutrient transport and waste removal by decreasing diffusion distances [162]. This in turn leads to more homogeneous cell differentiation [163] and extracellular matrix deposition. The flexibility of printing allows constructs with various degrees of porosity to be fabricated, including non-porous (solid) constructs as is common when this fused

deposition modeling technique is employed for rapid prototyping purposes. The porosity and architecture of constructs will impact both the mechanical properties and diffusion, and the optimal parameters relevant for cartilage tissue engineering must be pursued in further research.

To print well-defined, gel-only constructs, 20% Gel-MA with 2.4% HA had to be used. However, previous studies have shown that highly crosslinked gels inhibit the secretion and formation of new ECM, and that hydrogels with lower crosslinking densities provide a more permissive environment for matrix formation [94, 122, 165]. To overcome this limitation, Gel-MA could be combined with another material to enhance the rheological and mechanical properties, for instance with gellan gum [124] or fibrin [166]. The characterisation of Gel-MA/HA and other additives will be subject of future investigation, aiming at improving both printing accuracy and neocartilage formation.

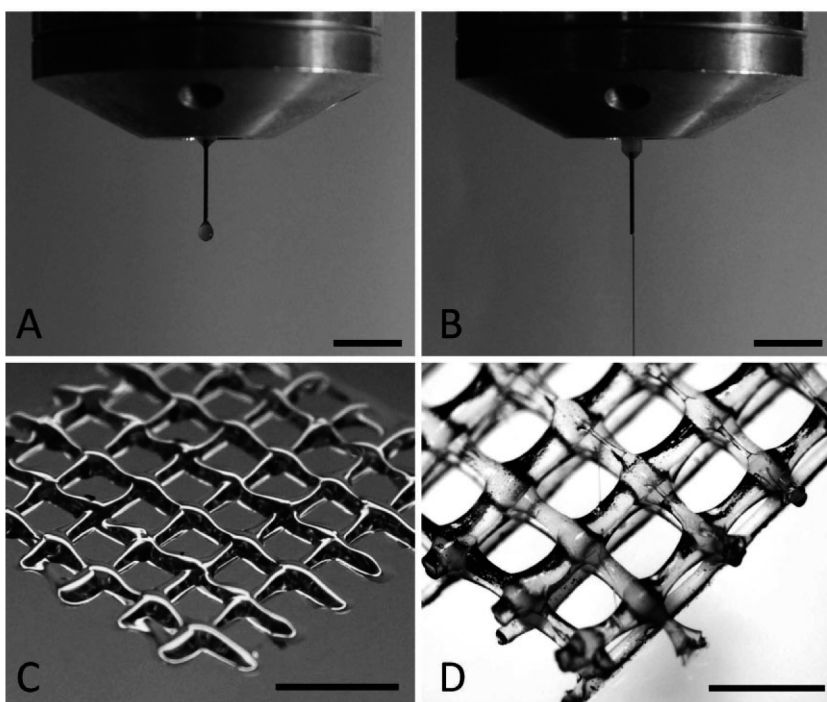


**Figure 4.4: Bioprinting of Gel-MA with or without HA.** Gel-MA on its own (20% w/v) formed droplets at the nozzle (A) and was deposited in flat lines that spread out on the surface (C). When 2.4% (w/v) HA was added, strands could be deposited from the nozzle (B), resulting in a construct of four layers (D). The scale bars in A–C represent 5 mm; the scale bar in D is 2 mm.



When constructs were fabricated using reinforcement with simultaneously deposited PCL fibers, the Gel-MA concentration could be lowered from 20 to 10% (still supplemented with 2.4% HA). Combining the hydrogel with the thermoplastic polymer also made it feasible to print more layers on top of each other, creating rectangular scaffolds ( $6 \times 60 \times 1.98$  mm), with separate Gel-MA/HA hydrogel parts, in which different components could be incorporated. Figure 4.5 shows cross-sections of such hybrid structures in which separate layers of gel can be discerned by different colored fluorescent beads (Figure 4.5A), or different coloured dyes (Figure 4.5B). The fabrication of distinct gel layers as shown here demonstrates the potential for capturing zone-specific components and material properties in printed constructs. The advantages of these hybrid constructs are two-fold: a wider range of hydrogels can be used for bioprinting, as shown here with a lower percentage of Gel-MA, and the stiffness of the resulting fiber-reinforced hydrogel is higher [160, 167] and hence better suited for musculoskeletal applications, in which the constructs bear considerable mechanical loads [160, 168-170]. The aim of this section of the study was to evaluate the potential to use Gel-MA or Gel-MA/HA mixtures in bioprinting, and the viability and differentiation of chondrocytes encapsulated in these materials. Although cell-laden, printed constructs were not fabricated in this study, cell viability has previously been shown to be similar in printed hybrid constructs and unprinted controls [144, 160], so similar cell viabilities would also be expected in printed, cell-laden constructs fabricated from these materials.

Figure 4.5 shows that hydrogels can be organised into layered structures with a total height of less than 2 mm, which is comparable to the thickness of articular cartilage in the human knee or hip [171]. Thus using these bioprinting techniques, layered structures for the repair of articular cartilage can be fabricated [118]. Bioprinting enables researchers to combine different materials and different cell types into one construct, thus facilitating the replication of the complex architecture of tissues. This can be of value for both *in vitro* models and for the engineering of neotissues for implantation. The hybrid approach allows for a wider range of hydrogel materials to be used with this technology and therefore expands the possibilities for models and implantable tissues.

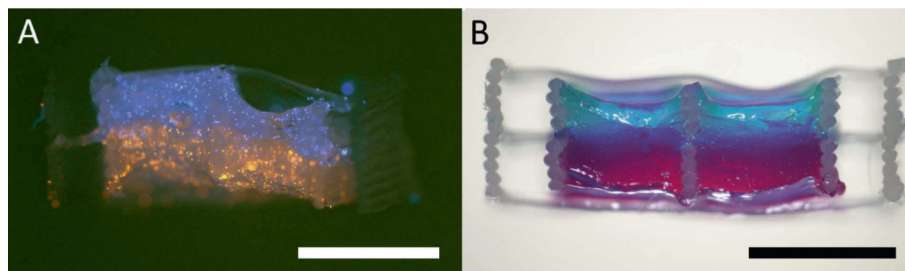


**Figure 4.5: Hybrid bioprinting of Gel-MA/HA (10%/2.4%) resulted in rectangular scaffolds with two separate Gel-MA/HA hydrogel parts.** Cross-sections of such constructs are shown, with incorporated blue and orange fluorescent beads (A) or basic fuchsin (pink) and fast green (B) to visualise the two Gel-MA hydrogels. The scale bars represent 2 mm.

### 4.3.5 Cell-laden Gel-MA Hydrogel Constructs

Chondrocyte viability in 10% Gel-MA was high, both with and without HA (Table 4.3). No significant differences were observed between days 1 and 3 of culture for either of the hydrogels ( $p = 0.320$  for Gel-MA,  $p = 0.662$  for Gel-MA/HA). Between materials there was no significant difference at day 1 ( $p = 0.946$ ), but at day 3 the cell viability was significantly higher in Gel-MA/HA ( $p = 0.045$ ). Viability was comparable to the values reported for the widely used calcium-crosslinkable [172] or photo-crosslinkable [173] alginate hydrogels, and at acceptable levels for both gel types. During photo-crosslinking, the radicals generated are quickly consumed in the crosslinking process, so cells are not adversely affected by UV exposure during crosslinking, whereas cells in monolayer cultures exposed to equivalent conditions are [65].

**Table 4.3: Cell viability and glycosaminoglycans per DNA for Gel-MA and Gel-MA/HA hydrogels.**

Hydrogel	Viability day 1 $\pm$ SD (%)	Viability day 3 $\pm$ SD (%)	GAG/DNA day 28 (g/g)
Gel-MA	$83 \pm 13$	$73 \pm 2$	$7.1 \pm 3.3$
Gel-MA/HA	$79 \pm 18$	$82 \pm 8^*$	$10.5 \pm 5.2$

\* Significantly different from Gel-MA day 3 ( $p = 0.045$ )

Cartilaginous tissue was formed after 4 weeks in both materials, indicated by the presence of glycosaminoglycans using Safranin-O staining (Figure 4.6A, B) and DMMB assay (Table 4.3), along with the presence of cartilage marker collagen type II (Figure 4.6C, D). No significant difference in the amount of GAGs retained, normalised to DNA, was observed between the Gel-MA and Gel-MA/HA hydrogels ( $p = 0.129$ ). Previously, HA has been reported to enhance

chondrogenesis, but its effects appear to be concentration dependent. Several studies have reported HA to have chondrogenic properties at low concentrations, while at higher concentrations HA has no effect, or may even inhibit chondrogenesis [101, 174-176]. A relatively high concentration of HA was required to give sufficient viscosity for printing, and this may explain why GAG/DNA values were similar in the presence or absence of HA. Overall, the high cell viability and the formation of cartilaginous tissue confirm the suitability of both tested materials for cartilage tissue engineering purposes. However, the limited connectivity of the newly formed extracellular matrix (Figure 4.6C, D) makes it clear that further optimisation of these materials or cell culture conditions is required.

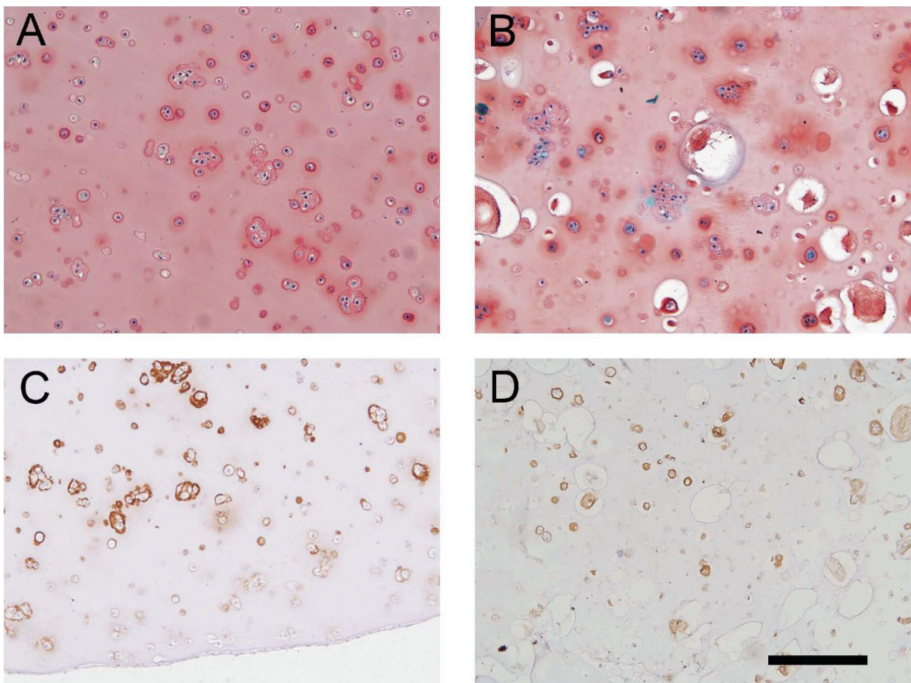


**Figure 4.6: Histology and immunohistochemistry of Gel-MA and Gel-MA/HA hydrogels after 4 weeks of culture.** Cells are stained blue in both cases. Safranin O staining indicating glycosaminoglycan formation (red) in Gel-MA (A) and Gel-MA/HA (B) hydrogels. Collagen type II immunostaining (brown) showing cartilaginous matrix production in Gel-MA (C) and Gel-MA/HA (D) hydrogels. The scale bar represents 200  $\mu\text{m}$  and applies to all panels.

Cell-based approaches in which chondrocytes are encapsulated in hydrogels have shown promise for cartilage regeneration [177], but must be able to withstand the harsh mechanical environment. As we have shown, hydrogels get

stiffer and stronger with increasing polymer content and crosslink density. However, for promoting the production of new matrix, polymer content and crosslink density should not be too high as this would impede the production and redistribution of extracellular matrix [120]. The crosslink density of polyethylene glycol gels has been shown to affect the distribution and composition of matrix deposited by encapsulated chondrocytes [120]. GAG distribution was homogeneous in loosely crosslinked PEG gels, with a modulus of 30 kPa, and localised to the pericellular regions in the more tightly crosslinked gels, with moduli of 360 and 960 kPa, respectively. Collagen type II deposition was also dependent on crosslink density, with the highest levels seen in the gels with an intermediate crosslink density (360 kPa). Thus a balance exists between optimizing gel properties for withstanding mechanical loads, and promoting synthesis and accumulation of new cartilage.

#### **4.4 Conclusion**

The physical properties of Gel-MA hydrogels can be controlled by manipulating the UV dose and concentration of Gel-MA in the precursor solution. Gels with compressive moduli in the range 5–180 kPa can be fabricated by varying the concentration of the precursor solution from 5 to 20%. Over this range of concentrations, the changes in gel dimensions caused by swelling are very small, facilitating the preparation of gel constructs with high shape fidelity. A mathematical model was developed that can be used to determine the concentration and UV exposure time required to give gels with a desired stiffness, as a useful tool for the development of Gel-MA-based hydrogel biomaterials in load bearing applications. The possibility to control the mechanical and swelling properties of the material, combined with the high cell survival and the formation of cartilaginous tissue make Gel-MA a candidate material for cartilage tissue engineering. When combined with viscosity-enhancing additives such as HA and/or a reinforcing support structure, such as PCL, Gel-MA can be fabricated into layered hydrogel structures, which could aid in the engineering of human cartilage.

#### **Acknowledgements**

The authors would like to thank the Australian Research Council and the European Union (Marie Curie Fellowship (PIOF-GA-2010-272286 to Melchels)) for funding. The support of the Dutch Arthritis Foundation is gratefully acknowledged. The antibody against collagen type II, developed by T. F. Linsenmayer, was obtained from the DSHB developed under the auspices of the NICHD and maintained by The University of Iowa, Department of Biology, Iowa City, IA 52242.

## Chapter 5

# A biomimetic extracellular matrix for cartilage regeneration centered on photo-curable gelatin, hyaluronic acid and chondroitin sulfate

---

Peter A. Levett<sup>1,2</sup>, Ferry P. W. Melchels<sup>1,2</sup>, Karsten Schrobback<sup>1</sup>, Dietmar W. Hutmacher<sup>1,3</sup>, Jos Malda<sup>1,2</sup> and Travis J. Klein<sup>1</sup>

Acta Biomaterialia (2014), Vol. 10, No. 1, p. 214-223.

<sup>1</sup> *Institute of Health and Biomedical Innovation, Queensland University of Technology, 60 Musk Ave, Kelvin Grove, QLD 4059, Australia*

<sup>2</sup> *Department of Orthopaedics, University Medical Center, Utrecht, P.O. Box 85500, 3508 GA, The Netherlands*

<sup>3</sup> *George W Woodruff School of Mechanical Engineering, Georgia Institute of Technology, Atlanta, Georgia, USA*

## Abstract

The development of hydrogels tailored for cartilage tissue engineering has been a research and clinical goal for over a decade. Directing cells towards a chondrogenic phenotype and promoting new matrix formation are significant challenges that must be overcome for the successful application of hydrogels in cartilage tissue therapies. Gelatin-methacrylamide (Gel-MA) hydrogels have shown promise for the repair of some tissues, but they have not been extensively investigated for cartilage tissue engineering. We encapsulated human chondrocytes in Gel-MA based hydrogels, and show that with the incorporation of small quantities of photo-crosslinkable hyaluronic acid methacrylate (HA-MA), and to a lesser extent chondroitin sulfate methacrylate (CS-MA), chondrogenesis and mechanical properties can be enhanced. The addition of HA-MA to Gel-MA constructs resulted in more rounded cell morphologies, enhanced chondrogenesis as assessed by gene expression and immunofluorescence, and increased quantity and distribution of the newly synthesised ECM throughout the construct. Consequently, while the compressive moduli of control Gel-MA constructs increased by 26 kPa after 8 weeks culture, constructs with HA-MA and CS-MA increased by 96 kPa. The enhanced chondrogenic differentiation, distribution of ECM, and improved mechanical properties make these materials potential candidates for cartilage tissue engineering applications.

**Keywords:** cartilage tissue engineering; hydrogels; photopolymerisation; gelatin; hyaluronic acid

## 5.1 Introduction

Articular cartilage is a collagen- and proteoglycan-rich tissue. More specifically though, collagen type II accounts for over 90% of total collagen in the mature tissue [178], and together with proteoglycans, the large quantity of collagen type II provides the tissue with the mechanical properties required to absorb impacts and withstand significant loads. In the superficial zone of cartilage, lubricating molecules such as proteoglycan 4 (PRG4) allow for low-friction movement in articulating joints. However, cartilage is frequently damaged through trauma or disease, and has little to no capacity for self-repair. Without intervention, damaged cartilage continues to degenerate to the point where pain and impaired mobility result, and a joint replacement is typically required. Cartilage tissue engineering is a promising approach to repair damaged cartilage, thereby alleviating the prolonged degeneration and ultimate joint replacement, and to this end, regenerative medicine approaches for cartilage repair have been widely studied and tested for over two decades [50, 179].

One of the major limitations of regenerative cartilage therapies has been the inability to regenerate tissue with the original composition and structure of articular cartilage. In approximately 50% of cases, the repair tissue from autologous chondrocyte implantation (ACI) [50] resembles fibrocartilage and is rich in collagen type I, instead of collagen type II [180, 181]. This is most likely due to chondrocyte dedifferentiation during expansion in two-dimensional cultures. Consequently, the repair tissue often lacks the biomechanical properties required to persist in a loaded joint. These inconsistent ACI results have prevented ACI procedures from becoming the routine first line of treatment for cartilage defects [180]. Thus, for cartilage tissue engineering to be ultimately successful, it will be critical to control the phenotype of chondrocytes, and the composition and organisation of the extracellular matrix (ECM) they produce [117]. The design of biomaterials to promote chondrogenic differentiation and guide cartilage ECM synthesis is a key approach to improve cartilage tissue engineering outcomes, and has attracted significant research interest in the past decade [118, 182-184]. Various materials have also been tested in next-generation ACI procedures, in which cells are seeded onto biomaterials prior to implantation [185]. Gelatin-methacrylamide (Gel-MA) hydrogels have attracted attention for tissue engineering applications in recent years [66]; however, their potential for application in cartilage tissue engineering has not been widely investigated.

Gelatin is produced by the hydrolysis of ECM-derived collagens, predominantly collagen type I. Gel-MA can be produced by chemical modification of gelatin,

allowing hydrogels to be covalently crosslinked in the presence of a photoinitiator and light [52]. During hydrolysis and chemical modification, some conformational structures are irreversibly altered, but Gel-MA hydrogels retain some properties of collagens and gelatin, such as cell adhesion domains [66], thermosensitivity [52] and enzymatic degradability [153]. Gel-MA hydrogels are gaining popularity as biomaterials, since they support the formation of new ECM, are enzymatically degradable, can be produced at low cost, are potentially injectable or printable, are easily crosslinked under physiological conditions, and show potential for cartilage tissue engineering [123].

In this study, we aimed to enhance chondrocyte behaviour in Gel-MA-based hydrogels by incorporating glycosaminoglycans (GAGs) into the hydrogels. Two of the most abundant GAGs in cartilage are hyaluronic acid (HA) and chondroitin sulfate (CS), and we incorporated these into Gel-MA hydrogels separately or together. We used methacrylated HA and CS (HA-MA and CS-MA, respectively) to allow covalent and stable incorporation of these GAGs into the Gel-MA hydrogels. Table 5.1 shows the composition and notation used for the hydrogel groups tested in this study.

## **5.2 Materials and Methods**

### **5.2.1 Macromer Synthesis**

Gelatin (porcine skin, type A), chondroitin sulfate A and methacrylic anhydride (MAAh) were purchased from Sigma Alrich (St Louis, MO, USA). Hyaluronic acid (molecular weight 0.86 MDa) was generously provided by Novozymes. Gel-MA, HA-MA and CS-MA were synthesised by reaction of gelatin, HA and CS, respectively, with MAAh, using protocols based on published methods [52, 56]. Briefly, gelatin, HA and CS were dissolved in phosphate-buffered saline (PBS, Invitrogen, Carlsbad, CA, USA) at 10%, 1% and 25% w/v, respectively. Gelatin was reacted with 0.6 g of MAAh per gram of gelatin for 1 h at 50 °C [52]. CS and HA were reacted with MAAh for 24 h on ice, with the pH regularly adjusted to 8 with 5 M sodium hydroxide [56, 186]. For HA and CS the molar excess of MAAh over the hydroxyl groups was 5- and 10-fold, respectively. After the reaction period, insoluble MAAh was removed by centrifugation, followed by dialysis against deionised water to remove remaining unreacted MAAh and methacrylic acid. The pH of the dialysed polymer solutions was adjusted to 7.4, after which they were freeze-dried and stored at -20 °C.



**Table 5.1: Composition and notation of hydrogels tested in this study.**

<b>Hydrogel Notation</b>	<b>Composition (% wt/vol)</b>
Gel-MA	10% Gel-MA
G-HA	9.5% Gel-MA, 0.5% HA-MA
G-CS	9.5% Gel-MA, 0.5% CS-MA
G-HA-CS	9% Gel-MA, 0.5% HA-MA, 0.5% CS-MA

### 5.2.2 Cell Isolation and Expansion

The procedure for isolating zonal chondrocytes from cartilage has been described in detail elsewhere [187]. Briefly, zonal cartilage samples were excised from the macroscopically normal regions of the femoral condyle of a patient undergoing knee replacement surgery, with consent and ethics approval from the Prince Charles Hospital and Queensland University of Technology [187]. Chondrocytes were expanded in low-glucose Dulbecco's Modified Eagle's Medium (DMEM) with 2 mM glutamax (Invitrogen), supplemented with 10% fetal bovine serum (Lonza, Waverly Australia), 10 mM 4-(2-hydroxyethyl)-1-piperazineethanesulfonic acid (HEPES), 0.1 mM non-essential amino acids, 0.5 µg/mL amphotericin B (Fungizone®), 50 U/mL penicillin G sodium, 50 µg/mL streptomycin (all Invitrogen), 0.4 mM L-proline and 0.1 mM ascorbic acid (both Sigma).

### 5.2.3 Cell Encapsulation and Culture

All hydrogel precursor solutions were prepared in PBS, and contained 0.05% (w/v) of the photoinitiator Irgacure 2959 (BASF, Ludwigshafen, Germany). Passage 1 chondrocytes were suspended in one of the four precursor solutions (Table 5.1) at a density of 7 million cells/mL. Hydrogels were crosslinked by 15 min exposure to 365 nm light at an intensity of 2.6 mW/ cm<sup>2</sup> in a CL-1000 crosslinker (UVP, Upland, CA, USA). The hydrogels were formed in a custom-manufactured Teflon mold covered by a glass slide, which produces gels with dimensions of 4 × 4 × 2 mm. The cell-hydrogel constructs were cultured for up to 8 weeks in defined chondrogenic differentiation media (high-glucose DMEM with 2 mM glutamax (Invitrogen), 10 mM HEPES, 0.1 mM non-essential amino acids, ITS-G (100× dilution), 0.5 µg/mL amphotericin B (Fungizone®), 50 U/mL penicillin G sodium, 50 µg/mL streptomycin (all Invitrogen), 1.25 mg/mL bovine serum albumin (BSA), 0.4 mM L-proline, 0.1 mM ascorbic acid, 0.1 µM dexamethasone (all Sigma) and 10 ng/mL TGF-β3 (GroPep, Adelaide, SA, Australia)). Cell-free hydrogels were cultured in high-glucose DMEM with 1.25 mg/mL BSA, 0.5 µg/mL amphotericin B, 50 U/mL penicillin G sodium and 50 µg/mL streptomycin.

### 5.2.4 Viability Assay

Live and dead cells were visualised with fluorescein diacetate (FDA) and propidium iodide (PI, both Sigma), respectively, at day 1, week 5 and week 8. Hydrogel constructs were washed in PBS, incubated in a solution of 10 µg/mL FDA and 5 µg/mL PI for 5 min at 37 °C, then washed twice in PBS. Images were captured using a Nikon Eclipse fluorescence microscope.

### 5.2.5 Biochemical Analyses

At each media change, the amount of GAGs secreted from cell-free and cell-laden constructs into the culture media was measured using the dimethyl-methylene blue (DMMB) assay (pH 1.5) [125]. Absorbances at 525 and 595 nm were measured, and the concentrations were calculated using the ratio of absorbances, compared to a quadratic standard curve prepared from chondroitin sulfate C (Sigma). Data from the first media change were excluded to allow for diffusion of unbound CS-MA from some gel groups. To quantify the retained GAGs and DNA, cultured constructs were weighed, frozen and freeze-dried. Dried constructs were digested overnight in 1 mg/mL hyaluronidase (Sigma) at 37 °C, followed by overnight digestion with 0.5 mg/mL proteinase K (Invitrogen) at 56 °C. GAG concentration in the digests was measured in the same way as media. For both GAGs secreted and retained, amounts from cell-free gels were subtracted from amounts from cell-laden constructs to determine the amount of GAGs produced by the cells. DNA concentration in the digests was measured using the Quant-iT™ PicoGreen® dsDNA quantification assay (Invitrogen).

### 5.2.6 Physical Properties

The compressive moduli of constructs were measured in an unconfined arrangement using an Instron 5848 microtester with a 5 N load cell. During testing constructs were submerged in PBS at 37 °C. A displacement rate of 0.01 mm/s was applied using a non-porous indenter, and the modulus taken from the linear region of the stress–strain curve from 10 to 15% strain [123].

### 5.2.7 Immunofluorescence

Constructs cultured for 8 weeks were frozen in Optimal Cutting Temperature compound (OCT, Sakura, Finetek, Tokyo, Japan) and sectioned. Sections were fixed by 10 minutes contact with ice-cold acetone, followed by antigen retrieval with 0.1% hyaluronidase (Sigma) for 30 min. Sections were blocked with 2% BSA in PBS for 1 h. Primary antibodies were diluted in 2% BSA in PBS, and applied overnight at 4 °C. Antibodies for collagen type II (II-II6B3,

Developmental Studies Hybridoma Bank (DSHB), Iowa City, IA, USA, 1:200 dilution), collagen type I (I-8H5, MP Biomedicals, Seven Hills, Australia, 1:300 dilution), aggrecan (MA75A95, Abcam/Sapphire Bioscience, Waterloo, Australia, 1:5 dilution) and CD44 (H4C4, DSHB, 1:200 dilution) were used. Cell membranes were visualised with CellMask<sup>TM</sup> Orange plasma membrane stain (Invitrogen, 1:400 dilution). A mouse IgG isotype control antibody (Jackson ImmunoResearch, West Grove, PA, USA, 1:1000 dilution) and secondary antibody only were used as negative controls. Sections were washed twice for 5 min in PBS. The goat anti-mouse secondary antibody (Alexa Fluor® 488, Invitrogen, 1:400 dilution) was diluted in 2% BSA in PBS containing 5 µg/mL 4',6-diamidino-2-phenylindole (DAPI, Invitrogen), and applied in the dark for 1 h. After rinsing and drying, sections were mounted with Prolong Gold (Invitrogen) and imaged using a Zeiss Axio microscope.

To quantify fluorescence intensities in the inter-territorial areas (minimum distance of 50 µm from cell nuclei), five regions (each 50 × 50 pixels) were selected from each of four different histological sections. The mean grey scale intensity of each region was calculated using ImageJ software (National Institutes of Health, USA). The circularity of cells was quantified by tracing only well defined cell membranes (n > 30) shown in CD44 immunofluorescence images using ImageJ.

### 5.2.8 Gene Expression

Total RNA was isolated from freshly trypsinised cells and from hydrogel constructs that were cultured for 5 weeks. Cells or hydrogel constructs were homogenised in 1 mL of TRIzol reagent (Invitrogen), and RNA was isolated according to the manufacturer's instructions. SuperScript<sup>TM</sup> III First Strand Synthesis System (Invitrogen) was used to synthesise complementary DNA (cDNA). DNase and RNase digestions were performed before and after cDNA synthesis, respectively. Real-time polymerase chain reaction (PCR) was performed using SybrGreen<sup>®</sup> Mastermix (Applied Biosystems/Invitrogen). Expression of all genes was normalised to the housekeeping gene RPL13A [126]. The primer sequences (5' → 3') used for PCR were as follows:

RPL13A: F: CATAGGAAGCTGGGAGCAAG,

R: GCCCTCCAATCAGTCTTCTG;

COL2A1: F: GGCAATAGCAGGTTACGTACA,

R: CGATAACAGTCTTGCCCCACTT;

COL1A1: F: CAGCCGCTTCACCTACAGC,

R: TTTTGTATTCAATCACTGTCTTGCC;

COL10A1: F: ACCCAACACCAAGACACAGTT-CT,

R: TCTTACTGCTATACCTTTACTCTTTATGGTGTA;  
ACAN: F: GCCTGCGCTCC-AATGACT,  
R: TAATGGAACACGATGCCTTTCA;  
PRG4: F: GAGTACCCAATCAAGG-CATTATCA,  
R: TCCATCTACTGGCTTACCATTGC;  
matrix metalloproteinase (MMP) 13:F: ACTTCACGATGGCATTGCTG,  
R: CATAATTGGCCCAGGAGGA [188].

### **5.2.9 EPIC- $\mu$ CT**

The distribution of fixed negative charges in the constructs was visualised using equilibrium partitioning of an ionic contrast agent microcomputed tomography (EPIC- $\mu$ CT) [128]. Constructs were incubated in a mixture of 40% (v/v) ioxaglate (Hexabrix, Aspen, Australia) in PBS at 37 °C overnight on a moving plate. Constructs were imaged in a  $\mu$ CT 40 scanner (Scanco Medical, Brüttsellen, Switzerland) at 45 kV and analysed using Scanco  $\mu$ CT software.

### **5.2.10 Macromer Synthesis**

Statistical analyses were performed using SPSS software (version 20, IBM Corporation, USA). Differences between groups were determined using analysis of variance and Tukey's or Dunnet's T3 post-hoc tests as appropriate, with a significance level of 0.05. Statistically significant differences are indicated in figures using Roman numerals or symbols. Any two groups labelled with the same Roman numeral are statistically similar, and groups without a like numeral are statistically different.

## **5.3 Results**

Chondrocytes from the superficial and middle/deep zones responded to the different hydrogels in a similar manner. Thus, data from experiments using chondrocytes from the middle/deep zone, which represents the bulk of the cartilage volume, are presented here.

### **5.3.1 Cell Numbers, Viability and Morphology**

High cell viabilities (80–90%) were observed in all constructs after 1 day, 5 weeks and 8 weeks of culture, with no differences between groups. Images of live and dead chondrocytes after 8 weeks culture are shown in Figure 5.1A–D. The DNA content in all groups increased between day 1 and week 8 (Figure 5.1I, all  $p < 0.05$ ), although relatively modestly, with less than 2-fold increases in each group.

The cell membrane receptor CD44 was stained with an antibody to visualise the morphology of the encapsulated cells after 8 weeks culture (Figure 5.1E-H), and the average circularity values of at least 30 cells per condition are shown in Figure 5.1J. In Gel-MA and G-CS constructs, cell morphologies varied between irregular, stretched morphologies and rounded morphologies (Figure 5.1E, G). In gels containing HA-MA, cells had more rounded morphologies (Figure 5.1F, H), and the average circularity was higher in these constructs (Figure 5.1J). Similarly, the viability images in Figure 5.1 show that cells had more rounded morphologies with HA-MA. Although HA-MA influenced the morphology of encapsulated cells, all cells at the surface of all constructs had highly stretched morphologies, as shown by membrane staining (Fig. S5.1).

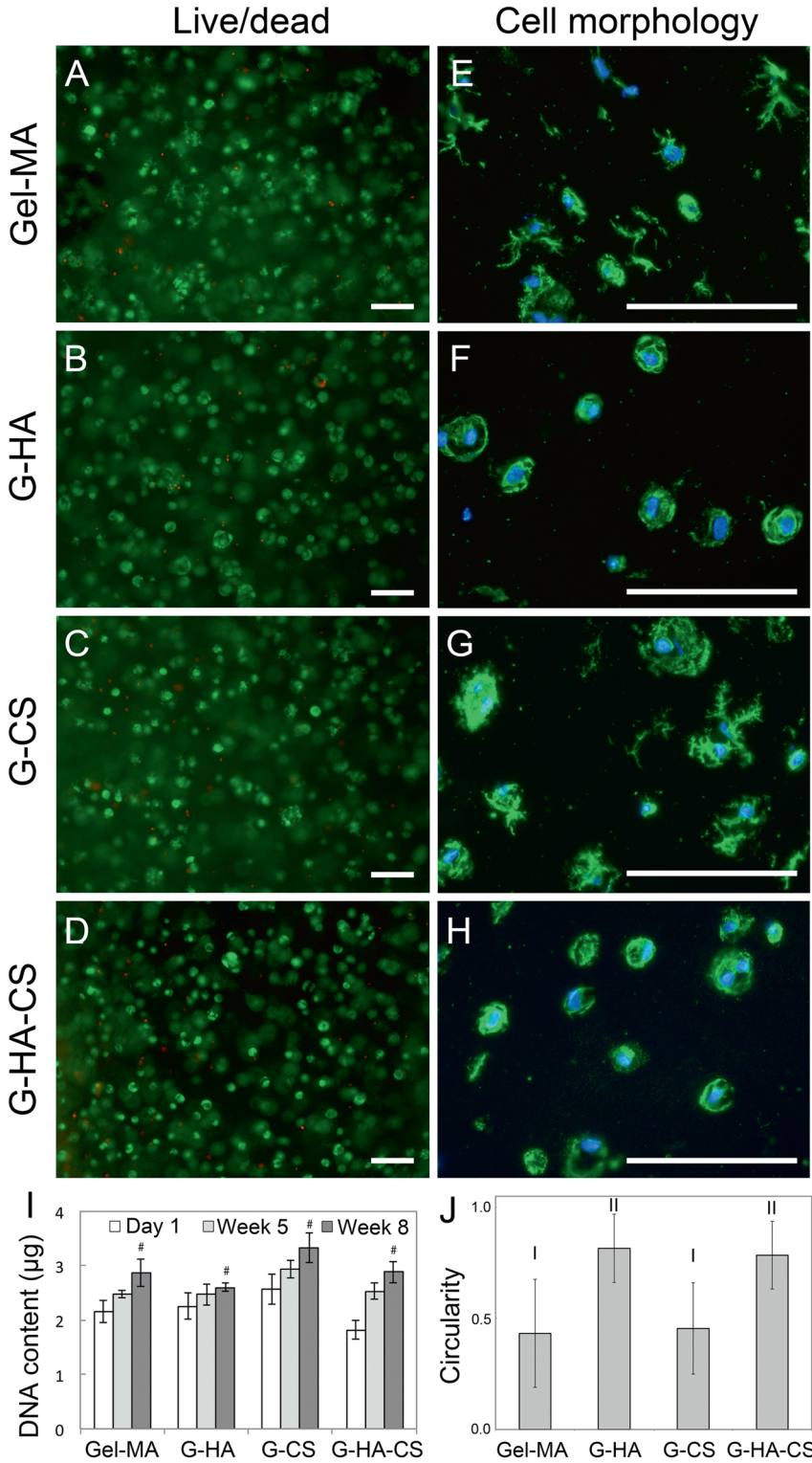


**Figure 5.1 (previous page): Viability (A–D) and morphology (E–H) of chondrocytes cultured for 8 weeks.** Total DNA content (I) after 1 day, 5 weeks and 8 weeks culture, and circularity of cells after 8 weeks culture (J). In live/dead images, living cells appear green and dead cells appear red. In cell morphology images, immunoreactive regions to the membrane receptor CD44 are shown in green, and nuclei were counterstained with DAPI, shown in blue. Scale bars: 100  $\mu$ m. For DNA quantification, bars and error bars show the mean and standard deviation of four samples, and # indicates that within each group, DNA content is different to the value at day 1 ( $p < 0.05$ ). In (J), groups without a like Roman numeral are statistically different ( $p < 0.05$ ).

### 5.3.2 Matrix Production and Accumulation

Gel-MA-based hydrogels supported the deposition of new matrix by chondrocytes; however, the composition and distribution of the cell-secreted matrix varied between hydrogels. Strong collagen type II and aggrecan immunoreactivity was observed in all gel constructs; however, in Gel-MA and G-CS constructs, strong staining was only observed in the regions close to cells, with very little immunoreactivity in the regions between cells (Figure 5.2A, C, E, G). In gels containing HA-MA, collagen type II and aggrecan were more homogeneously distributed (Figure 5.2B, D, F, H). The average fluorescence intensities of collagen type II and aggrecan in the inter-territorial regions were higher in constructs with HA-MA than those without (Figure 5.2M, N). In Gel-MA and G-CS constructs, collagen type I antibodies reacted strongly (Figure 5.2I, K). The intensity of collagen type I staining was markedly lower in gels with HA-MA (Figure 5.2J, L), and the intensity in the inter-territorial regions was also lower with HA-MA (Figure 5.2O). In sections treated with only the secondary antibody, the fluorescence intensities of inter-territorial regions were similar for all hydrogel formulations (data not shown). In addition, in constructs with HA-MA, inter-territorial intensities were higher for collagen type II and aggrecan, yet were lower for collagen type I, allowing us to conclude that differences were due to differential binding of the primary antibodies, rather than background or non-specific interactions. In all constructs, collagen type I staining was strong at the outer surface (Fig. S5.1).

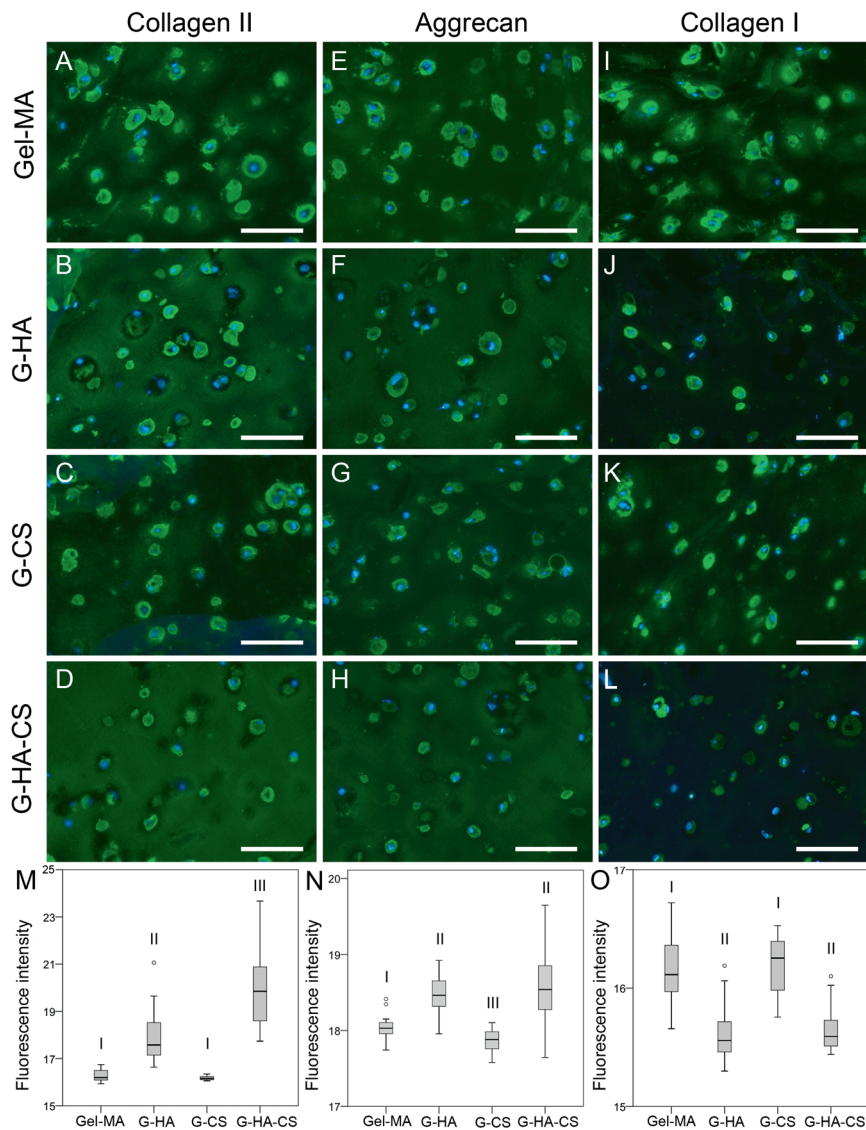


**Figure 5.2: Extracellular matrix production after 8 weeks culture.** Immunoreactive regions for collagen type II (A–D), aggrecan (E–H) and collagen type I (I–L) appear green, and nuclei were counterstained with DAPI (blue). The fluorescence intensities in the regions between cells (inter-territorial regions) were quantified for collagen type II (M), aggrecan (N) and collagen type I (O). Scale bars: 100  $\mu\text{m}$ . Box plots show data from a total of 20 regions from four different histological sections. Groups without a common Roman numeral are statistically different ( $p < 0.05$ ).



### 5.3.3 GAG Production

Figure 5.3 shows GAG production after 8 weeks culture, with all values corrected using cell-free gels. GAG content prior to correction with cell-free gels is shown in Figure S5.2, and GAG secretion profiles are shown in Figure S5.3. The amount of GAGs retained and secreted (both normalised to wet weight) was higher in G-HA constructs compared to Gel-MA (Figure 5.3A). The fraction of the total GAGs that were retained was 60-70% in all constructs, and was not influenced by the presence of HA-MA or CS-MA. When normalised to DNA content, the amount of GAGs retained was also higher in G-HA constructs compared to Gel-MA (Figure 5.3B).

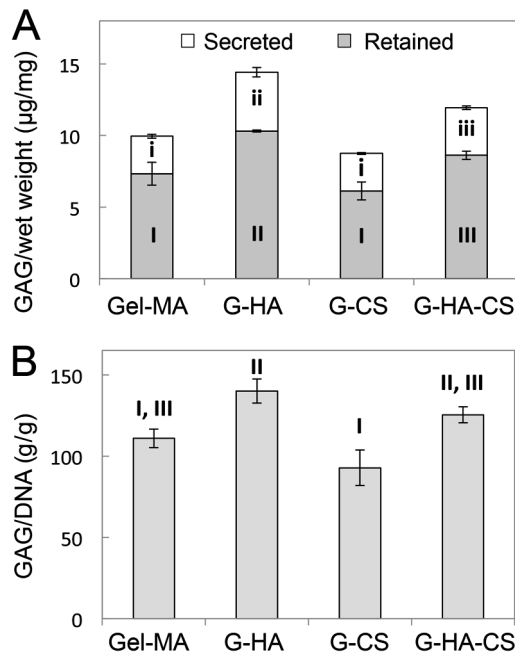


**Figure 5.3: GAG synthesis in hydrogel constructs after 8 weeks culture, with all values corrected using cell-free gels.** Total GAG production (A) after 8 weeks, shown as GAGs retained in the construct or GAGs secreted into the media. The GAGs retained in the constructs were normalised to the DNA content (B) after 8 weeks culture. Bars and error bars show the means and standard deviations of four samples, respectively. Groups without a common Roman numeral are statistically different ( $p < 0.05$ ). In (A), lower- and uppercase letters are used for GAGs secreted and retained, respectively.

### 5.3.4 EPIC- $\mu$ CT

Cell-free and chondrocyte-laden constructs were scanned using EPIC- $\mu$ CT [25] after 2, 5 and 8 weeks culture, using the negatively charged contrast agent ioxaglate. The intensity of the ioxaglate signal is inversely proportional to the concentration of groups with a fixed negative charge in the constructs. Figure 5.4 shows the scans of Gel-MA and G-HA constructs with middle/deep cells at 2, 5 and 8 weeks, and cell-free constructs at 2 weeks (images from all groups and time points are shown in Figures S5.5–S5.7). Attenuation levels in cell-free Gel-MA constructs are higher than in G-HA constructs (Figure 5.4A, E), due to the repulsion of ioxaglate by the negative charges of HA-MA. With increasing culture time, the difference in attenuation levels between Gel-MA and G-HA constructs becomes more pronounced, as a result of enhanced GAG synthesis and deposition in G-HA constructs. Thus EPIC- $\mu$ CT is a viable tool to visualise differences in fixed negative charges between different cell-free hydrogels, and matrix accumulation in tissue-engineered constructs.

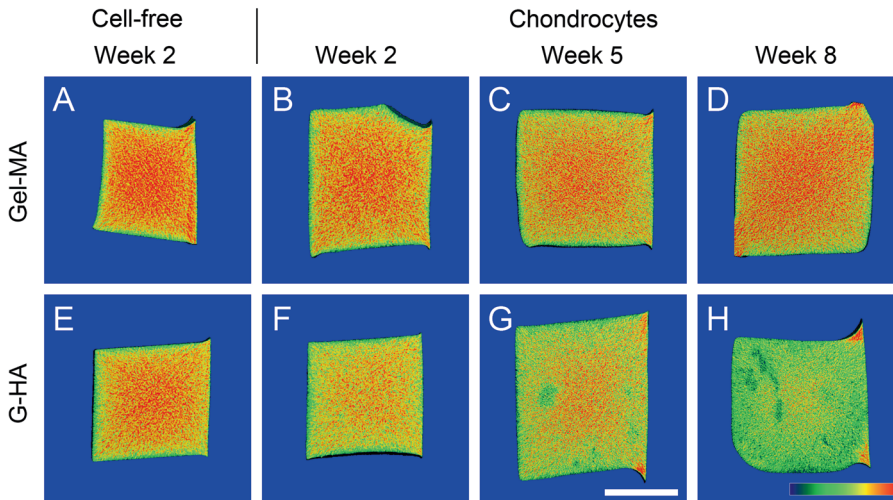


**Figure 5.4: EPIC- $\mu$ CT scans of cell-free hydrogel constructs (A, E) or cell-laden constructs (B–D, F–H).** Constructs were scanned after 2 weeks (A, B, E, F), 5 weeks (C, G) or 8 weeks culture (D, H). Constructs were Gel-MA (A–D) or G-HA (E–H). The scale bar in G is 2 mm and the scale is the same for all panels. The attenuation scale in (H) ranges from 10,000 (blue) to 22,000 (red), and applies to all panels. Figures S5.5–S5.7 show the images for all constructs at the time points evaluated.

### 5.3.5 Gene Expression

The expression levels of chondrogenic marker genes were highly dependent on the hydrogel composition, with greater chondrogenesis occurring in constructs containing HA-MA (Figure 5.5). COL2A1 expression was 9-fold higher in G-HA constructs compared to Gel-MA (Figure 5.5A). Addition of CS-MA to Gel-MA had a smaller (3-fold increase), but significant effect on COL2A1 expression. ACAN expression was upregulated by the addition of either HA-MA or CS-MA, or both, compared to Gel-MA alone (Figure 5.5B), while COL1A1, a dedifferentiation marker, was expressed at lower levels in gels with HA-MA (Figure 5.5C). Expression of the superficial zone marker PRG4 was higher in gels containing HA-MA (Figure 5.5D). PRG4 expression in G-CS gels was intermediate, and statistically similar to both the Gel-MA controls and constructs containing HA-MA. The addition of HA-MA, CS-MA or both lowered the expression of COL10A1 compared to Gel-MA controls (Figure 5.5E). Expression of the hypertrophy marker MMP13 was lower in gels containing HA-MA, and expression in these gels was unchanged from day 0 (Figure 5.5F). CS-MA had no influence of MMP13 expression compared to Gel-MA controls, and expression was upregulated in these groups compared to day 0.

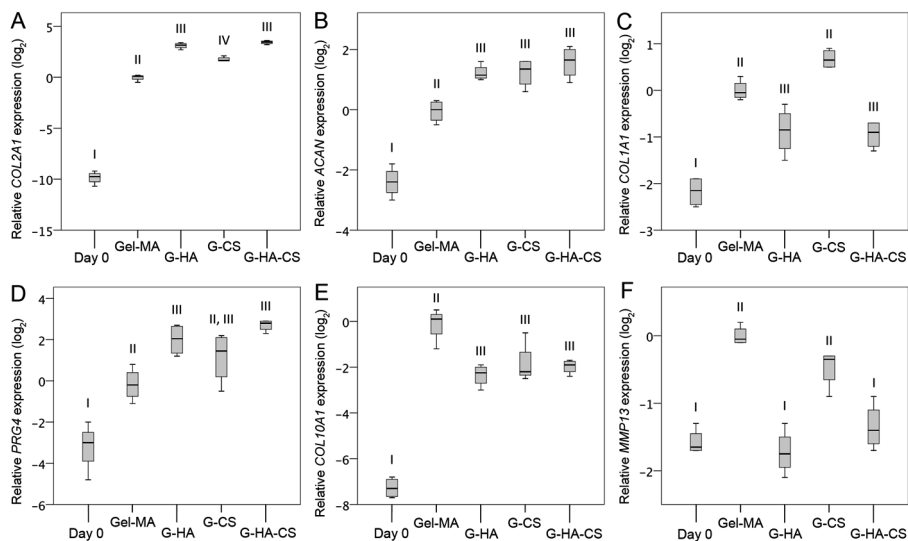


**Figure 5.5: Relative expression levels of collagen type II (A), aggrecan (B), collagen type I (C), PRG4 (D), collagen type 10 (E) and MMP13 (F) at day 0 and after 5 weeks culture.** Expression of each gene was normalised to the Gel-MA control, and presented on a log<sub>2</sub> scale. Box plots show data from four samples, and groups without a common Roman numeral are statistically different ( $p < 0.05$ ).

### 5.3.6 Physical Properties

Gel-MA hydrogels are sensitive to MMP degradation, yet significant gel degradation was not observed in either the cell-free or cell-laden constructs. Hydrogel constructs were easy to handle at each time point, and swelling after crosslinking was negligible.

The addition of HA-MA increased the stiffness of cell-free gels, and cell-laden gels on day 1 by ~10–15 kPa, while the addition of CS-MA had no effect on day 1 (Figure 5.6A, B). However, HA-MA had a much greater impact on the change in stiffness of cell-laden hydrogels after 8 weeks culture (Figure 5.6A, B). After 8 weeks culture, the moduli of Gel-MA constructs increased by 26 kPa, whereas G-HA constructs increased by 96 kPa (Figure 5.6B). The addition of CS-MA had a smaller, but significant effect on stiffness, with G-CS constructs increasing by 47 kPa. The largest change in the stiffness was seen in G-HA-CS constructs, which increased by 114 kPa during 8 weeks culture.

HA-MA also had an impact on the changes in the wet weights and swelling ratios of constructs during culture (Figure 5.6C, D; Figure S5.4). The increase in the wet weights of G-HA and G-HA-CS were lower than those of Gel-MA and

G-CS constructs. Similarly, during culture, the swelling ratio of Gel-MA constructs increased by more than G-HA and G-HA-CS constructs, while the increase in swelling ratio of G-CS constructs was similar to Gel-MA. Thus after 8 weeks, Gel-MA and G-CS constructs tended to be softer and more highly swollen than those containing HA-MA.

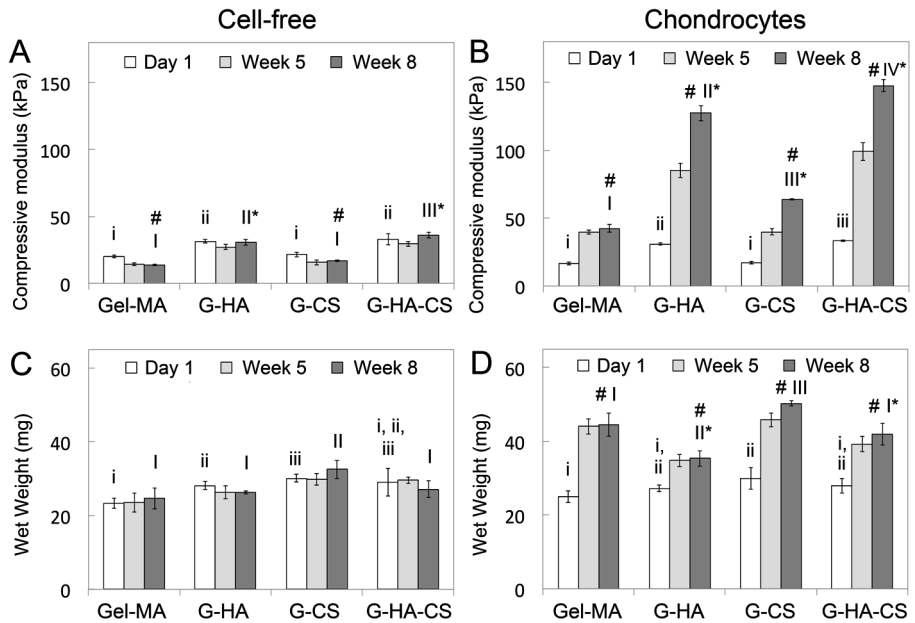


**Figure 5.6: Compressive moduli (A, B) and wet weights (C, D) of cell-free hydrogels (A, C) and cell-laden hydrogel constructs (B, D).** Compressive moduli and wet weights are shown after 1 day, 5 weeks and 8 weeks of culture. Bars and error bars show the mean and standard deviation of four samples, respectively. At day 1 and week 8, statistically significant differences between the hydrogel groups are indicated by different Roman numerals, using lower and upper case, respectively. At week 8, # indicates a significant difference from day 1, while \* indicates that the change during culture is significantly different to the change in the corresponding Gel-MA constructs.

## 5.4 Discussion

HA and CS are abundant GAGs in cartilage ECM, and they have been incorporated into hydrogels and scaffolds with the intention of creating a biomimetic environment to enhance chondrogenesis [54]. However, there is no clear consensus on the effect that incorporation of GAGs in hydrogels has on chondrogenic differentiation and matrix production. Gel-MA, derived from collagen type I, was the main component in each of the hydrogels used in this study, accounting for at least 90% of the polymer content by mass. This study shows that, when used alone, Gel-MA does not support complete chondrogenesis *in vitro*. However with the addition of small quantities of HA-MA, and to a lesser extent CS-MA, Gel-MA-based hydrogels can provide a supportive environment for the deposition of cartilage-like extracellular matrix.

HA is implicated in a vast number of biological processes, including cell proliferation, attachment, migration, differentiation, and tissue homeostasis [18, 189]. The influence of HA on chondrogenesis appears to be dose or concentration dependent, with several studies showing that low concentrations of HA promote chondrogenesis, while higher concentrations have no effect or even inhibit chondrogenesis [101, 174-176]. Despite these complications, HA incorporation into hydrogels has promoted chondrogenesis in several promising studies [190-192], and it remains a key material in cartilage tissue engineering research and clinical application. In this study, gene expression, protein deposition and cell morphology collectively demonstrated that HA-MA significantly enhanced chondrogenesis in the predominantly Gel-MA hydrogels tested. The benefits of HA-MA were exhibited in three ways: promoting the chondrocyte phenotype; increasing matrix accumulation; and enhancing matrix distribution.

Chondrocytes are highly differentiated cells with a distinct phenotype and cell morphology. The rounded morphology observed in healthy cartilage appears to be intrinsically linked to cell phenotype [53]. When placed on two-dimensional surfaces coated with ECM molecules, sub-populations of rounded and spread cells can be observed [193]. While rounded cells continue producing predominantly collagen type II, spread cells produce collagen type I and fibronectin [193], suggesting that reacquiring a rounded morphology may be essential for redifferentiation.

HA has been shown to play a critical role in cell attachment to the surrounding matrix [189, 194, 195]. During mitosis and cell migration, cells secrete a thin layer of an HA-rich matrix that mediates detachment and cell rounding [195]. In

cartilage, CD44 cell receptors bind HA, which results in the chondrocytes being surrounded by a gel-like layer [196]. Removing this layer rapidly alters the homeostasis of the tissue [196], indicating that HA is critical for regulation of biosynthesis and MMP production. In this study, inclusion of HA-MA supported rounded cell morphologies, and cell morphology correlated well with other measures of chondrogenic differentiation. We hypothesise that the enhanced chondrocyte morphology in constructs containing HA-MA may be the result of an intrinsic mixing incompatibility between the two polymers. Mixtures of gelatin and HA are cloudy, and, if left to settle in a solution state, eventually phase separate. The phase separation phenomenon may make cell adhesion sites on gelatin less available to cells, resulting in the rounded morphologies.

In G-HA constructs, the main chondrogenic marker, COL2A1, was upregulated 9-fold, whereas the main dedifferentiation marker, COL1A1, was down-regulated compared to Gel-MA constructs. While collagen type I staining was markedly reduced in constructs containing HA-MA, two cell subpopulations with different phenotypes were observed. Encapsulated cells had a predominantly rounded morphology and produced only low amounts of collagen type I, while cells at the surface had a fibroblast-like morphology, and secreted high levels of collagen type I. Fibroblastic morphologies and high levels of collagen type I were observed at the surface of all constructs, regardless of hydrogel composition (not shown). Thus at the surface, which is effectively a curved two-dimensional environment, chondrocytes adopt a dedifferentiated phenotype and produce collagen type I, as they do when cultured on tissue culture plastic [116]. This *in vitro* result is particularly relevant when compared to some current clinical practices, such as matrix-induced autologous chondrocyte implantation (MACI<sup>®</sup>), in which chondrocytes are seeded onto a collagen scaffold [197]. These cells attach to the scaffold, thus effectively being at a surface, rather than encapsulated in a three-dimensional environment. This may partly account for the limited success of cartilage tissue engineering attempts to date, in which predominantly fibrous cartilage, rather than the desired articular cartilage, is regenerated in the joint.

Incorporation of HA-MA resulted in increased accumulation of cartilage matrix molecules and increased compressive modulus. In addition to higher expression of cartilage-specific genes COL2A1 and ACAN, total GAG production and the GAG/DNA ratio were higher in constructs with HA-MA, indicating that HA-MA promoted increased biosynthesis of cartilage-specific matrix molecules. HA interacts with components of the ECM, particularly aggrecan and hyaladherins

[198], which may play a role in matrix retention [199], but HA-MA did not appear to impact matrix retention in these gels. Of the total amount of GAGs produced during 8 weeks of culture, 60–70% were retained in all constructs, with no significant effect of HA-MA (or CS-MA) on GAG retention. This may be due to the methacrylate modification of HA-MA, which is further discussed in Chapter 8.

Mechanical properties are a critical metric to assess the quality of tissue-engineered cartilage. Cartilage from bovine femoral condyles has a Young's modulus of approximately 0.3 MPa [200], and by attracting water, GAGs account significantly for the compressive stiffness of the tissue [14]. However, in this study, higher GAG levels did not fully account for changes in mechanical properties. After 8 weeks culture, differences in compressive moduli were much more pronounced than differences in GAG content. For example, the concentration of GAGs in G-HA constructs was 43% higher than in Gel-MA constructs, while, the increase in compressive moduli of G-HA constructs was 270% greater than the increase in Gel-MA constructs.

An explanation for the discrepancy in construct modulus and GAG content may lie in the third beneficial effect of HA-MA: enhancing matrix distribution. In addition to GAGs, the collagen network is also expected to contribute to the stiffness of the constructs, and thus GAG content alone is not always an accurate predictor of mechanical properties. HA-MA enhanced the distribution of collagen type II and aggrecan, shown by the higher levels of these components in the inter-territorial regions of constructs with HA-MA. As a result, the mechanical properties of constructs with HA-MA increased significantly more during culture than those without. The newly synthesised matrix is expected to be more interconnected in constructs with HA-MA, and hence provide greater mechanical reinforcement.

The mechanisms by which HA-MA enhanced the distribution of new matrix and improved the mechanical properties are not clear, but we hypothesise that the microscale phase separation of Gel-MA and HA-MA helped facilitate distribution of the ECM. In Chapter 3, in which hydrogels were prepared from either Gel-MA or HA-MA, we found that collagen type II and aggrecan were highly localised to the pericellular regions of HA-MA, suggesting that HA-MA alone does not facilitate larger-scale matrix distribution [188]. Similarly, other studies have shown that HA-MA hydrogels alone do not necessarily promote matrix distribution, but lower crosslink densities, and hence larger pore sizes, do allow for more matrix diffusion [122]. Further discussion about the potential



microstructure of these hydrogels can be found Section 8.2.

Both the hydrogel biomaterial and the cell-secreted ECM are sensitive to enzymatic degradation [201], so the changes in mechanical properties of the constructs during culture are a result of the balance between anabolic and catabolic factors, combined with hydrolytic degradation. The compressive moduli of all cell-laden constructs increased during culture, whereas cell-free constructs decreased slightly or were unchanged. The increase in stiffness of cell-laden constructs can therefore be attributed to the matrix deposited by the cells, suggesting that in all gels, regardless of composition, there was a net shift in favour of anabolic processes.

Constructs with HA-MA expressed lower levels of MMP13 than those without. MMP13, also called collagenase-3, is a marker of chondrocyte hypertrophy [202, 203], and is up-regulated in osteoarthritis, where it is a key mediator of cartilage degradation [204]. In this study, constructs with elevated MMP13 expression levels were also softer and more swollen; thus cell-mediated degradation of both the gelatin, as well as the newly produced ECM, may be a key factor limiting matrix accumulation and mechanical property development in these constructs. Exposure to collagen types I and II can upregulate MMP13 production via integrins or discoidin domain receptor 2 (DDR2) [205, 206], but exposure to denatured collagens and gelatin do not have the same effect [205]. Thus, although the cause of MMP13 upregulation in Gel-MA and G-CS constructs is unknown, it could be a result of the high levels of collagen type I that are produced in these gels.

The initial mechanical properties of hydrogels are dependent on the crosslink density, and hence pore size, of the hydrogel, and as expected, larger pore sizes facilitate more diffusion of newly secreted matrix [80, 122, 207]. Therefore, hydrogels that are initially the softest can become the stiffest after a period of *in vitro* culture, while hydrogels that are initially very stiff may impede the formation and distribution of new ECM [80, 122]. Interestingly, in this study the opposite trend was observed, with the stiffness increasing more in the gels that were initially stiffer, showing that HA-MA was facilitating matrix organisation by other means. When optimising the initial crosslink density for the purposes of cartilage repair, it is important to consider both the initial and developed mechanical properties, along with the overall strategy for cartilage repair.

The incorporation of CS-MA had fewer and less significant effects on chondrocyte and construct properties than HA-MA. This could be because CS does not participate in cell–matrix interactions to the same extent as HA. It

could also be because mixtures of gelatin and CS-MA are fully miscible, thus if the phase separation phenomenon observed for HA-MA was indeed important, it would be expected that chondrocytes would respond differently to CS-MA and HA-MA. The solubility limit of CS is substantially higher than that of HA, so much higher concentrations of CS-MA could potentially be incorporated into Gel-MA hydrogels. Thus although the effects of CS-MA were comparatively minor at 0.5%, higher concentrations may elicit stronger chondrocyte responses, and further studies should evaluate the concentration-dependent influence of CS-MA.

The incorporation of CS-MA increased COL2A1 and ACAN gene expression compared to Gel-MA controls; however, COL1A1 and MMP13 expression levels were unchanged. Previous studies using polyethylene glycol-based hydrogels have shown CS-MA to have variable effects on bovine chondrocytes. In one study, CS-MA was shown to strongly upregulate the expression of collagen type II and aggrecan [106], while in another study, CS-MA reduced proteoglycan synthesis by bovine chondrocytes by 22–50%, depending on CS-MA concentration [186].

When both HA-MA and CS-MA were included in the hydrogel construct, cells showed a similar response to those in G-HA constructs, indicating that HA-MA was a more potent modulator of differentiation and physical properties than CS-MA. The greatest increase in stiffness was seen in G-HA-CS constructs, suggesting that there may be advantages including both GAGs in the hydrogels.

Mesenchymal precursor cells (MPCs) have been widely investigated as a potential cell source for the repair of cartilage defects. Since G-HA hydrogels promote the chondrogenic redifferentiation of expanded chondrocytes, further studies could evaluate the potential for these hydrogels to be used to guide chondrogenic differentiation of MSCs. In addition, further studies should validate whether the *in vitro* results shown here can be translated to enhanced quality of repair tissue *in vivo*.

## 5.5 Conclusion

This study highlights the potential for multiple-component photocrosslinkable hydrogels based primarily on Gel-MA to be used in cartilage tissue engineering. Encapsulated chondrocytes remain viable for up to 8 weeks in culture, and produce a significant amount of ECM. Incorporation of a relatively small proportion of HA-MA into these hydrogels significantly enhances chondrogenesis and facilitates matrix distribution, with corresponding

improvements to mechanical properties. Incorporation of CS-MA enhances some aspects of chondrocyte redifferentiation, though to a lesser extent than HA-MA.

### **Acknowledgements**

The research leading to these results has received funding from the European Union's Seventh Framework Programme (FP7/2007-2013) under grant agreement no. 309962 (project HydroZONES). In addition, the authors would like to thank the Australian Research Council, the European Union (Marie Curie Fellowship PIOF-GA-2010-272286 to F.P.W.M.), and the Dutch Arthritis Foundation (J.M.) for funding. They are also grateful to Prof. Ross Crawford for obtaining cartilage tissue. The antibodies against collagen type II and CD44 were obtained from the Developmental Studies Hybridoma Bank, which is maintained by the University of Iowa, Department of Biology, Iowa City, IA 52242, USA.



## Chapter 6

# Hyaluronic acid enhances the mechanical properties of tissue-engineered cartilage constructs

---

Peter A. Levett<sup>1,2</sup>, Dietmar W. Hutmacher<sup>1</sup>, Jos Malda<sup>1,2</sup> and Travis J. Klein<sup>1</sup>

PlosOne (2014), DOI: 10.1371/journal.pone.0113216

<sup>1</sup> *Institute of Health and Biomedical Innovation, Queensland University of Technology, 60 Musk Ave, Kelvin Grove, QLD 4059, Australia*

<sup>2</sup> *Department of Orthopaedics, University Medical Center, Utrecht, P.O. Box 85500, 3508 GA, The Netherlands*

## Abstract

There is a need for materials that are well suited for cartilage tissue engineering. Hydrogels have emerged as promising biomaterials for cartilage repair, since, like cartilage, they have a high water content and they allow cells to be encapsulated within the material in a genuinely three-dimensional microenvironment. In this study, we investigated the mechanical properties of tissue-engineered cartilage constructs using *in vitro* culture models incorporating human chondrocytes from osteoarthritis patients. We evaluated hydrogels formed from mixtures of photocrosslinkable gelatin-methacrylamide (Gel-MA) and varying concentrations (0-2%) of hyaluronic acid methacrylate (HA-MA). Initially, only small differences in the stiffness of each hydrogel existed. After 4 weeks of culture, and to a greater extent 8 weeks of culture, HA-MA had striking and concentration dependent impact on the changes in mechanical properties. For example, the initial compressive moduli of cell-laden constructs with 0 and 1% HA-MA were 29 and 41 kPa, respectively. After 8 weeks culture, the moduli of these constructs had increased to 66 and 147 kPa respectively, representing a net improvement of 69 kPa for gels with 1% HA-MA. Similarly the equilibrium modulus, dynamic modulus, failure strength and failure strain were all improved in constructs containing HA-MA. Differences in mechanical properties did not correlate with glycosaminoglycan content, which did not vary greatly between groups, yet there were clear differences in aggrecan intensity and distribution as assessed using immunostaining. Based on the functional development with time in culture using human chondrocytes, mixtures of Gel-MA and HA-MA are promising candidates for cartilage tissue-engineering applications.

**Keywords:** Hydrogels, gelatin, hyaluronic acid, cartilage, tissue engineering

## 6.1 Introduction

Articular cartilage is a load bearing tissue. In articulating joints, cartilage provides low friction surfaces for efficient movement, and effective impact absorption and load dissipation. Unfortunately, cartilage is susceptible to damage, and has a very limited capacity to heal. To address this clinical need, researchers and clinicians have developed methods to potentially regenerate or tissue-engineer new cartilage, but currently there remains a shortage of materials that are well suited for guiding effective regeneration of high quality, hyaline cartilage [54].

The mechanical properties of cartilage are crucial to its ability to withstand the compressive and shear loads to which it is routinely subjected in the joint environment. It has been noted elsewhere that the importance of mechanical properties in tissue-engineered cartilage is often overlooked [129], and has even been suggested that mechanical properties should be viewed as the most important metric for assessing the quality of tissue-engineered cartilage [129]. Studies to identify materials for cartilage tissue engineering commonly characterise the mechanical properties of cell-free scaffolds or hydrogels, but frequently do not examine how the mechanical properties change with time [208]. While the optimal mechanical properties for a cartilage scaffold or tissue engineered cartilage are not known, healthy cartilage is a common reference, which has an equilibrium compressive modulus in the order of 0.1 – 2 MPa, varying significantly with depth from the articular surface [82]. Implanting a construct that has matured for four weeks *in vitro* showed better integration with the surrounding cartilage compared to implanting a freshly crosslinked construct [209], which may be partially a result of the mechanical properties developed over four weeks culture protecting the construct from damage once implanted.

The mechanical properties of tissue-engineered cartilage can be considered in two distinct elements. Firstly, the biomaterial has some inherent mechanical properties, and generally the mechanical properties of the newly formed construct will be derived from these inherent properties. Secondly, over time, the mechanical properties of the construct will change, due to material degradation, production of proteins and assembly of extracellular matrix via the cell machinery, and matrix remodelling.

The first element, the initial mechanical properties, is relatively simply altered by changing the materials used, the way in which they are constructed, or the way in which they are held together. For example, thermoplastic polymers can be used to produce very stiff constructs, which can easily match the stiffness of

articular cartilage [210], but fail to adequately match the low friction properties and shock absorption characteristics. Hydrogels, meanwhile, have been extensively investigated for cartilage repair, but the mechanical properties of these typically soft and highly water-swollen materials have limited their clinical impact. To overcome the limitation of the mechanical properties, strategies to enhance the mechanical properties of hydrogels have been keenly investigated. For example, double network hydrogels have been developed that have excellent compliance, high water content and remarkable failure strengths [83], however the process for producing these gels is not easily adapted for cell encapsulation and the strength is reduced upon repeated loading [211]. Very stiff and strong hydrogels can also be produced from polyvinyl alcohol, and promising short term clinical results have been reported [212], but these materials replace cartilage, rather than regenerate the original tissue. Similarly, polyethylene glycol diacrylate (PEGDA) hydrogels formed from a high concentration (40% w/v) of low molecular weight PEGDA (508 Da) have mechanical properties that are comparable to cartilage [82], but the potential to successfully encapsulate cells in such stiff gels remains uncertain, and exposure to low molecular weight PEG may also limit cell compatibility. Yet another approach has been to combine soft, cell compatible hydrogels with stronger materials, such as thermoplastic polymers [123, 213], to produce constructs in which the hydrogel contributes negligibly to the overall mechanical properties.

In parallel, research efforts have also been directed towards developing materials that allow an increase in the mechanical properties of tissue-engineered constructs with time, usually mediated by the deposition of extracellular matrix from embedded or invading cells. For hydrogels, one common method to allow for greater increases in mechanical properties has been to *lower* the initial stiffness of the gels, usually by lowering the concentration of polymer [80, 122]. The basic principle is that reducing the polymer concentration results in a hydrogel that is not only softer, but also has larger pores, therefore allowing more diffusion of extracellular matrix into and throughout the hydrogel, which ultimately accounts for the bulk of the mechanical strength.

Hyaluronic acid (HA) is a ubiquitous component of extracellular matrices, and performs important functions in cartilage. By binding and immobilising aggrecan, HA mediates the formation of massive aggregates of fixed negative charge that retain water and is a critical extracellular matrix (ECM) component for cartilage mechanical properties. Meanwhile, the collagen network acts to resist this swelling tendency and provides tensile strength. In this study, we



evaluated hydrogels formed from mixtures of photocrosslinkable derivatives of gelatin and HA (gelatin-methacrylamide (Gel-MA) and HA-methacrylate (HA-MA), respectively). In particular, we aimed to investigate in detail the role of HA-MA in the developed mechanical properties of engineered cartilage constructs using chondrocytes from four human patients. Based on our previous studies [214], we hypothesised that HA-MA would significantly enhance the mechanical properties of cultured constructs, and that the influence would be concentration dependent.

## **6.2 Materials and Methods**

### **6.2.1 Study Design**

The main aim of this study was to evaluate the importance of a hyaluronic acid derivative on the impact of developed mechanical properties of tissue-engineered cartilage constructs, and can be considered in two parts. The objective of the first part was to characterise the mechanical properties of cell-free hydrogel constructs after 1 and 28 days in culture, including compressive modulus, swelling ratio, and also the release profile of non-covalently bound HA from Gel-MA hydrogels. The objective of the second part was to encapsulate human chondrocytes in Gel-MA/HA-MA constructs and evaluate the impact of HA-MA on the change in mechanical properties and matrix production. For the cellular experiments, the compressive modulus and swelling ratio were tested on days 1, 28 and 56, and failure strength was measured after 63 days. ECM production was assessed in constructs cultured for 28 days.

### **6.2.2 Macromer Synthesis**

Gelatin and methacrylic anhydride (MAAh) were purchased from Sigma Aldrich (St Louis, MO, USA). Hyaluronic acid was purchased from Novozymes Biopharma (Bagsvaerd, Denmark). Irgacure 2959 was purchased from BASF (Ludwigshafen, Germany). Gelatin-methacrylamide (Gel-MA) and hyaluronic acid methacrylate (HA-MA) were synthesised using protocols based on previous methods [52, 56, 188]. Unless otherwise stated, all concentrations are given as percentage weight per volume (% w/v). Gelatin was dissolved in phosphate buffered saline (PBS, Invitrogen, Carlsbad, CA, USA) at 10% and reacted with 0.6 g MAAh per gram of gelatin for 1 hour at 50 °C under constant stirring. After the reaction period, excess MAAh was removed by centrifugation, and the Gel-MA was exhaustively dialysed against distilled water at 40 °C. The pH of the dialysed Gel-MA solution was adjusted to 7.4, and Gel-MA was recovered by lyophilisation. HA was dissolved in distilled water at 2% and reacted with

MAAh on ice for 8 hours under constant stirring. HA-MA was precipitated in an excess of cold 100% ethanol, redissolved, then exhaustively dialysed against distilled water. The pH of dialysed HA-MA was adjusted to 7.4, and HA-MA was recovered by lyophilisation. Following lyophilisation, HA-MA was washed with acetone and allowed to dry overnight in a biological safety cabinet to ensure sterility. Each polymer was dissolved separately at 10 mg/mL in deuterium oxide (Sigma) and proton nuclear magnetic resonance spectra were recorded on a Mercury 300 MHz instrument (Varian Associates Inc., CA, USA).

### **6.2.3 Ethics Statement**

Ethics approval was granted from the Queensland University of Technology and the Prince Charles Hospital (both Brisbane, Australia).

### **6.2.4 Cell Isolation and Expansion**

Human chondrocytes were isolated and expanded as described in detail elsewhere [187]. Cartilage with a macroscopically normal appearance was excised from the femoral condyles of four osteoarthritis (OA) patients that had undergone knee replacement surgery. The cartilage was diced with a scalpel and digested overnight with 0.15% collagenase type II (Worthington, NJ, USA) in high glucose Dulbecco's modified eagle medium (DMEM, Invitrogen). Chondrocytes from the four patients were kept separate for the entirety of the study, and were expanded in low-glucose DMEM with 2 mM glutamax (Invitrogen), supplemented with 10% fetal bovine serum (Lonza, Waverly Australia), 10 mM 4-(2-hydroxyethyl)-1-piperazineethanesulfonic acid (HEPES), 0.1 mM non-essential amino acids, 0.5 µg/mL amphotericin B (Fungizone), 50 U/mL penicillin G sodium, 50 µg/mL streptomycin (all Invitrogen), 0.4 mM L-proline and 0.1 mM ascorbic acid (both Sigma).

### **6.2.5 Hydrogel Formation**

All hydrogels were crosslinked in a custom made Teflon mould by 15 minutes exposure to 2.6 mW/cm<sup>2</sup> 365 nm light (UVP CL-1000, Upland, CA, USA). All gel precursor solutions had a total polymer concentration of 10% and contained 0.05% of the photoinitiator Irgacure 2959. Passage one chondrocytes were released from monolayer culture by 5 minutes incubation with 0.25% trypsin (Invitrogen). The cells were washed with DMEM containing FBS, then washed a further two times with serum-free DMEM. The cells were counted using a hemocytometer, and encapsulated by combining one millilitre of gel precursor solution with 10<sup>7</sup> cells and photocrosslinking. Initially gels had dimensions of approximately 4 × 4 × 2 mm. Cell-hydrogel constructs were cultured for up to 9

weeks in defined chondrogenic differentiation media (high-glucose DMEM with 2 mM glutamax (Invitrogen), 10 mM HEPES, 0.1 mM nonessential amino acids, ITS-G (100 × dilution), 0.5 µg/mL amphotericin B (Fungizone), 50 U/mL penicillin G sodium, 50 µg/mL streptomycin (all Invitrogen), 1.25 mg/mL bovine serum albumin (BSA), 0.4 mM L-proline, 0.1 mM ascorbic acid, 0.1 µM dexamethasone (all Sigma) and 10 ng/mL TGF-β3 (GroPep, Adelaide, Australia)). Cell-free hydrogels were cultured in high-glucose DMEM with 1.25 mg/mL BSA, 0.5 µg/mL amphotericin B, 50 U/mL penicillin G sodium and 50 µg/mL streptomycin.

### **6.2.6 Viability Analysis**

After 28 days culture, cell-laden hydrogel constructs were halved with a scalpel, incubated in a solution of 10 µg/mL fluorescein diacetate and 5 µg/mL propidium iodide (both Sigma) in PBS for 10 minutes, and imaged using a Zeiss Axio microscope. The cut face of each hydrogel construct was imaged to visualise the cell viability in the centre of the construct.

### **6.2.7 Mechanical Testing**

All hydrogels were tested in an unconfined arrangement between non-porous platens while submerged in PBS at 37 °C, using an Instron 5848 microtester (Instron, Melbourne, Australia). The compressive modulus was determined by compressing gels at 0.01 mm/s, and calculating the slope of the stress-strain curve between 10-15% strain. The cross-sectional area of each gel was calculated from the ratio of wet weight to height. After testing, the gels were lyophilised to determine the dry weight. The (mass) swelling ratio was determined as the ratio of wet weight to dry weight. The following procedure was used to determine the equilibrium modulus, dynamic modulus, failure strength and failure strain for each gel, using a displacement rate of 0.01 mm/s. Gels were compressed to 5% strain, held for 10 minutes, compressed to 10% strain, and held for 10 minutes. Fifty cycles of a sinusoidal waveform with an amplitude of 2% and frequency of 1 Hz was applied, centred about 10% strain. Gels were then compressed to 15% strain, held for 10 minutes, and compressed to 20% strain and held for 10 minutes. The load was released completely, and the gels were compressed until failure using a displacement rate of 0.01 mm/s. For each gel, the equilibrium modulus was determined from the slope of the residual stress-strain curve between 10 and 15% strain. The dynamic modulus was determined as the slope of the stress strain curve between 9 and 11% strain during dynamic compression. The failure force and displacement were taken as the point of a clear discontinuity of the force-displacement curve, from which

failure strength and strain were calculated based on cross-sectional area and height.

### **6.2.8 Immunofluorescence**

Constructs were snap frozen in Optimal Cutting Temperature (OCT) compound (Sakura, Finetek, Tokyo, Japan) and sectioned. Sections were fixed with ice-cold acetone for 10 minutes, and washed in PBS. Antigen retrieval was performed for collagen type II, using 0.1% hyaluronidase (Sigma) for 30 minutes at room temperature. All sections were blocked with 2% bovine serum albumin (BSA, Sigma) in PBS for 1 hour at room temperature. Primary antibodies were diluted in 2% BSA in PBS and applied overnight at 4 °C. Antibodies for aggrecan (969D4D11, Invitrogen, 1:300 dilution), collagen type II (II-II6B3, Developmental Studies Hybridoma Bank (DSHB), Iowa City, IA, USA, 1:200 dilution), CD44 (H4C4, DSHB, 1:200 dilution) and collagen type X (Abcam, polyclonal in rabbit, 1:100 dilution) were used. Slides were washed three times in PBS for 5 minutes each. The goat anti-mouse secondary antibody (Alexa Fluor488, Invitrogen, 1:400 dilution) was diluted in 2% BSA in PBS containing 5 µg/mL 4,6-diamidino-2-phenylindole (DAPI, Invitrogen), and applied in the dark for 1 hour. For collagen type X, the secondary antibody was Cy3 conjugated anti rabbit IgG (Abcam, 1:500 dilution). Slides were washed a further 3 times in PBS for 5 minutes each, and after drying, mounted with Prolong Gold (Invitrogen) and imaged using a Zeiss Axio microscope. Confocal microscopy was used to image the morphology of encapsulated cells and cells at the surface of constructs. Whole constructs were incubated in PBS containing 5 µg/mL DAPI and 0.8 U/mL rhodamine phalloidin for 1 hour then washed three times in PBS. Images were captured on a Leica SP5 laser scanning confocal microscope.

### **6.2.9 Biochemical Analyses**

GAG content was measured quantitatively using the dimethylmethylene blue (DMMB, Sigma) assay and a standard curve of chondroitin-6-sulfate (Sigma) and the ratio of absorbance at 525 nm to 590 nm. For HA/HA-MA retention experiments the assay was performed at pH 3.0, and for cell culture experiments pH 1.5 was used, since unsulfated GAGs bind with DMMB at a pH of 3.0 but not 1.5 [125]. For the retention experiments, cell-free gels were incubated in PBS at 37 °C for up to two weeks. At each time point, four gels were removed from PBS, weighed, and digested with papain (250 µg/mL, Sigma) at 60 °C overnight. GAG content was measured in cell-laden constructs after 1 and 28 days culture. The constructs weighed, lyophilised, weighed again, and digested

with 0.5% hyaluronidase (Sigma) in PBS at 37 °C for 48 hours, followed by digestion with proteinase K (Invitrogen) overnight at 56 °C. DNA content in the digests was measured using the Quant-iT™ PicoGreen® dsDNA assay (Invitrogen).

#### **6.2.10 EPIC- $\mu$ CT**

Equilibrium partitioning of an ionic contrast agent (EPIC) microcomputed tomography ( $\mu$ CT) was used to visualise the concentration and distribution of negative charge, as a measure for proteoglycan content in hydrogel constructs [128, 215]. This technique uses a negatively charged contrast agent to indicate the amount and distribution of fixed negative charge in the hydrogel construct. Since cartilage ECM is negatively charged, gels with a higher amount of ECM, and therefore a higher negative charge, have a lower signal strength of contrast agent. Gels were incubated in a mixture of 40% Ioxaglate (Hexabrix, Aspen, Australia) in PBS at 37 °C overnight with constant mixing, and imaged using a Scanco  $\mu$ CT 40 scanner (Scanco Medical, Brüttisellen, Switzerland).

#### **6.2.11 Statistical Analyses**

All statistical analyses were performed using SPSS v20 (IBM corporation, Armonk), with a statistical significance level of 0.05. Differences between hydrogel groups (0-2% HA-MA) were determined using ANOVA. Tukey's posthoc test was used in instances where the p-value for Levene's test was greater than 0.05, and Tamhane's T2 posthoc test was used where the p-value for Levene's test was less than 0.05. Statistically significant differences from the appropriate posthoc test are indicated in Figures using Roman numerals. Independent samples t-tests were used for comparisons within groups or between days, and statistically significant differences were indicated in figures using the symbols \*, # and †.

### **6.3 Results**

#### **6.3.1 Retention of HA**

When unmodified HA was incorporated into Gel-MA hydrogels, a portion diffuses out of the gels over the first 1-3 days, but some HA is stably incorporated (Figure 6.1). HA-MA content could not be quantified using the DMMB assay after papain digestion, since after digestion of gels containing HA-MA, a soft, yet stable hydrogel remained, most probably a crosslinked network of HA-MA. This nevertheless provides reasonable evidence that HA-

MA is stably incorporated, and in all studies with chondrocytes, HA-MA was therefore, used.

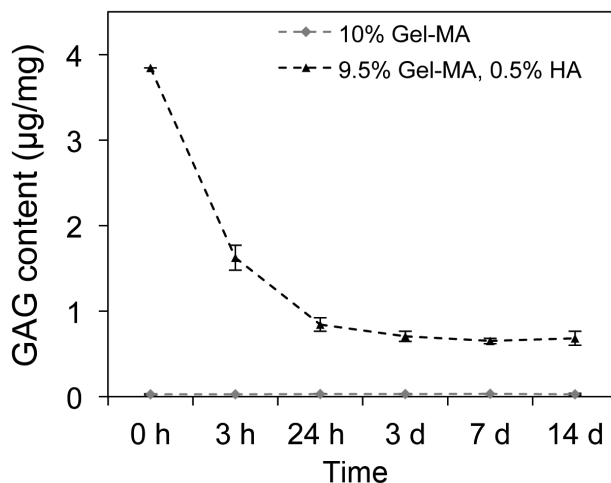


**Figure 6.1: Retention of HA in cell-free Gel-MA hydrogels over 14 days.** HA content per wet weight, determined using a quantitative GAG assay at a number of time points. The retention of HA-MA was not measureable, since the HA-MA appears to become crosslinked, and does not dissolve after proteinase K or papain digestion. Each point represents the mean of four samples, and error bars show standard deviations.

### 6.3.2 Viability and Cell Morphology

Cell viability was not dependent on HA-MA concentration, and was high in all groups after 28 days (Figure 6.2A). The morphologies exhibited by cells in all gels fell into one of two major categories: encapsulated cells displayed a predominantly rounded morphology, while cells at the surface of constructs had highly spread, fibroblastic morphologies (Figure 6.2B, C). Some encapsulated cells showed slight deviations from rounded morphology, with some non-circular actin structures and cell membrane extensions observed, particularly in constructs with 0% HA-MA.

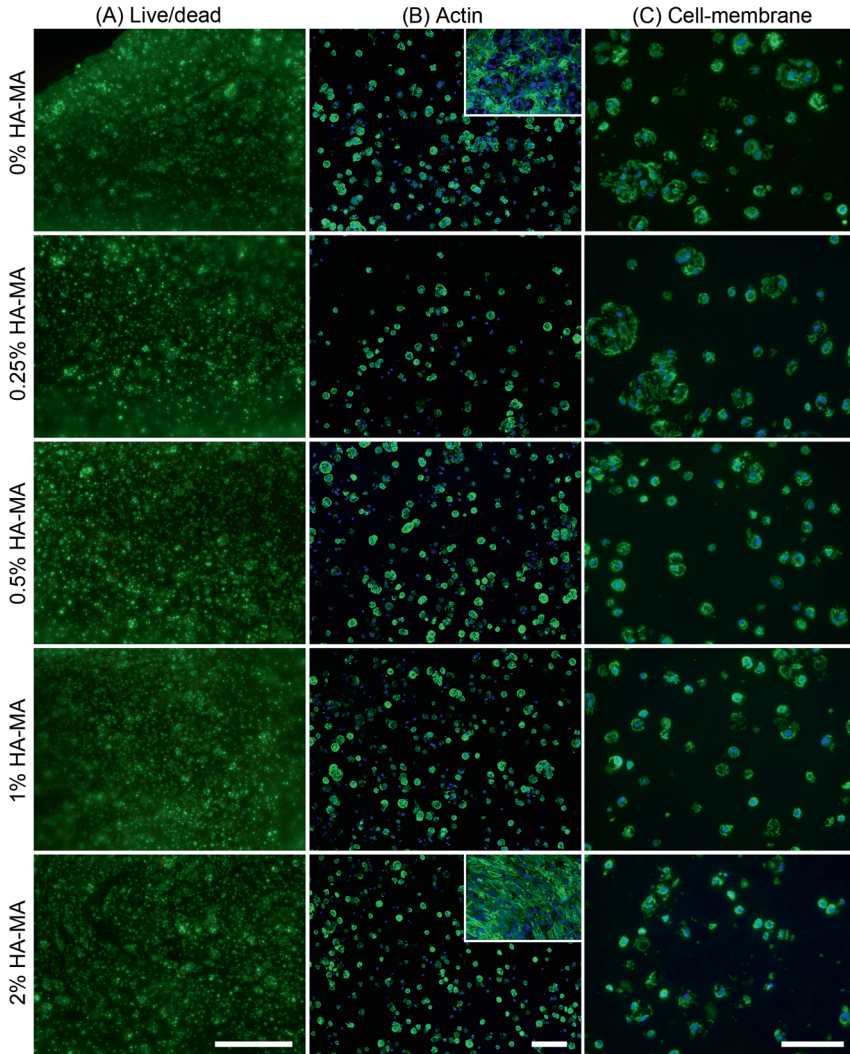


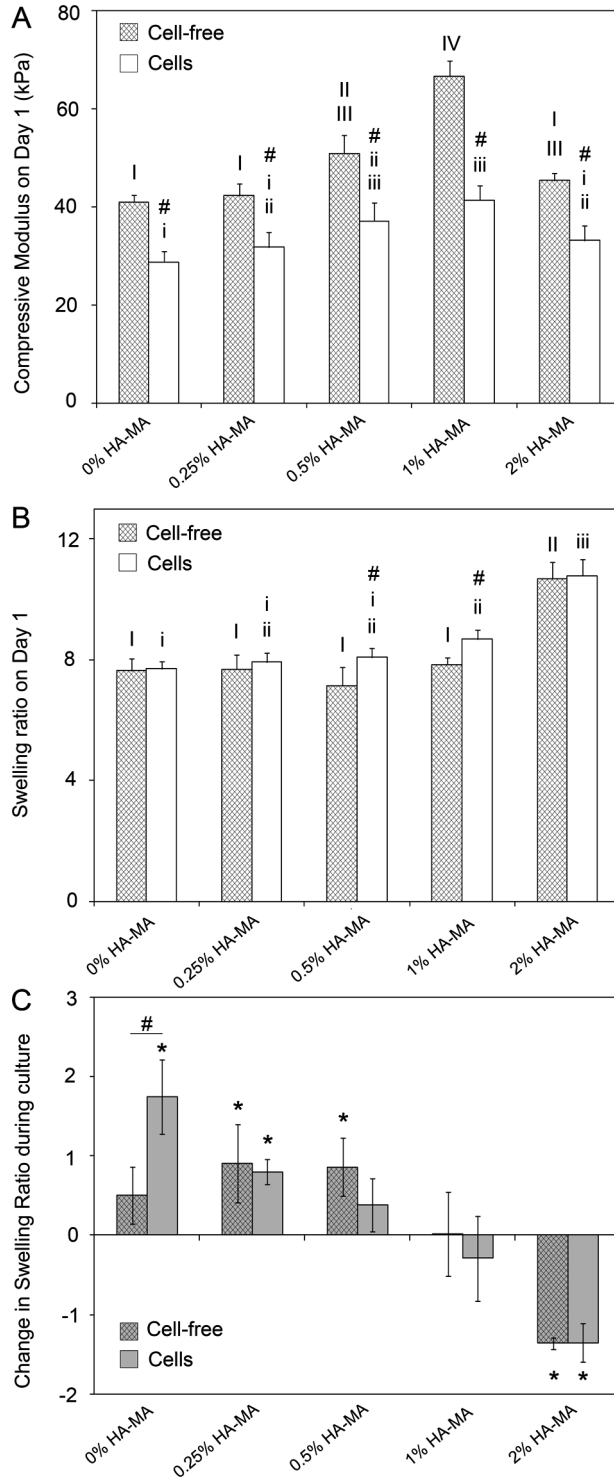
**Figure 6.2: Viability and morphology of chondrocytes after 28 days culture in Gel-MA hydrogels with 0-2% HA-MA.** (A) Viability images from the centre of hydrogel constructs, in which living cells appear green (stained with fluorescein diacetate) and dead cells appear red (stained with propidium iodide). (B) Confocal microscopy showing actin filaments (green) and nuclei (blue) showing the morphology of encapsulated chondrocytes inside the gels and at the surface of the gels (insets for 0 and 2% HA-MA). (C) CD44 immunostaining (green) and nuclei (blue) showing the cell membrane morphology of encapsulated cells. The scalebar in (A) represents 500  $\mu\text{m}$ , and scalebars in (B) and (C) represent 100  $\mu\text{m}$ .

### 6.3.3 Physical Properties

On day 1, HA-MA had a relatively minor, but statistically significant impact on the compressive modulus of cell-free and cell-laden hydrogels (Figure 6.3A). For HA-MA concentrations up to 1%, compressive modulus increased with HA-MA concentration. Constructs with 2% HA-MA were softer than those with 1% HA-MA, which was driven by substantially greater swelling in the 2% HA-MA hydrogels (Figure 6.3C). On day 1, all cell-laden hydrogels were softer than their cell-free counterparts (Figure 6.3A), but the effect was not a consequence of differential swelling. On day 1, swelling ratios of cell-free and cell-laden gels were generally similar, with only a few small, but statistically significant differences (Figure 6.3C).

**Figure 6.3 (next page): Physical properties of cell-free and cell-laden gels after 1 and 28 days culture *in vitro*.** (A) Compressive modulus of cell-free and cell-laden gels on day 1; (B) swelling ratio of cell-free and cell-laden gels on day 1; and (C) change in swelling ratio between days 1 and 28 of culture. Bars and error bars represent the mean and standard deviation of data from four patients. The symbol # indicates a significant difference between cell-free and cell-laden gels. In (C), a value of 2 represents an increase in swelling ratio, for example from 8 on day 1 to 10 on day 28, and \* represents a difference from day 0.

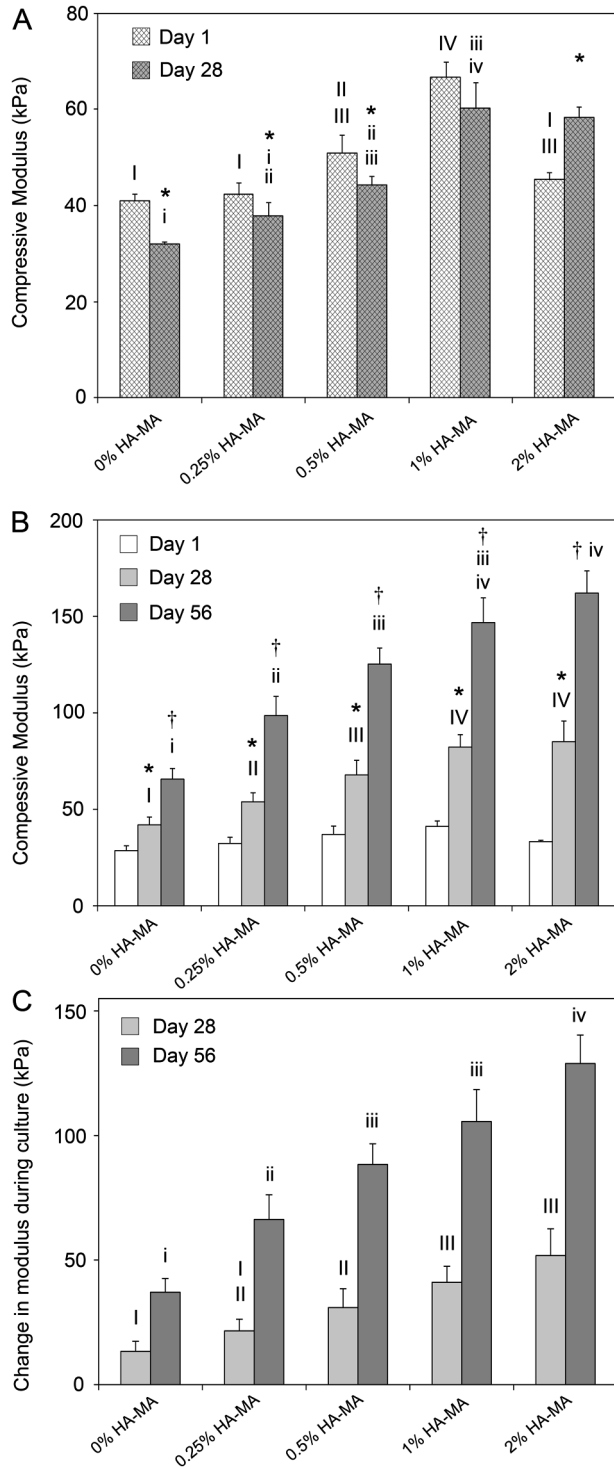




After 28 days culture, cell-free gels with 0-0.5% HA-MA were softer than on day 1, while 1% HA-MA gels were unchanged, and 2% HA-MA increased in stiffness (Figure 6.3B). The increase of gels with 2% HA-MA was consistent with a notable reduction in the swelling ratio, whereas the swelling ratios of other hydrogels either increased or were unchanged (Figure 6.3D). For each group with HA-MA, the change in swelling ratio during culture was the same for cell-free and cell-laden gels. For the Gel-MA only group, however, the cells caused the swelling ratio to increase significantly more during culture than the cell-free gels.

The most striking effect of HA-MA was apparent for the changes in the compressive moduli of cell-laden gels during culture. HA-MA had a strong and concentration dependent effect on the developed mechanical properties after 28 and 56 days culture (Figure 6.4). The stiffness of all groups increased during culture, but the increases were substantially greater in constructs containing HA-MA, and generally, the change in modulus increased as HA-MA concentration increased (Figure 6.4C). After 56 days culture, the compressive modulus of Gel-MA only constructs (0% HA-MA) increased by an average of 37 kPa, whereas constructs with 2% HA-MA increased by an average of 129 kPa during the same period.

**Figure 6.4 (next page): Compressive modulus of cell-free and cell-laden gels throughout *in-vitro* culture.** (A) The compressive modulus of cell-free gels on days 1 and 28; (B) compressive modulus of cell-laden gels on days 1, 28 and 56; and (C) change in modulus between day 1 and day 28 and day 1 and day 56. Bars and error bars represent the mean and standard deviation of data from four patients. The compressive modulus increased in all gels with culture time, and HA-MA had a significant impact on the rate of increase. The symbol \* indicates a difference between days 1 and 28, and † indicates a difference between days 28 and 56. In each panel, groups without a like Roman numeral are significantly different, and upper and lower cases should be considered separately.



After 63 days culture, the dynamic and equilibrium moduli of cell-laden constructs were measured (Figure 6.5A, B). Both dynamic and equilibrium moduli tended to increase with HA-MA concentration, although for higher HA-MA concentrations, the differences were smaller and less likely to be statistically significant. The presence of clear differences in the equilibrium moduli confirms that the differences in compressive and dynamic moduli are not just a result of increased resistance to fluid flow, but also stem from increased rigidity of the network. For hydrogel materials, the compressive modulus measured at a given strain will always be equal to or higher than the equilibrium modulus at the same strain. On day 63, the equilibrium modulus of gels with 1% HA-MA was 86 kPa, significantly higher than the compressive modulus of the same gels on day 1 (41 kPa), which also confirms that a substantial component of the equilibrium stiffness can be attributed to the cell-secreted extracellular matrix.

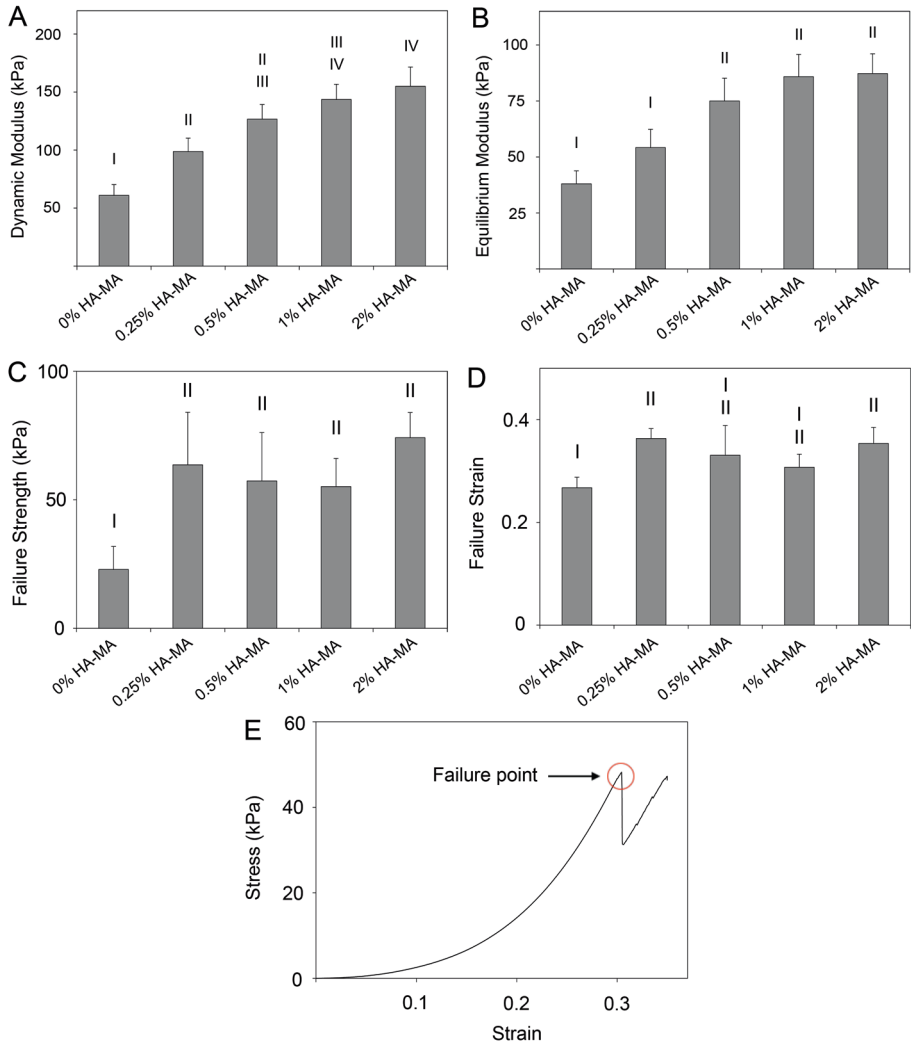


**Figure 6.5: Physical properties of cell-laden gels after 63 days of culture.** (A) Dynamic and (B) equilibrium moduli (B); (C) failure strength and (D) failure strain. An example stress-strain curve for a compression-to-failure test is shown in (E). Bars and error bars represent the mean and standard deviation of data from four patients. Differences between groups are indicated using Roman numerals; groups with a common numeral are significantly similar, and groups without a common numeral are significantly different.

HA-MA also had a significant impact on the failure properties of cell-laden constructs on day 63, but unlike the moduli measurements, was not strongly dependent on HA-MA concentration (Figure 6.5C). On average, the failure stress of gels with any concentration of HA-MA was 63 kPa, which represents a substantial increase from the failure strength of gels without HA-MA (23 kPa). Failure strains followed a similar pattern to failure strength, although not all differences were statistically significant (Figure 6.5D).

#### **6.3.4 Matrix Production**

After 4 weeks of culture, immunofluorescence was used to visualise the presence and distribution of the major cartilage matrix components aggrecan and collagen type II. For all hydrogel compositions, the intensity of both aggrecan and collagen type II immunofluorescence was greater towards the outer regions of the construct than in the centre (Figure 6.6). HA-MA appeared to influence the distribution of aggrecan, with more staining in the ECM as opposed to the pericellular matrix in constructs with HA-MA. Hydrogel composition appeared to have only minor impacts on the staining patterns of collagen type II, and the staining patterns of collagen type II and aggrecan were quite distinct.

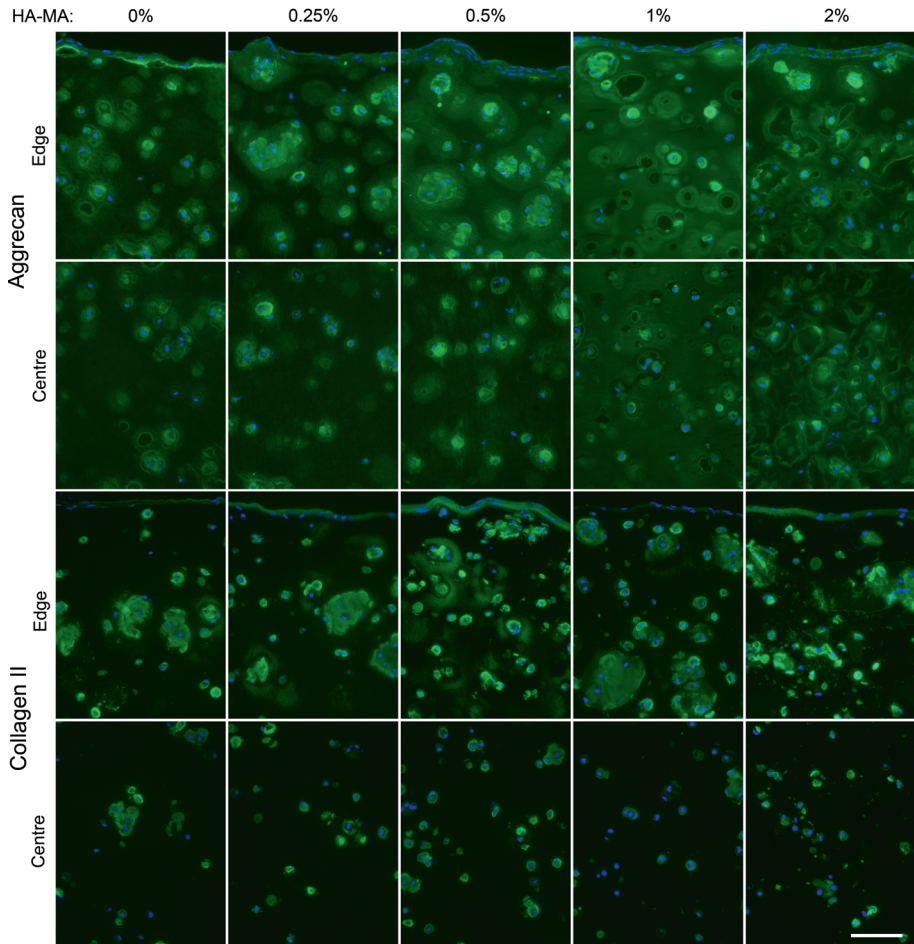


**Figure 6.6: Aggrecan and collagen type II immunofluorescence in constructs after 28 days of culture.** Aggrecan and collagen type II are shown in green, and nuclei are shown in blue. Regions at the edge and centre of each construct are shown. The scalebar represents 100  $\mu\text{m}$  and applies to all panels.

Collagen type I immunofluorescence was strong at the outermost edge of the constructs (Figure 6.7), consistent with the stretched chondrocyte morphologies observed on the surface of all gels. Collagen type I was also more strongly and widely stained in gels without HA-MA, especially compared to those with 0.5% and 1% HA-MA (Figure 6.7). Collagen type X was present throughout the cultured constructs (Figure 6.7), indicating that cells may be undergoing hypertrophy and potential for the ECM to be partially mineralised.

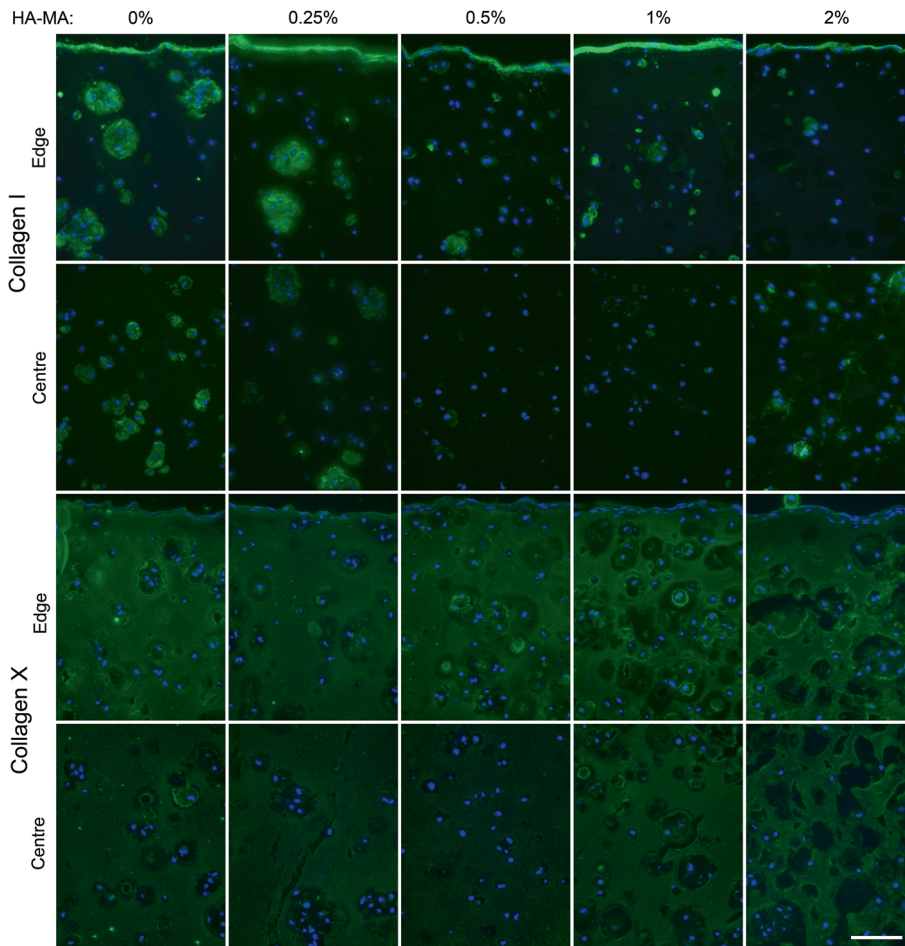


**Figure 6.7: Collagen type I and type X immunofluorescence in constructs after 28 days of culture.** Collagen type I and type X are shown in green and nuclei are shown in blue. Regions at the edge and centre of each construct are shown. The scalebar represents 100  $\mu\text{m}$  and applies to all panels.

### 6.3.5 GAG Production

The amount of GAGs that accumulated in the constructs over 28 days culture was quantified, and DNA content was quantified on days 1 and 28. In all gels, DNA content increased by a similar amount during 28 days culture (Figure 6.8A). Total GAG content was statistically similar in all groups (Figure 6.8B), and GAG content normalised to dry weight was also similar in all groups (Figure 6.8C). When normalised to the total GAG content to the 0% HA-MA group for each patient to account for inter-patient variability, a modest increase



is apparent in gels with 0.5% HA-MA compared to Gel-MA only gels (Figure 6.8D).

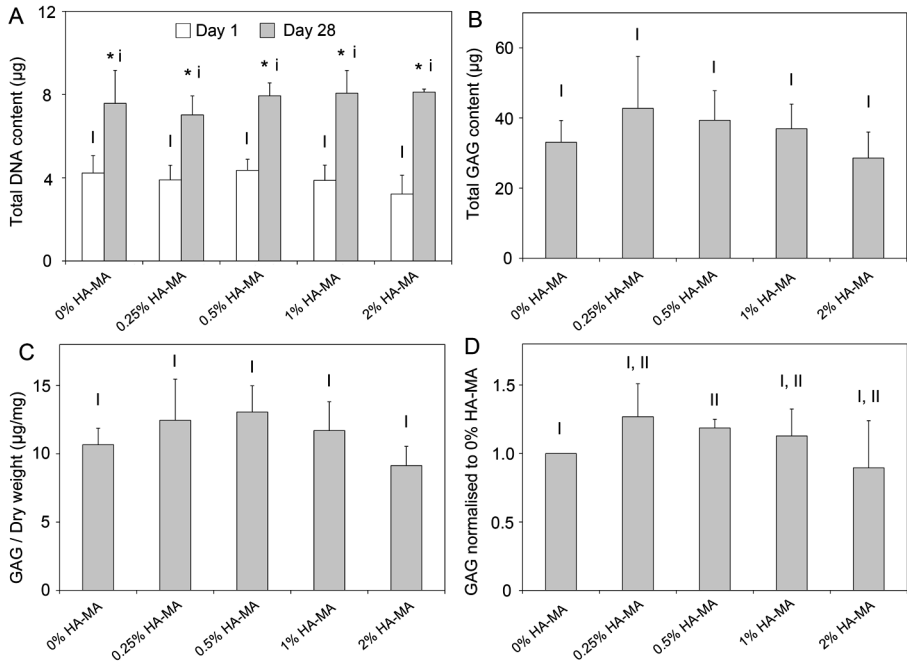


**Figure 6.8: (A) DNA content of constructs on days 1 and 28. (B) Total GAG content in each hydrogel construct after 28 days of culture; (C) GAG content normalised to dry weight, and (D) GAG content normalised to the GAG content for 0% HA-MA hydrogels for each patient (D). Bars and error bars represent the mean and standard deviation of four patients. Groups without a like Roman numeral are significantly different, and those with a like numeral are statistically similar. In (A), \* indicates a significant difference in the DNA content in a hydrogel group between days 1 and 28.**

### 6.3.6 EPIC- $\mu$ CT

EPIC- $\mu$ CT was used as a tool to visualise and semi-quantify differences in GAG content between hydrogels. In cell-free gels, the intensity of the negatively charged contrast agent Ioxaglate varies with HA-MA (Figure 6.9A). For example, 0% HA-MA gels show considerably more red colouration than 2% HA-MA gels. EPIC- $\mu$ CT can also give an indication of charge distribution, with more red coloration generally visible in the center regions of cell-laden constructs, where matrix synthesis was observed to be much lower (Figure 6.9B).

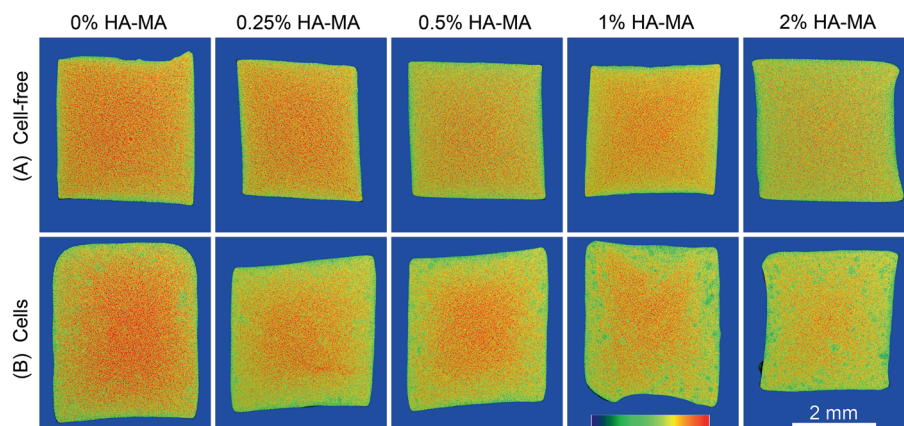


**Figure 6.9: EPIC- $\mu$ CT scans of cell-free (A) and cell-laden (B) constructs after 28 days culture.** The scans show intensity of the negatively charged contrast agent loxaglate, and attenuation range in each panel is from 5,000 (blue) to 22,000 (red). The 2 mm scalebar applies to all panels.

#### 6.4 Discussion

Hyaluronic acid (HA) is one of the most commonly studied biomaterials in cartilage tissue engineering, yet we are still discovering aspects of its significance for cartilage biology. In healthy cartilage, aggrecan is non-covalently bound to HA to create massive aggregates of fixed negative charge which provide compression resistance and swelling properties, both of which are key to its mechanical properties [12]. Many biomaterials for cartilage tissue engineering have been produced partly or wholly from HA or HA derivatives, some of which have progressed to clinical trials [73, 122, 216]. In addition, lightly crosslinked HA is an effective viscosupplementation agent for diseased or damaged joints, including those with OA [217].

In this study, a photocrosslinkable HA derivative has been shown to be a valuable addition to gelatin-based hydrogels, and specifically, has shown that the addition of HA-MA results in a substantial improvement in the developed mechanical properties, as measured using a number of different parameters. This is relevant for tissue-engineered cartilage *in vivo*, which must routinely withstand considerable stresses. After 9 weeks of culture, construct dynamic and equilibrium moduli significantly increased in a HA-MA concentration-dependent manner. After this time in culture, the majority of the compressive modulus was due to cell-secreted ECM. Additionally, inclusion of HA-MA increased failure strength relative to Gel-MA constructs, but strength was independent of HA-MA concentration over the range 0.25-2%. Although the

failure strength of cell-free gels was not measured, it is likely that the cell secreted ECM is also a major factor in determining the failure strength of the cell-hydrogel constructs.

While it is clear that the mechanical properties of the constructs in this study improve with time in culture, the exact mechanism for this improvement is not clear. GAG content in articular cartilage is correlated with compressive properties [218, 219] and GAG content is the most commonly used method to measure the functional development of tissue-engineered cartilage. However the importance of total GAG content for the mechanical properties of tissue-engineered cartilage is unclear, and an important distinction was observed in this study. In contrast to the role of GAGs in cartilage, the total GAG content had very little, if any, correlation with mechanical properties of the tissue-engineered constructs in this study. GAG content was relatively similar for each patient and hydrogel composition, with no significant differences in total GAG content or GAG/dry weight. When normalised within each patient, a slight increase in GAG/dry weight was observed for gels with 0.5% HA-MA, which is roughly in line with previous results from a single patient [214]. Other studies have shown that in pure HA-MA hydrogels, the correlation between mechanical properties and GAG content was also highly non-linear [122]. This must be considered when assessing the quality of tissue-engineered cartilage throughout the literature, where GAG content has been measured but not mechanical properties. Along with GAGs, the collagen network is also important for providing cartilage with mechanical strength. Total collagen content was not measured in this study, but it is likely that both the collagen content and its distribution throughout the gels contribute substantially to the mechanical properties. The hydroxyproline assay is the most common technique to measure total collagen content, but this is not practical for gels containing such a large amount of gelatin.

Cell viability was high after 28 days, indicating that the crosslinking process is well tolerated and that cells receive sufficient nourishment by diffusion through the gel. The crosslinking process has been previously shown to yield high cell viabilities [63, 65], but no study has definitely shown that no adverse cell outcomes occur. Meanwhile, photoinitiators that are active in the visible region of the spectrum are being investigated to further remove the potential for UV or radical induced cell damage [220].

Immunofluorescence analysis showed that aggrecan distribution was enhanced in gels with HA-MA, particularly towards the outer edges, and in the 1% HA-

MA group, in which an almost continuous aggrecan staining can be observed. This enhanced ECM distribution may be responsible for the increases in mechanical properties when HA-MA was included. Less staining was consistently observed in the centre of the constructs, and this is most likely a consequence of lower nutrient concentrations due to diffusion gradients within the gels. Constructs with 2% HA-MA appeared to inhibit the diffusion of OCT into the tissue; this adversely affected the quality of the sections from gels with 2% HA-MA, and as such, limited emphasis should be placed on images from these gels. Cell viability, however, was not reduced in the centre regions of all tested gels, perhaps unsurprisingly, since chondrocytes habitually withstand hypoxic conditions in native cartilage. Mechanical stimulation using bioreactors or perfused medium culture systems could be used to increase mass transfer throughout these constructs, potentially further improving mechanical properties [122]. Mechanical stimulation may also simultaneously enhance chondrogenesis and matrix synthesis by mimicking the natural strains that are applied to cartilage [187], and further studies should investigate bioreactor systems to progress these materials towards regenerative medicine applications.

Collagen type X was observed in all hydrogels in this study, which could potentially be a consequence of prolonged TGF- $\beta$ 3 exposure or the presence of reactive oxygen species during crosslinking. Other studies have indicated that reactive oxygen species may promote hypertrophy and collagen type X production [221, 222], thereby reducing the quality of the resulting tissue. Importantly, using alternative chemical groups for photocrosslinking can reduce hypertrophy and collagen type X production. Thiol groups, for example, can quench reactive oxygen species during crosslinking, whereas acrylate-based chemistries cannot [222]. HA can be modified with thiol groups using simple procedures [223] or purchased, and could be used instead of HA-MA [224]. Such a study would also provide insight into the importance of network topology on the developed mechanical properties and cell responses [222], since a substantial proportion of the crosslinks would be expected to occur between HA and Gel-MA macromers. In addition, oxygen inhibition results in a several-minute delay in the onset of crosslinking of acrylate (and methacrylamide) systems [123, 224]. By using thiolated HA this delay is effectively removed, which would greatly reduce the required UV exposure [222] and make the process safer.

Biological variation, or donor-to-donor variation, presents a significant challenge for biomedical research. Previously, it has been identified that HA-MA can improve the stiffness of cultured Gel-MA/HA-MA constructs, but these

results were obtained using chondrocytes from a single patient [214], and thus uncertainty remained over how applicable the findings were to cells from other patients. In the present study, we used chondrocytes from four patients to measure the importance of donor-to-donor variation. The similar response of each patient to these materials confirms that material composition has a significant influence on construct maturation. It is reasonable to expect that the differences observed here using *in vitro* methods would also translate to substantial differences in an *in vivo* setting, but this remains to be verified.

Cell source is an important consideration for cartilage repair, and a number of different clinically driven routes have been explored. Therefore, this study also provides further evidence of the potential to use chondrocytes from elderly patients and OA joints. Initially, expanded autologous chondrocytes were used for cartilage repair [50], but since then allogeneic chondrocytes [225] and mesenchymal stem cells [226] have been investigated. Cells from young donors are thought to be more biologically active and have greater potential for regeneration, and thus cartilage from juvenile donors has been preferred for some clinical treatments [227]. Although we have no comparative data from juvenile patients, in this study all cells were isolated from elderly patients with OA, and the cells from all patients were able to secrete ECM that significantly increased the construct stiffness. This reinforces the potential for using autologous chondrocytes even in elderly patients in combination with biomimetic hydrogels.

The hydrogels formed in this study are crosslinked using two very similar chemistries. The gelatin component is modified with predominantly methacrylamide groups, while HA is modified with methacrylate groups. Both groups are crosslinked via the reaction of unsaturated vinyl bonds however the reactivity of methacrylamide is reduced by resonance stabilisation with the adjacent nitrogen. Theoretically, methacrylamide can crosslink with methacrylate, and this has recently been demonstrated using Gel-MA and methacrylate functionalised polycaprolactone [228]. Should no preference exist, Gel-MA – HA-MA gels would be randomly inter-crosslinked on a molecular level. However, it is possible that the methacrylate groups preferentially crosslink with other methacrylate groups, or that due to their higher reactivity, methacrylate groups are favoured, particularly during the early stages of crosslinking. In this case, the network would resemble a double-network hydrogel, in which the first network is formed by crosslinked HA-MA, and the second network is crosslinked Gel-MA.

The degradation characteristics lend some weight to the hypothesis that two distinct networks may exist. For example, if the gelatin component of a gel with a composition of 9.5% Gel-MA, 0.5% HA-MA is removed by papain or proteinase K digestion, an intact, stable network of crosslinked HA-MA remains. The existence of a stable HA-MA network, even when HA-MA accounts for only one twentieth of the total dry mass indicates that the HA-MA network exists independently of the Gel-MA network. Of course this is also facilitated by the high molecular weight of the HA used here, increasing the likelihood and occurrence of HA chains overlapping.

The extent of mixing between Gel-MA and HA-MA is temperature dependent. Mixtures of these polymers have a degree of turbidity, which increases as temperature is reduced, probably as a result of the thermal gelation response of Gel-MA (Figure S6.1). This suggests that the network structure of crosslinked Gel-MA – HA-MA hydrogels may be temperature dependent, and possibilities may exist to further improve mechanical property development by adjusting the crosslinking temperature.

An important question also remains about the functionality of HA-MA compared to HA, and the mechanism by which HA-MA improves the mechanical properties. In cartilage, for instance, the non-covalent interaction between aggrecan and HA is stabilised by link protein [25], and HA turnover is mediated by enzymatic degradation by hyaluronidase and replacement with high molecular weight HA [229]. Preliminary data from our research (not shown) indicates that HA-MA is much less readily degraded by hyaluronidase than HA, and that link protein does not strongly bind to or recognise HA-MA. The reduced susceptibility of HA-MA to hyaluronidase has been noted in other studies, and appears, as one might expect, to depend on the degree of functionalisation [230]. Thus if HA-MA has altered functionality to HA, the mechanisms by which HA-MA improves the matrix organisation and function when added to Gel-MA gels requires further research.

There is a strong need for improved materials for cartilage tissue engineering, and biomimetic materials are a promising strategy to deliver these improvements. Currently, fibrin glue is one of the most commonly used gels to deliver cells to cartilage defects [51]. This usage is based on the familiarity of fibrin glue to orthopaedic surgeons and existing regulatory approval, rather than solid evidence demonstrating the suitability of fibrin glue for cartilage repair. Individually, Gel-MA and HA-MA are both interesting materials for tissue engineering [66, 129, 188], and here and elsewhere, mixtures of these two

materials have been identified as having particularly intriguing properties [123, 201, 214]. The crosslinked hydrogels appear to be quite stable in PBS, with cell-free gels of all compositions maintaining their shape and structure for at least six months at room temperature (data not shown). The gels are susceptible to enzymatic degradation, which can be manipulated by varying the relative amount of HA-MA [201] or incorporating polymers that are not susceptible to enzymatic degradation, such as PEG [231]. Further research should consider the mechanisms by which HA-MA exerts an impact on developed mechanical properties, possibilities to enhance diffusion throughout the gel, and direct comparisons between these gels and existing clinically used materials in large preclinical animal models.

## **6.5 Conclusion**

In summary, combinations of Gel-MA and HA-MA are promising candidates for cartilage tissue engineering. Encapsulated chondrocytes display a predominantly rounded morphology, and secrete extracellular matrix that increases the compressive modulus by up to three-fold over 8 weeks culture. Importantly, different patients respond similarly to HA-MA, and cells from all patients were capable of substantially increasing the stiffness of Gel-MA – HA-MA hydrogels.

### **Acknowledgements**

The authors are grateful to Professor Ross Crawford for facilitating the collection of knee tissue and to Kristel Boere for facilitating the NMR analyses. The antibody for collagen type II (developed by T. F. Linsenmayer) was obtained from the DSHB developed under the auspices of the NICHD, which is maintained by the University of Iowa, Department of Biology, Iowa City, IA 52242, USA.





## Chapter 7

# Crosslinkable hydrogels derived from cartilage, meniscus and tendon tissue

---

Jetze Visser<sup>1</sup>, Peter A. Levett<sup>1,2</sup>, Nikae C te Moller<sup>4</sup>, Jeremy Besems<sup>1</sup>, Kristel Boere<sup>3</sup>, Janny C. de Grauw<sup>4</sup>, P. René van Weeren<sup>4</sup>, Wouter J. A. Dhert<sup>1,4</sup> and Jos Malda<sup>1,2,4</sup>

Tissue Engineering – Part A (2015), Vol. 21, No. 7-8, p. 1195-1206.

<sup>1</sup> *Department of Orthopaedics, University Medical Center, Utrecht, P.O. Box 85500, 3508 GA, The Netherlands*

<sup>2</sup> *Institute of Health and Biomedical Innovation, Queensland University of Technology, 60 Musk Ave, Kelvin Grove, QLD 4059, Australia*

<sup>3</sup> *Department of Pharmaceutics, Utrecht University, 3508 TB, Utrecht, The Netherlands*

<sup>4</sup> *Department of Equine Sciences, Faculty of Veterinary Sciences, Utrecht University, Utrecht, The Netherlands*

---

This publication is also a Chapter in the doctoral thesis of Jetze Visser.

## Abstract

Decellularised tissues have proven to be versatile matrices for the engineering of tissues and organs. These matrices usually consist of collagens, matrix-specific proteins, and a set of largely undefined growth factors and signaling molecules. Although several decellularised tissues have found their way to clinical applications, their use in the engineering of cartilage tissue has only been explored to a limited extent. We set out to generate hydrogels from several tissue-derived matrices, as hydrogels are the current preferred cell carriers for cartilage repair. Equine cartilage, meniscus, and tendon tissue was harvested, decellularised, enzymatically digested, and functionalised with methacrylamide groups. After photo-crosslinking, these tissue digests were mechanically characterised. Next, gelatin methacrylamide (Gel-MA) hydrogels were functionalised with these methacrylated tissue digests. Equine chondrocytes and mesenchymal stromal cells (MSCs) (both from three donors) were encapsulated and cultured *in vitro* up to 6 weeks. Gene expression (COL1A1, COL2A1, ACAN, MMP-3, MMP-13, and MMP-14), cartilage-specific matrix formation, and hydrogel stiffness were analysed after culture. The cartilage, meniscus, and tendon digests were successfully photo-crosslinked into hydrogels. The addition of the tissue-derived matrices to Gel-MA affected chondrogenic differentiation of MSCs, although no consequent improvement was demonstrated. For chondrocytes, the tissue-derived matrix gels performed worse compared to Gel-MA alone. This work demonstrates for the first time that native tissues can be processed into crosslinkable hydrogels for the engineering of tissues. Moreover, the differentiation of encapsulated cells can be influenced in these stable, decellularised matrix hydrogels.

**Keywords:** Decellularised tissues cartilage, chondrocytes, hydrogels

## 7.1 Introduction

In tissue engineering, there is a rationale for designing [232, 233] biomimetic materials that recreate the native cell niche. Tissue-derived matrices, for example, can provide structural and biological support for matrix formation by embedded or invading cells [234]. Native tissues that have been decellularised while maintaining the natural growth factors and signaling molecules may thus provide the ultimate biomimetic environment [235]. Despite the clinical translation of decellularised materials for the repair of skin, bone, heart valves, and so on, the application in the field of cartilage regeneration has only been explored to a limited extent [236, 237].

There is a strong need for novel biomaterials for cartilage tissue engineering [46, 54]. Hydrogels are good potential candidates, since they can support the chondrogenic morphology and simultaneously serve as a temporary scaffold for matrix formation. Moreover, hydrogels are easily delivered to a cartilage defect and allow for engineering of advanced cartilage constructs [211]. Currently, fibrin glue is the clinical standard for cell delivery to cartilage defects [51]. However, this gel is relatively unstable with a high degradation rate and is thus a delivery vehicle rather than a support structure for cartilage matrix formation [238, 239]. Therefore, several new hydrogels are being designed, in which ideally the degradation rate is balanced with active cartilage matrix formation, and biochemical cues are incorporated to direct the behavior of encapsulated cells [184, 240]. Hydrogels derived from natural tissues are interesting candidates to meet these requirements, as they may form a potential scaffold for cells and include the appropriate biochemical cues. To this end, native matrix gels have been acquired from several tissues through digestion with pepsin enzymes [241-243]. These hydrogels allowed the invasion of cells and subsequent matrix deposition. However, tissue-derived matrix gels so far have only been physically cross-linked resulting in low shape stability, which is a serious drawback.

In this study, decellularised matrices were derived from cartilage, meniscus, and tendon tissues. Cartilage has a high level of collagen II and glycosaminoglycans (GAGs); meniscus has an intermediate level of GAGs, and a mixture of collagen types I and II, whereas tendon is predominantly composed of collagen type I and a small amount of GAGs [244]. Decellularised cartilage tissue may contain the biochemical cues that are present in the native chondrocyte niche. Intuitively, a collagen type II scaffold would be the scaffold of choice for cartilage engineering, whereas there are indications that this type of collagen induces catabolic pathways in cultured chondrocytes [245-247]. On the other

hand, collagen type I scaffolds have proven efficacy in the regeneration of cartilage tissue [248, 249]. Therefore, both types of collagen and a mixed composition (meniscus tissue) were evaluated here. The tissue-derived matrices were used for the functionalisation of gelatin methacrylamide (Gel-MA) hydrogels. Gel-MA has been identified as a stable, versatile hydrogel for tissue regeneration [66, 228, 250]. It can be synthesised at low cost and gelatin is widely available as a substrate; cell adhesion sites are abundant and cells are allowed to migrate through the hydrogel and remodel the newly formed tissue. We previously showed that functionalising Gel-MA with GAGs can substantially improve cartilage matrix formation in *in vitro* models [214]. In this study, cartilage, meniscus, and tendon tissues were processed into hydrogels that were covalently crosslinked to Gel-MA hydrogel. The potential of these matrices to enhance cartilage tissue formation by chondrocytes and mesenchymal stromal cells (MSCs) *in vitro* was evaluated.

## 7.2 Materials and Methods

### 7.2.1 Development of crosslinkable tissue-derived matrix hydrogels

Stifle joints (n = 8; age 3–10 years) were obtained from horses that had died or were euthanised due to nonorthopedic ailments. Consent was obtained from the owner before tissue harvest and tissue was only obtained from macroscopically healthy joints. The stifle joints were dissected and the full-thickness cartilage was harvested from the entire femoral condyles. Also, both complete menisci and the patellar tendons were harvested, 0.5 cm from their anchoring site in the bone. The tissues were dissected into small pieces (5×5×5 mm for meniscus and tendon, and 5×5×2 mm for cartilage tissue) and all donors were pooled. Three random samples were taken from each tissue type to measure the GAG and DNA content. The obtained values will thus reflect the variability between donors and sample location (e.g., cartilage from the medial or lateral condyle). Then the tissues were separately milled in liquid nitrogen (A11 basic analytical mill; IKA). The cartilage fragments were subsequently sieved through pores of 710 µm. Cells were removed from the tissues by treatment with 10 mM Tris/1% triton on a roller bench for 24 h; sonication for 2 h at 55 ± 10 kHz and a nuclease solution consisting of 1 U/mL deoxyribonuclease and 1 U/mL ribonuclease in phosphate-buffered saline (PBS) on a roller bench for 72 h at 37 °C. The resulting matrices (from cartilage, meniscus, and tendon tissue) were freeze-dried and digested with pepsin (Sigma-Aldrich) in a 0.01 M hydrochloric acid solution at 37 °C on a roller

bench, until clear suspensions were obtained. The pH of the solutions was raised to 9.0 for 1 h (using 1 M NaOH), to irreversibly inactivate the remaining pepsin enzymes [251], before adjustment to 7.5 (using 1 M HCl). Next, methacrylic anhydride (Sigma) was added dropwise (2.5 mL/g matrix) and was allowed to react with the matrices under constant stirring for 1 h. The methacrylated tissue-derived matrices (CartMA, MenMA and TendMA) were dialysed against distilled water for 7 days at 40 °C to remove unreacted methacrylic acid and anhydride. After freeze-drying, the tissue digests were dissolved in PBS 10% (w/v), containing photoinitiator Irgacure 2959 (0.1% [w/v], Ciba; BASF). A schematic overview of the experimental set-up is presented in Figure 7.1.

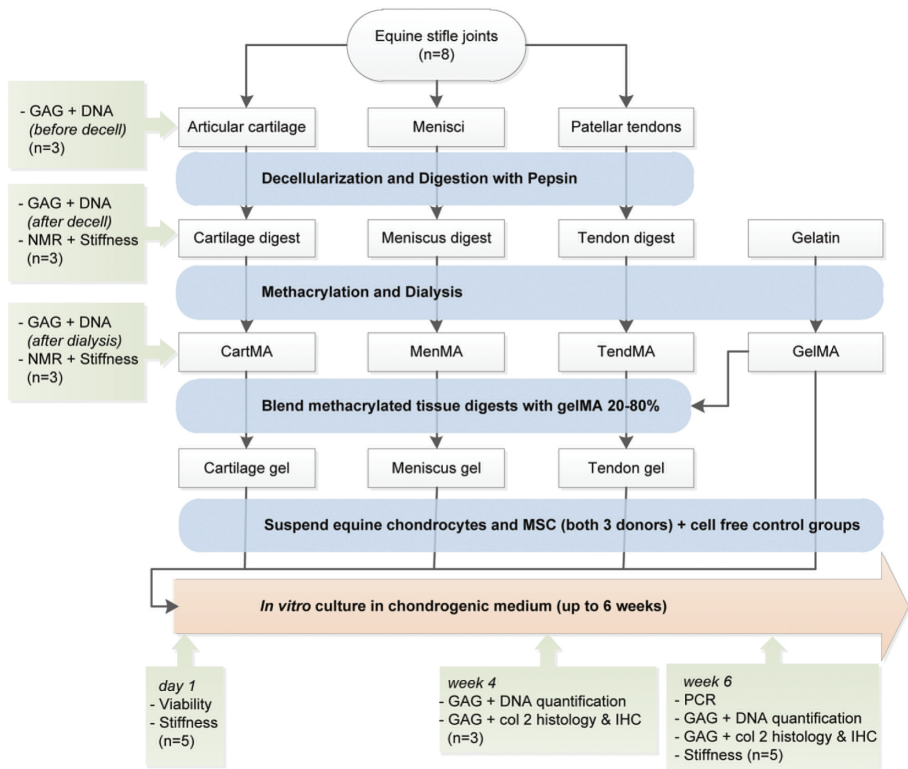


**Figure 7.1: Experimental setup of the study.** Col, collagen; GAG, glycosaminoglycans; IHC, immunohistochemistry; MES, mesenchymal stromal cells; n, the number of analysed samples per donor; NMR, nuclear magnetic resonance; PCR, polymerase chain reaction.

### 7.2.2 Characterisation of tissue derived matrices

Collagen type I (rat tail; BD Biosciences), collagen type II (from chicken sternal cartilage; Sigma), meniscus, tendon, and cartilage digests (not methacrylated) were electrophoresed on a Bolt 4–12% BisTris Plus gel (Novex; Life Technologies) under reducing conditions (1.25% 2-mercaptoethanol). The proteins were visualised with Page Blue (Thermo Scientific) and compared to a multicolour High Range protein ladder (Thermo Scientific). Images were recorded using an Epson perfection 4490 Photo scanner.

The success of the methacrylation procedure was evaluated using proton nuclear magnetic resonance ( $^1\text{H}$  NMR).  $^1\text{H}$  NMR spectra of 10 mg/mL solutions of decellularised cartilage, meniscus, and tendon tissue digests, and their methacrylated equivalents (respectively cartMA, menMA, and tendMA), were recorded on a Mercury 300 MHz instrument (Varian Associates, Inc.; NMR Instruments). Chemical shifts were recorded in ppm with reference to the solvent peak ( $\delta = 4.8$  ppm for  $\text{D}_2\text{O}$ ).

### 7.2.3 Blending of tissue digests with Gel-MA

For cellular differentiation experiments, the methacrylated tissue digests (cartMA, menMA, and tendMA), were separately blended with Gel-MA at 37 °C, and will be referred to as the cartilage, meniscus, and tendon group, respectively. Gel-MA was synthesised by reaction of type A gelatin (Sigma) with methacrylic anhydride as described previously [52, 123]. The final composition of the hydrogels was 8% Gel-MA and 2% tissue digest in 1×PBS with 0.1% photoinitiator (all w/v). Gel-MA (10% w/v) was used as a control.

### 7.2.4 Photocrosslinking of hydrogels

Photocrosslinking of all hydrogels was performed for 15 min in a custom-made Teflon mold (width × height = 4×2 mm) using 365 nm UV light in a UVP CL-1000L cross-linker (UVP). The crosslinked samples were stored overnight at 37 °C in PBS before analysing the compressive modulus.

### 7.2.5 Compressive mechanical testing

The compressive modulus of all three uncrosslinked and crosslinked (-MA) tissue digests was measured, and compared to crosslinked Gel-MA gels (all  $n = 5$ ). The compressive modulus was also measured at day 1 and week 6 of *in vitro* culture for all experimental groups (cross-linked cartilage, meniscus, tendon, and Gel-MA gels, all  $n = 5$ ). Measurements were performed by uniaxial unconfined compression in air at room temperature. Hydrogels and hydrogel-

cell constructs were compressed to ~20% strain in 2 min using a Dynamic Mechanical Analyser (DMA 2980; TA Instruments). The compressive modulus was calculated from the linear derivative of the stress/strain curve at 10–15% strain.

### **7.2.6 Isolation of equine chondrocytes and multipotent stromal cells**

Full-thickness cartilage was harvested under sterile conditions from the stifle joint of fresh equine cadavers (n = 3, age 3–10 years) with macroscopically healthy cartilage and with consent of the owners. After overnight digestion in 0.15% type II collagenase (Worthington Biochemical Corp) at 37 °C, the suspension was filtered, stored at -196 °C, and encapsulated in the hydrogels at passage 1, according to a previously described protocol [228].

With approval of the Institutional Animal Ethical Committee, bone marrow aspirates were obtained from the iliac crest of healthy horses under general anesthesia (n = 3). The mononuclear fraction was isolated according to a previously described protocol [252]. The cells were stored at -196 °C and encapsulated in the hydrogels at passage 3–4. The multi-lineage potential of cells cultured from the bone marrow aspirates was confirmed by a three-way differentiation assay as previously described [252, 253].

### **7.2.7 Viability assay**

To evaluate the effect of the addition of the methacrylated tissue digests to Gel-MA on embedded cells, the viability of chondrocytes and MSCs (both three donors) was analysed on day 1. The cells had been encapsulated in the cartilage, meniscus, tendon, and Gel-MA hydrogels at a concentration of  $5 \times 10^6$  cells/mL. A LIVE/DEAD Viability Assay (Molecular Probes MP03224) was performed according to the manufacturer's instructions. Live and dead cells were counted for three samples per time point, at four locations within each construct. Viability was calculated as follows: (live cells/total cells)  $\times$  100.

### **7.2.8 Cellular differentiation experiments**

Equine chondrocytes and MSCs (both three donors,  $15 \times 10^6$  cells/mL) were embedded in the cartilage, meniscus, tendon, and Gel-MA groups. The gels were cultured *in vitro* for up to 6 weeks in chondrogenic differentiation medium. For chondrocyte-laden hydrogels this consisted of Dulbecco's modified Eagle's medium (DMEM) (41965; Invitrogen) supplemented with 0.2 mM l-ascorbic acid 2-phosphate, 0.5% human serum albumin (SeraCare Life Sciences),  $1 \times$  ITS-

X (Invitrogen), 100 U/mL penicillin, 100 mg/mL streptomycin, 25 mM 4-(2-hydroxyethyl)-1-piperazineethanesulfonic acid (Invitrogen), and 5 ng/mL transforming growth factor  $\beta$ -2 (TGF- $\beta$ 2, R&D Systems). MSC-laden samples were cultured in DMEM (31966; Invitrogen) supplemented with 0.2 mM l-ascorbic acid 2-phosphate, 1 $\times$ ITS + premix (BD Biosciences), 0.1  $\mu$ M dexamethasone, 100 U/mL penicillin and 100  $\mu$ g/mL streptomycin, and 10 ng/mL TGF- $\beta$ 2 (R&D Systems). Cell-free hydrogels cultured for 6 weeks served as a negative control group.

### **7.2.9 Histology, immunohistochemistry and biochemistry**

After 4 and 6 weeks of culture (three and five replicates respectively), the DNA and GAG content was quantified for all donors and groups. To this end, the samples were digested overnight in papain solution (200  $\mu$ L per sample [0.01 M cysteine, 250  $\mu$ g/mL papain, 0.2 M  $\text{NaH}_2\text{PO}_4$ , and 0.01 M ethylenediaminetetraacetic acid] at 60  $^\circ\text{C}$ ). Total DNA was quantified using the Picogreen DNA assay (Invitrogen) according to the manufacturer's instructions. Total GAG content was determined by photospectrometry at 525 and 595 nm, after reaction with dimethylmethylene blue using a microplate reader (Biorad). The ratio of both absorbances was calculated and the GAG content was quantified using a chondroitin sulfate (Sigma) standard. The concentrations of GAG and DNA in each papain digest were normalised per donor to the 4-week Gel-MA control group. GAG/DNA was calculated to display the single cell synthetic activity for the production of cartilage-specific matrix.

After 6 weeks of culture, three samples from each donor were taken for histology and immunohistochemistry. Samples were dehydrated through a graded ethanol series, cleared in xylene, and embedded in paraffin. The samples were sectioned into 5  $\mu$ m slices and a triple stain of hematoxylin (Klinipath BV), fast green and Safranin-O (Merck) was applied to identify GAG deposition. The stained sections were examined using a light microscope (Olympus BX51).

Collagen type II was stained by immunohistochemistry after deparaffinisation and rehydration of the sections, according to a previously described protocol [228] (primary antibody: 1:100, monoclonal mouse, II-II6B3; Developmental Studies Hybridoma Bank (DSHB); secondary antibody: 1:200, P0447; Dako). Isotype controls were performed by using mouse isotype IgG1 monoclonal antibody at concentrations similar to those used for the stainings.



### **7.2.10 Gene expression**

After 6 weeks of culture, the samples were homogenised in TRIzol reagent (Invitrogen). The best-performing chondrocyte and MSC donors were selected for polymerase chain reaction (PCR) analysis, based on a safranin-O staining of the Gel-MA control groups at week 6. The RNA was isolated according to the manufacturer's guidelines (chloroform was substituted by 3-bromo-chloropropane [254]). RNA was cleared of any DNA contamination by DNase digestion. Total RNA yield was determined spectrophotometrically (NanoDrop ND1000; Isogen Life Science) and 500 ng total RNA per sample was reverse transcribed into complementary DNA (cDNA) using Superscript III (Invitrogen) and random primers. SybrGreen quantitative real-time PCR was subsequently performed on an iQ-5 real time PCR detection system (Bio-Rad Laboratories). Each sample was run in duplicate and a three-fold serial dilution of pooled cDNA was used as a standard curve.

Primers were designed using computer software (primer BLAST, [www.ncbi.nlm.nih.gov/tools/primer-blast](http://www.ncbi.nlm.nih.gov/tools/primer-blast)) and obtained from Eurogentec. The specific genes of interest were collagen type IA1 (COL1A1), collagen type IIA1 (COL2A1), aggrecan (ACAN), matrix metalloproteinase-3 (MMP-3), MMP-13, and MMP-14. Hypoxanthine-guanine-phosphoribosyltransferase 1 (HPRT-1) and signal recognition particle 14 kDa (SRP-14) were selected as reference genes. Following fold-change calculation using the standard curve method, the geometric mean of these two reference genes was used to calculate the normalised mRNA expression of each target gene. Primer sequences of selected genes are provided in Supplementary Table S7.1.

### **7.2.11 Statistical analyses**

An independent samples T-test, assuming unequal variances, was performed to compare the DNA and GAG content of the tissues before and after the decellularisation protocol and also to compare the stiffness of cross-linked and uncrosslinked cell-free hydrogels. A Univariate Analysis of Variance with a Tukey HSD post hoc test was performed to compare GAG, DNA, GAG/DNA, and the compressive modulus between the groups of the cell culture experiments. Because the level of matrix formation differed significantly between the cell donors, a randomised block design was used, correcting for donor effects. GAG and DNA were normalised to the Gel-MA control group at week 4 for each separate cell donor; the compressive modulus was normalised to Gel-MA day 1. The statistical analyses were done using SPSS statistics (IBM, version 20). For the PCR data, Kruskal Wallis and Dunn's multiple comparison

post hoc tests were used to test differences between experimental conditions for each primer pair using Graphpad software (Graphpad Prism version 5.2 for Windows). Differences were considered significant when  $p < 0.05$  for all tests.

## **7.3 Results**

### **7.3.1 Decellularisation procedure**

The DNA content of the cartilage, meniscus, and tendon tissues significantly decreased after decellularisation, to values below 50  $\mu\text{g}/\text{mg}$  dry weight (Figure 7.2A). The DNA content was unaltered by the subsequent dialysis. The GAG content of all three tissues showed large variations between donors and/or sample location (Figure 7.2B). Yet, the variation and the absolute GAG content decreased considerably after the decellularisation procedure and remained unaltered after dialysis. About 58 – 10% of methacrylated and decellularised material could be obtained from the original tissues (expressed in dry weight).

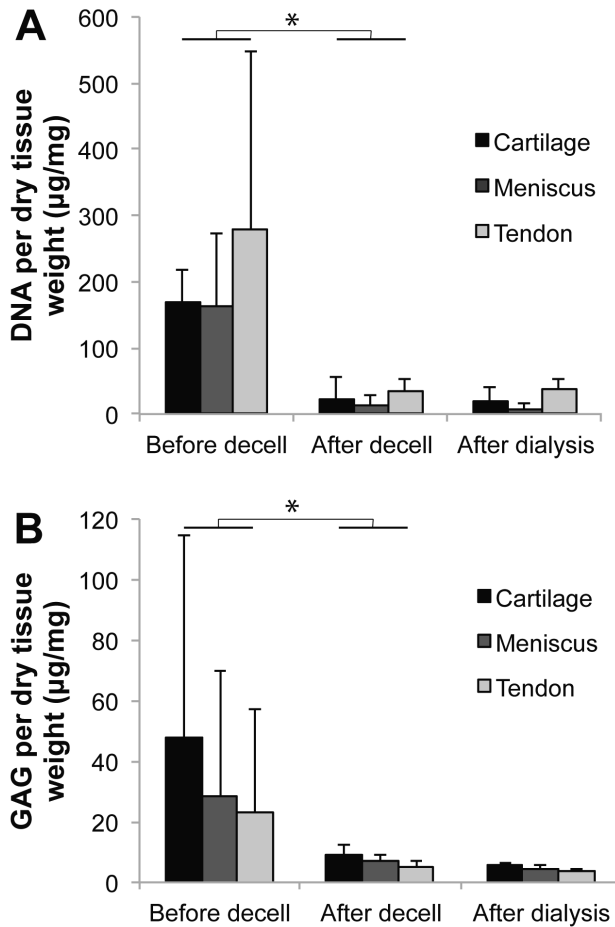


**Figure 7.2: The effect of the decellularisation protocol on DNA and glycosaminoglycan (GAG) content of equine cartilage, meniscus and tendon tissues.** (A) The DNA content of all tissues was significantly reduced by the decellularisation protocol. (B) The GAG content of all tissues directly after harvesting from the knee joint (before decell) shows large standard deviations, caused by donor and location variations. The subsequent decellularisation procedure significantly reduced and standardised the GAG contents.

### 7.3.2 Characterisation of tissue derived matrices

The decellularised cartilage, meniscus, and tendon matrices were successfully digested with pepsin enzymes until clear or close to clear solutions were obtained. Short treatment of the tissue particles (cartilage) or fibers (meniscus and tendon) with pepsin resulted in viscous substances, whereas overnight treatment resulted in low-viscosity solutions. Overnight digestion was used to

facilitate the methacrylation procedure. Gel electrophoresis showed that all digested tissues consisted of polymers with a molecular weight predominantly in the range of 130–300 kDa (Figure 7.3A). The profile of the collagen I solution reflects the collagen monomers (two subunits), dimers (two subunits), and trimers. This typical profile can also be observed in the tendon and meniscus digests. The collagen type II control only displays monomers with one subunit. This single unit monomer can also be found in the cartilage digest. Successful methacrylation of the solutions was confirmed with NMR by the double peak that emerged between 5 and 6 ppm after methacrylation of all three tissue digests (Figure 7.3B-G). Comparing the stiffness of methacrylated tissue digests (cartMA, menMA, and tendMA) with Gel-MA and nonmethacrylated tissue digests revealed significant variations (Figure 7.4). CartMA was stiffer than all other groups (66.2 – 11.9 kPa,  $p < 0.05$ ) and Gel-MA was stiffer (33.8 – 6.5 kPa,  $p < 0.05$ ) compared to menMA (15.1–5.4 kPa) and tendMA (11.4–0.6 kPa). The non-methacrylated tissue digests remained low-viscosity solutions after treatment with UV light and, therefore, their stiffness could not be determined. Considering the variable degree of stiffness and to functionalise the existing Gel-MA hydrogel platform, the methacrylated tissue digests were blended with Gel-MA for the cellular differentiation experiments.

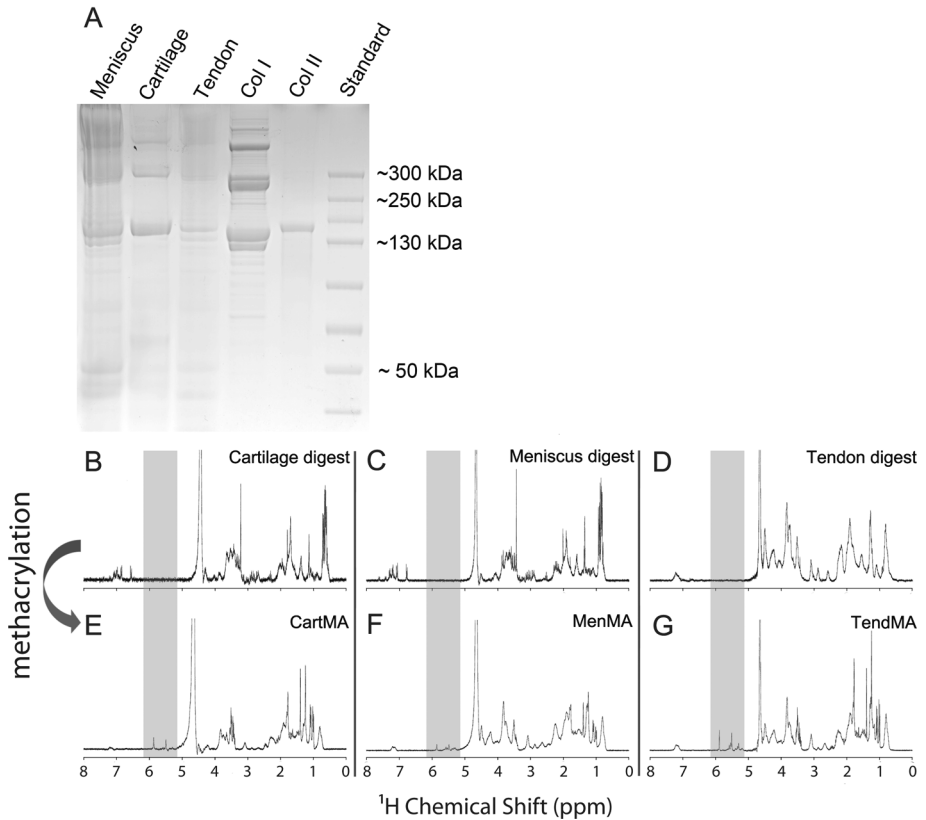


**Figure 7.3: Characterisation of tissue-derived matrices.** (A) Protein gel of tissue digests, collagen type I and II. (B-D) Nuclear Magnetic Resonance (NMR) of the tissue digests shows an inhomogeneous tissue profile after the decellularisation procedure, reflecting the natural polymers. (E-G) The two peaks that appeared after methacrylation (shaded area, between 5-6 ppm) show the presence of vinyl protons, and confirm the success of the methacrylation procedure.

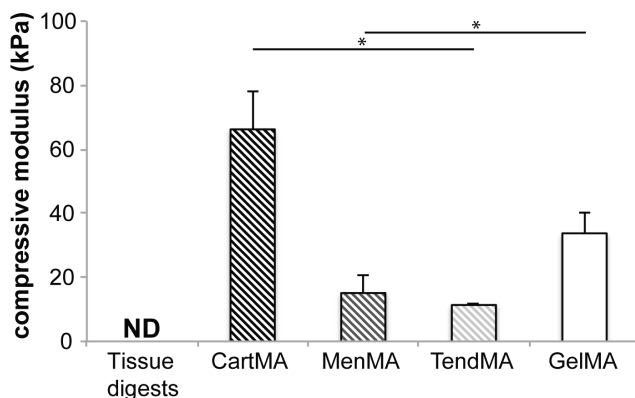


**Figure 7.4: Compressive modulus of photocrosslinked 10% hydrogels.** Non-methacrylated tissue digests were not crosslinkable and hence their compressive modulus could not be determined (ND). The compressive modulus of crosslinked tissue digests (cartMA, menMA and tendMA) and Gel-MA varied significantly.

### 7.3.3 Viability and cartilage matrix formation by embedded chondrocytes

Encapsulation of chondrocytes resulted in high viability at day 1 in all tissue-derived matrix hydrogels (Figure 7.5A). During *in vitro* culture, the tendon samples rapidly disintegrated for all chondrocyte donors and could, therefore, not be included in the differentiation analysis. Gel-MA gels had a higher stiffness 1 day after cell encapsulation compared to the cartilage, meniscus, and tendon groups (Figure 7.5B). A comparable pattern was observed after 6 weeks of culture. The DNA and GAG content and GAG/DNA of hydrogels was comparable for all groups after 4 weeks, but it was significantly higher in the Gel-MA group compared with cartilage and meniscus after 6 weeks (Figure 7.5C-E). The absolute GAG content in the Gel-MA control samples was 1.17 – 0.28  $\mu\text{g}/\text{mg}$  wet weight after 4 weeks and increased to 2.73 – 2.13  $\mu\text{g}/\text{mg}$  after 6 weeks of culture. GAG and DNA in all experimental groups were significantly higher than the cell free control samples. The superior cartilage-specific matrix formation after 6 weeks in the Gel-MA group was confirmed by histology for GAGs (Figure 7.5F) and immunohistochemistry for collagen type II (Figure 7.5G). The differences between the experimental groups at week 4 were comparable to week 6. Therefore, only week 6 data were presented for both cell types. The cell free cartilage gels contained no significant traces of GAGs and collagen type II after 6 weeks.

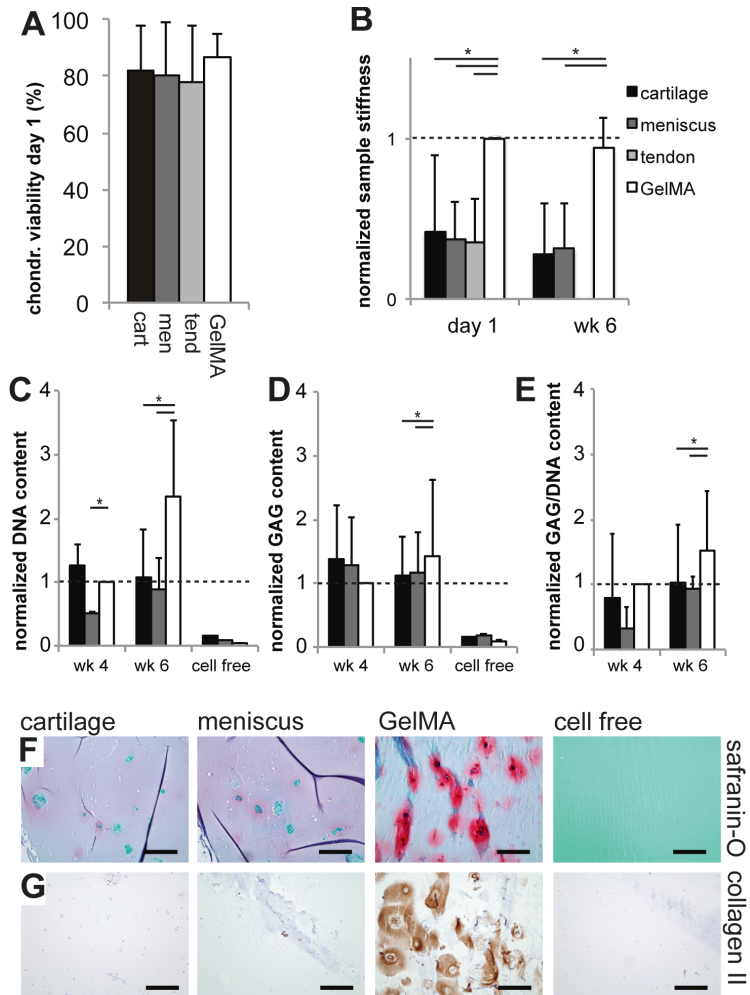


**Figure 7.5: Survival and chondrogenic differentiation of chondrocytes embedded in the tissue-derived matrix gels.** (A) The cartilage, meniscus and tendon gels were not cytotoxic for embedded chondrocytes; (B) the stiffness of the tissue-derived hydrogels was lower than Gel-MA directly after encapsulation (day 1) and after 6 weeks of culture; (C-E) the DNA, GAG and GAG/DNA values after 6 weeks of culture were lower in both experimental groups compared to the Gel-MA group; (F) GAG formation (red) and (G) collagen type II content (brown) were superior in the Gel-MA group after 6 weeks. The tendon group disintegrated during culture of chondrocytes and is therefore not displayed for GAG and DNA content. The DNA, GAG and GAG/DNA content were normalised per donor to Gel-MA week 4; sample stiffness was normalised to Gel-MA day 1. All scale bars are 200  $\mu\text{m}$ ; "cell free" sample is cartilage gel.

### **7.3.4 Viability and cartilage matrix formation by embedded MSCs**

MSCs in all experimental groups retained a high viability 1 day after encapsulation in the hydrogels (Figure 7.6A). The stiffness of Gel-MA gels was highest 1 day after encapsulation of the MSCs (Figure 7.6B). Gel-MA and tendon gels showed superior stiffness after 6 weeks of cell culture. The DNA content was higher in the tendon and Gel-MA gels compared to the cartilage and meniscus gels, both after 4 and 6 weeks of culture (Figure 7.6C). A comparable amount of GAG was measured for all groups; only the cartilage gels had a statistically lower amount than the Gel-MA group (Figure 7.6D). The absolute GAG content in the Gel-MA control samples was 3.48 – 3.62  $\mu\text{g}/\text{mg}$  wet weight after 4 weeks and 3.82 – 4.38  $\mu\text{g}/\text{mg}$  after 6 weeks of culture. The GAG/DNA values for the cartilage and meniscus gels were larger than found in the Gel-MA group (due to a lower DNA content in cartilage and meniscus gels), although these differences were not statistically significant. Staining of GAGs and collagen type II showed abundant cartilage-specific matrix formation by MSCs in all groups (Figure 7.6F, G).



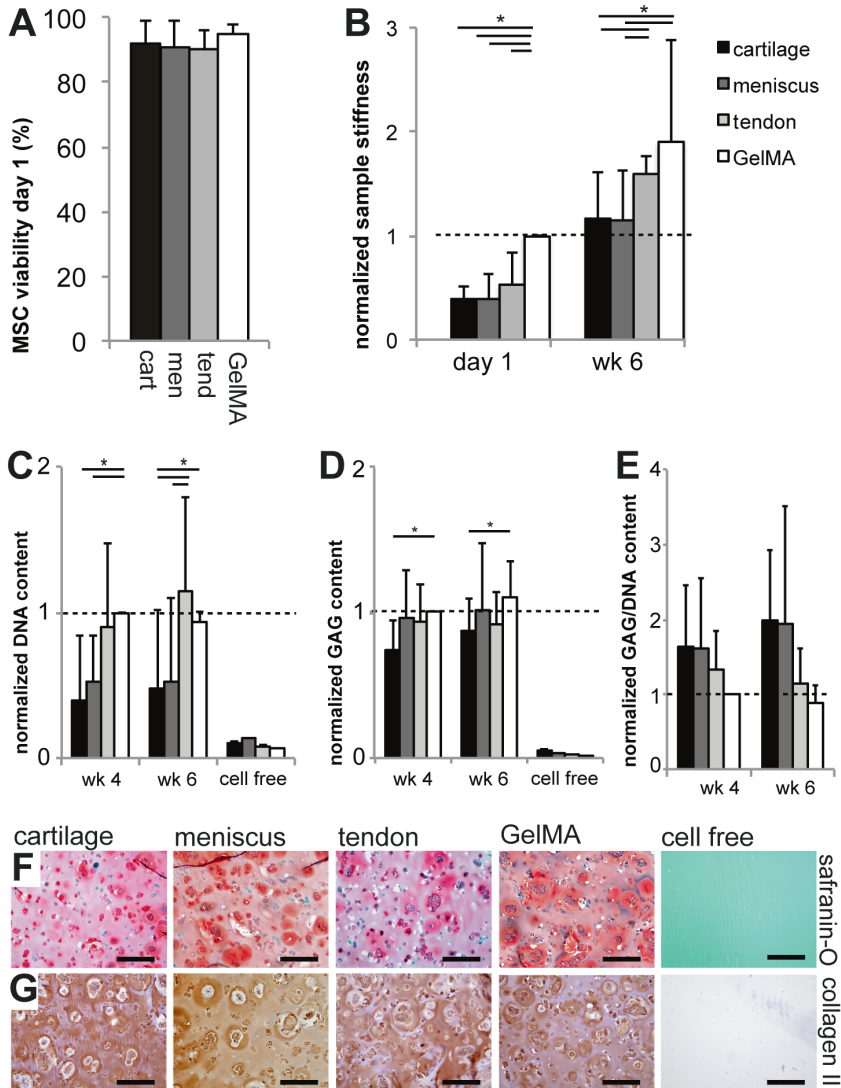


**Figure 7.6: Survival and chondrogenic differentiation of MSCs embedded in the tissue-derived matrix gels.** (A) The cartilage, meniscus and tendon gels were not cytotoxic for embedded MSCs; (B) directly after encapsulation of the MSCs (day 1), the stiffness of Gel-MA samples was highest; after 6 weeks of culture, Gel-MA as well as the tendon group were stiffer; (C-D) differences were observed in the DNA and GAG content of the experimental groups; (E) GAG/DNA content was higher in the cartilage and meniscus gels, although this difference was not statistically significant; (F) GAGs (red) and (G) collagen type II (brown) localisation in all groups after 6 weeks. The DNA and GAG content were normalised per donor to Gel-MA week 4; sample stiffness was normalised to Gel-MA day 1. All scale bars are 200  $\mu$ m; “cell free” sample is cartilage gel.

### 7.3.5 Gene expression levels

The poor interaction of the chondrocytes with the various tissue cultures (Figure 7.5) led to insufficient RNA yields in the cartilage and meniscus groups (the tendon group having disintegrated and not being available for that reason), so that the chondrocytes were excluded from the gene expression analysis. In contrast, the RNA yields of MSCs were sufficient for all samples. ACAN, and COL2 expression was similar for all experimental groups (Figure 7.7). The expression of COL1A1 was significantly lower in meniscus than in cartilage gels. Catabolic enzyme MMP-13 and MMP-14 expression was significantly lower in the tendon group compared with Gel-MA and the cartilage group respectively. These were the only target genes for which a significant difference existed between the experimental conditions.

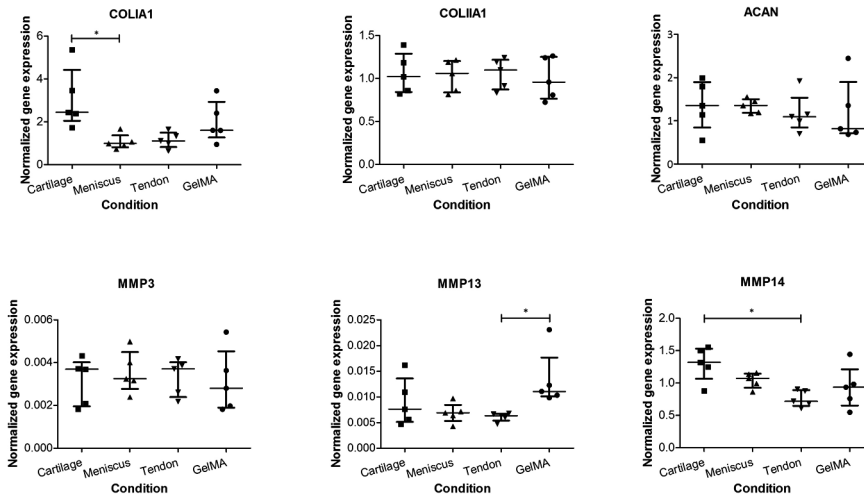


**Figure 7.7: Gene expression by MSCs in tissue-derived matrix gels.** Gene expressions for aggrecan and collagen type II were similar in all hydrogels cultured with MSCs. Collagen I expression was higher in the cartilage hydrogel compared to meniscus. MMP-3 expression was similar in all cultures, whereas expression of MMP-13 and MMP-14 was lower in tendon gels compared to Gel-MA and cartilage respectively. Separate data points were presented (n=5) including the median and interquartile range.

## 7.4 Discussion

In this study, crosslinkable hydrogels were created, based on matrix derived from cartilage, meniscus, and tendon tissues. These substrates allowed the biological functionalisation of the existing Gel-MA hydrogel system, in which they influenced the quantity and quality of matrix produced by embedded cells. All tissue types negatively influenced outcomes for chondrocytes, whereas encapsulated MSCs exhibited variable differentiation patterns, depending of the type of tissue the matrix gel was derived from.

To our knowledge, this is the first report in which decellularised tissues are covalently cross-linked into stable hydrogels. Previously, the Badylak group has derived hydrogels from the extracellular matrix of the dermis, urinary bladder, and the central nervous system [241, 242, 255]. These hydrogels allowed the infiltration and adhesion of cells and influenced their differentiation. In addition, hydrogels derived from heart, cartilage, and adipose were recently shown capable of supporting tissue formation by embedded cells [243]. Analogous to our work, the hydrogels were obtained by pepsin digestion of the respective tissues. However, only physical crosslinking of the natural polymers was accomplished, resulting in considerable contraction of the hydrogel constructs during culture. This behavior is comparable to other natural polymer networks like collagen gels and fibrin glue [239, 254, 256]. The resulting shape instability, however, is unfavourable for the sustainable filling and regeneration of a tissue defect, especially for load-bearing tissues such as cartilage. We have now successfully overcome this issue by covalent cross-linking of the matrix-derived hydrogels through the addition of methacrylamide groups. These substrates were subsequently incorporated into Gel-MA hydrogel, because we aimed to further develop this versatile hydrogel, which was proven efficient for cartilage matrix formation by embedded cells [123, 214, 228]. The methacrylation procedure resulted in a very substantial increase in the compressive modulus, which was largest in the cartilage-derived matrix and of the same order of magnitude as occurring in the Gel-MA reference matrix. The methacrylation procedure can hence be considered as an important asset in the production of extracellular matrices for tissues that have to withstand biomechanical forces.

The chondrogenic potential of MSCs in extracellular matrix gels was greater than that of chondrocytes. MSCs have previously shown capable of forming a cartilage specific matrix in 3D-hydrogel systems [257]. The quality and quantity of cartilaginous tissue formed by MSCs was found comparable to that of chondrocytes, although dependent on the type of hydrogel [258]. From our work

we can conclude that equine MSCs thrive relatively well in Gel-MA gels. Nevertheless, chondrocytes from the different donors did show less donor variation than the MSCs, which is a known phenomenon for the latter cell type [259]. Still, MSCs are of great interest as an allogeneic cell source for the single-stage repair of cartilage tissue [260]. A limitation for the application of MSCs *in vivo* is that they require the addition of growth factors to be directed toward the chondrogenic lineage [253]. Recently, chondrocytes have shown they are capable of guiding MSC differentiation, and therefore, a coculture of MSCs and chondrocytes holds promise for the repair of cartilage tissue [260].

The absolute GAG production by chondrocytes embedded in the Gel-MA hydrogels is similar to the amounts reported in previous *in vitro* studies [123, 214]. However, a consistent negative effect of the incorporation of all three tissue derived components was observed on the differentiation of chondrocytes. This is in line with previous reports on the culture of chondrocytes on collagen matrices [245-247]. Collagen type II matrix induces catabolic pathways in cultured articular chondrocytes, including the upregulation of MMP-3, MMP-13, and MMP-14 [246, 247]. In addition, earlier work from our group showed poor GAG production of chondrocytes cultured on decellularised cartilage matrix scaffolds (collagen type II) and even accelerated degradation of the scaffolds [245]. In the current work, scaffold (i.e., hydrogel) disintegration was observed only for the tendon hydrogels (collagen type I), which may be a result of the catabolic activities of the chondrocytes, analogous to those observed in osteoarthritis [261, 262]. Unfortunately, we were unable to analyse MMP expression by chondrocytes, since the tendon gels had disintegrated and RNA yield was too low in the cartilage and meniscus groups. In contradiction to these findings, successful cultures of chondrocytes were shown on synthetic collagen type I and II matrices [263-266]. The literature is thus inconclusive about the effect of collagen matrices on chondrocyte behavior, although the upregulation of inflammatory pathways has been clearly indicated.

In interpreting cell–matrix interactions, the difference between pure collagen scaffolds and tissue-derived matrices should be taken into account. In the latter, other matrix components, growth factors and/or signaling molecules may contribute to effects on cell behavior [233, 235]. For example, it was shown that several growth factors were retained in decellularised bladder submucosamatrix [267] and small intestinal submucosa matrix [268]. The decellularisation protocol in this study was relatively mild compared to previous studies [237]. Therefore, a panel of growth factors is likely to be retained within the matrix, although this was not specifically studied here. The main components of the

tissue-derived matrices were shown to be collagens type I and II, the proportions depending on the original tissue. However, the exact biochemical composition of the polymers, for example, the amount of available reactive amines to be methacrylated, remains unknown. As a result, the degree of methacrylation of the tissue-derived matrices was not controlled, and will hence vary between tissue types and tissue donors. This limitation should be taken into account during the interpretation of the responses of embedded cells.

The absence of trypsin as a protein-cleaving enzyme in the current protocol lead to the preservation of some of the GAGs (~10%, compared to 0% when treated with trypsin [245]) while the DNA content could be decreased to acceptable standards, that is, below 50 µg/mg dry tissue [237]. Chondrocytes probably benefit more from GAG than collagen components in hydrogel cultures [123, 214]. Therefore, the current outcomes could be improved by a modified decellularisation protocol, preserving still more GAGs.

For the chondrogenic differentiation of MSCs, our results show a slight preference for a collagen type I rich matrix (tendon gels) over collagen type II (cartilage gels). For example, MSCs proliferated more in tendon and Gel-MA gels and the sample stiffness was higher after culture, compared to meniscus and cartilage gels. In addition, MSCs in the tendon gels showed reduced expression of MMP-13 and MMP-14, although gene expression of cartilage-specific matrix genes was similar. Recently, Yang et al. also analysed the effects of tendon-derived matrix on MSCs and found a reduced expression of collagen type I, which is considered a marker for inferior fibrocartilage formation [256]. The lowest GAG production by MSCs was observed in the cartilage matrix gels, along with a higher gene expression of collagen type I. Previous research, however, revealed a stimulatory effect of cartilage matrix on the chondrogenic differentiation of MSCs *in vivo* [269, 270]. In addition, other work showed that chondrogenesis of bovine MSCs was slightly enhanced in collagen type II compared with collagen type I gels [271]. It appears that certainly collagens influence the differentiation of MSCs, yet the optimal collagen composition still needs to be unraveled and will require specific tailoring for the target tissue to be engineered.

Further research should identify the specific biological cues in native tissues that are favorable to cells in tissue engineering. Unfortunately, the specific factors responsible for the cell behavior in decellularised tissues are still largely unknown. A better understanding of the native cell niche can guide the process of producing biomimetic materials.

## 7.5 Conclusion

Crosslinkable hydrogels were created from cartilage, meniscus, and tendon tissue through a process that included enzymatic digestion and methacrylation. The methacrylation procedure successfully increased the stiffness of these matrices, which is a critical factor in the manufacturing of scaffolds for use in musculoskeletal tissue repair. Moreover, a stable hydrogel platform was created by covalent incorporation of these tissue-derived matrices in versatile Gel-MA hydrogels. The response of embedded cells to these matrices depended on the cell type and the matrix components. Chondrocytes performed relatively poor in the tissue-derived matrix gels compared with the Gel-MA control group. The chondrogenic differentiation capacity of MSCs was comparable across all hydrogels.

### Acknowledgements

The authors would like to thank Karin van Leersum and Trudy van Ruiten for their assistance in the experimental work. The antibody against collagen type II (II-II6B3), developed by T.F Linsenmayer, was obtained from the DSHB developed under the auspices of the NICHD and maintained by The University of Iowa, Department of Biology, Iowa City, IA 52242. Jetze Visser was supported by a grant from the Dutch government to the Netherlands Institute for Regenerative Medicine (NIRM, grant No. FES0908) and Jos Malda was supported by the Dutch Arthritis Foundation.

## **Chapter 8**

### Discussion and future work

---

## **Discussion and future work**

The development of hydrogels and other biomaterials for cartilage tissue engineering is an active field of research, with universities and companies around the world striving to find the optimal materials for replacing or regenerating cartilage. This Chapter summarises some of the recent findings related to the development of hydrogels for cartilage regeneration.

### **8.1 Hydrogel composition**

In cartilage tissue engineering, hydrogels are being widely used as both models and as biomaterials for clinical application. The composition and biochemical properties of hydrogels vary enormously, and Chapters 3 and 5 show that these properties have major consequences for chondrocyte differentiation and matrix production. Despite this, there is relatively little evidence and research underpinning the materials that are currently used for clinical cartilage repair.

Aims iii) and iv) of this thesis were to functionalise Gel-MA hydrogels with moieties to promote chondrogenesis and matrix production. In order to incorporate these moieties stably into Gel-MA, it was necessary for them to be covalently crosslinked into the hydrogel network. To achieve this, we used methacrylic anhydride to conjugate methacrylate (or methacrylamide) groups to each of the target moieties. The importance of covalent attachment, as opposed to physical entanglement, was displayed using low and high molecular weight polysaccharides, namely heparin (MW ~ 17-19 kDa, Sigma) and HA (MW 950 kDa, Novozymes). When unmodified heparin was incorporated into Gel-MA hydrogels, virtually all of the heparin diffused out of the gels within 24 hours (Figure 8.1). Modification of heparin with methacrylate groups (Hep-MA) resulted in stable incorporation, with no change in GAG content over 14 days (Figure 8.1). In comparison, incorporation of unmodified HA, with a much higher molecular weight, resulted in a more gradual and ultimately incomplete loss of HA from Gel-MA hydrogels (Figure 8.1). Nevertheless, ~80% of the HA initially incorporated diffused out of the gels within 14 days. In contrast, the presence of a hydrogel network in gels containing HA-MA following papain or proteinase K digestion indicates that the HA-MA is independently covalently crosslinked. It was not possible to quantify HA-MA in the gels using the DMMB assay, since once crosslinked, HA-MA is not digested by papain or proteinase K, and upon mechanical disruption does not re-enter solution. These retention studies highlight the importance of covalent bonding for stable incorporation, but we cannot be certain of the effect that modification has on the interactions with biological systems.



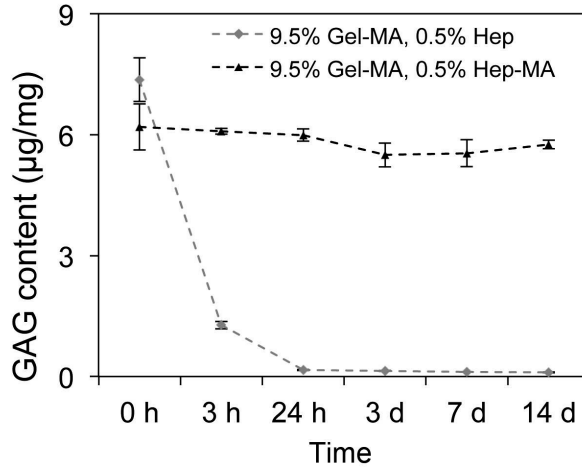


**Figure 8.1: Retention of heparin and heparin-methacrylate in cell-free Gel-MA hydrogels in PBS over 2 weeks.**

This is particularly important since the mechanisms by which HA-MA enhanced outcomes in Chapter 5 are not yet understood. Preliminary evidence suggests that link protein, which stabilises the binding of aggrecan to HA in cartilage, cannot bind to HA-MA (immunostaining results – data not shown). Further, other studies have shown that as the degree of functionalisation increases, the rate of digestion with hyaluronidase decreases [272]. In a preliminary study using PEG-based hydrogels (Qgel, Switzerland), the addition of 3.3 mg/mL HA (Novozymes) into the hydrogels had no effect on GAG production or changes in construct stiffness during 14 days culture (data not shown). In addition, in Chapter 4, we did not observe differences in the cultures with or without HA, although this may be a result of an overly high HA concentration, which was chosen primarily to facilitate printing.

## 8.2 Hydrogel structure and properties

Hydrogels are inherently ‘soft and watery’ materials, with a generally low modulus and fracture energy (Figure 8.2). Mechanical properties are often cited as a limitation of hydrogels for cartilage applications, given the loads that this tissue must withstand. Like cartilage, damage to Gel-MA hydrogels is not easily repaired, so the gel construct must be sufficiently strong to withstand the loads within the joint. The stiffness of Gel-MA based hydrogels have been investigated in some detail in this thesis, including the changes in stiffness are a product of cell-secreted ECM.

One of the advantages of synthetic hydrogels over natural hydrogels is the ability to tightly control the properties – such as polymer chemistry, molecular weight, cross-link density, and degradation mechanisms and kinetics [273]. In contrast, with the notable exception of ionic crosslinking, most conventional crosslinking mechanisms for natural hydrogels have traditionally been incompatible with cells. The most commonly used crosslinking mechanisms for natural hydrogels include glutaraldehyde, carbodiimide, low-wavelength UV irradiation or heating [273]. While it is undeniable that synthetic hydrogels offer a degree of versatility that natural hydrogels cannot, in this thesis we have shown that it is possible to tailor both the mechanical properties and biochemical composition of Gel-MA hydrogels. In Chapter 4 we show that the compressive modulus of Gel-MA hydrogels can be easily manipulated over a wide range (5 to 180 kPa), and by increasing the precursor concentration beyond 20% (w/v), we expect that the stiffness can be further increased.

Double network hydrogels offer marked improvements in strength compared to their single network counterparts. Double network hydrogels consist of two interpenetrating, crosslinked polymer networks. Double network hydrogels are most commonly fabricated by crosslinking each network sequentially: the first polymer is crosslinked to produce a single network hydrogel; it is then swelled in a solution of the second polymer, followed by crosslinking of the second network. Most double networks are produced from synthetic polymers, and by carefully selecting materials with appropriate properties, along with concentrations and crosslink densities, hydrogels with failure strengths approaching those of rubbers can be produced (Figure 8.2) [83]. Although double-network hydrogels were not studied in this thesis, the combination of Gel-MA and HA-MA leads naturally to the question of whether they can be used to form double network hydrogels. One of the key requirements for formation is that the second polymer must be small enough to diffuse into and throughout the first network, at a concentration high enough for the second network to be formed. The high molecular weight of HA-MA would likely necessitate that it is used as the first network, and Gel-MA is used as the second. This technique may also offer biological advantages, since encapsulated cells would be expected to have more exposure and contact with the first network (HA-MA), which may further improve cell differentiation compared to mixtures of Gel-MA and HA-MA

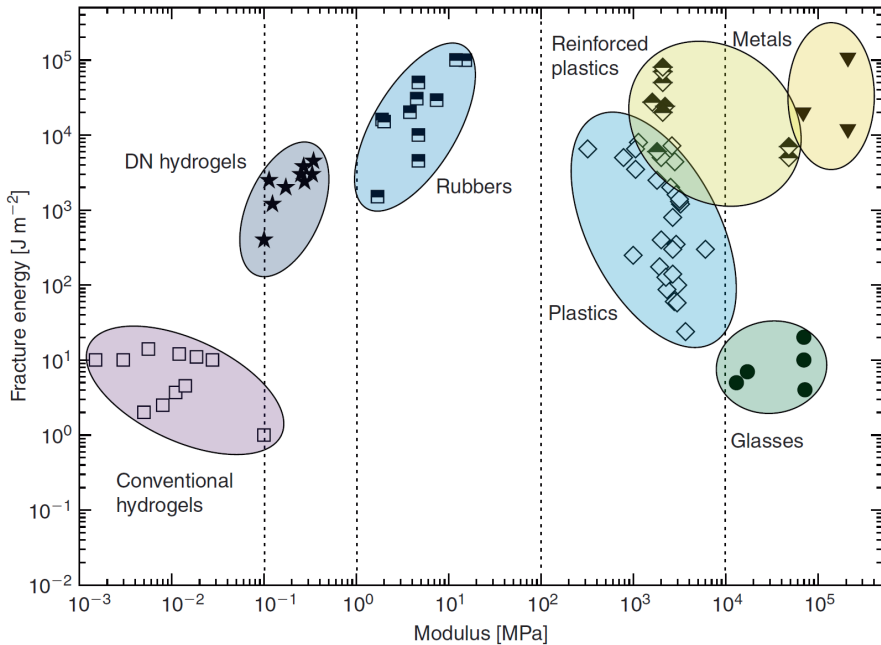


**Figure 8.2: Fracture energy and modulus of common groups of biomaterials, displaying the soft and weak properties typical of hydrogels (from [81]).**

A similar approach was recently reported by Shin et al [124], who formed a first network from gellan-methacrylate, followed by swelling for 2 days in 5-20% Gel-MA, which was crosslinked to form the second network. Single network Gel-MA hydrogels formed from 20% Gel-MA had a swollen polymer content of approximately 10% and a failure stress of approximately 3 MPa. In contrast, double network hydrogels produced using 0.5% gellan-methacrylate and 20% Gel-MA had a swollen polymer content of approximately 15%, and the failure stress increased to nearly 7 MPa. Interestingly, the failure strains were comparable for the single and double network gels, whereas typically failure strains are higher in double network hydrogels. This leads to uncertainty over whether the double network structure provides any real additional benefit over simply mixing the two components in one solution, and performing a single crosslinking step, which was not tested in this study [124].

When interpreting the results of this thesis, in particular the significant impact that a relatively small proportion of HA-MA can have, it is appropriate to ask what the structure of the Gel-MA/HA-MA hydrogels is on a micro-scale. There is some indirect evidence from experimental observations that suggests there may be more to the microstructure than a simple, homogeneously inter-

crosslinked mixture. Firstly, the two polymers, gelatin and hyaluronic acid, are functionalised with slightly different photocrosslinkable groups. Gelatin is predominantly functionalised with methacrylamide groups, while hyaluronic acid is functionalised with more reactive methacrylate groups. Thus during the early stages of photo-crosslinking, methacrylate groups may react more readily than methacrylamide groups. Secondly, the hydrogels mixtures studied here were predominantly Gel-MA, with relatively small quantities of HA-MA. For example, in Chapter 6, two of the experimental groups were 10% Gel-MA and 9.75% Gel-MA with 0.25% HA-MA. The hydrogel constructs made from 10% Gel-MA are very rapidly and completely digested by proteinase K – they are typically solubilised in approximately 1 hour. In the Gel-MA/HA-MA mixture, there is an approximately 40-fold mass excess of Gel-MA over HA-MA. If we assume that they are crosslinked with no preference or distinction between the two polymers, then we would expect that due to this significant excess of Gel-MA, that relatively few methacrylate groups on HA-MA would be crosslinked to other methacrylate groups on HA-MA. As such, when the Gel-MA component is removed via proteinase digestion, we would expect the entire network to fall apart. Contrary to this expectation, this does not happen; when the Gel-MA component of hydrogels formed from 9.75% Gel-MA and 0.25% HA-MA is digested away, a much softer, yet stable hydrogel remains. The presence of this hydrogel after digestion indicates that perhaps the methacrylate groups on hyaluronic acid do preferentially crosslink with other methacrylate groups, resulting in a network of crosslinked hyaluronic acid that is in part independent from the Gel-MA network.

If this were the case, then the structure of hydrogels formed from mixtures of Gel-MA and HA-MA would show some elements of double network hydrogels, with two interpenetrating, partly independently crosslinked networks. This would very likely have major implications for cell encapsulation, and potentially help interpret an otherwise unexplained finding from Chapter 5: the impact that a small amount of HA-MA had on chondrocyte phenotype, and in particular, cell morphology. In Chapter 5, chondrocytes had remarkably different morphologies when encapsulated in 10% Gel-MA compared to 9.5% Gel-MA with 0.5% HA-MA. In the mixture of Gel-MA and HA-MA, why should the presence of 0.5% HA-MA prevent the chondrocytes and attaching to Gel-MA, as they do in 10% Gel-MA hydrogels, when Gel-MA accounts for 95% of the polymer content? Is HA-MA somehow shielding the chondrocytes from Gel-MA? This question has particular relevance when we consider the hypothesis described above on the microstructure of Gel-MA/HA-MA hydrogels. If the hypothesis were correct, then, during crosslinking, the more reactive

methacrylate groups would crosslink first, forming an initial network of HA-MA, and thereby encapsulating the chondrocytes in a network of predominantly hyaluronic acid. The secondary network of Gel-MA would crosslink next, but crosslinking of the Gel-MA network next to chondrocytes would be restricted by the existing HA-MA network. Thus on a macro scale, the chondrocytes are embedded in a hydrogel that contains 95% Gel-MA by mass and only 5% HA-MA, whereas their pericellular environment, which is critical for cell attachment, cell morphology and differentiation, could actually contain a higher proportion of HA-MA. Furthermore, this suggests that the methacrylation of hyaluronic acid is critical for its function in the gel, and may help explain why we saw no impact on cell differentiation, matrix production or mechanical properties when we added unmodified HA to PEG (data not shown) and Gel-MA hydrogels (Chapter 4).

Importantly, though the discussion above is not implausible, it is based on limited evidence. However given the remarkable impact on cell morphology, further studies to characterise the microstructure of the hydrogels are justified.

### **8.3 Matrix organisation**

The ECM of cartilage is highly organised over several length scales. At the cellular level, the matrix composition and structures depend on the proximity of the matrix to cells, ranging from the pericellular matrix to the more distant interterritorial matrix. On a larger scale, cartilage tissue is organised into distinct zonal structures, with different matrix physicochemical properties and cell phenotypes within each zone.

#### *Spatial organisation*

Controlling the spatial distribution of the ECM produced within a hydrogel is a crucial requirement for tissue engineering. In living tissues, the ECM occupies the bulk of the space between cells, and in cartilage, the ECM accounts for the large majority of the tissue volume. Allowing the cell-secreted matrix to spread throughout hydrogel constructs has been a challenge, with matrix typically being confined to the pericellular regions. In Chapter 3, Alcian Blue staining showed that ECM was well distributed through Gel-MA constructs, concurrent with a dramatic increase in stiffness during 3 weeks culture. In Chapter 5, however, the stiffness of Gel-MA-only constructs changed much less during culture. This difference is most likely caused by differences in the initial stiffness of each group of hydrogels, along with differences in the way in which they were crosslinked. In Chapter 3, Gel-MA hydrogels were relatively soft on day 1 (~1.5 kPa), while in Chapter 5 they were significantly more rigid (~15

kPa), in part because the gels in Chapter 3 were exposed to air during crosslinking, while those in Chapter 5 were enclosed. This indicates that the initial stiffness influences matrix organisation, and probably also chondrogenesis. Studies with other hydrogel materials have shown similar outcomes using different hydrogels, with better matrix distribution in gels that have lower initial crosslinking densities [80, 122].

In Chapter 5, the distribution of collagen type II was much better in Gel-MA constructs containing HA-MA than in Gel-MA controls. We expect this to be a result of the formation of larger pore sizes; a consequence of the lack of mixing that Gel-MA and HA-MA display. This represents the most important finding in this thesis, and creates the possibility phase for separation to be a design specification for biomedical hydrogels. This concept of using phase-separated polymer mixtures to enhance ECM distribution, to our knowledge, has not been explored elsewhere.

### *Zonal organisation and structure*

Recreating the zonal structure of cartilage in engineered cartilage tissue has not been displayed thus far, and traditionally it has perhaps been a secondary requirement to generating hyaline cartilage as opposed to fibrous tissue. Nevertheless, zonal organisation is responsible for a critical part of cartilage function, and recreating the zonal organisation is a key goal of next generation cartilage therapies. Previous studies have reported that zonal chondrocytes respond differently to HA and CS [106], and that these GAGs can guide the differentiation of MSCs towards chondrocytes with zonal phenotypes [184]. Both superficial and deep zone chondrocytes responded most positively to CS, however it was unclear from this report what concentration of CS was used, making comparisons difficult to make [106]. Using MSCs, Nguyen et al. concluded that 9% PEG hydrogels supplemented with 9% CS and 2% MMP degradation sequences were suitable for promoting the superficial zone phenotype, while 19% PEG hydrogels with 1% HA were optimal for deep zone differentiation [184]. These selections were based on the relative expression/production of collagen type II and GAGs, with low GAG content and high collagen type II expression being indicative of the superficial phenotype, and high GAG content and low collagen type II indicating the deep zone phenotype. These metrics are not well established as markers for distinguishing between different zones of cartilage, and further evaluation is required to establish the true zonal phenotype of MSCs in these gels.

Based on these reports, in Chapter 5 we isolated and separately encapsulated cells from the superficial and middle/deep zones. The inclusion of HA-MA had a significant impact on chondrocyte phenotype and matrix production, but the responses shown by superficial chondrocytes were closely mirrored by middle/deep chondrocytes. This may also be a consequence of the cell source, since it remains unclear how much of the true zonal phenotype is retained in osteoarthritic cartilage. Hydrogel printing is a promising technology for the assembly of zonal structures, but at this stage, the optimal hydrogel compositions required to direct zonal differentiation are not yet known.

#### **8.4 Photocrosslinking mechanisms**

Depending on the chemical moieties used for crosslinking, hydrogels networks can either form via step or chain growth. Polymers can be readily functionalised with acrylate, methacrylate and methacrylamide functional groups, and as a result these functionalities have been commonly used for photocrosslinking in the past decade. More recently there has been interest in hydrogels that are crosslinked via orthogonal chemical groups, such as thiol-norbornene [274] and thiol-(meth)acrylates [222]. These hydrogels are predominantly crosslinked via the reaction of thiols to either (meth)acrylate or norbornene, and thus polymerisation proceeds via step growth rather than chain growth. Step growth hydrogels have emerged as a promising system for the next phase of hydrogel research and development, and recent studies suggest that both mechanical properties [275] and cell responses, which are particularly relevant for cartilage biology [222], may be superior in step polymerised hydrogels.

To increase crosslinking kinetics, thiol acrylate/norbornene hydrogels are still generally crosslinked by UV light in the presence of a photoinitiator, such as IC2959, but critically, the role of reactive oxygen species (ROS) is very different to (meth)acrylate crosslinking. In aqueous systems containing oxygen, the photo-generated radicals react rapidly with oxygen to form ROS. Despite being highly reactive, ROS cannot initiate crosslinking of (meth)acrylates, and therefore they accumulate and potentially react with cells. This results in a lag phase during crosslinking, in which few photo-radicals initiate polymerisation. In Chapter 4, this lag phase was found to be approximately 4 minutes in our empirical model using Gel-MA hydrogels. The crosslinking mechanism in thiol-norbornene or thiol-(meth)acrylate systems is somewhat different: photogenerated radicals abstract a hydrogen atom from thiol groups, forming thiyl radicals, which react with the unsaturated carbon moiety, such as (meth)acrylate or norbornene. The key distinction is that ROS can also abstract a hydrogen atom from thiol groups, and thus any ROS that are generated are

consumed in the crosslinking reaction. This eliminates the oxygen inhibition issues for which (meth)acrylate systems are notorious [224], and crucially for cell-encapsulation, prevents the accumulation of intracellular ROS.

Hydrogels that are polymerised via step or chain growth have been compared in a number of recent publications [222, 275]. Chain polymerised hydrogels contain regions of high and low crosslink densities, and during loading, the weak points fracture relatively easily [276]. In contrast, step polymerised hydrogels display a higher degree of homogeneity in the network topology, leading to more robust mechanical properties [275]. The tensile toughness of step polymerised PEG hydrogels were consistently higher than their chain polymerised counterparts [275], but it is unclear whether the distinction between the network structures formed from step or chain crosslinked PEG hydrogels would also apply to Gel-MA. The PEG hydrogels are typically linear polymers that are functionalised at each end. In comparison, Gel-MA contains a number of crosslinkable domains along each chain, and it is perceivable that the network structure resulting from chain polymerised Gel-MA may be significantly different to that resulting from chain crosslinked PEG diacrylate. More specifically, crosslinked Gel-MA networks may be inherently more homogeneous than PEG diacrylate.

Roberts and Bryant have recently investigated the role of ROS on chondrocytes during crosslinking of PEG diacrylate compared to PEG-thiol-norbornene (PEG-TNB) [222]. When present in high concentrations, ROS can be involved with cell signalling and regulatory pathways, and can have deleterious effects on cell structures. In both hydrogels, photocrosslinking was achieved by 10 minutes exposure to 352 nm light at an intensity of 6 mW/cm<sup>2</sup>, in the presence of 0.05% IC2959 [222]. As expected from the differences in crosslinking mechanisms, ROS accumulation was greater in the PEG diacrylate hydrogels. More striking, though, was the difference in the composition of the matrix secreted by bovine chondrocytes in each of the hydrogels over 14 days (Figure 8.3). In both degradable and non-degradable gels, the matrix produced in the chain-polymerised hydrogels stained strongly for collagen type X, a marker of hypertrophic differentiation. No collagen type X was detected in the step polymerised PEG hydrogels, indicating that crosslinking chemistry had a remarkable impact on biological outcomes (Figure 8.3). The authors suggest that the intracellular ROS produced during crosslinking was likely to be responsible for the differences, but further studies are required to confirm this hypothesis.



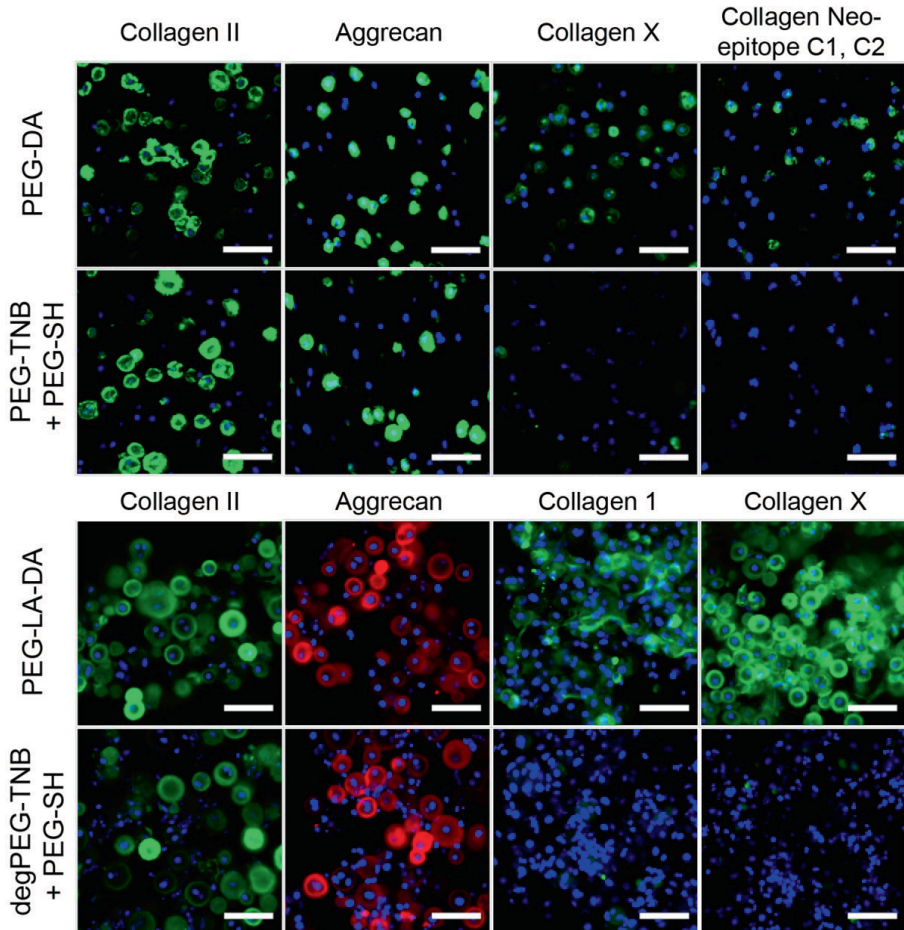


**Figure 8.3: The role of crosslinking mechanism and reactive oxygen species in ECM production by chondrocytes.** Immunofluorescence staining of extracellular matrix proteins secreted by bovine chondrocytes encapsulated in either chain or step crosslinked PEG-based hydrogels. Upper panels: chain crosslinked PEG-DA, or step crosslinked PEG-TNB + PEG-SH; lower panels: degradable, chain crosslinked PEG-LA-DA or degradable, step crosslinked PEG-TNB + PEG-SH. Scalebars represent 50  $\mu\text{m}$ . Figure from [222].

These studies have several implications for the research presented within this thesis. Firstly, these studies evaluated hydrogels formed from relatively small PEG chains (in the order of 3 – 10 kDa), whereas the hydrogels we have used are formed from much larger macromers, some with considerably higher viscosity than PEG solutions. In addition, it is difficult to directly compare the rate of ROS generation in our hydrogels during crosslinking. We used the same concentration of photoinitiator, but since we used a lower intensity (~2.7

mW/cm<sup>2</sup>) and longer wavelength light, we would expect that the rate of radical formation would be significantly lower in our system, potentially resulting in lower peak ROS concentrations. Finally, the role of ROS in the signalling pathways of primary bovine chondrocytes may be substantially different to the expanded human chondrocytes evaluated here.

In light of the accumulation of ROS during IC2959-initiated crosslinking of PEG diacrylate hydrogels, along with the extensive deposition of collagen type X, perhaps the low crosslinking efficiencies that we have (unintentionally) used are beneficial for cell encapsulation. ROS are present in all tissues at some level, and are a routine by-product of oxygen metabolism. At low levels they are an important element of cell signalling pathways, but at high concentrations can cause cell damage, direct cell fate, or even initiate apoptosis. In cartilage, high levels of ROS have been shown to disrupt cell signalling, cause inflammation and tissue degradation [277] and importantly, can induce hypertrophy [221]. Cells possess mechanisms to eliminate ROS, and thus the accumulation is a balance between the rate of generation and rate of elimination. Avoiding cell damage and apoptosis during cell encapsulation is critical, and thus lower rates of radical formation may limit the maximum ROS concentration by allowing temporal elimination by cells.

Recent studies on chain and step polymerised hydrogels highlight possible avenues of future research for the hydrogels biomaterials described in this thesis. The mechanical properties of Gel-MA/HA-MA hydrogels require more comprehensive characterisation, including evaluation of failure strength and strain. The potential for step polymerised Gel-MA and HA-MA hydrogels could be investigated using thiolated HA, or thiolated crosslinkers, such as pentaerythritol tetrakis(3-mercaptopropionate) (available from Sigma Alrich). Thiolated HA can be purchased (for example Glyosil® from Glycosan), or for consistency, prepared by the addition of cysteine to HA using EDAC/NHS crosslinking (1-ethyl-3-(3-dimethylaminopropyl) carbodiimide (EDAC), and N-hydroxysuccinimide (NHS)). [223]. Using thiolated HA may result in a combination of crosslinking mechanisms, since based on the ratio of Gel-MA to HA used in this thesis, we would expect a higher number of methacrylamide groups than thiol groups. Following complete conversion of thiols by reaction with methacrylamide, crosslinking would proceed solely via methacrylamide groups. The addition of a thiolated crosslinker could be used to further promote thiol-to-methacrylamide crosslinking.

Methacrylamide modified gelatin is the major component of the materials investigated in this thesis. Gelatin can alternatively be functionalised with methacrylate or acrylamide groups, with differences in the reactivity of the resulting polymers [110, 278]. Methacrylate modification has been achieved via the conversion of carboxyl groups using a linker molecule, such as ethanolamine, followed by conversion of hydroxyls on the linker to methacrylate [110]. No advantages of this indirect modification have been shown, and it has the distinct disadvantage of being more difficult to produce. A detailed comparison of Gel-MA and gelatin-acrylamide has recently been published [278]. As one would expect, gelatin-acrylamide derivatives are more reactive than Gel-MA, thus requiring shorter UV crosslinking times or lower concentrations to achieve gels with similar mechanical properties, but with some compromise of cell viability. For high degrees of functionalisation, both the molecular weight and polydispersity of gelatin-acrylamide increased during functionalisation, suggesting some spontaneous crosslinking. Overall, the slight increase in reactivity of gelatin-acrylamide does not appear to convey substantial benefits compared with Gel-MA.

## **8.5 Clinical status and regulatory pressures**

Clinically, cartilage tissue engineering therapies represent a diverse range of treatment strategies, rationales and outcomes. For the past two decades, cartilage therapies have been at the forefront of translational tissue engineering – albeit with mixed success. To avoid the complexity of OA, most therapies target patients with a single, symptomatic lesion of the femoral condyle or trochlea, with minimal co-morbidities. It is a changing landscape, and competition to gain regulatory approval and bring products to market is fierce. Modern cartilage tissue regeneration therapies are classified as single or two stage therapies, depending on the number of surgeries required. Tables 8.1 and 8.2 summarise the current status of single and two stage cartilage tissue therapies.

Tissue engineering has an indisputable potential to change the healthcare industry, but is far from exempt from market and regulatory forces. The rapid development in the field in the last decade has, to some degree, outpaced the regulatory processes that serve to administer it, and the costs and challenges of gaining regulatory approval and widespread uptake have been the downfall of many ventures [279]. In this challenging and highly fluid field, the companies driving these products are frequently subject to mergers and acquisitions, while others, without prior warning, may cease to exist.

The regulatory framework in place in Europe has made it the first-choice jurisdiction for commercialisation of many regenerative medicine therapies. In 2007, the EU introduced a category called Advanced Therapy Medicinal Products (ATMP) which is the approval required for complex tissue engineered products that include cultured cells or tissues. In comparison, products classed as medical devices are required to obtain a CE mark, which is a far easier approval process. Current cartilage therapies may be classed as an ATMP or medical device, depending on whether cells or tissues are used, and the extent to which they are manipulated or cultured outside of the body. Expansion of cells *in vitro*, as is common in ACI-based therapies, classes these therapies as ATMPs in the EU. The approval process for ATMPs requires rigorous evaluation, including clinical trials, and typically takes many years.

Any therapies with approval prior to the introduction of ATMPs in 2007 were required to undergo re-assessment, and in 2009, after extensive testing, the cell-based cartilage therapy ChondroCelect became the very first ATMP to gain approval. In June 2013, Matrix Applied Characterised Autologous Cultured Chondrocytes (MACI, Genzyme Europe B.V.) became the second ATMP approved for cartilage repair, and also the first combined tissue-engineered medicine approved in the European Union. While some therapies, such as ChondroCelect and MACI, have been able to meet the stringent requirements, others that entered clinical trials, such as Hyalograft C and Cartipatch have been withdrawn from the market (summarised in Table 8.1 and Table 8.2).

In contrast to ATMPs, cell-free therapies are classified as medical devices, and as such only require a CE mark for approval. This is a far simpler, cheaper and faster regulatory approval process, and is a major advantage for cell-free therapies. Chondux and GelrinC use photocrosslinkable hydrogels for cartilage repair, but instead of including cells in the therapy, they are intended to be used in conjunction with microfracture (Table 8.2).

### **8.6 Single vs. two-stage therapies**

Microfracture is the benchmark treatment for isolated cartilage lesions, and benefits from being a relatively simple, quick and low cost procedure. In contrast, tissue engineering approaches were first envisioned as two-stage therapies, in which tissue was harvested during the first surgery, cells were isolated and expanded *ex vivo*, and implanted some weeks later during the second surgery [50].

Two-stage procedures are expensive and inefficient, and for the most part, have failed to conclusively establish that they offer substantial improvements over microfracture. A significant portion of the cost of two-stage cartilage treatment therapies arises from the need for two surgeries, and the cost of expanding cells *ex vivo*. In Europe, the cost of the leading cell-based cartilage repair therapy, ChondroCelect (Tigenix, Belgium), is approximately €30,000. The reduced cost and increased efficiency of single-stage therapies have increased the interest and research efforts in this area [280]. Clearly, the common element among single stage therapies is that the use of expanded autologous chondrocytes has been removed. Several strategies to negate this requirement are:

- Delivering cell-free biomaterials to fill the defect. These can be delivered in combination with microfracture, thus providing an artificial ECM to allow cell invasion and guide remodelling.
- Using alternative cell sources, such as allogeneic cells, or autologous stem/stromal cells that can be isolated from other tissues, such as bone marrow aspirates or adipose tissue.
- Using techniques to ‘particulate’ cartilage, which can then be seeded/incorporated into a biomaterial to fill the lesion. Both autograft cartilage (for example CAIS) and allogeneic donor cartilage are being investigated (for example *DeNovo* NT).
- Rapid digestion protocols for isolating chondrocytes or chondrons from autologous cartilage intra-operatively.
- Combinations of the above strategies, such as rapid digestion of chondrocytes, combined with allogeneic stromal cells (for example the IMPACT trial [51] – **I**nstant **M**SC **P**roduct accompanying **A**utologous **C**hondron **T**ransplantation).

With the exception of microfracture, single-stage cartilage therapies are in the early stages of development and testing, so it is too early to tell what clinical significance they may have. Another relevant consideration is the relative importance of cost versus repair tissue quality. These therapies are substantially cheaper than their two-stage counterparts, but if clinical outcomes from single-stage therapies are inferior to two-stage treatments, what weightings should be applied to determine the ‘best’ treatment?

**Table 8.1: Current status of two-stage clinical treatments for cartilage repair.**

<b>Product</b>	<b>Brief description and regulatory status</b>	<b>References</b>
Carticel® <sup>a</sup>	Original commercial product for autologous chondrocyte implantation. In 1997 it became the first ever cell therapy to receive FDA approval.	[281]
Chondro-Select® <sup>b</sup>	Expanded, autologous chondrocytes, which are characterised using propriety technology and inserted into the lesion. The area is sealed with a collagen membrane. In October 2009 it became the first advanced therapy medicinal product (ATMP) to receive EU approval.	[282, 283]
MACI <sup>c</sup>	Expanded autologous chondrocytes are seeded onto a bilayered collagen I/III scaffold (porcine) (ACI-Maix, Matricel, Germany). The scaffold is trimmed to shape, implanted cell-side down, and fixed in the defect using fibrin glue. Approved in the EU (June 2013).	[282]
Hyalograft® C <sup>d</sup>	Expanded autologous chondrocytes seeded onto a Hyaff 11 scaffold (esterified hyaluronic acid) and pressed into the defect. Withdrawn from European market in January 2013, with focus shifting to single stage therapy.	[216]
NeoCart® <sup>e</sup>	Expanded autologous chondrocytes seeded onto a bovine collagen type I scaffold, cultured in a high-pressure bioreactor with perfusion and controlled oxygen tension. Multicentre, phase III clinical trial (US).	[284, 285]
BioCart™ II <sup>e</sup>	Autologous chondrocytes expanded with autologous serum and FGF2. Cells are seeded onto a fibrin/hyaluronic acid matrix. Multicentre, phase II clinical trial underway (US and Israel); commercially available in Israel.	[286, 287]
Cartipatch® <sup>f</sup>	Expanded autologous chondrocytes suspended within an alginate-agarose hydrogel and implanted. Phase III trials (EU) commenced, but development of this product has ceased.	[288, 289]
CaReS <sup>g</sup>	Primary autologous chondrocytes seeded onto a collagen type I membrane (rat tail), cultured using autologous serum for up to 2 weeks <i>in vitro</i> and implanted with fibrin glue.	[290]
Novocart® 3D <sup>h</sup>	Expanded autologous chondrocytes seeded onto a collagen type I-chondroitin sulfate sponge. Phase III trial (EU).	[291, 292]

<sup>a</sup>Genzyme Biosurgery, U.S.; <sup>b</sup>TiGenix, Belgium; <sup>c</sup>Genzyme Europe B.V.; <sup>d</sup>Anika Therapeutics, US.; <sup>e</sup>Histogenics, Waltham, MA, USA; <sup>f</sup>TBF Genie Tissulaire, France; <sup>g</sup>Arthro Kinetics, Germany; <sup>h</sup>B Braun-Tetec, Germany.

**Table 8.2: Current status of single-stage clinical treatments for cartilage repair.**

<b>Product</b>	<b>Brief description and regulatory status</b>	<b>References</b>
Cartilage autograft implantation system (CAIS) <sup>a</sup>	Particulated autologous cartilage that is distributed onto a PGA-PCL foam (65% PGA, 35% PCL). Particulated cartilage is glued with fibrin, and the implant is immobilised in the defect with staples. Phase III clinical trial (Singapore) vs microfracture.	[293, 294]
<i>DeNovo</i> NT <sup>b</sup>	Particulated cartilage from a juvenile, allogeneic donor, sealed within fibrin glue. Large, multicentre, phase IV clinical trial underway (US).	[227, 295, 296]
RevaFlex <sup>TM c</sup>	Originally called Neocartilage implant; until recently was called <i>DeNovo</i> ET. Allogeneic chondrocytes isolated from juvenile donors, seeded at $0.5-1 \times 10^6$ cells/cm <sup>2</sup> and cultured for ~50 days in defined medium. Neotissue is implanted using fibrin glue. Phase III clinical trial (US).	[225, 297, 298]
GelrinC <sup>d</sup>	Adjunct to microfracture. Cell-free photocrosslinkable hydrogel composed of denatured fibrinogen conjugated to polyethylene glycol. Phase I/II clinical trial underway (EU and Israel).	[299, 300]
Autologous Matrix Induced Chondrogenesis (AMIC®) <sup>e</sup>	Adjunct to microfracture. A collagen I/III, cell-free matrix (ChondroGide®, Geistlich) stabilised with stitches and fibrin glue. Phase II/III clinical trial underway (EU).	[301, 302]
BST-CarGel <sup>f</sup>	Adjunct to microfracture. A thermosensitive chitosan-glycerophosphate hydrogel is mixed with whole blood (1:3 ratio) and crosslinked <i>in situ</i> . Phase III clinical trial (Canada, EU).	[303, 304]
Chondux <sup>TM g</sup>	Adjunct to microfracture. A chondroitin sulfate adhesive is applied to the microfractured defect, which is then filled with a cell-free, photocrosslinkable PEG-DA hydrogel containing 0.5% HA. Clinical trials in EU have been prematurely terminated.	[73, 305]
RepliCart <sup>TM h</sup>	Injection of allogeneic MSCs after reconstruction of the anterior cruciate ligament following keen injury. Strictly aims to prevent degeneration and onset of OA in this at risk group, rather than regenerate damaged cartilage. Phase II clinical trials.	[306, 307]
VeriCart <sup>i</sup>	Double-structured collagen scaffold that can be combined with microfracture or seeded with bone marrow derived cells. Application underway for CE mark in Europe.	[308, 309]
CaReS-1S <sup>j</sup>	One-step procedure with the collagen type I matrix used in CaReS. CE mark awarded in EU.	[290, 310]

<sup>a</sup>Depuy Mitek, MA, USA; <sup>b</sup>Zimmer Orthobiologics, Inc, IN, USA; <sup>c</sup>ISTO Technologies, MO, USA; <sup>d</sup>Regentis Biomaterials, Haifa, Israel; <sup>e</sup>Geistlich Pharma AG, Wolhusen, Switzerland; <sup>f</sup>Piramal Healthcare; <sup>g</sup>Biomet Inc, IN, USA; <sup>h</sup>Mesoblast; <sup>i</sup>Histogenics; <sup>j</sup>Arthro Kinetics, Germany.

Many clinical trials have shown that symptomatic lesions *can* be regenerated with excellent, hyaline cartilage. However, these outcomes are not consistently achieved, and in a large proportion of patients, the outcomes are not dissimilar to microfracture. The challenge is to identify and exploit mechanisms that can be used to increase the proportion of patients with excellent repair tissue. This may be through selecting a subpopulation of patients or indications that are most suited for a certain therapy, or through different rehabilitation programs. To this end, studies are underway to identify molecular markers and patient characteristics that can be used to predict the chance of success prior to surgery [311]. Similarly, characterised chondrocyte implantation was shown to be superior to microfracture for patients treated within 3 years of injury, while outcomes were similar with either treatment for those with delayed treatment (> 3 years) [312]. These studies aim to identify subpopulations that are particularly likely to benefit from the additional expense, risk and time associated with cartilage tissue engineering therapies.

Much remains to be done for cartilage tissue engineering to be adopted as a widespread and mainstream therapy. In a recent review of the clinical status of cartilage repair, Mollon and co-authors state that “The notion that ACI-like procedures produce hyaline-like cartilage in humans remains unsupported by high quality clinical research” [313]. This is not through lack of effort – cartilage tissue engineering has been the subject of intense basic and translational research for two decades – but rather a reflection of the substantial challenges facing cartilage repair. Many of these are unique to cartilage, and the title of another recent review gives a succinct picture of the progress in engineering cartilage compared to bone: “Unlike bone, cartilage regeneration remains elusive” [46]. Nevertheless, efforts to regenerate cartilage are steadily increasing [314], and it is hoped that increased understanding of biological processes and scaffold requirements will deliver meaningful advances in cartilage tissue engineering.

### **8.7 Clinical application of photocrosslinkable hydrogels**

Recently, two photocrosslinkable hydrogel systems (GelrinC and ChonDux<sup>TM</sup>) have been applied in clinical cartilage repair. The surgical procedure used is an evolution of conventional microfracture; following debridement and perforation of the subchondral bone, the void volume is filled with a cell-free hydrogel precursor and crosslinked with UV light.

The research group led by Professor Jennifer Elisseeff has been at the forefront of research in photocrosslinkable hydrogels for the past decade, and among



other interests, has a strong reputation for cartilage research. Her group's work in this area has focused largely on PEGDA-based hydrogels, in which chondrocytes or MSCs are encapsulated. In 2013, Sharma et al., from the Elisseff group, published a study in which PEGDA hydrogels were used clinically in combination with microfracture (Chondux™) [73]. The PEGDA hydrogel was mixed with 5 mg/mL of unmodified 1.2 MDa HA to increase viscosity, and thus ease of handling of the precursor solution. Notably, this is the same concentration of HA that was used in Chapter 5 (0.5% w/v), but no mention is made of the potential biological function of the HA [73], whereas in Chapter 5, the addition of methacrylated HA was shown to have a substantial impact on chondrocyte phenotype and matrix synthesis and properties. The hydrogel was applied in combination with an adhesive based on chondroitin sulfate to enhance attachment with the surrounding tissues [315]. Repair was evaluated *in vitro*, in a goat model, and subsequently in 15 human patients. A larger clinical trial of ChonDux commenced in Europe, but for unknown reasons has been prematurely terminated [305].

GelrinC is a hydrogel composed of PEGDA that has been covalently bound to denatured fibrinogen ('PEGylated' fibrinogen) [316]. The material was developed primarily by Professor Dror Seliktar, and is being commercialised by Regentis Biomaterials. Similarly to Chondux™, is crosslinked *in situ* using UV light following conventional microfracture [300]. The gel degrades over 6 – 12 months, and is replaced with repair tissue. The results 24 months after operation were reported at the International Cartilage Repair Society in September 2013, and appear promising, with significant improvement in patient-reported metrics after 24 months, and continued improvement between 18 and 24 months [317]. It is a versatile hydrogel platform, and the degradation kinetics can be tailored by altering the amount of fibrinogen. The repair of several tissues, including bone, nerve, cartilage and cardiac tissue has been investigated using this material, but cartilage repair is the current focus for Regentis Biomaterials.

It is promising to see photocrosslinked hydrogels being used for clinical cartilage repair, since these materials offer meaningful improvements over those that are currently commonly used. UV light has been used to crosslink the hydrogels *in situ*, which allows the hydrogel to mold precisely to the shape and size of the defect, assuring complete fill and enhancing attachment. However this exposes the patients' tissue to some level of UV radiation, with associated safety implications. By using a cell-free hydrogel, the possibility for UV-induced cell damaged is reduced, and the road to clinical translation is significantly simplified. Photocrosslinked hydrogels are establishing a presence

in clinical cartilage repair in the form of cell-free, hydrogel seals for microfracture, but cell-encapsulated hydrogels are still in preclinical development, and are subject to considerable additional challenges.

## **8.8 Bioprinting**

In Chapter 4 we investigated the potential to print Gel-MA based hydrogel structures. Because Gel-MA solutions have a relatively low viscosity, we printed Gel-MA in combination with HA to increase viscosity, with and without PCL as a support structure. Using these methods, it was possible to print constructs with transverse porosity using 20% Gel-MA with HA. Layered constructs without porosity could be printed using 10% Gel-MA with HA and a PCL support. Recently, the printability of Gel-MA without viscosity enhancers or support structures has been demonstrated, using a system that allows a high degree of control over printing parameters, such as pressure, temperature, and stage speed [112]. The main advantage that this system has over the BioScaffolder used in Chapter 4 is that the temperature is controlled right up until the point that the gel is dispensed from the needle, giving a much greater level of temperature control. In the BioScaffolder, the temperature of the bio-ink reservoir in the syringe is maintained by liquid heating/cooling, but the needle is exposed to ambient conditions, and the water temperature of the water bath fluctuates to a degree and cannot be quickly changed. As the solution flows through the needle it cools, and has a tendency to gel and block the needle, causing uneven flow rates. To prevent blockages, the temperature of the reservoir is increased to compensate for cooling in the needle, thus precise control of the temperature at the needle exit point is difficult to achieve. The study by Billiet et al. [112] demonstrates the importance of precise control over multiple parameters for high resolution hydrogel printing.

Hydrogels have a number of properties that make them particularly suited for the fabrication of bioprinted cartilage constructs. They allow cells to be encapsulated in a native three-dimensional state, are highly cell compatible, and generally the surfaces have a very low friction coefficient. However, as previously discussed, the mechanical properties are a limitation. Bioprinting offers possibilities to utilise the low friction and cell-compatible properties of hydrogels, while using stronger and stiffer materials such as PCL to provide mechanical reinforcement [213]. In Chapter 4, we have printed hybrid structures composed of an outer shell of rigid PCL, filled with two layers of hydrogel. In this way, the cells can be maintained in a highly hydrated and diffusive environment, while the mechanical strength is provided by the PCL shell. Clear limitations are that the high friction of the PCL would likely cause unacceptable

wear if congruent with opposing cartilage surfaces, and stable integration with surrounding tissues may be more challenging with PCL than hydrogels. Ideally the PCL support structures would be wholly encompassed by the hydrogel, and current research efforts are directed towards developing such materials [318].

Printed Gel-MA constructs can be crosslinked by UV light and IC2959. As previously discussed, this mechanism is subject to oxygen inhibition, and this is particularly relevant for printed structures, which have a significantly larger surface area to volume ratio. This allows increased diffusion of oxygen into the construct, with additional crosslinking inhibition, and potentially inhomogeneous crosslinking. The use of thiol-containing crosslinkers may offer additional advantages overcoming oxygen inhibition in the crosslinking of printed structures.

## 8.9 Limitations

The primary goal of this thesis is to make a contribution to the field of cartilage tissue engineering research. In carrying out the studies described within, we have also gained some insight into hydrogel properties, chondrocyte biology, and cell-material interactions, as assessed using *in vitro* culture models. *In vitro* studies allow materials to be compared in controlled and consistent conditions, and enable more detailed evaluations than are possible *in vivo*. They are a valuable, if not essential step in the development of tissue engineered therapies, and by increasing the level of evidence used to select materials for *in vivo* studies and clinical therapies, *in vitro* models should contribute to improved clinical outcomes in the future. On the down side, the full complexity and challenges of cartilage tissue engineering cannot be entirely recreated in an *in vitro* environment. In particular, the *in vitro* models used here completely remove the immune response of the patient, which is a critical factor for success of tissue engineering therapies. Thus, although it was outside of the scope of this project, the *in vitro* studies described within must be complemented with subsequent *in vivo* repair studies before conclusions can be drawn on the suitability of these materials for cartilage tissue engineering. *In vivo* studies of Gel-MA/HA-MA hydrogels for cartilage tissue engineering have begun at Utrecht University, and future work using *in vivo* models will show the true potential of the materials discussed in this thesis.

Biological variation – that is the inherent variability between individuals – is a significant limitation of the work described in this thesis. Human chondrocytes were sourced from OA patients receiving knee replacements, so the potential for donor variation is further increased by taking cells from patients with different

stages of OA and potentially different co-morbidities. In Chapters 3 and 5, we used a single, different biological donor, and measured the difference in the performance of this donor using different hydrogels. This decision was made to allow a larger number of hydrogel groups to be included, and the hydrogel groups that were identified as the most promising were subsequently investigated using a greater number of donors. Pleasingly, good consistency was observed between the four donors used in Chapter 6.

IC2959 is the most widely used photoinitiator for cell encapsulation, and was used in all studies in this thesis. Ultimately, it is likely that despite its extensive use, IC2959 is not an ideal photoinitiator for cell-encapsulation. Developing and evaluating water-soluble photoinitiators for biomedical use is an active research area in its own right. In 1991, a lithium acylphosphinate salt (LAP) was shown to act as a water soluble, visible light photoinitiator, but no mention was initially made of its potential application for cell-encapsulation [319]. More recently, there has been renewed interest in this photoinitiator from tissue engineering research groups, who have demonstrated cell encapsulation using visible light, with good cytocompatibility [220]. VA-086 has also shown advantages to IC2959 for crosslinking alginate methacrylate, and is another photoinitiator that is of increasing interest in this field. Fortunately, we expect that as improved photoinitiators become increasingly available, they should be compatible with Gel-MA based hydrogels.

According to the manufacturer, the output from the UVP longwave crosslinker is centred about 365 nm, which lies right at the edge absorption region of IC2959 (Figure 8.4). We therefore expect the crosslinking efficiency at this wavelength to be very low, and the UV exposure required to attain a given degree of crosslinking is likely to be much higher than the exposure required at lower wavelengths. While this may have been beneficial in some aspects, such as lower rates of ROS formation, ultimately minimising UV exposure is going to be highly advantageous.

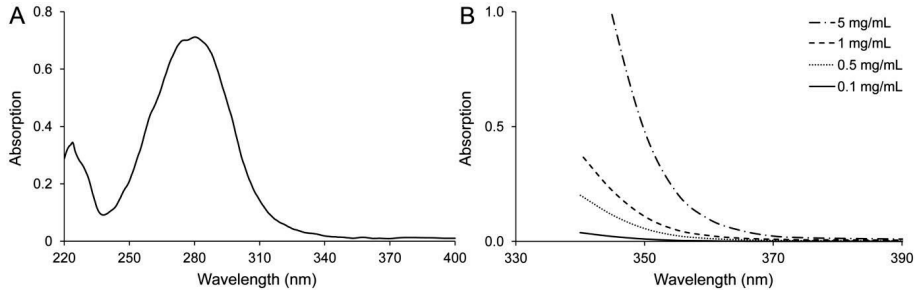


**Figure 8.4: Absorption spectrum of Irgacure 2959 at 0.1 mg/mL (A), and absorption between 340 - 390 nm for concentrations of 0.1 – 5 mg/mL (B).**

The production of GAGs is a hallmark of chondrocytes, and for over two decades, staining and quantifying GAG production has been a fundamental tool for cartilage regeneration and tissue engineering research. Significantly, in this thesis GAG production did not correlate well with chondrogenesis in several instances. We believe that this is an important limitation of ‘total GAG’ measurements, which may be especially relevant when using chondrocytes. Several ratios have been suggested as being indicative of the differentiation state of chondrocytes, namely the ratio of collagen type II to type I expression [116], and the ratio of aggrecan to versican expression [320]. In the latter, aggrecan is expressed in differentiated chondrocytes, while versican is expressed in dedifferentiated chondrocytes. Notably, however, these are both GAG-rich proteoglycans. Therefore quantifying the total amount of GAGs produced in constructs does not necessarily provide any insight into the differentiation state of the chondrocytes, in the same way that quantifying total collagen content cannot. Interestingly, total collagen content assays have fallen out of use with many cartilage research groups, but GAG measurements are still common. The difference may lie in an easily overlooked detail: quantitative GAG assays using DMMB are simple, fast, sensitive and cheap, but total collagen (hydroxyproline) assays are very time consuming and labour intensive.

In this thesis we have primarily used hydrogels based on gelatin, thus the hydroxyproline assay is not a feasible method for quantifying total collagen content. Nevertheless, collagen quantification is important for cartilage tissue engineering, since whereas GAG content of tissue-engineered cartilage often approaches the level in native cartilage, the collagen content is often substantially lower [47]. In particular, since it is far more valuable to know collagen type II content rather than total collagen, future studies should aim to quantify collagen type II in the constructs, for example using enzyme linked immunosorbent assays (ELISA).

In Chapter 3 it was evident that dedifferentiated chondrocytes produce substantial amounts of GAGs in Gel-MA. From these results, we concluded that the GAG assay and Alcian Blue were acceptable for measuring how much matrix was produced, which is important, but does not reflect the matrix quality. This trend was recently observed in a study comparing two different PEG hydrogels. The hydrogel group with the higher GAG content showed significantly *less* staining for aggrecan, and the overall tissue quality appeared lower in this group [222]. These results demonstrate the clear limitation of GAG measurements, and highlight the importance of combining these measurements with more reliable indicators of differentiation state – such as immunohistochemistry or gene expression.

From a practical perspective, experience is important with Gel-MA hydrogels. Gel-MA is sensitive to temperature, light, and enzymatic degradation, and thus handling can influence gel properties. For cell culture, it is important to make every effort to standardise procedures and handling. This is further complicated by the addition of other components, such as HA-MA, which appear to alter the kinetics and nature of the temperature sensitivity – mixtures of Gel-MA and HA-MA, for example, form thermal gels more rapidly than Gel-MA solutions alone. Furthermore, stability and sterility are practical challenges for using polymers in cell culture. HA-MA has limited stability, even when dried and stored at low temperatures, and so should be used as soon as practicable after functionalisation. Maintaining the sterility of HA-MA is also a practical challenge when used on a small, laboratory scale. Conventional approaches for sterilising cell culture materials, such as autoclaving, short wave UV exposure and gamma irradiation are not compatible with HA-MA solutions. For low concentrations (<~1%), filter sterilisation is possible, however for higher concentrations, the high viscosity makes filtration difficult.

Finally, it is worth re-iterating the two cell subpopulations that emerge on Gel-MA based constructs. Cells at the surface of the hydrogel readily attached and spread, as they do on two dimensional surfaces and adopt a dedifferentiated phenotype. This is not ideal for cartilage tissue engineering, and complicates the interpretation of some results, such as gene expression, in which these two subpopulations are pooled. It remains to be seen whether this is phenomenon would be observed for a hydrogel crosslinked within a cartilage defect, in which case only the articulating surface would not be adjacent to other structures.

## 8.10 Future directions

Further research is required to advance our understanding of the hydrogels used in this thesis, and progress their application towards cartilage repair.

*In vitro* studies should assess the impact that UV exposure and photocrosslinking has on encapsulated cells, particularly in light of the recent comparison of photocrosslinked PEG hydrogels [222]. Following this finding, possibilities to enhance chondrogenic outcomes should be studied, including the use of thiolated HA or thiol crosslinkers, and/or other methods to reduce ROS during crosslinking, such as mixing endogenous superoxide dismutase into the hydrogel precursor solution.

The optimum conditions for photocrosslinking Gel-MA based hydrogels should be investigated in detail. For example, it remains to be shown whether it is preferable to use a shorter period exposure to 350 nm light, or a longer period of exposure to 360 nm light. Such studies should use the exposure period required to produce gels with similar stiffness, which would be indicative of similar degrees of crosslinking.

The prolonged delivery of growth factors is a common feature of *in vitro* studies, especially in cartilage, and of course is not possible in clinical situations. Ideally, the growth factor would be immobilised within the defect, and continue guiding regeneration over the weeks following implantation. As a consequence of its negative charge, heparin displays a high affinity for many growth factors, and has been incorporated into various hydrogels for the retention and gradual release of growth factors, including FGF-2, VEGF, TGF- $\beta$ 1 and BMP-2, among others [321]. In preliminary studies, we have functionalised Gel-MA hydrogels with photocrosslinkable heparin, and shown that the heparin remains stably bound in the gel. Using this platform, co-encapsulation of cells with growth factors should be investigated to determine whether the need for continual growth factor delivery can be reduced.

MSCs are a potential cell source for cartilage regeneration, and can be used in combination with or instead of chondrocytes. Directing the differentiation of MSCs towards a chondrogenic lineage is a prerequisite for their use, and is commonly achieved using growth factors. It would be interesting to evaluate the differentiation of MSCs encapsulated in Gel-MA – HA-MA hydrogels. Previous work has shown that when MSCs are encapsulated in Gel-MA and implanted subcutaneously in mice, they attach, spread and undergo osteogenic

differentiation [322], so the potential for HA-MA to promote chondrogenic rather than osteogenic differentiation would be an interesting line of research.

Thorough *in vivo* studies with these hydrogels will be essential for assessing the true potential of these materials to be used in cartilage regeneration. Early studies should focus on cell viability, the production of ECM, and critically, methods to secure the hydrogels within the defect. Following these pilot studies, comparisons with other treatments, such as microfracture, should be investigated.

### **8.11 Conclusion**

Gel-MA based hydrogels have been identified as potential materials for cartilage tissue engineering applications. When used alone, Gel-MA hydrogels support significantly more matrix production than other commonly used hydrogel systems. Controlling the physical and swelling properties of Gel-MA can be achieved through two simple means: adjusting the concentration of the precursor solution, or the length of UV exposure. Further, Gel-MA retains its temperature sensitivity, allowing printed structures to be formed. The incorporation of small quantities of HA-MA and to a much lesser extent, CS-MA, markedly improves chondrogenesis, matrix production and developed mechanical properties. Finally, tissue from cartilage, tendon and meniscus can be solubilised, functionalised and incorporated into Gel-MA hydrogels, although outcomes for chondrogenesis do not appear to be promising.

Cartilage tissue engineering is an exciting and dynamic field. Over the past decade, it has been at the forefront of clinical tissue engineering and regenerative medicine. There is an increasing level of activity across the entire field, from molecular studies of cell signalling and differentiation pathways, right through to clinical trials and commercial products for cartilage repair. Much of the progress in biomaterials for cartilage regeneration has yet to be realised in clinical practice, and we expect this to continue to fuel new products and techniques in cartilage repair in the coming years.



## Summary & Samenvatting in het Nederlands

---

## Summary

The materials used throughout this thesis are photocrosslinkable hydrogels that are based predominantly on photocrosslinkable gelatin, or Gel-MA. In Chapter 3, Gel-MA hydrogels stood out as the material in which chondrocytes produced the most ECM and had the greatest increase in compressive stiffness. These are key metrics used to assess tissue-engineered cartilage, and as a consequence, Gel-MA became the core component of the hydrogels investigated in this thesis. The limited extent of chondrogenic redifferentiation in Gel-MA was a key limitation, with chondrocytes appearing to redifferentiate best when encapsulated in HA-MA.

Exploring the properties and versatility of Gel-MA hydrogels was the subject of Chapter 4. In this study we showed that the physical properties of Gel-MA hydrogels could be varied over a wide range by making simple adjustments to the polymer concentration and UV crosslinking time. In addition, physical properties were dependent on the temperature at which the UV crosslinking took place. This allows the thermosensitivity of gelatin to be used as a means to increase the stiffness of covalently crosslinked hydrogels. The potential for Gel-MA hydrogels to be used as a bioink for printing defined constructs was also tested, using a commercially available printing device (BioScaffolder). Controlling the temperature is critical for achieving the appropriate rheological properties for printing, and this was very challenging with this device. To overcome this, the viscosity of the Gel-MA solution was dramatically increased by adding HA. This reduced the rate at which Gel-MA flows under gravity, allowing more time for the Gel-MA to cool and thereby preserve the geometry and architecture of the structure. When Gel-MA/HA mixtures were printed into PCL support structures, layered constructs could be printed with a reasonable degree of separation between the layers. Finally, the effect of adding 2.4% HA on matrix production and viability was investigated using equine chondrocytes, although no clear differences were observed with or without HA.

In Chapter 5 we investigated the impact of functionalising Gel-MA hydrogels with two of the most abundant and important GAGs in cartilage, HA and CS. In order to achieve stable and lasting incorporation of these GAGs, particularly the much smaller CS, they were first modified with methacrylate groups, to produce HA-MA and CS-MA. The differences in the impact of HA-MA vs. CS-MA could not have been more apparent. HA-MA had a strongly positive influence on the production of ECM, the cell morphology and chondrogenic differentiation. Most strikingly, HA-MA resulted in substantially improved mechanical properties, which was supported by an increased distribution of

collagen type II and aggrecan. In comparison, CS-MA had only very minor impacts on cell phenotype and matrix production, although much higher concentrations of CS-MA could potentially be used with this polymer. Chondrocytes from the superficial and mixed middle/deep zones were treated separately in this study, but no notable differences were observed between these cell subpopulations.

The development of mechanically strong and functional constructs is of critical importance when trying to regenerate a load-bearing tissue, and the findings from Chapter 5, in which HA-MA substantially improved the developed mechanical properties throughout culture, was the focus of a more detailed investigation in Chapter 6. Specifically, we sought to investigate in further detail the impact that HA-MA has on the developed mechanical properties, including failure strength, compressive modulus, dynamic modulus and equilibrium modulus. In addition, we used 0, 0.25, 0.5, 1 or 2% (w/v) HA-MA, and used chondrocytes from four different donors to compare donor-to-donor variability. Changes in compressive, dynamic and equilibrium modulus all tended to increase with culture time and HA-MA concentration. Across all four patients, HA-MA resulted in substantial improvements to mechanical properties. For example the compressive modulus of constructs with 0% HA-MA increased by an average of 37 kPa over 8 weeks culture, while those with 2% HA-MA increased by an average of 129 kPa. The failure strength was approximately two-fold higher in all groups with HA-MA, but was not dependent on HA-MA concentration. Collectively, these results confirmed that the addition of HA-MA to Gel-MA constructs is a useful way to improve the mechanical functionality of the cell-synthesised ECM.

Producing biomaterials and scaffolds from decellularised tissues is potentially an ideal way to recreate a specific cell niche. This has not been investigated widely for cartilage applications, and in Chapter 7 we functionalised Gel-MA hydrogels with tissue derivatives from three equine tissues: cartilage, meniscus and tendon. The tissues were enzymatically digested and decellularised, then functionalised to include photocrosslinkable methacrylate and/or methacrylamide groups. Functionalising tissue-extracts to allow them to be directly covalently crosslinked is a novel approach, and to our knowledge has not been demonstrated before. Equine chondrocytes and MSCs were encapsulated in hydrogels composed of 8% Gel-MA blended with 2% of either of the functionalised cartilage, meniscus or tendon tissue. Although substantial improvements in cell responses were not observed, the focus of this study was

developing the process for producing the functionalised tissues, and stably incorporating these tissue derivatives into hydrogels.

In summary, this thesis has identified hydrogel materials that are promising for cartilage tissue engineering. In particular, blends of photocrosslinkable gelatin and hyaluronic acid performed well in *in vitro* models, with significant formation of new ECM and substantial improvements in the developed mechanical properties. When either material was used alone, both had significant limitations, but together the materials appear very promising.

## Samenvatting

De foto-polymeriseerbare hydrogelen die in dit proefschrift zijn beschreven bestaan voornamelijk uit foto-crosslinkbare gelatine, genaamd Gel-MA. In Hoofdstuk 3 viel Gel-MA hydrogel op als het materiaal waarin chondrocyten een hoge extracellulaire matrix productie toonden die gepaard ging met een toename in stijfheid. Dit zijn belangrijke parameters die gebruikt worden om gekweekt kraakbeenweefsel te evalueren, met als gevolg dat Gel-MA verder onderzocht is als dragermateriaal in dit proefschrift. Echter, de beperkte mate van chondrogene redifferentiatie in Gel-MA bleek een belangrijke limitatie, en chondrocyten leken beter te redifferentiëren wanneer zij ingekapseld zijn in foto-polymeriseerbaar hyaluronzuur (HA-MA).

Het onderzoeken van de eigenschappen en de veelzijdigheid van Gel-MA hydrogelen werd het onderwerp van Hoofdstuk 4. In deze studie hebben we aangetoond dat de fysische eigenschappen van Gel-MA hydrogelen sterk gevarieerd kunnen worden door simpele aanpassingen aan de polymeerconcentratie en UV polymerisatietijd. Bovendien waren de fysische eigenschappen afhankelijk van de temperatuur waarop UV crosslinking plaats vond. Hierdoor kan de thermosensitiviteit van Gel-MA gebruikt worden als een middel om de stijfheid van covalent gecrosslinkte netwerken te verhogen. De potentie van Gel-MA hydrogelen om gebruikt te worden als bioinkt voor geprinte driedimensionale constructen werd getest met behulp van een commercieel verkrijgbare bioprinter (BioScaffolder). Een nauwkeurige controle over de printtemperatuur bleek cruciaal om de juiste reologische eigenschappen voor printen te verkrijgen, wat erg uitdagend bleek. Door de viscositeit van de Gel-MA oplossing sterk te verhogen door de toevoeging van hyaluronzuur (HA) kon de printbaarheid sterk worden verbeterd. Deze toevoeging vermindert de snelheid waarmee Gel-MA stroomt onder zwaartekracht, waardoor de gel meer tijd had om af te koelen, en de geometrie en ordening van de structuur behouden konden worden. Door Gel-MA/HA mengsels te printen samen met verstevigende PCL netwerken konden gelaagde constructen geprint worden met een redelijke mate van scheiding tussen de lagen. Er werden geen duidelijke verschillen waargenomen van het toevoegen van 2,4% HA op matrix productie en levensvatbaarheid van equine chondrocyten.

In Hoofdstuk 5 onderzochten we het effect van het toevoegen van twee van de meest voorkomende en belangrijke glycosaminoglycanen (GAG's) in kraakbeen, HA en chondroitinesulfaat (CS), aan Gel-MA hydrogelen. Om stabiele en duurzame opname van deze GAG's in de hydrogel te verkrijgen, werden zij eerst gemodificeerd met methacrylaatgroepen (MA), waardoor HA-

MA en CS-MA ontstonden. HA-MA had een sterk positieve invloed op extracellulaire matrix productie, celmorfologie en chondrogene differentiatie. Daarnaast resulteerde de toevoeging van HA-MA in aanzienlijk verbeterde mechanische eigenschappen van de hydrogel-constructen. Daarentegen had CS-MA slechts geringe invloed op het fenotype van de cel en op matrix productie. Dit werd afzonderlijk onderzocht met chondrocyten uit de oppervlakkige en middel/diepe kraakbeenzones, maar er werden desondanks geen noemenswaardige verschillen waargenomen in de respons van deze cel subpopulaties.

De ontwikkeling van mechanisch sterke en functionele constructen is van cruciaal belang voor de regeneratie van dragende weefsels. De resultaten van Hoofdstuk 5, waarin HA-MA de ontwikkelde mechanische eigenschappen sterk verbeterde, leidden tot een meer gedetailleerd onderzoek in Hoofdstuk 6. In het bijzonder wilden we de impact die HA-MA heeft op de ontwikkelde mechanische eigenschappen nader onderzoeken, waaronder de materiaalsterkte, compressiemodulus, dynamische modulus en evenwichtsmodulus. Daarnaast gebruikten we 0, 0.25, 0.5, 1 of 2% (w/v) HA-MA en chondrocyten van vier verschillende donoren om donor-tot-donor variabiliteit te vergelijken. Aanpassingen in compressie-, dynamische en evenwichtsmodulus hadden allen de neiging om te stijgen met kweektijd en HA-MA concentratie. In de experimenten met cellen van alle vier patiënten leidde HA-MA tot een aanzienlijke verbetering van de mechanische eigenschappen. De compressiemodulus van constructen met 0% HA-MA steeg bijvoorbeeld met gemiddeld 37 kPa gedurende 8 weken in kweek, terwijl die met 2% HA-MA een stijging lieten zien van gemiddeld 129 kPa. De materiaalsterkte was ongeveer twee keer zo hoog van alle groepen met HA-MA, maar was niet afhankelijk van de HA-MA concentratie.

Het produceren van scaffolds gebaseerd op gedecellulariseerd weefsel is potentieel een ideale manier om een specifieke celomgeving te creëren. Dit is echter slechts in beperkte mate onderzocht voor kraakbeentoepassingen, en in Hoofdstuk 7 hebben we daarom Gel-MA gefunctionaliseerd met weefselderivaten van drie equine weefsels: kraakbeen, meniscus en pees. De weefsels werden enzymatisch gedegradeerd en gedecellulariseerd, en vervolgens gefunctionaliseerd met fotocrosslinkbaar methacrylaat- en/of methacrylamidegroepen. Het functionaliseren van weefselderivaten om hen in staat te stellen covalent te crosslinken is een nieuwe aanpak. Equine chondrocyten en mesenchymale stamcellen (MSCs) werden ingebed in hydrogelen die bestonden uit 8% Gel-MA gemengd met 2% van het

gefunctionaliseerde (en gedecellulariseerde) kraakbeen-, meniscus- of peesweefsel. Hoewel aanzienlijke verbeteringen in celreacties niet werden waargenomen, was de focus van deze studie om het proces van productie van gefunctionaliseerde weefsels en stabiele opname van deze weefselderivaten in hydrogelen te ontwikkelen.

Samenvattend heeft dit proefschrift hydrogel materialen geïdentificeerd die veelbelovend zijn voor tissue engineering van kraakbeen. Mengsels van fotocrosslinkbare gelatine en hyaluronzuur presteerden goed in *in vitro* modellen, met aanzienlijke extracellulaire matrix vorming en forse verbeteringen van de mechanische eigenschappen. Beide materialen hadden belangrijke beperkingen wanneer ze niet in combinatie gebruikt werden. Echter, samengevoegd lijken de materialen veelbelovend.





## References

---

## References

- [1] Donaldson J. The use of gold in dentistry: An historical overview, Part 1. *Gold Bulletin* 1980;13:117-24.
- [2] Hildebrand HF. Biomaterials – a history of 7000 years. *BioNanoMaterials* 2013;13:119-33.
- [3] Ratner BD. A history of biomaterials. In: Ratner BD, Hoffman AS, Schoen FJ, Lemons JE, editors. *Biomaterials science: an introduction to materials in medicine*. 2nd ed. New York: Academic Press; 2004.
- [4] Marketsandmarkets. Biomaterials Market [By Products (Polymers, Metals, Ceramics, Natural Biomaterials) & Applications (Cardiovascular, Orthopedic, Dental, Plastic Surgery, Wound Healing, Tissue Engineering, Ophthalmology, Neurology Disorders)] – Global Forecasts to 2017. 2013.
- [5] Langer R, Vacanti J. *Tissue Engineering*. *Science* 1993;260:920-6.
- [6] Williams DF. *Williams dictionary of biomaterials*: Liverpool University Press; 1999.
- [7] Roth V, Mow V. The intrinsic tensile behaviour of the matrix of bovine articular-cartilage and its variation with age. *Journal of Bone and Joint Surgery* 1980;62:1102-17.
- [8] Schumacher B, Block J, Schmid T, Aydelotte M, Kuettnner K. A novel proteoglycan synthesised and secreted by chondrocytes of the superficial zone of articular cartilage. *Archives of Biochemistry and Biophysics* 1994;311:144-52.
- [9] Buckwalter J, Mankin H. Articular Cartilage Part I: Tissue design and chondrocyte-matrix interactions. *Journal of Bone and Joint Surgery* 1997;79:600-11.
- [10] Muir H. The chondrocyte, architect of cartilage. *Biomechanics, structure, function and molecular biology of cartilage matrix macromolecules*. *BioEssays* 1995;17:1039-48.
- [11] Cancedda R, Dozina B, Giannonia P, Quarto R. Tissue engineering and cell therapy of cartilage and bone *Matrix Biology* 2003;22:81-91.
- [12] Poole AR, Kojima T, Yasuda T, Mwale F, Kobayashi M, Lavery S. Composition and structure of articular cartilage: A template for tissue repair. *Clinical Orthopaedics and Related Research* 2001:S23-S33.
- [13] Goldring M. The role of the chondrocyte in osteoarthritis. *Arthritis and Rheumatism* 2000;43:1916-26.
- [14] Watanabe H, Yamada Y, Kimata K. Roles of aggrecan, a large chondroitin sulfate proteoglycan, in cartilage structure and function *Journal of Biochemistry* 1998;124:687-93.
- [15] Muir H. Proteoglycans as organizers of the intercellular matrix. *Biochemical Society Transactions* 1983;11:613-22.
- [16] Laurent TC, Fraser JR. Hyaluronan. *FASEB Journal* 1992;6.
- [17] Fraser JR, Laurent TC, Laurent UBG. Hyaluronan: Its nature, distribution, functions and turnover *Journal of Internal Medicine* 1997;242:27-33.
- [18] Toole BP. Hyaluronan: From extracellular glue to pericellular cue *Nature Reviews Cancer* 2004;4:528-39.

- [19] Chen WYJ, Abatangelo G. Functions of hyaluronan in wound repair Wound Repair and Regeneration 1999;7:89-.
- [20] Aruffo A, Stamenkovic I, Melnick M, Underhill CB, Seed B. CD44 is the principal cell surface receptor for hyaluronate Cell 1990;61:1303-13.
- [21] Kielty CM, Whittaker SP, Grant ME, Shuttleworth CA. Type VI collagen microfibrils: Evidence for a structural association with hyaluronan The Journal of Cell Biology 1992;118:979-90.
- [22] McDevitt CA, Marcelino J, Tucker L. Interaction of intact type VI collagen with hyaluronan FEBS Letters 1992;294:167-70.
- [23] Lee Y-T, Shao H-J, Wang J-H, Liu H-C, Hou S-M, Young T-H. Hyaluronic acid modulates gene expression of connective tissue growth factor (CTGF), transforming growth factor-1 (TGF-1), and vascular endothelial growth factor (VEGF) in human fibroblast-like synovial cells from advanced-stage osteoarthritis in vitro. Journal of Orthopaedic Research 2010;28:492-6.
- [24] Mow V, Ratcliffe A, Poole A. Cartilage and diarthrodial joints as paradigms for hierarchical materials and structures. Biomaterials 1992;13:67-97.
- [25] Hardingham T. The role of link-protein in the structure of cartilage proteoglycan aggregates. Biochemical Journal 1979;177:237-47.
- [26] Bassar P, Schneiderman R, Bank R, Wachtel E, Maroudas A. Mechanical properties of the collagen network in human articular cartilage as measured by osmotic stress technique. Archives of Biochemistry and Biophysics 1998;351:207-19.
- [27] Maroudas A. Balance between swelling pressure and collagen tension in normal and degenerate cartilage. Nature 1976;260:808-9.
- [28] Comper WD, Williams PWW, Zamparo O. Water transport in extracellular matrices. Connective Tissue Research 1990;25:89-102.
- [29] Collins D. The pathology of articular and spinal diseases London: Arnold; 1949.
- [30] Meachim G, Stockwell R. The Matrix. In: Freeman M, editor. Adult Articular Cartilage. 1st edition ed. London: Pitman; 1973. p. 1-50.
- [31] Aspden RM, Hukins DWL. Collagen organization in articular cartilage, determined by x-ray diffraction, and its relationship to tissue function. Proceedings of the Royal Society of London Series B-Biological Sciences 1981;212:229-304.
- [32] Maroudas A. Physicochemical properties of articular cartilage. In: Freeman MAR, editor. Adult Articular Cartilage. 2nd Edition ed. Tunbridge Wells: Pitman Medical; 1979. p. 215-90.
- [33] Schinagl R, Gurskis D, Chen A, Sah R. Depth-dependent confined compression modulus of full-thickness bovine articular cartilage. Journal of Orthopaedic Research 1997;15:499-506.
- [34] Heinegard D, Paulsson M. Cartilage. Methods in Enzymology 1987;145:336-63.
- [35] Weightman B, Kempson GE. Load Carriage. In: Freeman MAR, editor. Adult Articular Cartilage. 2nd Edition ed. Tunbridge Wells: Pitman Medical; 1979. p. 291-332.

- [36] Dowthwaite GP, Bishop JC, Redman SN, Khan IM, Rooney P, Evans DJR, et al. The surface of articular cartilage contains a progenitor cell population *Journal of Cell Science* 2004;117:889-97.
- [37] Poole CA, Flint M, Beaumont B. Chondrons in Cartilage: Ultrastructural Analysis of the Pericellular Microenvironment in Adult Human Articular Cartilages. *Journal of Orthopaedic Research* 1987;5:509-22.
- [38] Wang Q, Nguyen B, Thomas C, Zhang Z, Haj A, Kuiper N. Molecular profiling of single cells in response to mechanical force: Comparison of chondrocytes, chondrons and encapsulated chondrocytes. *Biomaterials* 2010;31:1619-25.
- [39] Kvist AJ, Nyström A, Hultenby K, Sasaki T, Talts JF, Aspberg A. The major basement membrane components localize to the chondrocyte pericellular matrix — A cartilage basement membrane equivalent? *Matrix Biology* 2008;27:22-33.
- [40] Irawan D, Hutmacher D, Klein T. Matrices for zonal cartilage tissue engineering. In: Khang T, editor. *Handbook of Intelligent Scaffolds for Tissue Engineering and Regenerative Medicine*: Pan Stanford Publishing; 2010.
- [41] Poole CA. Articular cartilage chondrons: Form, function and failure. *Journal of Anatomy* 1997;191:1-13.
- [42] Gelber AC, Hochberg MC, Mead LA, Wang N-Y, Wigley FM, Klag MJ. Joint injury in young adults and risk for subsequent knee and hip osteoarthritis. *Annals of Internal Medicine* 2000;135:321-8.
- [43] Buchanan WW, Kean WF, Palmer DG. The contribution of William Hunter (1718–1783) to the study of bone and joint disease. *Clinical Rheumatology* 1987;6:489-503.
- [44] Hunter W. On the structure and diseases of articulating cartilages. *Philosophical Transactions of the Royal Society of London* 1743;42B:5140521.
- [45] Shapiro F, Koide S, Glimcher M. Cell origin and differentiation in the repair of full-thickness defects of articular cartilage. *Journal of Bone and Joint Surgery* 1993;75:532-53.
- [46] Huey DJ, Hu JC, Athanasiou KA. Unlike bone, cartilage regeneration remains elusive. *Science* 2012;338:917-21.
- [47] Mahmoudifar N, Doran PM. Chondrogenesis and cartilage tissue engineering: the longer road to technology development. *Trends in Biotechnology* 2012;30:166-76.
- [48] Hunziker EB. The elusive path to cartilage regeneration *Advanced Materials* 2009;21:3419-24.
- [49] Bedi A, Feeley BT, Williams RJ. Management of articular cartilage defects of the knee. *Journal of Bone and Joint Surgery* 2010;94:994-1009.
- [50] Brittberg M, Lindahl A, Nilsson A, Ohlsson C, Isaksson O, Peterson L. Treatment of deep cartilage defects in the knee with autologous chondrocyte transplantation. *New England Journal of Medicine* 1994;331:889-95.
- [51] Mastbergen SC, Saris DBF, Lafeber FPJG. Functional articular cartilage repair: here, near, or is the best approach not yet clear? *Nature Reviews Rheumatology* 2013;9:277-90.

- [52] Van den Bulcke AI, Bogdanov B, Rooze ND, Schacht EH, Cornelissen M, Berghmans H. Structural and rheological properties of methacrylamide modified gelatin hydrogels. *Biomacromolecules* 2000;1:31-8.
- [53] Benya PD, Shaffer JD. Dedifferentiated chondrocytes reexpress the differentiated collagen phenotype when cultured in agarose gels. *Cell* 1982;30:215-24.
- [54] Spiller KL, Maher SA, Lowman AM. Hydrogels for the repair of articular cartilage defects. *Tissue Engineering - Part B* 2011;17:281-99.
- [55] Elisseeff J, McIntosh W, Anseth K, Riley S, Ragan P, Langer R. Photoencapsulation of chondrocytes in poly(ethylene oxide)-based semi-interpenetrating networks. *Journal of Biomedical Materials Research* 2000;51:164-71.
- [56] Smeds KA, Pfister-Serres A, Miki D, Dastgheib K, Inoue M, Hatchell DL, et al. Photocrosslinkable polysaccharides for in situ hydrogel formation *Journal of Biomedical Materials Research: Part A* 2001;54:115-21.
- [57] Cook WD. Spectral distributions of dental photopolymerization sources. *Journal of Dental Research* 1982;61:1436-8.
- [58] Birdsell D, Bannon P, Webb R. Harmful effects of near-ultraviolet radiation used for polymerization of a sealant and a composite resin. *The Journal of the American Dental Association* 1977;94:311-4.
- [59] Eriksen P, Moscato PM, Franks JK, Sliney DH. Optical hazard evaluation of dental curing lights. *Community Dentistry and Oral Epidemiology* 1987;15:197-201.
- [60] Besaratinia A, Yoon J-i, Schroeder C, Bradforth SE, Cockburn M, Pfeifer GP. Wavelength dependence of ultraviolet radiation-induced DNA damage as determined by laser irradiation suggests that cyclobutane pyrimidine dimers are the principal DNA lesions produced by terrestrial sunlight. *FASEB Journal* 2011;25:3079-91.
- [61] de Gruijl F. Photocarcinogenesis: UVA vs. UVB radiation. *Skin Pharmacology and Applied Skin Physiology* 2002;15:316-20.
- [62] Kielbassa C, Roza L, Epe B. Wavelength dependence of oxidative DNA damage induced by UV and visible light. *Carcinogenesis* 1997;18:811-6.
- [63] Bryant SJ, Nuttelman CR, Anseth KS. Cytocompatibility of UV and visible light photoinitiating systems on cultured NIH/3T3 fibroblasts in vitro. *Journal of Biomaterials Science, Polymer Edition* 2000;11:439-57.
- [64] Bahney CS, Lujan TJ, Hsu CW, Bottlang M, West JL, Johnstone B. Visible light photoinitiation of mesenchymal stem cell-laden bioresponsive hydrogels. *European Cells and Materials* 2011;22:43-55.
- [65] Fedorovich NE, Oudshoorn MH, Geemen Dv, Hennink WE, Alblas J, Dhert WJA. The effect of photopolymerization on stem cells embedded in hydrogels *Biomaterials* 2009;30:344-53.
- [66] Nichol JW, Koshy ST, Bae H, Hwang CM, Yamanlara S, Khademhosseini A. Cell-laden microengineered gelatin methacrylate hydrogels *Biomaterials* 2010;31:5536-44.

- [67] Elisseeff J, Anseth K, Sims D, McIntosh W, Randolph M, Langer R. Transdermal photopolymerization for minimally invasive implantation Proceedings of the National Academy of Sciences of the United States of America 1999;96:3104-7.
- [68] Chou AI, Akintoye SO, Nicoll SB. Photo-crosslinked alginate hydrogels support enhanced matrix accumulation by nucleus pulposus cells in vivo. Osteoarthritis and Cartilage 2009;17:1377-84.
- [69] Burdick JA, Chung C, Jia X, Randolph MA, Langer R. Controlled degradation and mechanical behavior of photopolymerized hyaluronic acid networks. Biomacromolecules 2005;6:386-91.
- [70] Amsden BG, Sukarto A, Knight DK, Shapka SN. Methacrylated glycol chitosan as a photopolymerizable biomaterial. Biomacromolecules 2007;8:3758-66.
- [71] Dijk-Wolthuis WNEv, Steenbergen MJv, Underberg WJM, Hennink WE. Degradation kinetics of methacrylated dextrans in aqueous solution. Journal of pharmaceutical sciences 1997;86:413-7.
- [72] Coutinho DF, Sant SV, Shin H, Oliveira JT, Gomes ME, Neves NM, et al. Modified gellan gum hydrogels with tunable physical and mechanical properties. Biomaterials 2010;31:7494-502.
- [73] Sharma B, Fermanian S, Gibson M, Unterman S, Herzka DA, Cascio B, et al. Human cartilage repair with a photoreactive adhesive-hydrogel composite. Science Translational Medicine 2013;5.
- [74] Skaalure SC, Dimson SO, Pennington AM, Bryanta SJ. Semi-interpenetrating networks of hyaluronic acid in degradable PEG hydrogels for cartilage tissue engineering. Acta Biomaterialia 2014.
- [75] Grigolo B, Roseti L, Fiorini M, Fini M, Giavaresi G, Aldini NN, et al. Transplantation of chondrocytes seeded on a hyaluronan derivative (Hyaff (R)-11) into cartilage defects in rabbits Biomaterials 2001;22:2417-24.
- [76] Nettles DL, Vail TP, Morgan MT, Grinstaff MW, Setton LA. Photocrosslinkable hyaluronan as a scaffold for articular cartilage repair. Annals of Biomedical Engineering 2004;32:391-7.
- [77] Chung C, Mesa J, Miller G, Randolph M, Gill T, Burdick J. Effects of auricular chondrocyte expansion on neocartilage formation in photocrosslinked hyaluronic acid networks. Tissue Engineering 2006;12:2665-73.
- [78] Erickson IE, Huang AH, Sengupta S, Kestle S, Burdick JA, Mauck RL. Macromer density influences mesenchymal stem cell chondrogenesis and maturation in photocrosslinked hyaluronic acid hydrogels. Osteoarthritis and Cartilage 2009;17:1639-48.
- [79] Toh WS, Lee EH, Guo X-M, Chan JKY, Yeow CH, Choo AB, et al. Cartilage repair using hyaluronan hydrogel-encapsulated human embryonic stem cell-derived chondrogenic cells Biomaterials 2010;31:6968-80.
- [80] Klein TJ, Rizzi SC, Schrobback K, Reichert JC, Jeon JE, Crawford RW, et al. Long-term effects of hydrogel properties on human chondrocyte behavior. Soft Matter 2010;6:5175-83.

- [81] Naficy S, Brown HR, Razal JM, Spinks GM, Whitten PG. Progress toward robust polymer hydrogels. *Australian Journal of Chemistry* 2011;64:1007-25.
- [82] Nguyen QT, Hwang Y, Chen AC, Varghese S, Sah RL. Cartilage-like mechanical properties of poly (ethylene glycol)-diacrylate hydrogels. *Biomaterials* 2012;33:668-6690.
- [83] Gong JP, Katsuyama Y, Kurokawa T, Osada Y. Double-network hydrogels with extremely high mechanical strength *Advanced Materials* 2003;15:1155-8.
- [84] Skaalure SC, Dimson SO, Pennington AM, Bryant SJ. Gel structure has an impact on pericellular and extracellular matrix deposition, which subsequently alters metabolic activities in chondrocyte-laden PEG hydrogels. *Acta Biomaterialia* 2011;7:492-504.
- [85] Kock LM, Geraedts J, Ito K, Donkelaar CCv. Low agarose concentration and TGF- $\beta$ 3 distribute extracellular matrix in tissue-engineered cartilage *Tissue Engineering Part A* 2013;19:1621-31.
- [86] Pierschbacher MD, Ruoslahti E. Cell attachment activity of fibronectin can be duplicated by small synthetic fragments of the molecule. *Nature* 1984;309:30-3.
- [87] Connelly JT, García AJ, Levenston ME. Inhibition of in vitro chondrogenesis in RGD-modified three-dimensional alginate gels *Biomaterials* 2007;28:1071-83.
- [88] Matsuki K, Sasho T, Nakagawa K, Tahara M, Sugioka K, Ochiai N, et al. RGD peptide-induced cell death of chondrocytes and synovial cells *Journal of Orthopaedic Science* 2008;13:524-32.
- [89] Callahan LAS, Childers EP, Bernard SL, Weiner SD, Becker ML. Maximizing phenotype constraint and extracellular matrix production in primary human chondrocytes using arginine-glycine-aspartate concentration gradient hydrogels. *Acta Biomaterialia* 2013;9:7420-8.
- [90] Villanueva I, Weigel CA, Bryant SJ. Cell-matrix interactions and dynamic mechanical loading influence chondrocyte gene expression and bioactivity in PEG-RGD hydrogels. *Acta Biomaterialia* 2009;5:2832-46.
- [91] Kock LM, Schulz RM, Donkelaar CCv, Thümmeler CB, Bader A, Ito K. RGD-dependent integrins are mechanotransducers in dynamically compressed tissue-engineered cartilage constructs *Journal of Biomechanics* 2009;42:2177-82.
- [92] Salinas CN, Cole BB, Kasko AM, Anseth K. Chondrogenic differentiation potential of human mesenchymal stem cells photoencapsulated within poly(ethylene glycol)-arginine-glycine-aspartic acid-serine thiol-ethacrylate mixed-mode networks *Tissue Engineering* 2007;13:1025-34.
- [93] Salinas CN, Anseth K. The enhancement of chondrogenic differentiation of human mesenchymal stem cells by enzymatically regulated RGD functionalities *Biomaterials* 2008;29:2370-7.
- [94] Park Y, Lutolf M, Hubbell J, Hunziker E, Wong M. Bovine primary chondrocyte culture in synthetic matrix metalloproteinase-sensitive poly(ethylene glycol)-based hydrogels as a scaffold for cartilage repair. *Tissue Engineering* 2004;10:515-23.

- [95] Chung C, Beecham M, Mauck RL, Burdick JA. The influence of degradation characteristics of hyaluronic acid hydrogels on in vitro neocartilage formation by mesenchymal stem cells. *Biomaterials* 2009;30:4287-96.
- [96] Cheng C-W, Lin K-C, Pan F-M, Sinchaikul S, Wong C-H, Su W-C, et al. Facile synthesis of metal-chelating peptides on chip for protein array *Bioorganic & Medicinal Chemistry Letters* 2004;14:1987-90.
- [97] Lee HJ, Yu C, Chansakul T, Hwang NS, Varghese S, Yu SM, et al. Enhanced chondrogenesis of mesenchymal stem cells in collagen mimetic peptide-mediated microenvironment *Tissue Engineering Part A* 2008;14:1843-51.
- [98] Salinas CN, Anseth K. Decorin moieties tethered into PEG networks induce chondrogenesis of human mesenchymal stem cells. *Journal of Biomedical Materials Research Part A* 2009;90A:456-64.
- [99] Mhanna R, Ozturk E, Vallmajo-Martin Q, Millan C, Muller M, Zenobi-Wong M. GFOGER-modified MMP-sensitive polyethylene glycol (PEG) hydrogels induce chondrogenic differentiation of human mesenchymal stem cells. *Tissue Engineering - Part A* 2013;20:1165-74.
- [100] Zhu J. Bioactive modification of poly(ethylene glycol) hydrogels for tissue engineering. *Biomaterials* 2010;31:4639-56.
- [101] Allemann F, Mizuno S, Eid K, Yates KE, Zaleske D, Glowacki J. Effects of hyaluronan on engineered articular cartilage extracellular matrix gene expression in 3-dimensional collagen scaffolds *Journal of Biomedical Materials Research* 2001;55:13-9.
- [102] Grigolo B, Lisignoli G, Piacentini A, Fiorini M, Gobbi P, Mazzotti G, et al. Evidence for redifferentiation of human chondrocytes grown on a hyaluronan-based biomaterial (HYAFF (R) 11): molecular, immunohistochemical and ultrastructural analysis *Biomaterials* 2002;23:1178-95.
- [103] Liao E, Yaszemski M, Krebsbach P, Hollister S. Tissue-engineered cartilage constructs using composite hyaluronic acid/collagen I hydrogels and designed poly(propylene fumarate) scaffolds. *Tissue Engineering* 2007;13:537-50.
- [104] Ko C-S, Huang J-P, Huang C-W, Chu I-M. Type II collagen-chondroitin sulfate-hyaluronan scaffold cross-linked by genipin for cartilage tissue engineering. *Journal of Bioscience and Bioengineering* 2008;107:177-82.
- [105] Angele P, Müller R, Schumann D, Englert C, Zellner J, Johnstone B, et al. Characterization of esterified hyaluronan-gelatin polymer composites suitable for chondrogenic differentiation of mesenchymal stem cells *Journal of Biomedical Materials Research: Part A* 2009;91A:416-27.
- [106] Hwang NS, Varghese S, Lee HJ, Theprungsirikul P, Canver AC, Sharma B, et al. Response of zonal chondrocytes to extracellular matrix-hydrogels. *FEBS Letters* 2007;581:4172-8.
- [107] Hwang NS, Varghese S, Li H, Elisseeff J. Regulation of osteogenic and chondrogenic differentiation of mesenchymal stem cells in PEG-ECM hydrogels. *Cell and Tissue Research* 2011;344:499-509.



- [108] Fedorovich NE, Swennen I, Girones J, Moroni L, Blitterswijk CA, Schacht E, et al. Evaluation of photocrosslinked lutrol hydrogel for tissue printing applications. *Biomacromolecules* 2009;10:1689-96.
- [109] Melchels FPW, Dhert WJA, Hutmacher DW, Malda J. Development and characterisation of a new bioink for additive tissue manufacturing. *Journal of Materials Chemistry B* 2014;2:2282-9.
- [110] Skardal A, Zhang J, McCoard L, Xu X, Oottamasathien S, Prestwich GD. Photocrosslinkable hyaluronan-gelatin hydrogels for two-step bioprinting *Tissue Engineering: Part A* 2010;16:2675-85.
- [111] Cui X, Breitenkamp K, Finn MG, Lotz M, D'Lima DD. Direct human cartilage repair using three-dimensional bioprinting technology. *Tissue Engineering - Part A* 2012;18:1304-12.
- [112] Billiet T, Gevaert E, Schryver TD, Cornelissen M, Dubrue P. The 3D printing of gelatin methacrylamide cell-laden tissue-engineered constructs with high cell viability. *Biomaterials* 2013.
- [113] Macmull S, Skinner J, Bentley G, Carrington R, Briggs T. Treating articular cartilage injuries of the knee in young people. *British Medical Journal* 2010;340:587-92.
- [114] Welsch GH, Mamisch TC, Zak L, Blanke M, Olk A, Marlovits S. Evaluation of cartilage repair tissue after matrix-associated autologous chondrocyte transplantation using a hyaluronic-based or a collagen-based scaffold with morphological MOCART scoring and biochemical T2 mapping: Preliminary results. *American Journal of Sports Medicine* 2010;38:934-42.
- [115] Behrens P, Bitter T, Kurz B, Russlies M. Matrix-associated autologous chondrocyte transplantation/implantation (MACT/MACI) - 5-year follow-up *Knee* 2006;13:194-202.
- [116] Darling EM, Athanasiou KA. Rapid phenotypic changes in passaged articular chondrocyte subpopulations. *Journal of Orthopaedic Research* 2005;23:425-32.
- [117] Demoor M, Maneix L, Ollitrault D, Legendre F, Duval E, Claus S, et al. Deciphering chondrocyte behaviour in matrix-induced autologous chondrocyte implantation to undergo accurate cartilage repair with hyaline matrix. *Pathologie Biologie* 2012;60:199-207.
- [118] Klein T, Rizzi S, Reichert J, Georgi N, Malda J, Schuurman W, et al. Strategies for zonal cartilage repair using hydrogels. *Macromolecular Bioscience* 2009;9:1049-58.
- [119] Ge Z, Li C, Heng BC, Cao G, Yang Z. Functional biomaterials for cartilage regeneration. *Journal of Biomedical Materials Research - Part A* 2012;100A:2526-36.
- [120] Bryant SJ, Anseth KS. Hydrogel properties influence ECM production by chondrocytes photoencapsulated in poly(ethylene glycol) hydrogels *Journal of Biomedical Materials Research Part A* 2002;59:63-72.
- [121] Leonard M, Boisseson MRD, Hubert P, Dalençon F, Dellacherie E. Hydrophobically modified alginate hydrogels as protein carriers with specific controlled release properties. *Journal of Controlled Release* 2004;98:395-405.

- [122] Erickson IE, Kestle SR, Zellars KH, Farrell MJ, Kim M, Burdick JA, et al. High mesenchymal stem cell seeding densities in hyaluronic acid hydrogels produce engineered cartilage with native tissue properties. *Acta Biomaterialia* 2012;8:3027-34.
- [123] Schuurman W, Levett PA, Pot MW, Weeren PRv, Dhert WJA, Hutmacher DW, et al. Gelatin-methacrylamide hydrogels as potential biomaterials for fabrication of tissue engineered cartilage constructs. *Macromolecular Bioscience* 2013;13:551-61.
- [124] Shin H, Olsen BD, Khademhosseini A. The mechanical properties and cytotoxicity of cell-laden double-network hydrogels based on photocrosslinkable gelatin and gellan gum biomacromolecules. *Biomaterials* 2012;33:3143-52.
- [125] Farndale R, Buttle D, Barrett A. Improved quantitation and discrimination of sulphated glycosaminoglycans by use of dimethylmethylene blue. *Biochimica et Biophysica Acta* 1986;883:173-7.
- [126] Curtis KM, Gomez LA, Rios C, Garbayo E, Raval AP, Perez-Pinzon MA, et al. EF1 alpha and RPL13a represent normalization genes suitable for RT-qPCR analysis of bone marrow derived mesenchymal stem cells. *BMC Molecular Biology* 2010;11:61.
- [127] Schrobback K, Malda J, Crawford RW, Upton Z, Leavesley DI, Klein TJ. Effects of oxygen on zonal marker expression in human articular chondrocytes. *Tissue Engineering Part A* 2012;18:920-33.
- [128] Palmer AW, Guldborg RE, Levenston ME. Analysis of cartilage matrix fixed charge density and three-dimensional morphology via contrast-enhanced microcomputed tomography. *Proceedings of the National Academy of Sciences of the United States of America* 2006;103:19255-60.
- [129] Kim IL, Mauck RL, Burdick JA. Hydrogel design for cartilage tissue engineering: A case study with hyaluronic acid. *Biomaterials* 2011;32:8771-82.
- [130] Little CJ, Bawolin NK, Chen X. Mechanical properties of natural cartilage and tissue-engineered constructs. *Tissue Engineering - Part B* 2012;17:213-27.
- [131] Mueller MB, Tuan RS. Functional characterization of hypertrophy in chondrogenesis of human mesenchymal stem cells *Arthritis and Rheumatism* 2008;58:1377-88.
- [132] Schulze-Tanzil G, Souza Pd, Castrejon HV, John T, Merker H-J, Scheid A, et al. Redifferentiation of dedifferentiated human chondrocytes in high-density cultures. *Cell and Tissue Research* 2002;308:371-9.
- [133] Kwiecinski JJ, Dorosz SG, Ludwig TE, Abubacker S, Cowman MK, Schmidt TA. The effect of molecular weight on hyaluronan's cartilage boundary lubricating ability – alone and in combination with proteoglycan 4. *Osteoarthritis and Cartilage* 2011;19:1356-62.
- [134] Coates EE, Riggin CN, Fisher JP. Matrix molecule influence on chondrocyte phenotype and proteoglycan 4 expression by alginate-embedded zonal chondrocytes and mesenchymal stem cells. *Journal of Orthopaedic Research* 2012;30:1886-97.

- [135] Williams GM, Klein TJ, Sah RL. Cell density alters matrix accumulation in two distinct fractions and the mechanical integrity of alginate–chondrocyte constructs. *Acta Biomaterialia* 2005;1:625-33.
- [136] Campoccia D, Doherty P, Radice M, Brun P, Abatangelo G, Williams DF. Semisynthetic resorbable materials from hyaluronan esterification *Biomaterials* 1998;19:2101-27.
- [137] Dhanasingh A, Salber J, Moeller M, Groll J. Tailored hyaluronic acid hydrogels through hydrophilic prepolymer cross-linkers. *Soft Matter* 2010;6:618-29.
- [138] Hench L. *Biomaterials*. Science 1980;208:826-31.
- [139] Fedorovich N, Alblas J, Wijn JD, Hennink W, Verbout A, Dhert W. Hydrogels as extracellular matrices for skeletal tissue engineering: State-of-the-art and novel application in organ printing. *Tissue Engineering* 2007;13:1905-25.
- [140] Melchels FPW, Domingos MAN, Klein TJ, Malda J, Bartolo PJ, Huttmacher DW. Additive manufacturing of tissues and organs. *Progress in Polymer Science* 2012;37:1079-104.
- [141] Mironov V, Reis N, Derby B. Bioprinting: A beginning *Tissue Engineering* 2006;12:631-4.
- [142] Guillotin B, Souquet A, Catros S, Duocastella M, Pippenger B, Bellance S, et al. Laser assisted bioprinting of engineered tissue with high cell density and microscale organization. *Biomaterials* 2010;31:7250-6.
- [143] Mironov V, Boland T, Trusk T, Forgacs G, Markwald RR. Organ printing: computer-aided jet-based 3D tissue engineering *Trends in Biotechnology* 2003;21:157-61.
- [144] Fedorovich NE, Schuurman W, Wijnberg HM, Prins H-J, Weeren PRv, Malda J, et al. Biofabrication of osteochondral tissue equivalents by printing topologically defined, cell-laden hydrogel scaffolds. *Tissue Engineering Part C - Methods* 2012;18:33-44.
- [145] Boland T, Xu T, Damon B, Cui X. Application of inkjet printing to tissue engineering. *Biotechnology Journal* 2006;1:910-7.
- [146] Guillotin B, Guillemot F. Cell patterning technologies for organotypic tissue fabrication. *Trends in Biotechnology* 2011;29:183-90.
- [147] Lee KC, Koh IB. Intravascular tumour targeting of aclarubicin-loaded gelatin microspheres. Preparation, biocompatibility and biodegradability. *Archives of Pharmacological Research* 1987;10:42-9.
- [148] Ratcliffe JH, Hunneyball IM, Smith A, Wilson CG, Davis SS. Preparation and evaluation of biodegradable polymeric systems for the intra-articular delivery of drugs. *Journal of Pharmacy and Pharmacology* 1984;36:431-6.
- [149] Gupta A, Mohanty B, Bohidar HB. Flory temperature and upper critical solution temperature of gelatin solutions. *Biomacromolecules* 2005;6:1623-7.
- [150] Mohanty B, Bohidar HB. Microscopic structure of gelatin coacervates. *International Journal of Biological Macromolecules* 2005;36:39-46.
- [151] Censi R, Schuurman W, Malda J, Dato Gd, Burgisser PE, Dhert WJA, et al. A printable photopolymerizable thermosensitive p(HPMAM-lactate)-PEG

- hydrogel for tissue engineering. *Advanced Functional Materials* 2011;21:1833-42.
- [152] Sutter M, Siepmann J, Hennink WE, Jiskoot W. Recombinant gelatin hydrogels for the sustained release of proteins. *Journal of Controlled Release* 2007;119:301-12.
- [153] Benton JA, DeForest CA, Vivekanandan V, Anseth KS. Photocrosslinking of gelatin macromers to synthesize porous hydrogels that promote valvular interstitial cell function. *Tissue Engineering Part A* 2009;15:3221-30.
- [154] Aubin H, Nichol JW, Hutson CB, Bae H, Sieminski AL, Cropek DM, et al. Directed 3D cell alignment and elongation in microengineered hydrogels. *Biomaterials* 2010;31:6941-51.
- [155] Qi H, Du Y, Wang L, Kaji H, Bae H, Khademhosseini A. Patterned differentiation of individual embryoid bodies in spatially organized 3D hybrid microgels. *Advanced Materials* 2010;22:5276-81.
- [156] Pescosolido L, Schuurman W, Malda J, Matricardi P, Alhaique F, Coviello T, et al. Hyaluronic acid and dextran-based semi-IPN hydrogels as biomaterials for bioprinting. *Biomacromolecules* 2011;12:1831-8.
- [157] Chung C, Erickson IE, Mauck RL, Burdick JA. Differential behavior of auricular and articular chondrocytes in hyaluronic acid hydrogels. *Tissue Engineering: Part A* 2008;14:1121-31.
- [158] Park S-H, Park SR, Chung SI, Pai KS, Min B-H. Tissue-engineered cartilage using fibrin/hyaluronan composite gel and its in vivo implantation. *Artificial Organs* 2005;25:838-45.
- [159] Bosch Evd, Gielens C. Gelatin degradation at elevated temperature. *International Journal of Biological Macromolecules* 2003;32:129-38.
- [160] Schuurman W, Khristov V, Pot MW, Weeren PRv, Dhert WJA, Malda J. Bioprinting of hybrid tissue constructs with tailorable mechanical properties. *Biofabrication* 2011;3.
- [161] Brinkman WT, Nagapudi K, Thomas BS, Chaikof EL. Photo-crosslinking of type I collagen gels in the presence of smooth muscle cells: Mechanical properties, cell viability, and function. *Biomacromolecules* 2003;5:890-5.
- [162] Lewis MC, MacArthur BD, Malda J, Pettet G, Please CP. Heterogeneous proliferation within engineered cartilaginous tissue: the role of oxygen tension. *Biotechnology and Bioengineering* 2005;91:607-15.
- [163] Carrier RL, Rupnick M, Langer R, Schoen FJ, Freed LE, Novakovic GV-. Perfusion improves tissue architecture of engineered cardiac muscle. *Tissue Engineering* 2002;8:175-88.
- [164] Obradovic B, Carrier RL, Vunjak-Novakovic G, Freed LE. Gas exchange is essential for bioreactor cultivation of tissue engineered cartilage. *Biotechnology and Bioengineering* 1999;63:197-205.
- [165] Bryant SJ, Chowdhury TT, Lee DA, Bader DL, Anseth KS. Crosslinking density influences chondrocyte metabolism in dynamically loaded photocrosslinked poly(ethylene glycol) hydrogels. *Annals of Biomedical Engineering* 2004;32:407-17.

- [166] Xu W, Wang X, Yan Y, Zheng W, Xiong Z, Lin F, et al. Rapid prototyping three-dimensional cell/gelatin/fibrinogen constructs for medical regeneration. *Journal of Bioactive and Compatible Polymers: Biomedical Applications* 2007;22:363-77.
- [167] Shim J-H, Lee J-S, Kim JY, Cho D-W. Bioprinting of a mechanically enhanced three-dimensional dual cell-laden construct for osteochondral tissue engineering using a multi-head tissue/organ building system. *Journal of Micromechanics and Microengineering* 2012;22.
- [168] Endres M, Hutmacher DW, Salgado AJ, Kaps C, Ringe J, Reis RL, et al. Osteogenic induction of human bone marrow-derived mesenchymal progenitor cells in novel synthetic polymer-hydrogel matrices. *Tissue Engineering* 2003;9:689-702.
- [169] Holloway JL, Lowman AM, Palmese GR. Mechanical evaluation of poly (vinyl alcohol)-based fibrous composites as biomaterials for meniscal tissue replacement. *Acta Biomaterialia* 2010;6:4716-24.
- [170] Schagemann JC, Chung HW, Mrosek EH, Stone JJ, Fitzsimmons JS, O'Driscoll SW, et al. Poly- $\epsilon$ -caprolactone/gel hybrid scaffolds for cartilage tissue engineering. *Journal of Biomedical Materials Research Part A* 2010;93A:454-63.
- [171] Shepherd DET, Seedhom BB. Thickness of human articular cartilage in joints of the lower limb. *Annals of the Rheumatic Diseases* 1999;58:27-34.
- [172] Heiligenstein S, Cucchiari M, Laschke MW, Bohle RM, Kohn D, Menger MD, et al. In vitro and in vivo characterization of nonbiomedical-and biomedical-grade alginates for articular chondrocyte transplantation. *Tissue Engineering Part C - Methods* 2011;17:829-42.
- [173] Rouillard AD, Berglund CM, Lee JY, Polacheck WJ, Tsui Y, Bonassar LJ, et al. Methods for photocrosslinking alginate hydrogel scaffolds with high cell viability. *Tissue Engineering Part C - Methods* 2011;17:173-9.
- [174] Callahan LAS, Ganos AM, McBurney DL, Dilisio MF, Weiner SD, Walter E, Horton J, et al. ECM production of primary human and bovine chondrocytes in hybrid PEG hydrogels containing type I collagen and hyaluronic acid. *Biomacromolecules* 2012;13:1625-31.
- [175] Akmal M, Singh A, Anand A, Kesani A, Aslam N, Goodship A, et al. The effects of hyaluronic acid on articular chondrocytes. *Journal of Bone and Joint Surgery - British Volume* 2005;87B:1143-9.
- [176] Kavalkovich KW, Boynton RE, Murphy JM, Barry F. Chondrogenic differentiation of human mesenchymal stem cells within an alginate layer culture system. *In Vitro Cellular & Developmental Biology - Animal* 2002;38:457-66.
- [177] Kim M, Kim SE, Kang SS, Kim YH, Tae G. The use of de-differentiated chondrocytes delivered by a heparin-based hydrogel to regenerate cartilage in partial-thickness defects. *Biomaterials* 2011;32:7883-96.
- [178] Eyre D. Collagen of articular cartilage. *Arthritis Research* 2002;4:30-5.
- [179] Steinmetz NJ, Bryant SJ. The effects of intermittent dynamic loading on chondrogenic and osteogenic differentiation of human marrow stromal cells

encapsulated in RGD-modified poly(ethylene glycol) hydrogels. *Acta Biomaterialia* 2011;7:3829-40.

[180] Vasiliadis HS, Wasiak J, Salanti G. Autologous chondrocyte implantation for the treatment of cartilage lesions of the knee: a systematic review of randomized studies. *Knee Surgery Sports Traumatology Arthroscopy* 2010;18:1645-55.

[181] Knutsen G, Engebretsen L, Ludvigsen TC, Drogset JO, Grøntvedt T, Solheim E, et al. Autologous chondrocyte implantation compared with microfracture in the knee - A randomised trial. *Journal of Bone and Joint Surgery - American Volume* 2004;86:455-64.

[182] Bryant S, Davis-Arehart K, Luo N, Shoemaker R, Arthur J, Anseth K. Synthesis and characterization of photopolymerized multifunctional hydrogels: Water-soluble poly(vinyl alcohol) and chondroitin sulfate macromers for chondrocyte encapsulation. *Macromolecules* 2004;37:6726-33.

[183] Varghese S, Hwang NS, Canver AC, Theprungsirikul P, Lin DW, Elisseeff J. Chondroitin sulfate based niches for chondrogenic differentiation of mesenchymal stem cells. *Matrix Biology* 2008;27:12-21.

[184] Nguyen LH, Kudva AK, Guckert NL, Linse KD, Roy K. Unique biomaterial compositions direct bone marrow stem cells into specific chondrocytic phenotypes corresponding to the various zones of articular cartilage. *Biomaterials* 2010.

[185] Albrecht C, Tichy B, Nürnberger S, Hosiner S, Zak L, Aldrian S, et al. Gene expression and cell differentiation in matrix-associated chondrocyte transplantation grafts: a comparative study. *Osteoarthritis and Cartilage* 2011;19:1219-27.

[186] Villanueva I, Gladem SK, Kessler J, Bryant SJ. Dynamic loading stimulates chondrocyte biosynthesis when encapsulated in charged hydrogels prepared from poly(ethylene glycol) and chondroitin sulfate. *Matrix Biology* 2010;29:51-62.

[187] Jeon JE, Schrobback K, Hutmacher DW, Klein TJ. Dynamic compression improves biosynthesis of human zonal chondrocytes from osteoarthritis patients. *Osteoarthritis and Cartilage* 2012;20:906-15.

[188] Levett PA, Melchels FPW, Schrobback K, Hutmacher DW, Malda J, Klein TJ. Chondrocyte redifferentiation and construct mechanical property development in single-component photocrosslinkable hydrogels. *Journal of Biomedical Materials Research - Part A* 2013;102:2544-53.

[189] Ponta H, Sherman L, Herrlich PA. CD44: From adhesion molecules to signalling regulators. *Nature Reviews: Molecular cell biology* 2003;4:33-45.

[190] Park H, Choi B, Hu J, Lee M. Injectable chitosan hyaluronic acid hydrogels for cartilage tissue engineering. *Acta Biomaterialia* 2013;9:4779-86.

[191] Jin R, Teixeira LSM, Dijkstra PJ, Blitterswijk CA, Karperien M, Feijen J. Enzymatically-crosslinked injectable hydrogels based on biomimetic dextran-hyaluronic acid conjugates for cartilage tissue engineering. *Biomaterials* 2010;31:3103-13.

- [192] Roberts JJ, Earnshaw A, Ferguson VL, Bryant SJ. Comparative study of the viscoelastic mechanical behavior of agarose and poly(ethylene glycol) hydrogels. *Journal of Biomedical Materials Research Part B: Applied Biomaterials* 2011;99:158-69.
- [193] Brodtkin KR, Garcia AJ, Levenston ME. Chondrocyte phenotypes on different extracellular matrix monolayers. *Biomaterials* 2004;25:5929-38.
- [194] Toole BP. Hyaluronan in morphogenesis. *Journal of Internal Medicine* 1997;242:35-40.
- [195] Evanko SP, Angello JC, Wight TN. Formation of hyaluronan- and versican-rich pericellular matrix is required for proliferation and migration of vascular smooth muscle cells. *Arteriosclerosis, thrombosis, and vascular biology* 1999;19:1004-13.
- [196] Knudson W, Loeser RF. CD44 and integrin matrix receptors participate in cartilage homeostasis. *Cellular and Molecular Life Sciences* 2002;59:36-44.
- [197] Brittberg M. Cell carriers as the next generation of cell therapy for cartilage repair: A review of the matrix-induced autologous chondrocyte implantation procedure. *The American Journal of Sports Medicine* 2010;38:1259-71.
- [198] Knudson CB, Knudson W. Hyaluronan-binding proteins in development, tissue homeostasis, and disease. *FASEB Journal* 1993;7:1233-41.
- [199] Roberts JJ, Nicodemus GD, Giunta S, Bryant SJ. Incorporation of biomimetic matrix molecules in PEG hydrogels enhances matrix deposition and reduces load-induced loss of chondrocyte-secreted matrix. *Journal of Biomedical Materials Research - Part A* 2011;97:281-91.
- [200] Korhonen RK, Laasanen MS, Töyräs J, Rieppo J, Hirvonen J, Helminen HJ, et al. Comparison of the equilibrium response of articular cartilage in unconfined compression, confined compression and indentation. *Journal of Biomechanics* 2002;37:903-9.
- [201] Camci-Unal G, Cuttica D, Annabi N, Demarchi D, Khademhosseini A. Synthesis and characterization of hybrid hyaluronic acid-gelatin hydrogels. *Biomacromolecules* 2013;14:1085-92.
- [202] D'Angelo M, Yan Z, Nooreyazdan M, Pacifici M, Sarment DS, Billings PC, et al. MMP-13 is induced during chondrocyte hypertrophy. *Journal of Cellular Biochemistry* 2000;77:678-93.
- [203] Johansson N, Saarialho-Kere U, Airola K, Herva R, Nissinen L, Westermarck J, et al. Collagenase-3 (MMP-13) is expressed by hypertrophic chondrocytes, periosteal cells, and osteoblasts during human fetal bone development. *Developmental Dynamics* 1997;208:387-97.
- [204] Billingham RC, Dahlberg L, Ionescu M, Reiner A, Bourne R, Rorabeck C, et al. Enhanced cleavage of type II collagen by collagenases in osteoarthritic articular cartilage. *The Journal of Clinical Investigation* 1997;99.
- [205] Xu L, Peng H, Wu D, Hu K, Goldring MB, Olsen BR, et al. Activation of the discoidin domain receptor 2 induces expression of matrix metalloproteinase 13 associated with osteoarthritis in mice. *Journal of Biological Chemistry* 2005;280:548-55.

- [206] Ronzière M-C, Aubert-Foucher E, Gouttenoire J, Bernaud J, Herbage D, Mallein-Gerin F. Integrin  $\alpha\beta 1$  mediates collagen induction of MMP-13 expression in MC615 chondrocytes. *Biochimica et Biophysica Acta - Molecular Cell Research* 2005;1746:55-64.
- [207] Bryant S, Anseth K. Controlling the spatial distribution of ECM components in degradable PEG hydrogels for tissue engineering cartilage. *Journal of Biomedical Materials Research Part A* 2003;64A:70-9.
- [208] Ahearne M, Kelly DJ. A comparison of fibrin, agarose and gellan gum hydrogels as carriers of stem cells and growth factor delivery microspheres for cartilage regeneration. *Biomedical Materials* 2013;8:035004.
- [209] Erickson IE, Kestle SR, Zellars KH, Dodge GR, Burdick JA, Mauck RL. Improved cartilage repair via in vitro pre-maturation of MSC-seeded hyaluronic acid hydrogels. *Biomedical Materials* 2012;7:024110.
- [210] Woodfield TBF, Malda J, Wijn Jd, Péters F, Riesle J, Blitterswijk CAv. Design of porous scaffolds for cartilage tissue engineering using a three-dimensional fiber-deposition technique. *Biomaterials* 2004;25:4149-61.
- [211] Malda J, Visser J, Melchels FP, Jüngst T, Hennink WE, Dhert WJA, et al. 25th anniversary article: engineering hydrogels for biofabrication. *Advanced Materials* 2013;25:5011-28.
- [212] Baker MI, Walsh SP, Schwartz Z, Boyan BD. A review of polyvinyl alcohol and its uses in cartilage and orthopedic applications. *Journal of Biomedical Materials Research Part B: Applied Biomaterials* 2012;100B:1451-7.
- [213] Kim M, Hong B, Lee J, Kim SE, Kang SS, Kim YH, et al. Composite system of PLCL scaffold and heparin-based hydrogel for regeneration of partial-thickness cartilage defects. *Biomacromolecules* 2012;13:2287-98.
- [214] Levett PA, Melchels FPW, Schrobback K, Hutmacher DW, Malda J, Klein TJ. A biomimetic extracellular matrix for cartilage tissue engineering centered on photocurable gelatin, hyaluronic acid and chondroitin sulfate. *Acta Biomaterialia* 2014;10:214-23.
- [215] Benders KEM, Malda J, Saris DBF, Dhert WJA, Steck R, Hutmacher DW, et al. Formalin fixation affects equilibrium partitioning of an ionic contrast agent-microcomputed tomography (EPIC- $\mu$  CT) imaging of osteochondral samples. *Osteoarthritis and Cartilage* 2010;18:1586-91.
- [216] Marcacci M, Berruto M, Brocchetta D, Delcogliano A, Ghinelli D, Gobbi A, et al. Articular cartilage engineering with Hyalograft (R) C - 3-year clinical results *Clinical Orthopaedics and Related Research* 2005:96-105.
- [217] Abate M, Pulcini D, Iorio AD, Schiavone C. Viscosupplementation with intra-articular hyaluronic acid for treatment of osteoarthritis in the elderly. *Current Pharmaceutical Design* 2010;16:631-40.
- [218] Williamson AK, Chen AC, Sah RL. Compressive properties and function—composition relationships of developing bovine articular cartilage. *Journal of Orthopaedic Research* 2001;19:1113-21.



- [219] Wilson W, Huyghe JM, Donkelaar CCv. Depth-dependent compressive equilibrium properties of articular cartilage explained by its composition. *Biomechanics and Modeling in Mechanobiology* 2007;6:43-53.
- [220] Fairbanks BD, Schwartz MP, Bowman CN, Anseth KS. Photoinitiated polymerization of PEG-diacrylate with lithium phenyl-2,4,6-trimethylbenzoylphosphinate: polymerization rate and cytocompatibility. *Biomaterials* 2009;30:6702-7.
- [221] Morita K, Miyamoto T, Fujita N, Kubota Y, Ito K, Takubo K, et al. Reactive oxygen species induce chondrocyte hypertrophy in endochondral ossification. *The Journal of Experimental Medicine* 2007;204:1613-23.
- [222] Roberts JJ, Bryant SJ. Comparison of photopolymerizable thiol-ene PEG and acrylate-based PEG hydrogels for cartilage development. *Biomaterials* 2013;34:9969-79.
- [223] Kafedjiiski K, Jetli RKR, Föger F, Hoyer H, Werle M, Hoffer M, et al. Synthesis and in vitro evaluation of thiolated hyaluronic acid for mucoadhesive drug delivery. *International Journal of Pharmaceutics* 2007;343:48-58.
- [224] O'Brien AK, Cramer NB, Bowman CN. Oxygen inhibition in thiol-acrylate photopolymerizations. *Journal of Polymer Science Part A: Polymer Chemistry* 2006;44:2007-14.
- [225] Adkisson HD, Martin JA, Amendola RL, Milliman C, Mauch KA, Katwal AB, et al. The potential of human allogeneic juvenile chondrocytes for restoration of articular cartilage. *The American Journal of Sports Medicine* 2010;38:1324-33.
- [226] Gobbi A, Karnatzikos G, Sankineani SR. One-step surgery with multipotent stem cells for the treatment of large full-thickness chondral defects of the knee. *The American Journal of Sports Medicine* 2014;42:648-57.
- [227] McCormick F, Yanke A, Provencher MT, Cole BJ. Minced articular cartilage - basic science, surgical technique, and clinical application. *Sports medicine and arthroscopy review* 2008;16:217-20.
- [228] Boere KWM, Visser J, Seyednejad H, Rahimian S, Gawlitta D, Steenbergen MJv, et al. Covalent attachment of a three-dimensionally printed thermoplast to a gelatin hydrogel for mechanically enhanced cartilage constructs. *Acta Biomaterialia* 2014;10:2602-11.
- [229] Bastow ER, Byers S, Golub SB, Clarkin CE, Pitsillides AA, Fosang AJ. Hyaluronan synthesis and degradation in cartilage and bone. *Cellular and Molecular Life Sciences* 2008;65:395-413.
- [230] Seidlits SK, Khaing ZZ, Petersen RR, Nickels JD, Vanscoy JE, Shear JB, et al. The effects of hyaluronic acid hydrogels with tunable mechanical properties on neural progenitor cell differentiation. *Biomaterials* 2010;31:3930-40.
- [231] Hutson CB, Nichol JW, Aubin H, Bae H, Yamanlar S, Al-Haque S, et al. Synthesis and characterization of tunable poly(ethylene glycol): Gelatin methacrylate composite hydrogels. *Tissue Engineering - Part A* 2011;17:1713-23.

- [232] DeForest CA, Anseth KS. Advances in bioactive hydrogels to probe and direct cell fate. *Annual Review of Chemical and Biomolecular Engineering* 2012;3:421-44.
- [233] Badylak SF, Weiss DJ, Caplan A, Macchiarini P. Engineered whole organs and complex tissues. *The Lancet* 2012;379:943-52.
- [234] Badylak SF, Freytes DO, Gilbert TW. Extracellular matrix as a biological scaffold material: Structure and function. *Acta Biomaterialia* 2009;5:1-13.
- [235] Badylak S, Brown B, Gilbert T, Daly K, Huber A, Turner N. Biologic scaffolds for constructive tissue remodeling. *Biomaterials* 2011;32:316-9.
- [236] Benders KEM, Weeren PRv, Badylak SF, Saris DIBF, Dhert WJA, Malda J. Extracellular matrix scaffolds for cartilage and bone regeneration. *Trends in Biotechnology* 2013;31:169-76.
- [237] Crapo PM, Gilbert TW, Badylak SF. An overview of tissue and whole organ decellularization processes. *Biomaterials* 2011;32:3233-43.
- [238] Deponti D, Giancamillo AD, Mangiavini L, Pozzi A, Frascini G, Sosio C, et al. Fibrin-based model for cartilage regeneration: tissue maturation from in vitro to in vivo. *Tissue Engineering Part A* 2012;11-12:1109-22.
- [239] Homminga GN, Buma P, Koot HWJ, Kraan PMvd, Berg WBvd. Chondrocyte behavior in fibrin glue in vitro. *Acta Orthopaedica* 1993;64:441-5.
- [240] Teixeira LSM, Leijten JCH, Wennink JWH, Chatterjea AG, Feijen J, Blitterswijk CAv, et al. The effect of platelet lysate supplementation of a dextran-based hydrogel on cartilage formation. *Biomaterials* 2012;33:3651-61.
- [241] Freytes DO, Martin J, Velankar SS, Lee AS, Badylak SF. Preparation and rheological characterization of a gel form of the porcine urinary bladder matrix. *Biomaterials* 2008;29:1630-7.
- [242] Wolf MT, Daly KA, Brennan-Pierce EP, Johnson SA, Carruthers CA, D'Amore A, et al. A hydrogel derived from decellularized dermal extracellular matrix. *Biomaterials* 2012;33:7028-38.
- [243] Pati F, Jang J, Ha D-H, Kim SW, Rhie J-W, Shim J-H, et al. Printing three-dimensional tissue analogues with decellularized extracellular matrix bioink. *Nature Communications* 2014;5:3935.
- [244] Mescher A. Junqueira's basic histology: Text & atlas. 12th Edition ed: McGraw Hill.
- [245] Benders KEM, Boot W, Cokelaere SM, Weeren PRV, Gawlitta D, Bergman HJ, et al. Multipotent stromal cells outperform chondrocytes on cartilage-derived matrix scaffolds. *Cartilage* 2014.
- [246] Klatt AR, Paul-Klausch B, Klinger G, Kühn G, Renno JH, Banerjee M, et al. A critical role for collagen II in cartilage matrix degradation: Collagen II induces pro-inflammatory cytokines and MMPs in primary human chondrocytes. *Journal of Orthopaedic Research* 2009;27:65-70.
- [247] Fichter M, Körner U, Schömburg J, Jennings L, Cole AA, Mollenhauer J. Collagen degradation products modulate matrix metalloproteinase expression in cultured articular chondrocytes. *Journal of Orthopaedic Research* 2006;24:63-70.

- [248] Delcogliano M, Caro Fd, Scaravella E, Ziveri G, Biase CFD, Marotta D, et al. Use of innovative biomimetic scaffold in the treatment for large osteochondral lesions of the knee. *Knee Surgery, Sports Traumatology, Arthroscopy* 2014;22:1260-9.
- [249] Zheng M-H, Willers C, Kirilak L, Yates P, Xu J, Wood D, et al. Matrix-induced autologous chondrocyte implantation (MACI®): Biological and histological assessment. *Tissue Engineering* 2007;13:737-46.
- [250] Nikkhah M, Eshak N, Zorlutuna P, Annabi N, Castello M, Kim K, et al. Directed endothelial cell morphogenesis in micropatterned gelatin methacrylate hydrogels. *Biomaterials* 2012;33:9009-18.
- [251] Piper D, Fenton B. pH stability and activity curves of pepsin with special reference to their clinical importance. *Gut* 1965;6:506-8.
- [252] Gawlitta D, Farrell E, Malda J, Creemers LB, Alblas J, Dhert WJA. Modulating endochondral ossification of multipotent stromal cells for bone regeneration. *Tissue Engineering Part B: Reviews* 2010;16:385-95.
- [253] Pittenger MF, Mackay AM, Beck SC, Jaiswal RK, Douglas R, Mosca JD, et al. Multilineage potential of adult human mesenchymal stem cells. *Science* 1999;284:143-7.
- [254] Chomczynski P, Mackey K. Substitution of chloroform by bromochloropropane in the single-step method of RNA isolation. *Analytical Biochemistry* 1995;225:163-4.
- [255] Medberry CJ, Crapo PM, Siu BF, Carruthers CA, Wolf MT, Nagarkar SP, et al. Hydrogels derived from central nervous system extracellular matrix. *Biomaterials* 2013;34:1033-40.
- [256] Yang G, Rothrauff BB, Lin H, Gottardi R, Alexander PG, Tuan RS. Enhancement of tenogenic differentiation of human adipose stem cells by tendon-derived extracellular matrix. *Biomaterials* 2013;34:9295-306.
- [257] Williams CG, Kim TK, Taboas A, Malik A, Manson P, Elisseff J. In vitro chondrogenesis of bone marrow-derived mesenchymal stem cells in a photopolymerizing hydrogel *Tissue Engineering* 2003;9:679-88.
- [258] Erickson IE, Huang AH, Chung C, Li RT, Burdick JA, Mauck RL. Differential maturation and structure-function relationships in mesenchymal stem cell- and chondrocyte-seeded hydrogels. *Tissue Engineering Part A* 2009;15:1041-52.
- [259] Carter-Arnold J, Neilsen N, Amelse L, Odoi A, Dhar MS. In vitro analysis of equine, bone marrow-derived mesenchymal stem cells demonstrates differences within age- and gender-matched horses. *Equine Veterinary Journal* 2013;46:589-95.
- [260] Windt TSd, Hendriks JAA, Zhao X, Vonk LA, Creemers LB, Dhert WJA, et al. Concise review: Unraveling stem cell cocultures in regenerative medicine: Which cell interactions steer cartilage regeneration and how? *Stem Cells Translational Medicine* 2014;3:723-33.
- [261] Xu L, Peng H, Glasson S, Lee P, Hu K, Ijiri K, et al. Increased expression of the collagen receptor discoidin domain receptor 2 in articular cartilage as a

- key event in the pathogenesis of osteoarthritis. Xu L1, Peng H, Glasson S, Lee PL, Hu K, Ijiri K, Olsen BR, Goldring MB, Li Y 2007;56:2663-73.
- [262] Zhang Y, Su J, Yu J, Bu X, Ren T, Liu X, et al. An essential role of discoidin domain receptor 2 (DDR2) in osteoblast differentiation and chondrocyte maturation via modulation of Runx2 activation. *Journal of Bone and Mineral Research* 2011;26:604-17.
- [263] Nehrer S, Breinan HA, Ramappa A, Shortkroff S, Young G, Minas T, et al. Canine chondrocytes seeded in type I and type II collagen implants investigated In Vitro. *Journal of Biomedical Materials Research* 1997;38:95-104.
- [264] Nehrer S, Breinan HA, Ramappa A, Young G, Shortkroff S, Louie LK, et al. Matrix collagen type and pore size influence behaviour of seeded canine chondrocytes. *Biomaterials* 1997;18:769-76.
- [265] Rutgers M, Saris DB, Vonk LA, Rijen MHv, Akrum V, Langeveld D, et al. Effect of collagen type I or type II on chondrogenesis by cultured human articular chondrocytes. *Tissue Engineering - Part A* 2013;19:59-65.
- [266] Schwarz S, Elsaesser AF, Koerber L, Goldberg-Bockhorn E, Seitz AM, Bermueller C, et al. Processed xenogenic cartilage as innovative biomatrix for cartilage tissue engineering: effects on chondrocyte differentiation and function. *Journal of Tissue Engineering and Regenerative Medicine* 2012.
- [267] Chun SY, Lim GJ, Kwon TG, Kwak EK, Kim BW, Atala A, et al. Identification and characterization of bioactive factors in bladder submucosa matrix. *Biomaterials* 2007;28:4251-6.
- [268] Voytik-Harbin S, Brightman A, Kraine M, Waisner B, Badylak S. Identification of extractable growth factors from small intestinal submucosa. *Journal of Cellular Biochemistry* 1997;15:478-91.
- [269] Chen C-C, Liao C-H, Wang Y-H, Hsu Y-M, Huang S-H, Chang C-H, et al. Cartilage fragments from osteoarthritic knee promote chondrogenesis of mesenchymal stem cells without exogenous growth factor induction. *Journal of Orthopaedic Research* 2012;30:393-400.
- [270] Xue JX, Gong YY, Zhou GD, Liu W, Cao Y, Zhang WJ. Chondrogenic differentiation of bone marrow-derived mesenchymal stem cells induced by acellular cartilage sheets. *Biomaterials* 2012;33:5832-40.
- [271] Bosnakovski D, Mizuno M, Kim G, Takagi S, Okumura M, Fujinaga T. Chondrogenic differentiation of bovine bone marrow mesenchymal stem cells (MSCs) in different hydrogels: Influence of collagen type II extracellular matrix on MSC chondrogenesis. *Biotechnology and Bioengineering* 2006;93:1152-63.
- [272] Leach JB, Bivens KA, Patrick CW, Schmidt CE. Photocrosslinked hyaluronic acid hydrogels: Natural, biodegradable tissue engineering scaffolds. *Biotechnology and Bioengineering* 2003;82:578-89.
- [273] Drury JL, Mooney DJ. Hydrogels for tissue engineering: scaffold design variables and applications *Biomaterials* 2003;24:4337-51.
- [274] Fairbanks BD, Schwartz MP, Halevi AE, Nuttelman CR, Bowman CN, Anseth KS. A versatile synthetic extracellular matrix mimic via thiol-norbornene photopolymerization. *Advanced Materials* 2009;21:5005-10.

- [275] Tibbitt MW, Kloxin AM, Sawicki LA, Anseth KS. Mechanical properties and degradation of chain and step-polymerized photodegradable hydrogels. *Macromolecules* 2013;46:2786-92.
- [276] Lin-Gibson S, Jones RL, Washburn NR, Horkay F. Structure-property relationships of photopolymerizable poly(ethylene glycol) dimethacrylate hydrogels. *Macromolecules* 2011;38:2897-902.
- [277] Henrotin YE, Bruckner P, Pujol J-PL. The role of reactive oxygen species in homeostasis and degradation of cartilage. *Osteoarthritis and Cartilage* 2003;11:747-55.
- [278] Billiet T, Gasse BV, Gevaert E, Cornelissen M, Martins JC, Dubrue P. Quantitative contrasts in the photopolymerization of acrylamide and methacrylamide-functionalized gelatin hydrogel building blocks. *Macromolecular Bioscience* 2013.
- [279] Lysaght M, Jaklenec A, Deweerd E. Great expectations: private sector activity in tissue engineering, regenerative medicine, and stem cell therapeutics. *Tissue Engineering Part A* 2008;14:305-15.
- [280] Meyerkort D, Wood D, Zheng M-H. One-stage vs two-stage cartilage repair: a current review. *Orthopedic Research and Reviews* 2010;2:95-106.
- [281] Browne JE, Anderson AF, Arciero R, Mandelbaum B, Moseley JB, Micheli MLJ, et al. Clinical outcome of autologous chondrocyte implantation at 5 years in US subjects. *Clinical Orthopaedics and Related Research* 2005;436:237-45.
- [282] Kassim SH, Somerville RPT. From lipoproteins to chondrocytes: A brief summary of the european medicines agency's regulatory guidelines for advanced therapy medicinal products *Human Gene Therapy* 2013;24:568-70.
- [283] Saris DBF, Vanlauwe J, Victor J, Haspl M, Bohnsack M, Fortems Y, et al. Characterized chondrocyte implantation results in better structural repair when treating symptomatic cartilage defects of the knee in a randomized controlled trial versus microfracture *American Journal of Sports Medicine* 2008;36:235-46.
- [284] Clinicaltrials.gov. Confirmatory study of NeoCart in knee cartilage repair. 2010.
- [285] Crawford D, DeBerardino T, Williams RJ. NeoCart, an autologous cartilage tissue implant, compared with microfracture for treatment of distal femoral cartilage lesions: An FDA phase-II prospective, randomized clinical trial after two years. *Journal of Bone and Joint Surgery - American Volume* 2012;94:979-89.
- [286] Nehrer S, Chiari C, Domayer S, Barkay H, Yayon A. Results of chondrocyte implantation with a fibrin-hyaluronan matrix: a preliminary study. *Clinical Orthopaedics and Related Research* 2008;466:1849-55.
- [287] Eshed I, Trattng S, Sharon M, Arbel R, Nierenberg G, Konen E, et al. Assessment of cartilage repair after chondrocyte transplantation with a fibrin-hyaluronan matrix – Correlation of morphological MRI, biochemical T2 mapping and clinical outcome. *European Journal of Radiology* 2011;81.
- [288] Selmi TAS, Verdonk P, Chambat P, Dubrana F, Potel J-F, Barnouin L, et al. Autologous chondrocyte implantation in a novel alginate-agarose hydrogel -

Outcome at two years *Journal of Bone and Joint Surgery - British Volume* 2008;90B:597-604.

[289] [Clinicaltrials.gov](#). Comparison of microfracture treatment and CARTIPATCH® chondrocyte graft treatment in femoral condyle lesions.

[290] Schneider U, Rackwitz L, Andereya S, Siebenlist S, Fensky F, Reichert J, et al. A prospective multicenter study on the outcome of type I collagen hydrogel-based autologous chondrocyte implantation (CaReS) for the repair of articular cartilage defects in the knee. *The American Journal of Sports Medicine* 2011;39:2558-65.

[291] Panagopoulos A, Niekerk Lv, Triantafillopoulos I. Autologous chondrocyte implantation for knee cartilage injuries: moderate functional outcome and performance in patients with high-impact activities. *Orthopedics* 2012;35:e6-14.

[292] [Clinicaltrials.gov](#). Safety and effectiveness study to evaluate NOVOCART® 3D plus compared to the microfracture to treat articular cartilage defects of the knee (N3D).

[293] Cole BJ, Jack Farr M, Winalski CS, Hosea T, Richmond J, Mandelbaum B, et al. Outcomes after a single-stage procedure for cell-based cartilage repair: a prospective clinical safety trial with 2-year follow-up. *The American Journal of Sports Medicine* 2011;39:1170-9.

[294] [Clinicaltrials.gov](#). Knee articular cartilage repair: Cartilage autograft implantation system versus conventional microfracture (CAIS).

[295] [Clinicaltrials.gov](#). DeNovo NT natural tissue graft stratified knee study.

[296] Farr J, Yao JQ. Chondral defect repair with particulated juvenile cartilage allograft. *Cartilage* 2011;2:346-53.

[297] McCormick F, BrianJ.Cole, Nwachukwu B, Harris JD, Adkisson HD, Farr J. Treatment of focal cartilage defects with a juvenile allogeneic 3-dimensional articular cartilage graft. *Operative Techniques in Sports Medicine* 2013;21:95-9.

[298] [Clinicaltrials.gov](#). Neocartilage implant phase III trial.

[299] [Clinicaltrials.gov](#). Study to evaluate the safety and performance of treatment of articular cartilage lesions located on the femoral condyle with gelrinC.

[300] McNickle AG, Provencher MT, Cole BJ. Overview of existing cartilage repair technology. *Sports Medicine and Arthroscopy Review* 2008;16:196-201.

[301] [Clinicaltrials.gov](#). ACI-C versus AMIC. A randomized trial comparing two methods for repair of cartilage defects in the knee.

[302] Gille J, Schuseil E, Wimmer J, Gellissen J, Schulz AP, Behrens P. Mid-term results of Autologous Matrix Induced Chondrogenesis for treatment of focal cartilage defects in the knee. *Knee Surgery Sports Traumatology Arthroscopy* 2010;18:1456-64.

[303] Shive MS, Hoemann CD, Restrepo A, Hurtig MB, Duval N, Ranger P, et al. BST-CarGel: In situ chondroInduction for cartilage repair. *Operative Techniques in Orthopaedics* 2006;16:271-8.

[304] Stanish W, McCormack R, Forriol F, Mohtadi N, Pelet S, Desnoyers J, et al. Novel scaffold-based BST-CarGel treatment results in superior cartilage

- repair compared with microfracture in a randomized controlled trial. *Journal of Bone and Joint Surgery - American Volume* 2013;95:1640-50.
- [305] [Clinicaltrials.gov](http://Clinicaltrials.gov). ChonDux for filling full thickness cartilage defects in the femoral condyle of the knee.
- [306] Prestwich GD, Erickson IE, Zarebinski TI, West M, Tew WP. The translational imperative: making cell therapy simple and effective. *Acta Biomaterialia* 2012;8:2000-7.
- [307] Lee JK, Responde DJ, Cissell DD, Hu JC, Nolta JA, Athanasiou KA. Clinical translation of stem cells: Insight for cartilage therapies. *Critical Reviews in Biotechnology* 2013;34:89-100.
- [308] Cascio BM, Sharma B. The future of cartilage repair. *Operative Techniques in Sports Medicine* 2008;16:221-4.
- [309] Irion VH, Flanigan DC. New and emerging techniques in cartilage repair: Other scaffold-based cartilage treatment options. *Operative Techniques in Sports Medicine* 2013;21:125-37.
- [310] Petri M, Broese M, Simon A, Liodakis E, Ettinger M, Guenther D, et al. CaReS® (MACT) versus microfracture in treating symptomatic patellofemoral cartilage defects: a retrospective matched-pair analysis. *Journal of Orthopaedic Science* 2013;18:38-44.
- [311] Windt TSd, Concaro S, Lindahl A, Saris DBF, Brittberg M. Strategies for patient profiling in articular cartilage repair of the knee: a prospective cohort of patients treated by one experienced cartilage surgeon. *Knee Surgery, Sports Traumatology, Arthroscopy* 2012;20:2225-32.
- [312] Vanlauwe J, Saris DBF, Victor J, Almqvist KF, Bellemans J, Luyten FP. Five-year outcome of characterized chondrocyte implantation versus microfracture for symptomatic cartilage defects of the knee: Early treatment matters. *The American Journal of Sports Medicine* 2011;39:2566-74.
- [313] Mollon B, Kandel R, Chahal J, Theodoropoulos J. The clinical status of cartilage tissue regeneration in humans. *Osteoarthritis and Cartilage* 2013;21:18224-1833.
- [314] Kon E, Filardo G, Matteo BD, Perdisa F, Marcacci M. Matrix assisted autologous chondrocyte transplantation for cartilage treatment: A systematic review. *Bone and Joint Research* 2013;2:18-25.
- [315] Wang D-A, Varghese S, Sharma B, Strehin I, Fermanian S, Gorham J, et al. Multifunctional chondroitin sulphate for cartilage tissue-biomaterial integration *Nature Materials* 2007;6:385-92.
- [316] Almany L, Seliktar D. Biosynthetic hydrogel scaffolds made from fibrinogen and polyethylene glycol for 3D cell cultures. *Biomaterials* 2005;26:2467-77.
- [317] [PRNewswire.com](http://PRNewswire.com). Hydrogel implant GelrinC demonstrates impressive recovery rates for patients with knee cartilage damage. 2013.
- [318] Visser J, Melchels FPW, Jeon JE, Bussel EMv, Kimpton LS, Byrne HM, et al. Reinforcement of hydrogels using three-dimensionally printed microfibrils. *Nature Communications* 2015;6:10.1038/ncomms7933.

- [319] Majima T, Schnabel W, Weber W. Phenyl-2,4,6-trimethylbenzoylphosphinates as water-soluble photoinitiators - generation and reactivity of  $O \frac{1}{4}P(C_6H_5)(O^-)$  radical-anions. *Macromolecular Chemistry and Physics* 1991;192:2307-15.
- [320] Barlic A, Drobni M, Maliev E, Kregar-Velikonja N. Quantitative analysis of gene expression in human articular chondrocytes assigned for autologous implantation *Journal of Orthopaedic Research* 2008;26:847-53.
- [321] Jeon O, Powell C, Solorio LD, Krebs MD, Alsberg E. Affinity-based growth factor delivery using biodegradable, photocrosslinked heparin-alginate hydrogels. *Journal of Controlled Release* 2011;154:258-66.
- [322] Visser J, Levett P, te Moller N, Besems J, Boere K, van Rigen M, et al. Crosslinkable hydrogels derived from cartilage, meniscus and tendon tissue. *Tissue Engineering - Part A* 2015;21:1195-206.



## **Appendix A**

### Supplementary Information

---

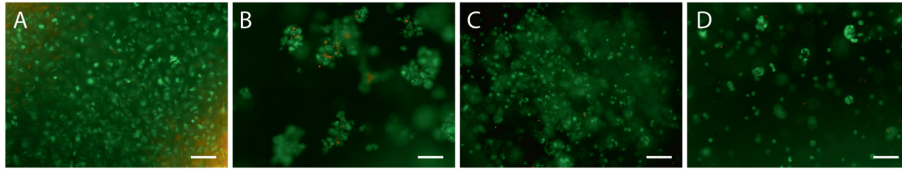


**Figure S3.1: Viability of chondrocytes after 4 weeks culture in gel-MA (A), PEG-MA (B), HA-MA (C) or AL-MA (D) hydrogel constructs.** Live cells appear green, and dead cells appear red. Scale bars represent 100  $\mu\text{m}$ .

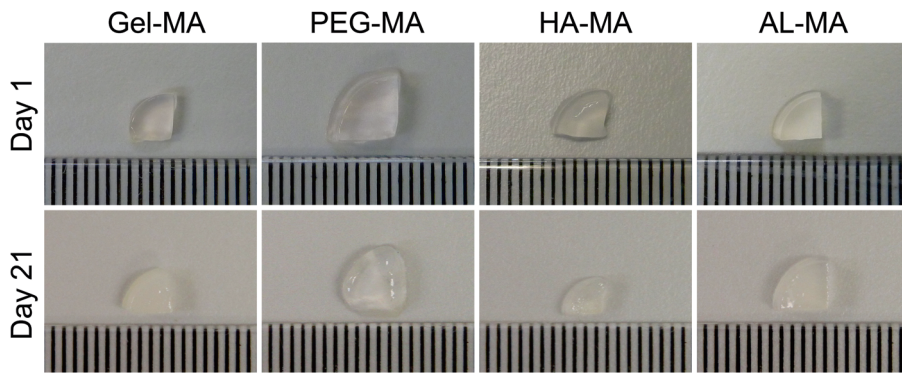


**Figure S3.2: Photographs of cell-laden hydrogel constructs on day 1 and day 21.** Intervals represent 1 mm.

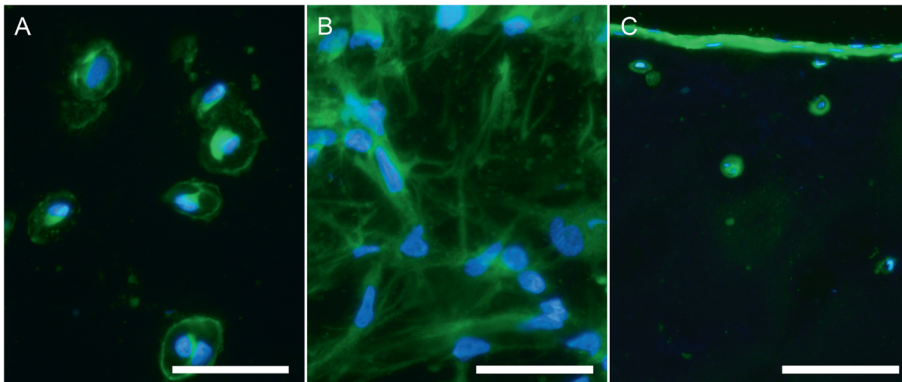


**Figure S5.1: Morphologies of chondrocytes that were encapsulated (A) or at the surface (B) of a G-HA construct, and collagen type I immunofluorescence showing strong staining at the edge of a G-HA-CS construct (C).** Constructs were cultured for 8 weeks, and in A and B, cell membranes were stained using cell mask (green) and nuclei were counterstained with DAPI (blue). Scale bars in A and B are 50  $\mu\text{m}$ , and C is 100  $\mu\text{m}$ .

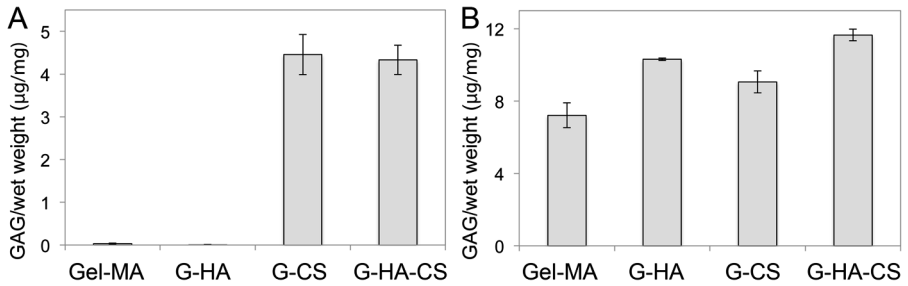


**Figure S5.2. Total GAG content at 8 weeks in cell-free hydrogels (A) and hydrogel constructs with middle/deep chondrocytes (B).** Bars and error bars show the means and standard deviations of 4 samples.

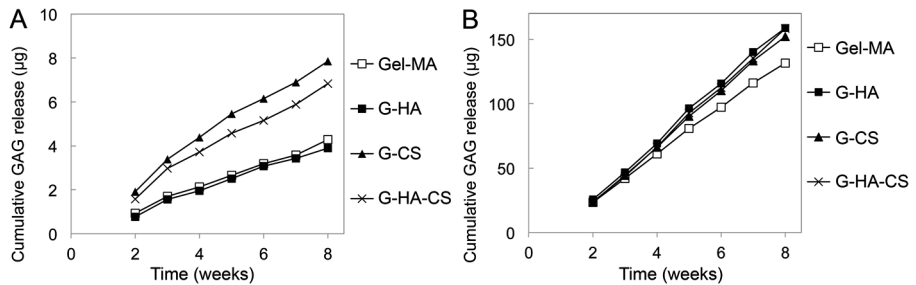


**Figure S5.3. Cumulative GAG release into culture media from cell-free gels (A), and corrected cumulative GAG release from chondrocyte laden constructs (B).** Corrected values were calculated as the difference between the amount of GAGs secreted from cell-laden constructs and cell-free gels. Each data point represents the mean of 4 samples.

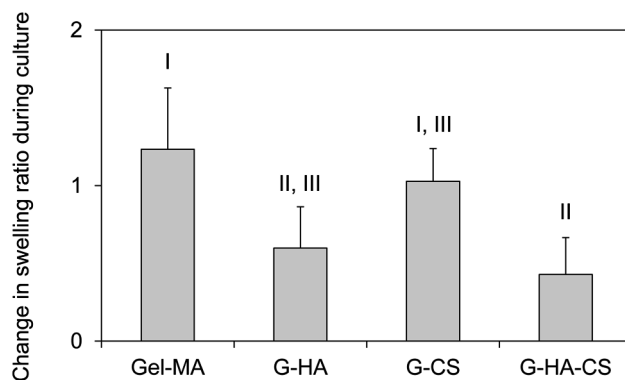


**Figure S5.4. Change in swelling ratios of cell-laden hydrogel constructs during 8 weeks culture.** Groups without a like Roman numeral are statistically different ( $p < 0.05$ ).

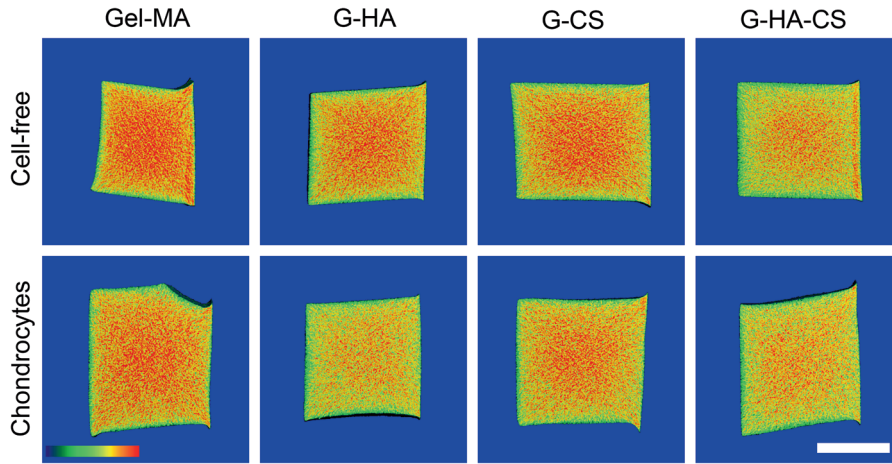


**Figure S5.5. EPIC- $\mu$ CT scans of hydrogel constructs cultured for 2 weeks.** The scale bar represents 2 mm, and the same scale applies to all panels. The attenuation range is 10,000 – 22,000 for all panels.

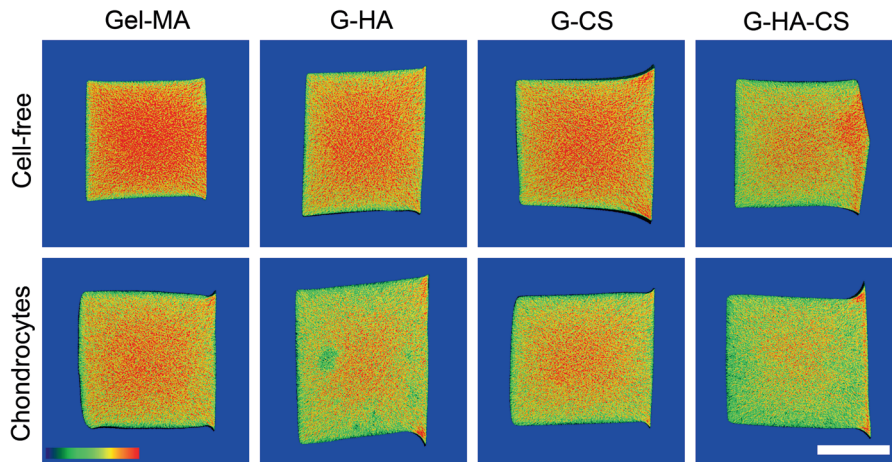


**Figure S5.6. EPIC- $\mu$ CT scans of hydrogel constructs cultured for 5 weeks.** The scale bar represents 2 mm, and the same scale applies to all panels. The attenuation range is 10,000 – 22,000 in all panels.

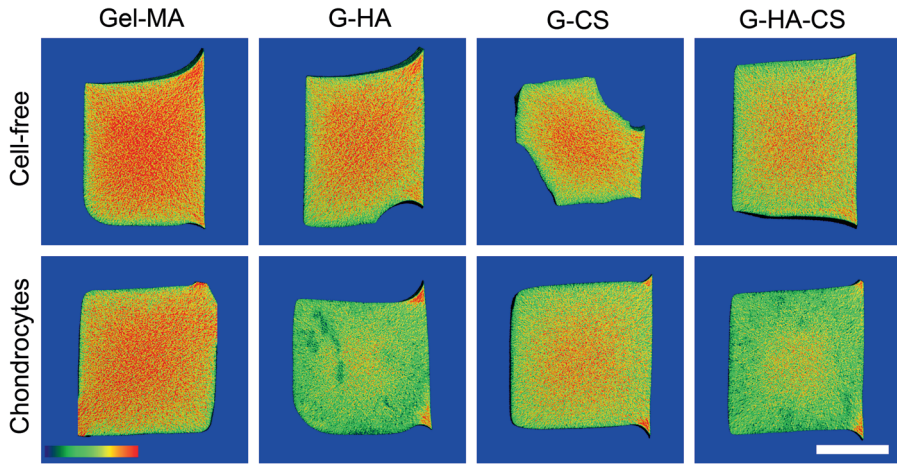


**Figure S5.7. EPIC- $\mu$ CT scans of hydrogel constructs cultured for 8 weeks.** The scale bar represents 2 mm, and the same scale applies to all panels. The attenuation range is 10,000 – 22,000 in all panels.

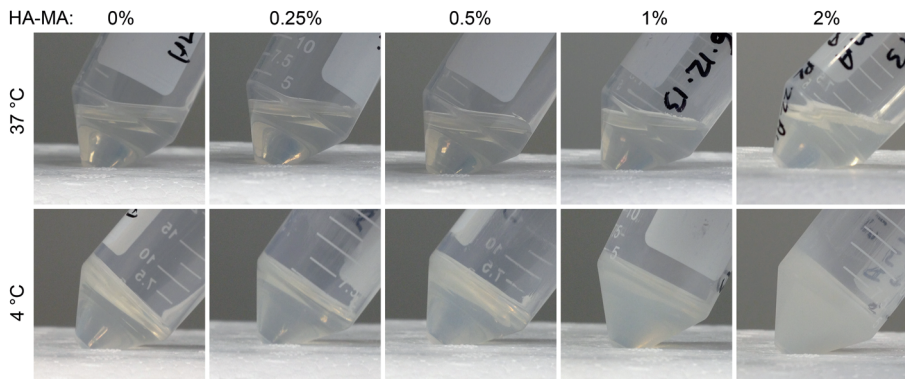


**Figure S6.1: Photographs of gel precursor solutions at 37 °C and 4 °C.** Mixing of Gel-MA and HA-MA is temperature dependent, with HA-MA causing much greater opacity when the mixtures are cool.

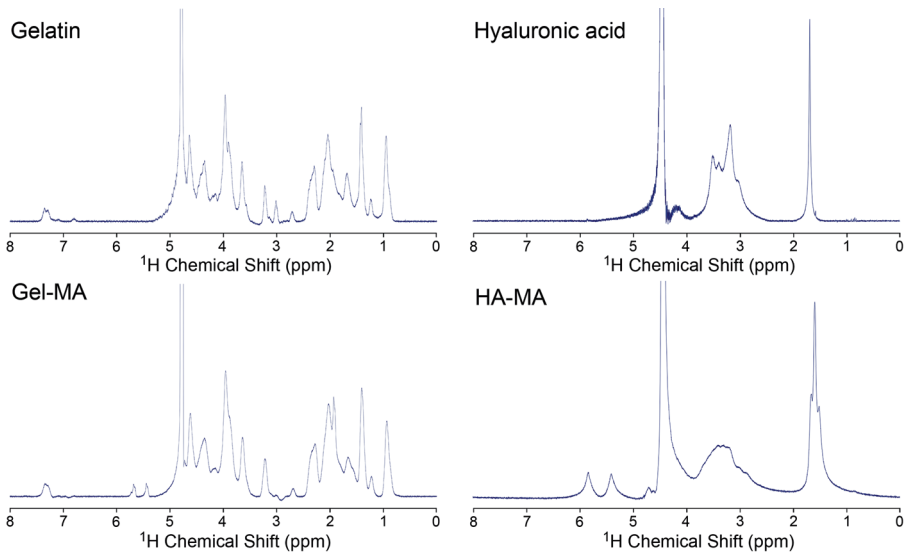


**Figure S6.2: Proton nuclear magnetic resonance spectra of gelatin and hyaluronic acid and their photocrosslinkable derivatives.** The appearance of two peaks in the region 5.5-6.5 ppm show the addition of unsaturated, photocrosslinkable groups.

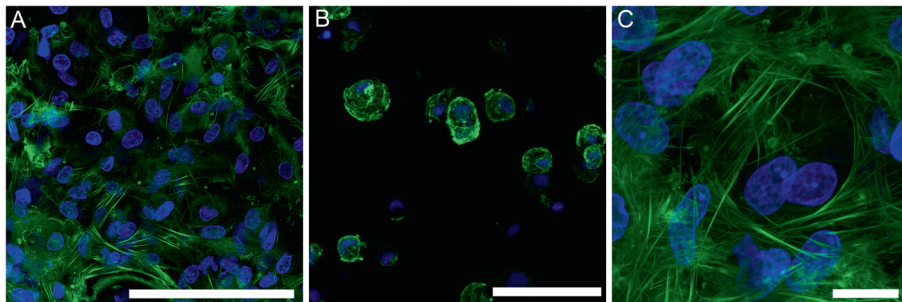


**Figure S6.3: High magnification confocal micrographs of actin structures from a 0% HA-MA construct cultured for 28 days.** Images were taken from the surface of the gel (A and C) or the centre (B). Scalebars represent 100  $\mu\text{m}$  (A), 50  $\mu\text{m}$  (B) or 10  $\mu\text{m}$  (C).

**Table S7.1: Names, symbols and primer sequences of selected genes for qRT-PCR analysis. For each primer pair, the top sequence denotes the forward primer and the bottom sequence the reverse.**

Gene name	Symbol	Primer sequence
Collagen type I A1	COL1A1	5'-AGCCAGCAAGATCGAGAACAT-3' 5'-CGTCTCCATGTTGCAGAAGA-3'
Collagen type II A1	COL2A1	5'-GGCAATAGCAGGTTACGTACA-3' 5'-CGATAACAGTCTTGCCCCACTT-3'
Aggrecan	ACAN	5'-AAGACAGGGTCTCGCTGCCCAA-3' 5'-ATGCCGTGCATCACCTCGCA-3'
Matrix metalloproteinase-3	MMP-3	5'-TTTTGGCCATCTCTTCCTTCA-3' 5'-TGTGGATGCCTTTGGGTATC-3'
Matrix Metalloproteinase-13	MMP-13	5'-CAAGGGATCCAGTCTCTCTATGGT-3' 5'-GGATAAGGAAGGGTCACATTTGTC-3'
Matrix Metalloproteinase-14	MMP-14	5'-GGACTGTCCGGAATGAGGATCT-3' 5'-TTGGAATGCTCAAGGCCCA-3'
Hypoxanthine-guanine-phosphoribosyltransferase 1	HPRT-1	5'-TGGACAGGACTGAACGGCTTGC-3' 5'-GCAGGTCAGCAAAGAATTTATAGCCCC-3'
Signal recognition particle 14 kDa	SRP-14	5'-TGCTGGAGAGCGAGCAGTTCCT-3' 5'-AGCCCTCCACGGAACCTTTCCT-3'





## **Appendix B**

# Contribution and Authorship

---

**Statement of Original Authorship**

To the best of my knowledge and belief, the thesis contains no material previously published or written by another person except where due reference is made. Multiple people contributed to the publications in this thesis. Each authors' contribution is to the publications in this thesis is described on the following pages.

Signature: \_\_\_\_\_

Date: \_\_\_\_\_

### Statement of Contribution of Co-Authors for Thesis by Published Paper

The authors listed below have certified that:

1. They meet the criteria for authorship in that they have participated in the conception, execution, or interpretation, of at least that part of the publication in their field of expertise;
2. They take public responsibility for their part of the publication, except for the responsible author who accepts overall responsibility for the publication;
3. There are no other authors of the publication according to these criteria that are not listed;
4. Potential conflicts of interest have been disclosed to (a) granting bodies, (b) the editor or publisher of journals or other publications, and (c) the head of the responsible academic unit, and
5. They agree to the use of the publication in the Peter Levett's thesis and its publication on the QUT ePrints database consistent with any limitations set by publisher requirements.

**Chapter 3: Chondrocyte redifferentiation and construct mechanical property development in single-component photocrosslinkable hydrogels**, published in the Journal of Biomedical Materials Research – Part A in September 2013.

Contributor	Statement of contribution
Peter A Levett	Experimental design, polymer synthesis, hydrogel construct fabrication, cell culture, construct analyses, data analysis and manuscript preparation.
Ferry PW Melchels	Experimental design, polymer synthesis, data analysis and manuscript editing.
Karsten Schrobback	Experimental design, data analysis and manuscript editing.
Dietmar W. Hutmacher	Experimental design and manuscript editing.
Jos Malda	Experimental design and manuscript editing.
Travis J. Klein	Experimental design, hydrogel construct fabrication, cell culture, construct analyses, data analysis and manuscript editing.

#### Principal Supervisor Confirmation

I have sighted email or other correspondence from all co-authors confirming their certifying authorship.

\_\_\_\_\_  
Name

\_\_\_\_\_  
Signature

\_\_\_\_\_  
Date

### Statement of Contribution of Co-Authors for Thesis by Published Paper

The authors listed below have certified that:

1. They meet the criteria for authorship in that they have participated in the conception, execution, or interpretation, of at least that part of the publication in their field of expertise;
2. They take public responsibility for their part of the publication, except for the responsible author who accepts overall responsibility for the publication;
3. There are no other authors of the publication according to these criteria that are not listed;
4. Potential conflicts of interest have been disclosed to (a) granting bodies, (b) the editor or publisher of journals or other publications, and (c) the head of the responsible academic unit, and
5. They agree to the use of the publication in the Peter Levett's thesis and its publication on the QUT ePrints database consistent with any limitations set by publisher requirements.

**Chapter 4: Gelatin-methacrylamide hydrogels as potential biomaterials for fabrication of tissue-engineered cartilage constructs**, published in *Macromolecular Biosciences* in February 2013.

Contributor	Statement of contribution
Peter A Levett	Experimental design, design of Teflon hydrogel molds, polymer synthesis, hydrogel construct fabrication, hydrogel mechanical testing and analyses and manuscript preparation.
Wouter Schuurman	Experimental design, printed hydrogel construct fabrication, cell culture, data analysis and manuscript preparation.
Michiel W. Pot	Printed hydrogel construct fabrication, cell culture, data collection and manuscript editing.
Paul René van Weeren	Experimental design and manuscript editing.
Wouter J.A. Dhert	Experimental design and manuscript editing.
Dietmar. W. Hutmacher	Experimental design and manuscript editing.
Ferry. P.W. Melchels	Experimental design, UV crosslinker procurement, polymer synthesis, printed hydrogel construct fabrication, data analysis and manuscript preparation.
Travis J. Klein	Experimental design, design of Teflon hydrogel molds, data analysis and manuscript editing.
Jos Malda	Experimental design and manuscript editing.

#### Principal Supervisor Confirmation

I have sighted email or other correspondence from all co-authors confirming their certifying authorship.

\_\_\_\_\_  
Name

\_\_\_\_\_  
Signature

\_\_\_\_\_  
Date

### Statement of Contribution of Co-Authors for Thesis by Published Paper

The authors listed below have certified that:

1. They meet the criteria for authorship in that they have participated in the conception, execution, or interpretation, of at least that part of the publication in their field of expertise;
2. They take public responsibility for their part of the publication, except for the responsible author who accepts overall responsibility for the publication;
3. There are no other authors of the publication according to these criteria that are not listed;
4. Potential conflicts of interest have been disclosed to (a) granting bodies, (b) the editor or publisher of journals or other publications, and (c) the head of the responsible academic unit, and
5. They agree to the use of the publication in the Peter Levett's thesis and its publication on the QUT ePrints database consistent with any limitations set by publisher requirements.

**Chapter 5: A biomimetic extracellular matrix for cartilage tissue engineering centered on photocurable gelatin, hyaluronic acid and chondroitin sulfate,** published in *Acta Biomaterialia* in October 2013.

Contributor	Statement of contribution
Peter A Levett	Experimental design, polymer synthesis, hydrogel construct fabrication, cell culture, construct analyses, data analysis and manuscript preparation.
Ferry. P. W. Melchels	Experimental design, polymer synthesis and manuscript editing.
Karsten Schrobback	Experimental design, data analysis and manuscript editing.
Dietmar. W. Hutmacher	Experimental design and manuscript editing.
Jos Malda	Experimental design and manuscript editing.
Travis J. Klein	Experimental design, construct analyses, data analysis and manuscript editing.

Principal Supervisor Confirmation

I have sighted email or other correspondence from all co-authors confirming their certifying authorship.

\_\_\_\_\_  
Name

\_\_\_\_\_  
Signature

\_\_\_\_\_  
Date

### Statement of Contribution of Co-Authors for Thesis by Published Paper

The authors listed below have certified that:

1. They meet the criteria for authorship in that they have participated in the conception, execution, or interpretation, of at least that part of the publication in their field of expertise;
2. They take public responsibility for their part of the publication, except for the responsible author who accepts overall responsibility for the publication;
3. There are no other authors of the publication according to these criteria that are not listed;
4. Potential conflicts of interest have been disclosed to (a) granting bodies, (b) the editor or publisher of journals or other publications, and (c) the head of the responsible academic unit, and
5. They agree to the use of the publication in the Peter Levett's thesis and its publication on the QUT ePrints database consistent with any limitations set by publisher requirements.

**Chapter 6: Hyaluronic acid enhances the mechanical properties of tissue-engineered cartilage constructs**, published in PlosONE in December 2014.

Contributor	Statement of contribution
Peter A Levett	Experimental design, polymer synthesis, hydrogel construct fabrication, cell culture, construct analyses, data analysis and manuscript preparation.
Dietmar. W. Hutmacher	Experimental design and manuscript editing.
Jos Malda	Experimental design and manuscript editing.
Travis J. Klein	Experimental design, construct analyses, data analysis and manuscript editing.

Principal Supervisor Confirmation

I have sighted email or other correspondence from all co-authors confirming their certifying authorship.

\_\_\_\_\_  
Name

\_\_\_\_\_  
Signature

\_\_\_\_\_  
Date

### Statement of Contribution of Co-Authors for Thesis by Published Paper

The authors listed below have certified that:

1. They meet the criteria for authorship in that they have participated in the conception, execution, or interpretation, of at least that part of the publication in their field of expertise;
2. They take public responsibility for their part of the publication, except for the responsible author who accepts overall responsibility for the publication;
3. There are no other authors of the publication according to these criteria that are not listed;
4. Potential conflicts of interest have been disclosed to (a) granting bodies, (b) the editor or publisher of journals or other publications, and (c) the head of the responsible academic unit, and
5. They agree to the use of the publication in the Peter Levett's thesis and its publication on the QUT ePrints database consistent with any limitations set by publisher requirements.

**Chapter 7: Crosslinkable hydrogels derived from cartilage, meniscus, and tendon tissue**, published in *Tissue Engineering – Part A* in January 2015.

Contributor	Statement of contribution
Jetze Visser	Experimental conception and design, cell culture, polymer synthesis, data analysis and manuscript preparation.
Peter A Levett	Experimental design, tissue preparation, polymer synthesis, construct analyses and manuscript editing.
Nikae C.R. te Moller	Data analysis: PCR.
Jeremy Besems	Tissue preparation, polymer synthesis, hydrogel construct fabrication, cell culture, construct analyses, data analysis and manuscript editing.
Kristel W.M. Boere	Polymer analysis and manuscript editing.
Mattie H.P. van Rijen	Data analysis: biochemistry and histology
Janny C. de Grauw	Experimental design and manuscript editing.
Wouter J.A. Dhert	Experimental design and manuscript editing.
Paul René van Weeren	Experimental design and manuscript editing.
Jos Malda	Experimental conception and design, manuscript editing.

Principal Supervisor Confirmation

I have sighted email or other correspondence from all co-authors confirming their certifying authorship.

\_\_\_\_\_  
Name

\_\_\_\_\_  
Signature

\_\_\_\_\_  
Date